AD NUMBER
ADC005410
CLASSIFICATION CHANGES
TO: unclassified
FROM: confidential
LIMITATION CHANGES
TO: Approved for public release, distribution unlimited
FROM: Controlling DoD Organization. Maury Center for Ocean Science, Washington, DC.
AUTHORITY
ONR ltr, 31 Jan 2006; ONR ltr, 31 Jan 2006

AD-C005410

SECURITY REMARKING REQUIREMENTS

DOD 5200.1-R, DEC 78

REVIEW ON 28 JUL 94

CONFIDENTIAL

MC Report 104
Copy No. 120

AD C005410

MEDITERRANEAN ENVIRONMENTAL ACOUSTIC SUMMARY (U)

July 1974

LONG RANGE ACOUSTIC PROPAGATION PROJECT

[redacted] SECURITY INFORMATION*

[redacted]thorized Disclosure Subject to Criminal [redacted]

AD No. ____ DDC FILE COPY

OCEAN SCIENCE PROGRAM

MAURY CENTER FOR OCEAN SCIENCE

Department of the Navy
Washington, D.C.

DDC
REPORT
MAR 30
RECEIVED
A

CONFIDENTIAL, classified by CNR
Exempt from GDS of E.O. 11652 by OP-095
Ex. Cat. (3), Auto. declass. cannot be predetermined

CONFIDENTIAL

In accordance with security regulations which apply to this document and must be observed by the holder [redacted] with special instructions from the Director [redacted] Project ONR Code 102-06 [redacted]

NATIONAL SECURITY INFORMATION

Unauthorized Disclosure Subject to Criminal Sanctions.

UNCLASSIFIED

SECURITY CLASSIFICATION OF THIS PAGE (When Data Entered)

REPORT DOCUMENTATION PAGE

READ INSTRUCTIONS BEFORE COMPLETING FORM

1. REPORT NUMBER: MC Report 104	2. GOVT ACCESSION NO.
3. RECIPIENT'S CATALOG NUMBER	
4. TITLE (and Subtitle): Mediterranean Environmental Acoustic Summary (U)	5. TYPE OF REPORT & PERIOD COVERED: Summary
6. PERFORMING ORG. REPORT NUMBER	
7. AUTHOR(s): Long Range Acoustic Propagation Project	8. CONTRACT OR GRANT NUMBER(s): N00014-71-C-0438
9. PERFORMING ORGANIZATION NAME AND ADDRESS: Tracor, Inc. 1601 Research Boulevard Rockville, Maryland 20850	10. PROGRAM ELEMENT, PROJECT, TASK AREA & WORK UNIT NUMBERS
11. CONTROLLING OFFICE NAME AND ADDRESS: Long Range Acoustic Propagation Project Maury Center for Ocean Science Dept. of the Navy, Washington, D.C.	12. REPORT DATE: July 1974
	13. NUMBER OF PAGES
14. MONITORING AGENCY NAME & ADDRESS(if different from Controlling Office)	15. SECURITY CLASS. (of this report): CONFIDENTIAL
	15a. DECLASSIFICATION/DOWNGRADING SCHEDULE: XGDS-3

16. DISTRIBUTION STATEMENT (of this Report)

In addition to security requirements which apply to this document, this document may not be released for further distribution by the holder or user without specific prior approval of the Director, Long Range Acoustic Propagation Project (Code 102-[illegible]).

17. DISTRIBUTION STATEMENT (of the abstract entered in Block 20, if different from Report)

Unlimited

18. SUPPLEMENTARY NOTES

None

19. KEY WORDS (Continue on reverse side if necessary and identify by block number)

Marine Climatology	Geophysics	Propagation Loss
Mediterranean Sea	Biology	Ambient Noise
Physical Oceanography	Shipping Distribution	
Geology	Sound Velocity Structure	

20. ABSTRACT (Continue on reverse side if necessary and identify by block number)

This report contains a compilation of environmental and acoustic data for the Mediterranean Sea. Environmental topics covered, both in text and graphically include marine climatology, physical oceanography, geology and geophysics, biology, and shipping distributions. The acoustic data include the sound velocity structure, propagation loss data, and ambient noise data. Variable environmental and acoustic data are presented on a monthly or seasonal basis.

DD FORM 1 JAN 73 1473 EDITION OF 1 NOV 65 IS OBSOLETE

S/N 0102-014-6601

UNCLASSIFIED

SECURITY CLASSIFICATION OF THIS PAGE (When Data Entered)

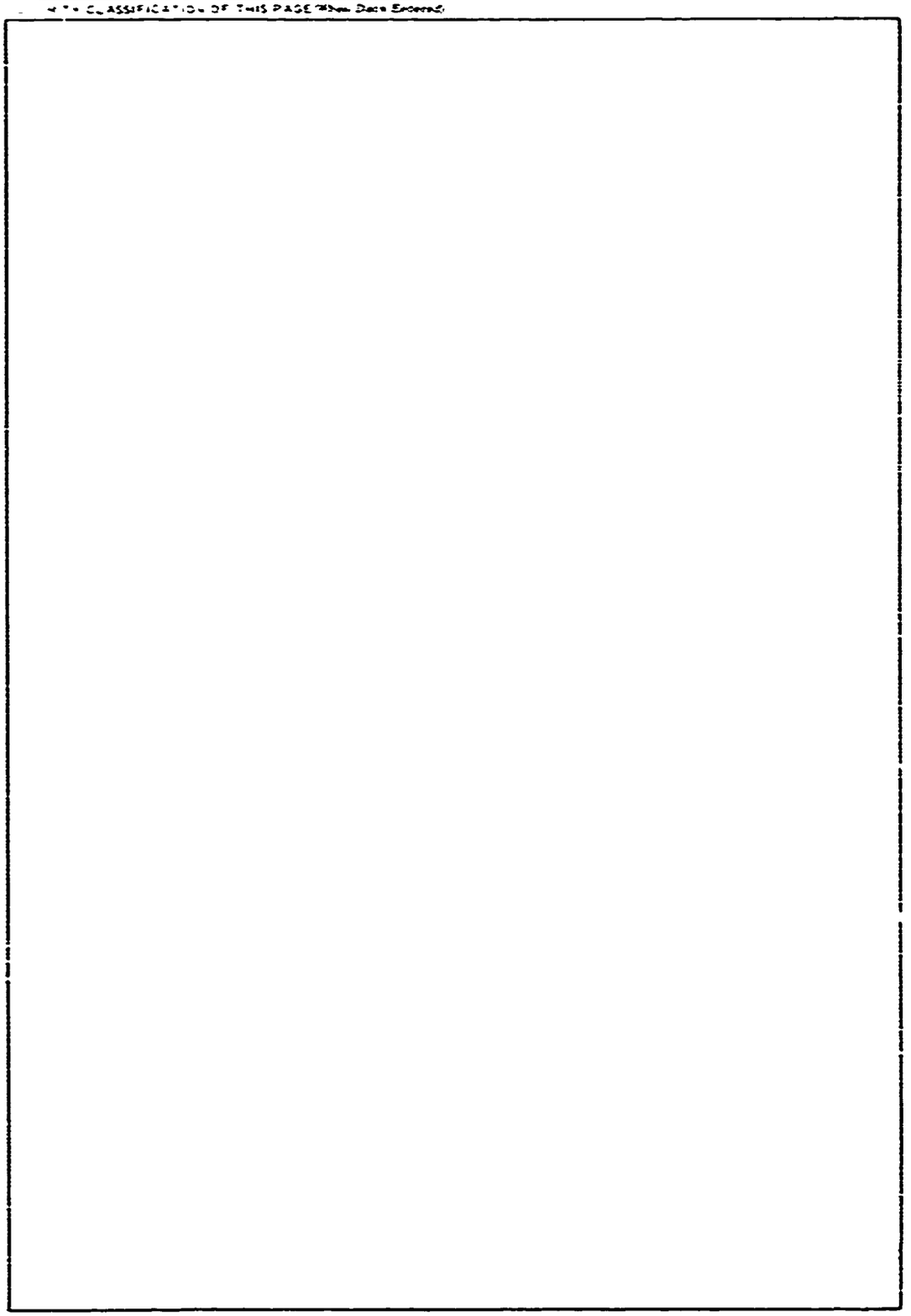

FOREWORD (U)

(U) In 1969 the Maury Center for Ocean Sciences issued a publication entitled "Mediterranean Sea Environmental Atlas for ITASS (U)". It was stated in the Foreword to this document that the presentation of the environmental and acoustic data was tailored solely to support a specific equipment system. Furthermore, the Atlas was considered as an interim document anticipating that it would be updated in the future.

(U) Since 1969, many new acoustic and oceanographic measurements have been made in the Mediterranean Sea. The Long Range Acoustic Propagation Project (LRAPP) itself participated in or sponsored three such efforts (IMP, IOMEDEX, and TASSRAP/DECKPLATE). These measurements have contributed significantly to our knowledge and understanding of sound transmission and ambient noise in the Mediterranean. This fact, coupled with the continued operational interest there, makes the issuance of an up-date to the Atlas worthwhile.

(U) In order to serve the variety of different needs of the operating Fleet as well as those of the scientific and planning community, while at the same time providing volumes which are convenient to use and easy to handle, the Atlas up-date will be issued as four separate companion reports, namely: "Mediterranean ASW Bibliography - Volume I", MC Report 101 (Unclassified); "Mediterranean ASW Bibliography - Volume II (U)", MC Report 102 (Secret); "Mediterranean Environmental Acoustic Data Catalog (U)", MC Report 103 (Confidential); and "Mediterranean Environmental Acoustic Summary (U)", MC Report 104 (Secret). These four volumes cover the many different aspects of environmental acoustics and include information reflecting the total oceanographic discipline as it supports the study of antisubmarine warfare. The information they contain was drawn from a broad spectrum of sources that originated in this country and elsewhere.

J. B. Hersey

J.B. Hersey
Deputy Assistant Oceanographer
for Ocean Science

Letter on file

9

PREFACE AND ACKNOWLEDGEMENTS (U)

(U) The inherent complexities involved in sound propagation in the ocean medium have made it necessary to use modeling as the basis for developing our understanding of this process and for evaluating the performance of underwater acoustic sensor systems. During the past several years we have made continuing progress in improving the accuracy and efficiency of these models. Such progress necessitates that, from time to time, the information that is available for the various ocean regions be recompiled in order to insure the continued adequacy of the basic input parameters to these models at their present state of development. The present report constitutes such a recompilation for the Mediterranean Sea. This specific area was chosen in order to support the Mediterranean ASW Program, conducted by LRAPP in 1974.

(U) The environmental acoustic data summary was derived from material supplied by a large number of people. The environmental and sound velocity structure data and references were compiled by the Undersea Surveillance Oceanographic Center of the U.S. Naval Oceanographic Office. The overall coordinator of this effort was CDR W.B. Matthews. The principal investigator for sound velocity, temperature, salinity and water masses was Mr. Don F. Fenner, with assistance from Messrs. Paul J. Bucca, William J. Cronin, Jr., Terry L. Kelley and William C. Lippert. Ocean fronts and internal waves was compiled by Mr. Alvin Fisher, sea and swell by Mr. Richard H. Holcombe, tides and currents by Mr. Theodore Frontenac, bathymetry and province charts by Mr. Reuben J. Busch, physiography by Mr. Robert N. Bergantino, geophysics and sediments by Mr. Patrick T. Taylor.

(U) Volume scattering was compiled by Mr. Richard H. Love and Mr. Wayne E. Renshaw, false targets and bioluminescence by Mr. William T. Leapley, bottom reverberation by Mr. Jonathan M. Berkson, bottom loss by Mr. Robert E. Christensen. Ms. Joanne V. Lackie and Mr. Douglas Kolk prepared the illustrations for the temperature, salinity and sound velocity sections.

(U) The data on ambient noise were compiled and summarized by Dr. William M. Carey, MAR, Inc. The data on propagation loss were compiled by Dr. Carey and summarized by Dr. August F. Wittenborn, Tracor, Inc. Shipping distributions were supplied by Dr. Lou P. Solomon, PSI and Mr. Paul Wolff, Ocean Data Systems, Inc. The project was under the direction of LCDR T.J. McCloskey, Long Range Acoustic Propagation Project. The overall coordinator for the preparation of this document was Mr. Jimmy T. Gottwald, Tracor, Inc., with assistance from Dr. August F. Wittenborn and Mr. A.N. Glennon, Tracor, Inc.

R. D. Gaul
Manager, Long Range Acoustic
Propagation Project

TABLE OF CONTENTS

TABLE OF CONTENTS (Continued)

LIST OF ILLUSTRATIONS

LIST OF ILLUSTRATIONS (Continued)

LIST OF ILLUSTRATIONS (Continued)

LIST OF ILLUSTRATIONS (Continued)

*These figures are inserted in the envelope bound at the back of this volume

LIST OF ILLUSTRATIONS (Continued)

LIST OF ILLUSTRATIONS (Continued)

*These figures are inserted in the envelope bound at the back of this volume.

LIST OF ILLUSTRATIONS (Continued)

LIST OF ILLUSTRATIONS (Continued)

LIST OF ILLUSTRATIONS (Continued)

LIST OF ILLUSTRATIONS (Continued)

LIST OF TABLES

MEDITERRANEAN ENVIRONMENTAL ACOUSTIC SUMMARY (U)

1.0(U) INTRODUCTION (U)

(U) This report contains a compilation of environmental and acoustic data for the Mediterranean Sea. Environmental topics covered, both in text and graphically, include marine climatology, physical oceanography, geology and geophysics, biology, and shipping distributions. The acoustic data include the sound velocity structure, propagation loss data, and ambient noise data. Variable environmental and acoustic data are presented on a monthly or seasonal basis.

(U) Many of the more common basins, seas, and local bays and gulfs of the Mediterranean Sea referred to in the text are identified in figure 1.0-1.

(U) For ASW purposes, the ultimate result of a data compilation such as is contained in this report is to develop subdivisions within an operating area, here the Mediterranean Sea, which are acoustically homogeneous to within certain bounds. The extent to which this can be achieved determines the number of different subdivisions which must be considered for sonar performance prediction and evaluation. Figure 1.0-2 shows the prediction areas in the Mediterranean as presently used by Fleet Numerical Weather Central (FNWC) for producing operational predictions. This chart is based on NAVOCEANO Chart NA8 p 2401. In principle, each area is intended to have, within prescribed limits, a uniform depth, uniform bottom reflection properties and uniform water column properties. The extent to which this has been achieved to date will be discussed further below.

(U) It should be noted that, in a volume of this nature, the data must be summarized over relatively large areas and over relatively long periods of time. Thus, the user cannot expect that environmental observations at a specific time and location will necessarily be exactly as shown herein for that location during the corresponding month. He should expect, however, that continuing observations over a period of a month would produce data similar to the data presented here for the corresponding month. Thus, although this volume is expected to be a useful aid in understanding the general performance of Fleet sonars in the Mediterranean, it must be recognized that any performance estimate based on this data must be tempered by consideration of the differences between the mean or representative data given here and the actual conditions that prevail in the operational environment.

Figure 1.0-1. Local Seas and Basins of the Mediterranean

ASW PREDICTION AREA INFORMATION					

Figure 1.0-2(C). Standard ASW Prediction Areas for the Mediterranean (U)

Section 2.1, Marine Climatology, begins overleaf.

2.0(U) MEDITERRANEAN SEA ENVIRONMENT (U)

(U) This section describes the environmental factors that establish and influence the propagation of sound in the Mediterranean Sea. These factors are discussed in the following sequence:

- Marine Climatology (2.1)
- Physical Oceanography (2.2)
- Geology/Geophysics (2.3)
- Biology (2.4)
- Shipping Distribution (2.5)

(U) The discussion in this section is oriented toward the occurrence and distribution of the factors. Their influence upon underwater sound is reflected in section 3.0.

2.1(U) Marine Climatology (U)

(U) The data on marine climate and waves are derived from synoptic meteorological observations made from ships, including, in particular, voluntary observations from merchantmen along primary shipping lanes. These observations are accumulated and combined into climatological data files at national repositories.

(U) The following discussion of the Mediterranean climate is based on the seasonal specification of the World Meteorological Organization, i.e., four-month winter and summer seasons (December through March and June through September), separated by two-month spring and autumn transitional seasons. For many of the parameters, however, graphic presentations of the data will be by the month.

2.1.1(U) Pressure (U). Throughout the year, the warm Azores high is the dominant climatic control in the Mediterranean. In winter, the cold Siberian high and, in summer, the thermal (monsoon) lows of northern Africa and southwestern Asia provide secondary controls of the Mediterranean climate.

(U) In winter, a trough of low pressure, oriented along the axis of the sea but favoring the northern coastal regions, generally separates the two highs and constitutes a secondary track for North Atlantic migratory storms. As exemplified by the region of the Ligurian Sea, most lows develop in the Mediterranean as secondaries on trailing cold fronts. However, other lows enter the Mediterranean either across southwestern France from the Bay of Biscay or through the Strait of Gibraltar.

(U) By summer, the intensified Azores high has moved northeastward, the Siberian high has disappeared, and shallow monsoon lows have formed over the Sahara and Arabian deserts. The Azores high now extends to the longitude of the Grecian peninsula and isobars are oriented generally north-south. As a consequence, the resulting pressure gradients cause a stable flow of air from the northwest in the Aegean and eastern Mediterranean Seas.

(U) The transitional seasons portend the seasons to follow, with autumn (October and November) and spring (April and May) resembling winter and summer, respectively.

2.1.2(U) Winds (U). Figures 2.1.2-1 through 2.1.2-6 present wind data showing the monthly percentage frequencies of wind speeds less than Beaufort Force 3 (<10 knots) and greater than Beaufort Force 8 (>34 knots) and three wind roses showing the percentage distribution of wind direction for the three relatively open water areas in the Algerian, Ionian and Tyrrhenian Basins. The vectors in the wind roses show the direction from which the winds blow.

(U) In winter, the convergent and variable winds associated with the relatively frequent lows are the strongest of the year. In February, a representative winter month, winds of gale force (equal to or greater than Beaufort Force 8), occur with frequencies exceeding five percent between France and Sardinia, between Sicily and Tunisia, and around Greece to Crete and Turkey. In the inner Gulf of Lion, gales occur 30 percent or more of the time.

(U) In summer, winds are in general lightest but most constant, under the influence of the stable pressure gradients between the Azores high and desert lows. Storm activity, hence gale occurrence, is at a yearly low during summer.

2.1.3(U) Air Temperature (U). The climate of the Mediterranean is characterized by relatively mild winters and hot summers.

(U) Isolines of mean surface air temperatures are shown by the month in figures 2.1.3-1 and 2.1.3-2. January and February are generally the coolest months. Mean air temperatures in February range from about 48°F (8.9°C) in the north Aegean and Adriatic Seas to about 60°F (15.6°C) off the coasts of Libya and Egypt. A high wind chill may sometimes be experienced in the northern gulfs and seas that are subject to the winter mistral and bora. Diurnal temperature variations are likewise greater in these regions during the winter months.

(U) July and August are usually the hottest months. Mean temperatures in August range from 72°F (22.2°C) in the Gulf of Lion to 82°F (27.8°C) east of Cyprus. Temperature contrasts are minimal, especially in the Adriatic and Aegean Seas. High temperatures are possible along

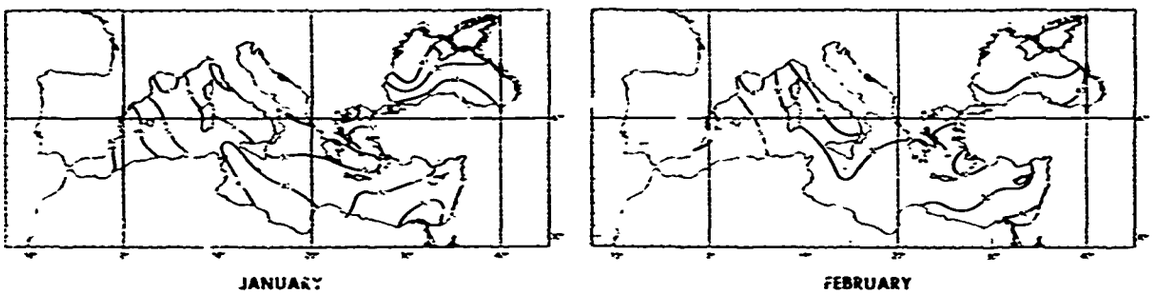

Percentage Frequency of Wind Speed Beaufort Force $\leq$ 3 ($\leq$ 10 kts)

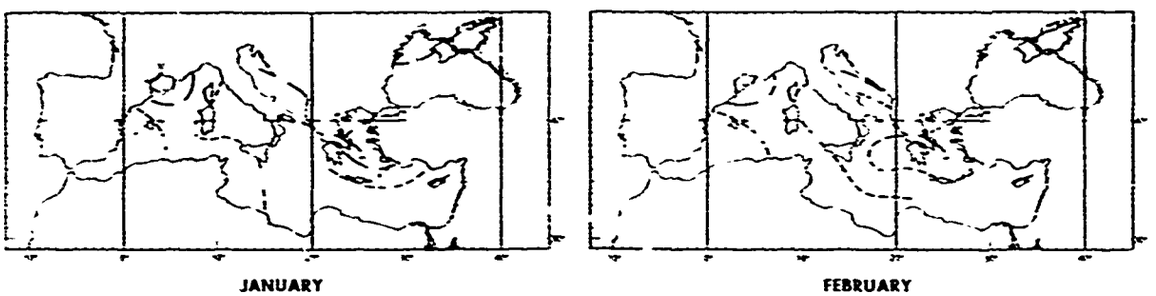

Percentage Frequency of Wind Speed Beaufort Force $\geq$ 8 ($\geq$ 34 kts)

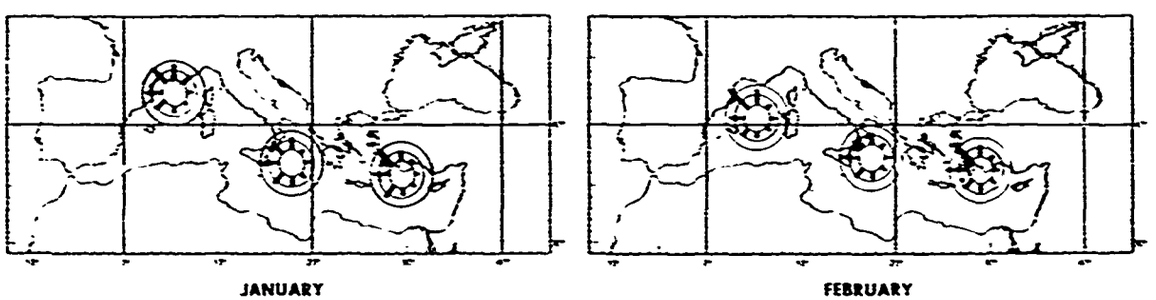

Directional Distribution (Circles at Frequency Intervals of 10%)

Figure 2.1.2-1. Wind Speed and Directionality for the Months of January and February

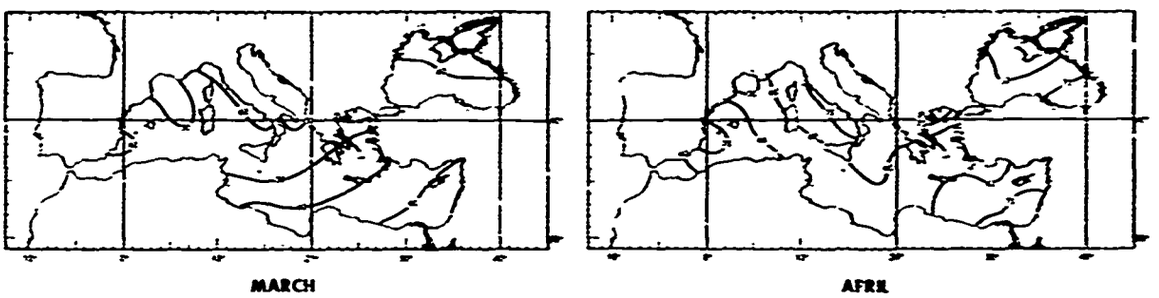

Percentage Frequency of Wind Speed Beaufort Force $\leq$ 3 ($\leq$ 10 kts)

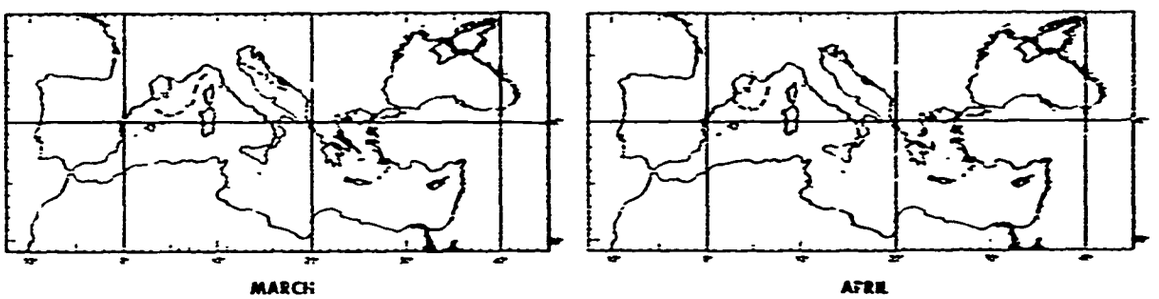

Percentage Frequency of Wind Speed Beaufort Force $\geq$ 8 ($\geq$ 34 kts)

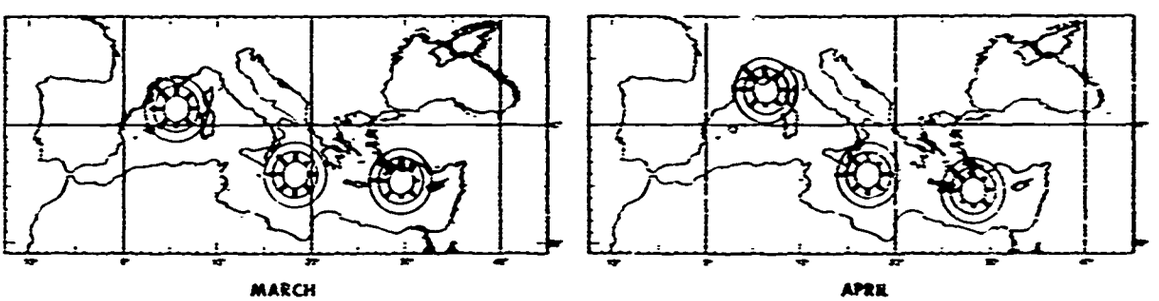

Directional Distribution (Circles at Frequency Intervals of 10%)

Figure 2.1.2-2. Wind Speed and Directionality for the Months of March and April

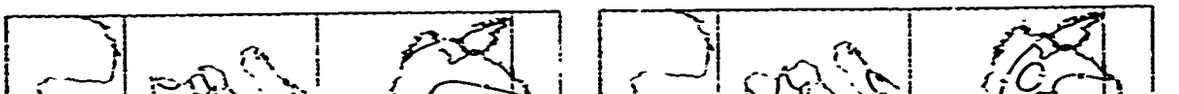

Percentage Frequency of Wind Speed Beaufort Force $\leq$ 5 ($\leq$ 10 kts)

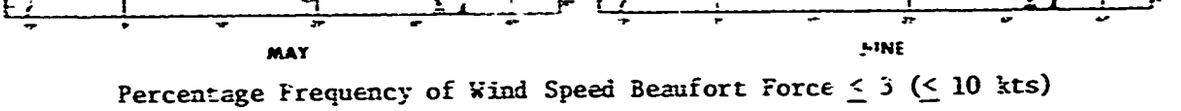

Percentage Frequency of Wind Speed Beaufort Force $\geq$ 8 ($\geq$ 34 kts)

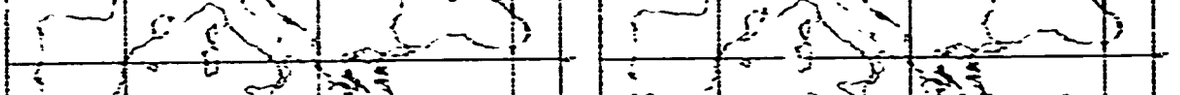

Directional Distribution (Circles at Frequency Intervals of 10%)

Figure 2.1.2-3. Wind Speed and Directionality for the Months of May and June

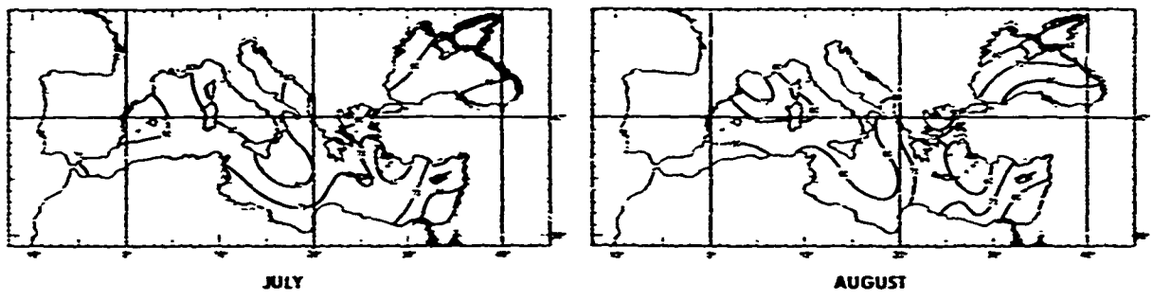

Percentage Frequency of Wind Speed Beaufort Force $\leq$ 3 ($\leq$ 10 kts)

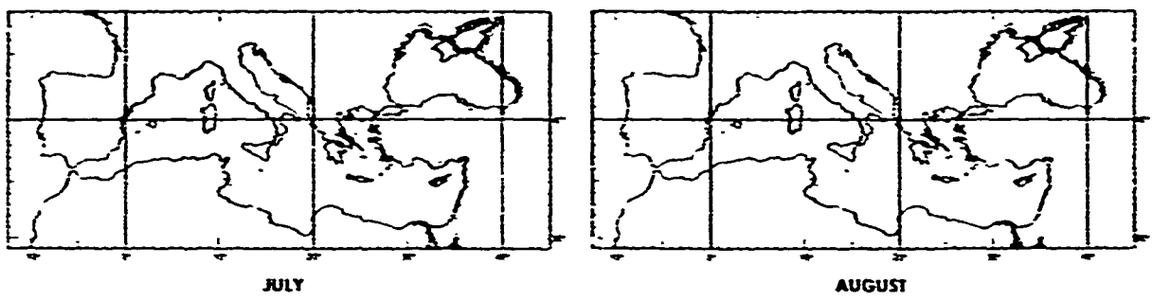

Percentage Frequency of Wind Speed Beaufort Force $\geq$ 8 ($\geq$ 34 kts)

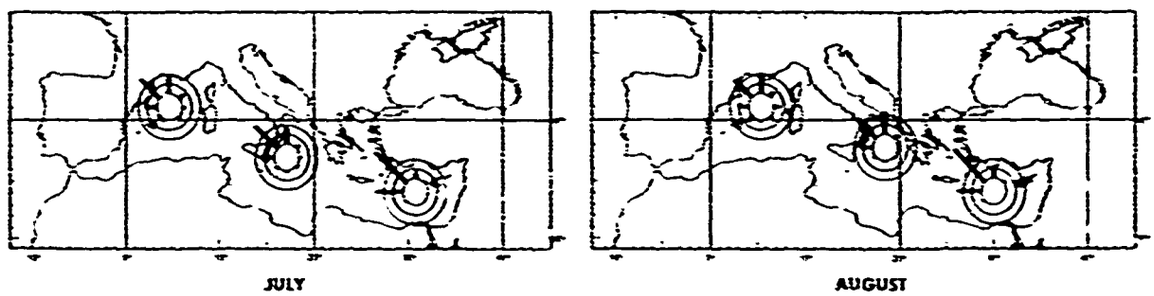

Directional Distribution (Circles at Frequency Intervals of 10%)

Figure 2.1.2-4. Wind Speed and Directionality for the Months of July and August

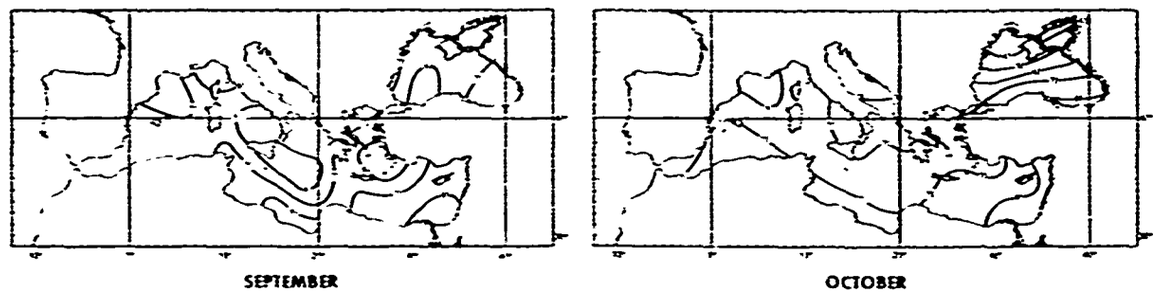

Percentage Frequency of Wind Speed Beaufort Force $\leq$ 3 ($\leq$ 10 kts)

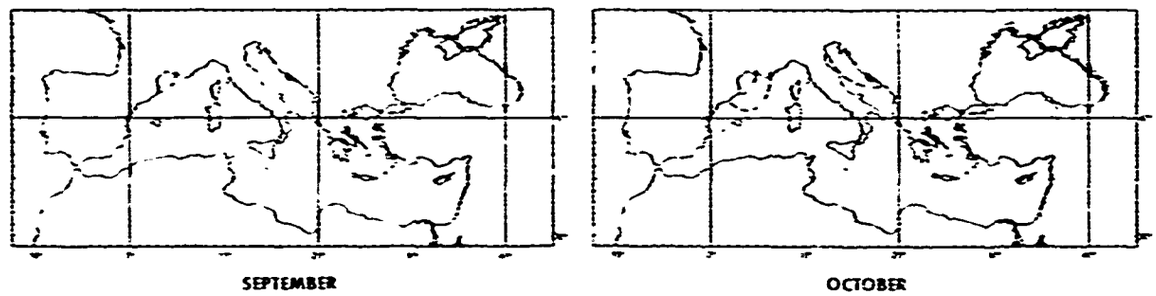

Percentage Frequency of Wind Speed Beaufort Force $\geq$ 8 ($\geq$ 34 kts)

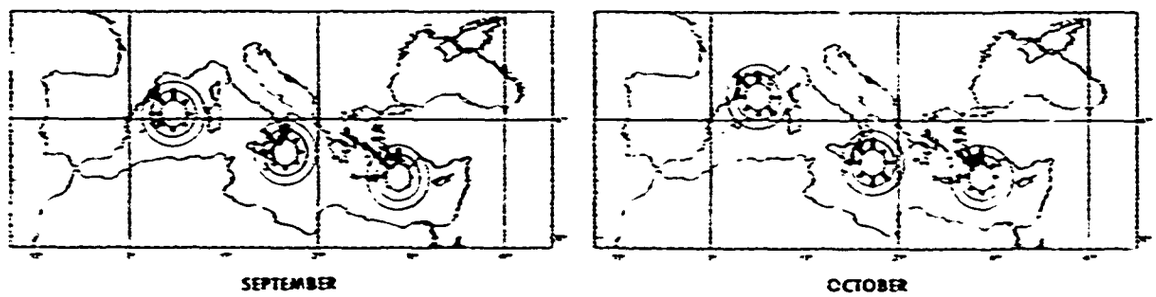

Directional Distribution (Circles at Frequency Intervals of 10%)

Figure 2.1.2-5. Wind Speed and Directionality for the Months of September and October

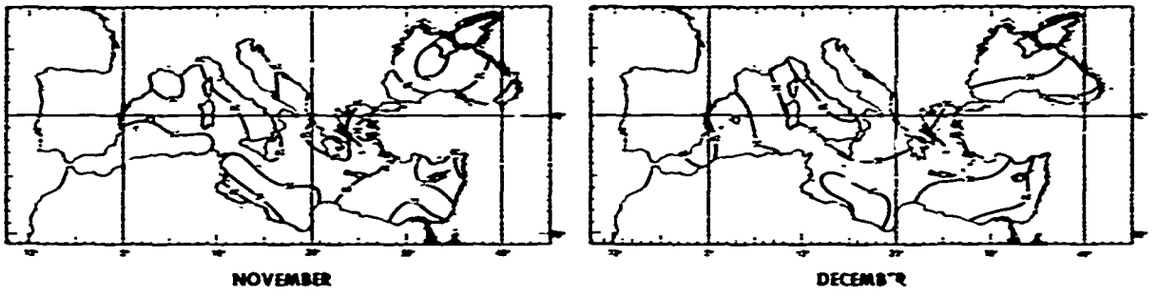

Percentage Frequency of Wind Speed Beaufort Force $\leq$ 3 ($\leq$ 10 kts)

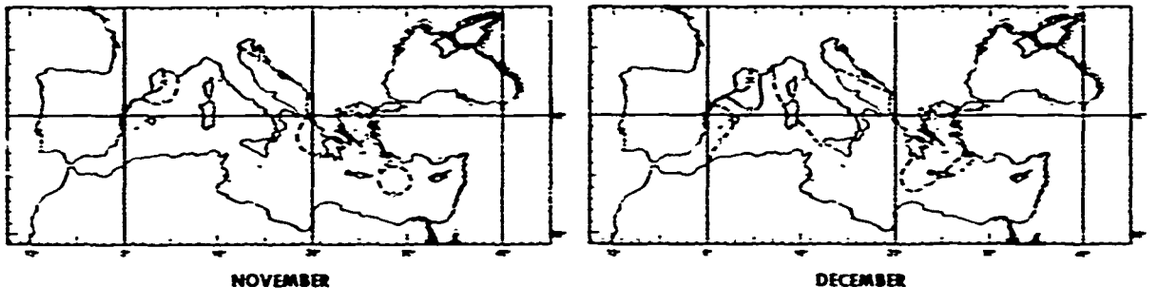

Percentage Frequency of Wind Speed Beaufort Force $\geq$ 8 ($\geq$ 34 kts)

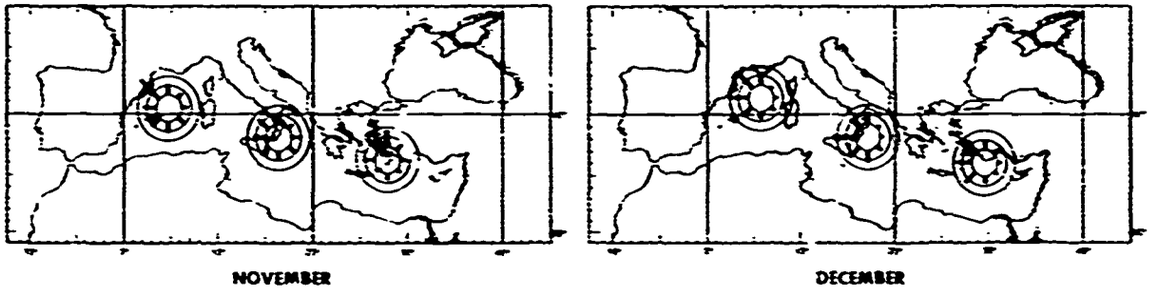

Directional Distribution (Circles at Frequency Intervals of 10%)

Figure 2.1.2-6. Wind Speed and Directionality for the Months of November and December

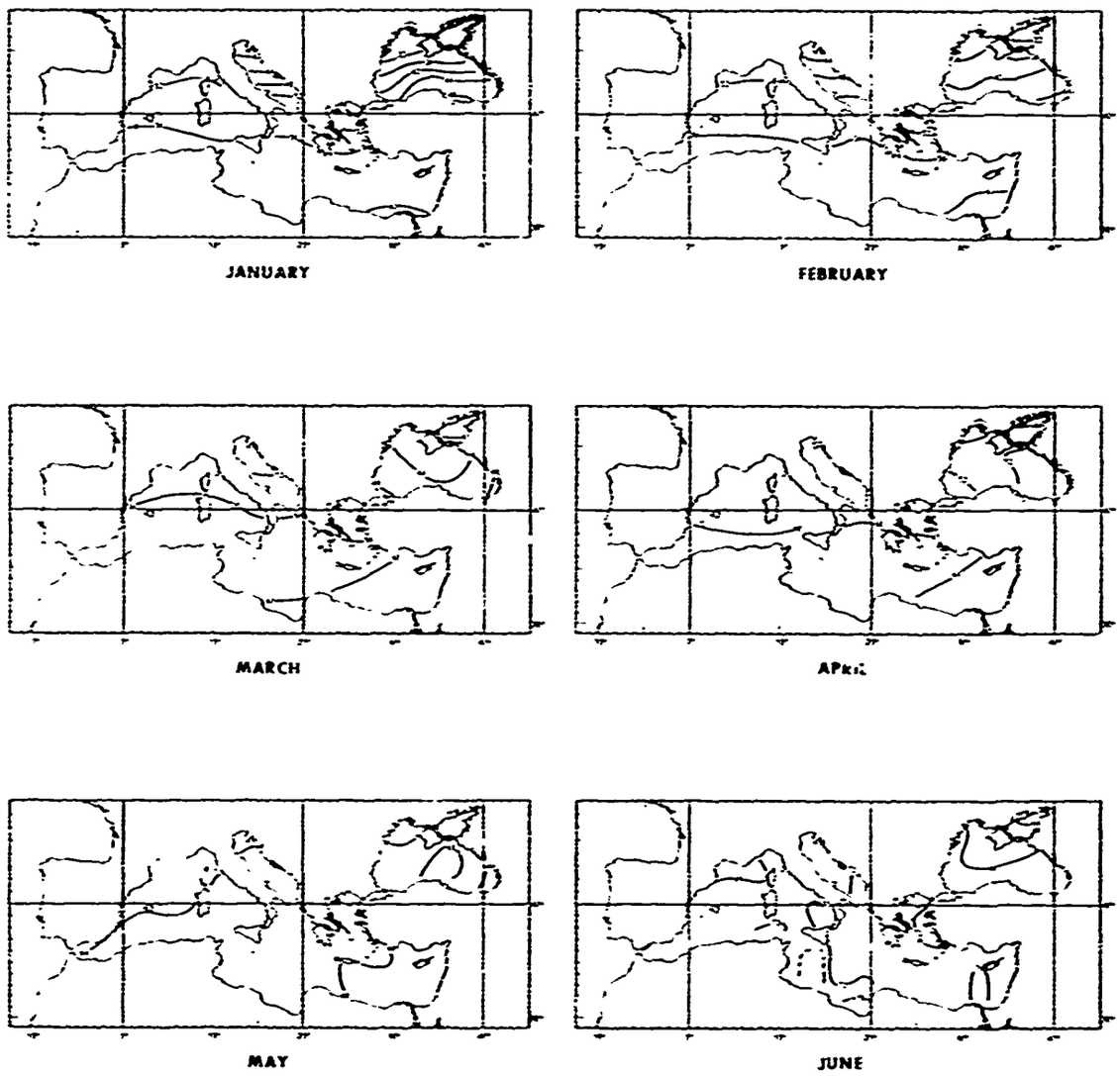

Figure 2.1.3-1. Mean Surface Air Temperature in Degrees Fahrenheit for the Months January through June

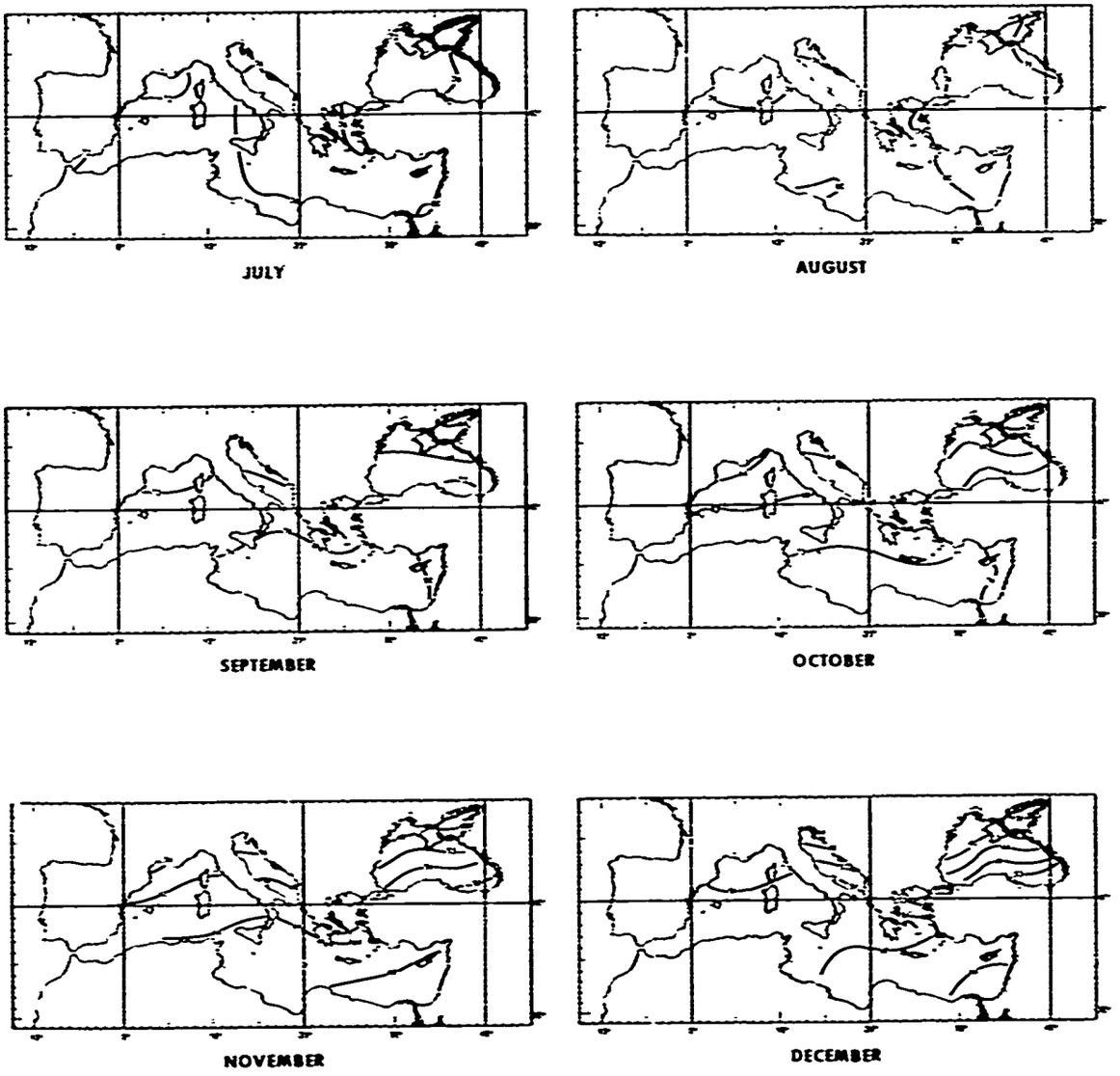

Figure 2.1.3-2. Mean Surface Air Temperature in Degrees Fahrenheit for the Months July through December

the North African coast, when the hot, desert wind (sirocco) is blowing offshore. Under such conditions, a maximum temperature of 118°F (47.8°C) has been recorded at Tunisian coastal points in July and August.

2.1.4(U) Cloudiness and Precipitation (U). The maximum frequency of cloudiness and precipitation occurs during winter, in association with the numerous low pressure systems. In January, the average total cloud amounts exceed five-tenths over the greater part of the Mediterranean Sea, and drizzle and light rain occur from five to 15 percent of the time. In summer, cloud cover averages less than three-tenths, and rainfall is rare. Figures 2.1.4-1 and 2.1.4-2 show regions of average cloud cover <0.2 by the month. Figures 2.1.4-3 and 2.1.4-4 show regions of average cloud cover >0.8 by the month. Figure 2.1.4-5 shows the percentage of climatological observations by the month which include precipitation.

2.1.5(U) Visibility (U). Atmospheric visibility generally exceeds five nautical miles throughout the Mediterranean but may occasionally be restricted by fog, haze, dust, or rain. Warm temperatures usually inhibit the occurrence of advection fog, so that visibilities are infrequently less than one-half nautical mile, except in the extreme north, during winter. Figures 2.1.5-1 and 2.1.5-2 show percentage of occurrence of visibility less than five nautical miles.

(U) Precipitation is the principal cause of reduced visibility in the north Aegean and Adriatic Seas during winter and early spring; however, sea fog may form over these cooler waters when warm, moist southerly air moves in. Thus, in the extreme north of the two seas, there is a five percent probability that visibility will be less than one-half nautical mile in December and March.

(U) Restricted visibility, due mainly to haze and fog, is least frequent in summer. During July and August, the likelihood that visibility will be less than five nautical miles exceeds five percent only in the northwestern gulfs and in the southwest part of the area (Strait of Gibraltar and Alboran Sea). In the same regions, visibility is less than one-half nautical mile about one percent of the time. Dust, haze, and even sand are the principal restrictions to visibility along the coasts of Morocco and Algeria.

2.1.6(U) Waves (U). Waves usually consist of sea and swell intermixed, where sea denotes those waves being raised or sustained by the existing wind, and swell refers to waves that have moved away from the generating area and are therefore decaying. Seas, also known as wind waves or wind seas, are short, sharp, and irregular waves; swells are long, smoother, and regular.

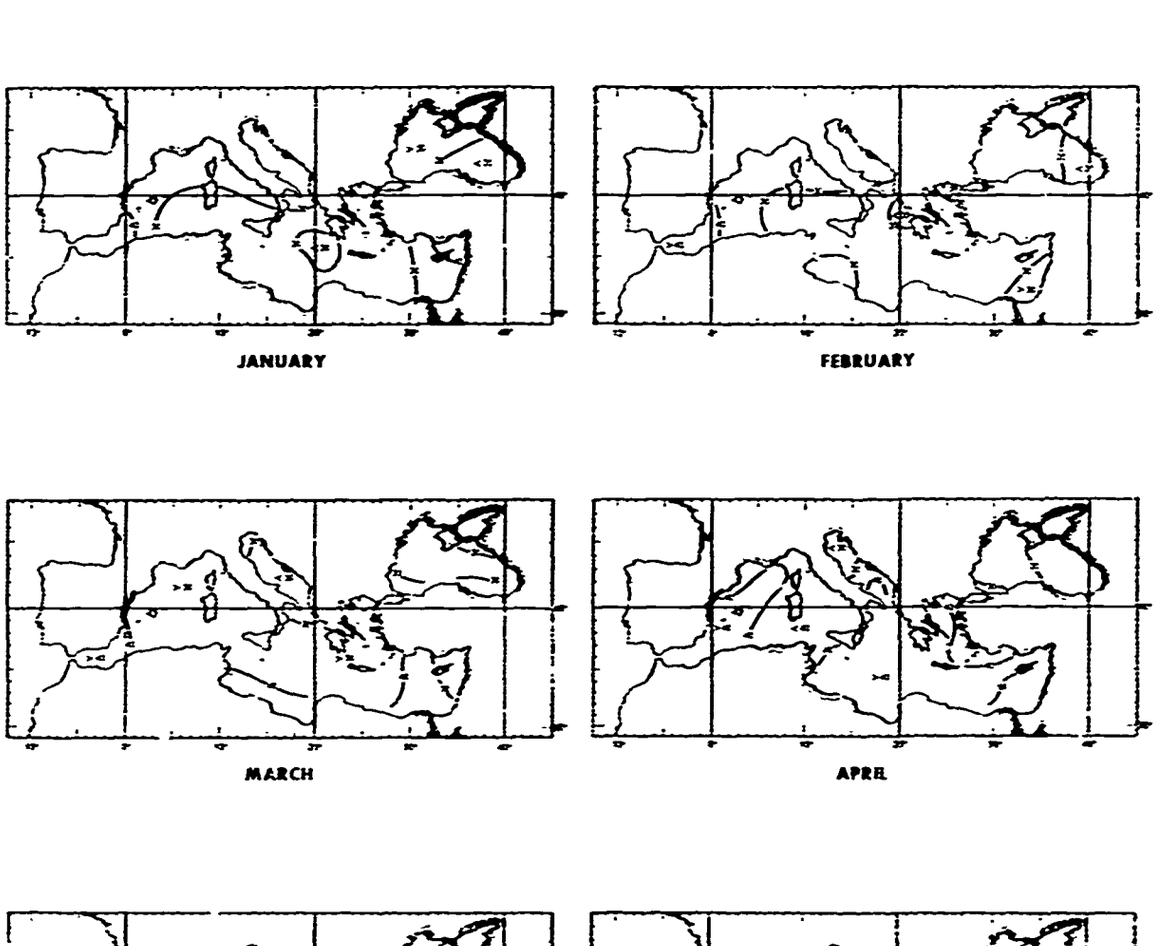

Figure 2.1.4-1. Percentage of Occurrence of Cloud Cover of ≤ 0.2 for the Months January through June

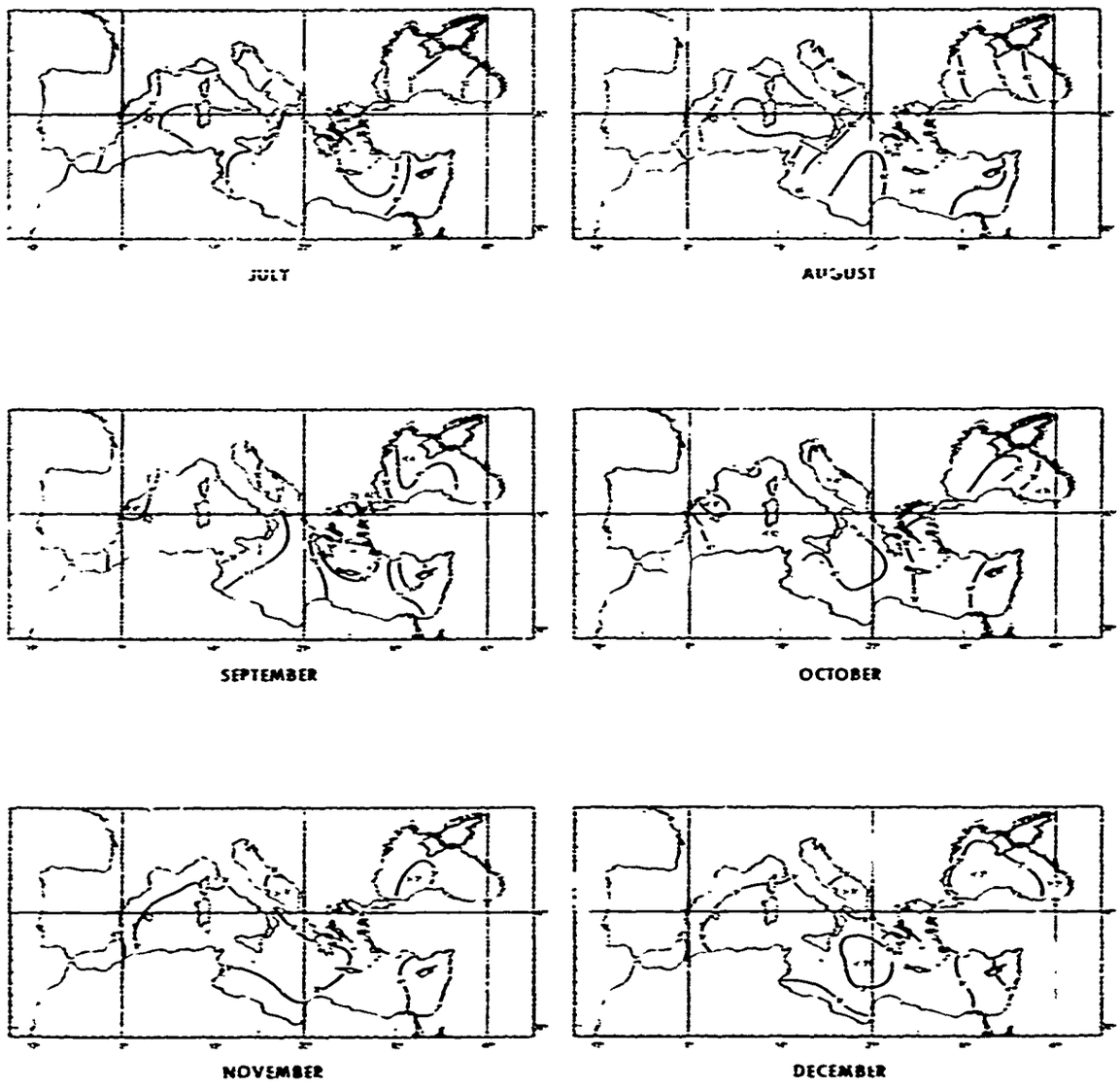

Figure 2.1.4-2. Percentage of Occurence of Cloud Cover of ≤ 0.2 for the Months July through December

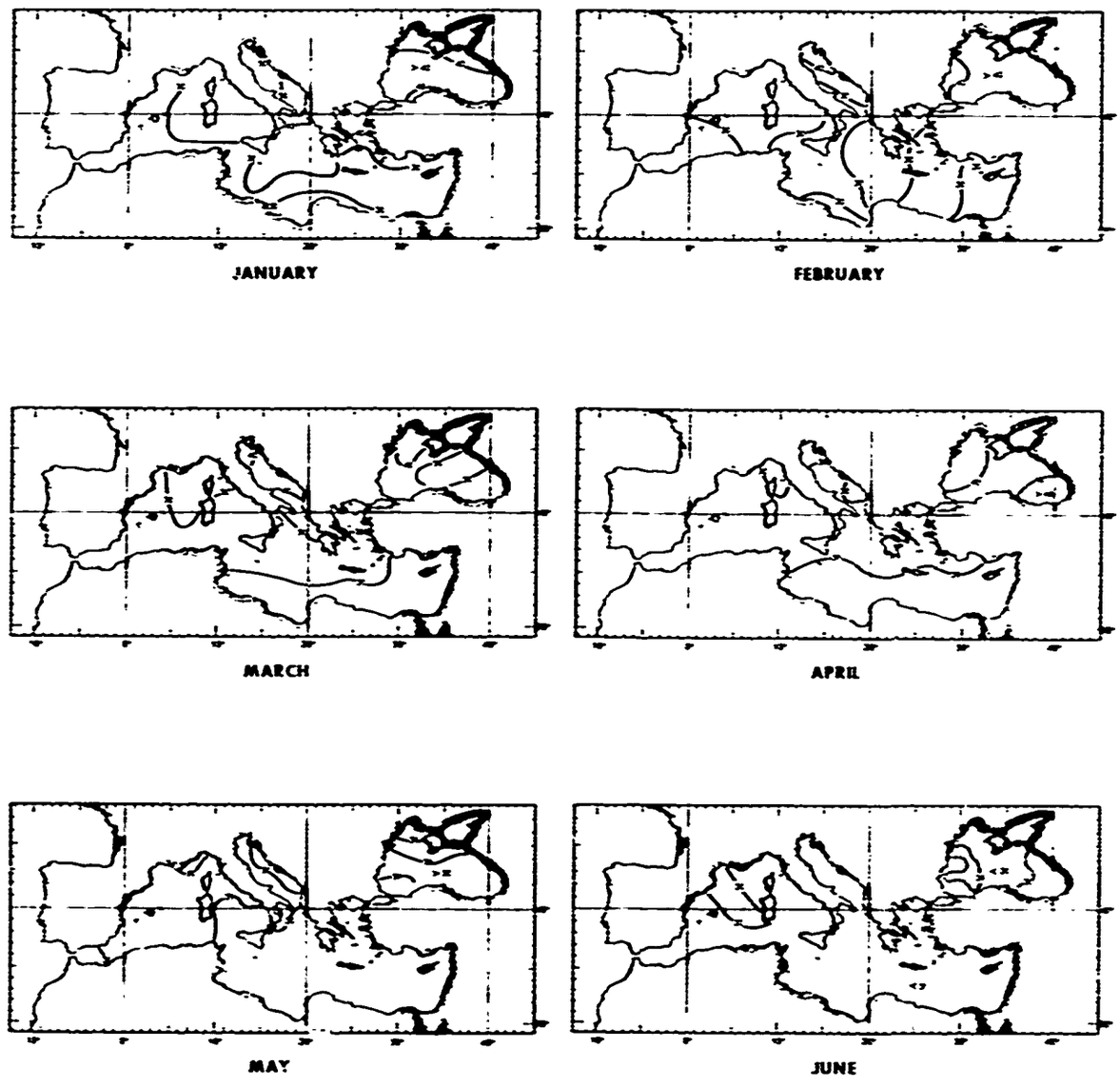

Figure 2.1.4-3. Percentage of Occurrence of Cloud Cover of $\geq$ 0.8 for the Months January through June

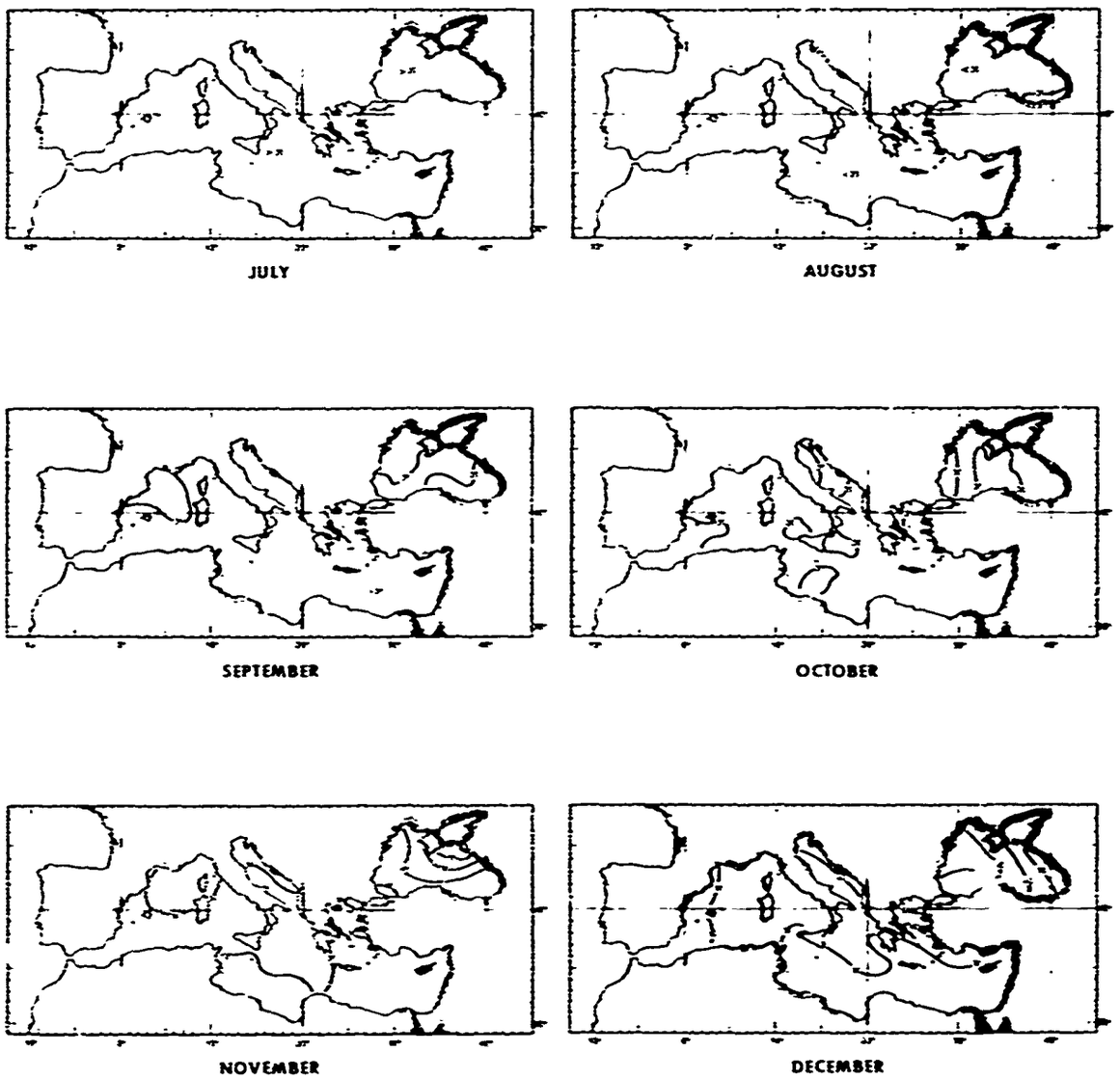

Figure 2.1.4-4. Percentage of Occurrence of Cloud Cover of $\geq$ 0.8 for the Months July through December

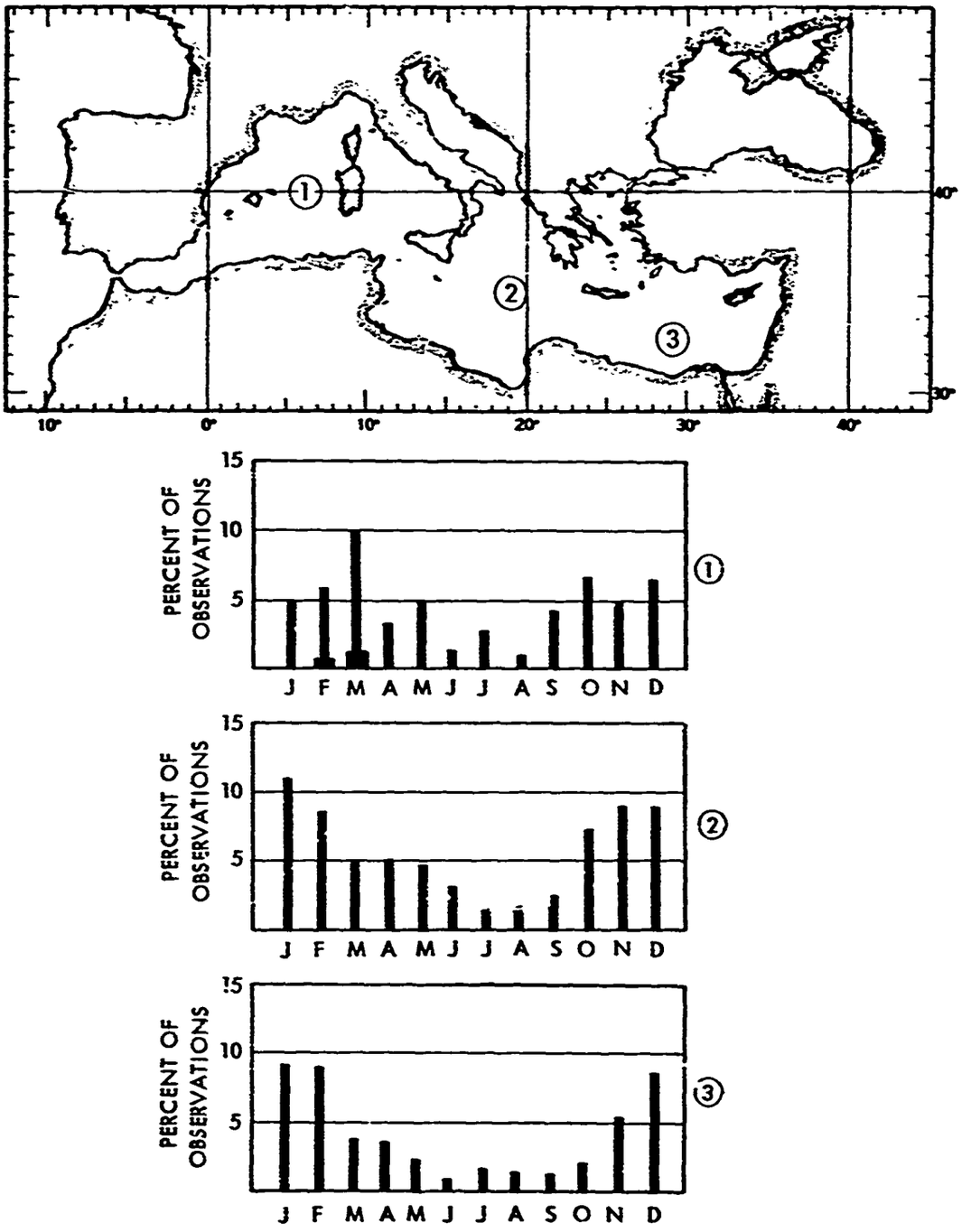

Figure 2.1.4-5. Percentage of Climatologica_ Observations by the Month Which Include Precipitation for the Indicated Basins (Narrow Bars Correspond to Liquid, Wide Bars to Frozen Precipitation)

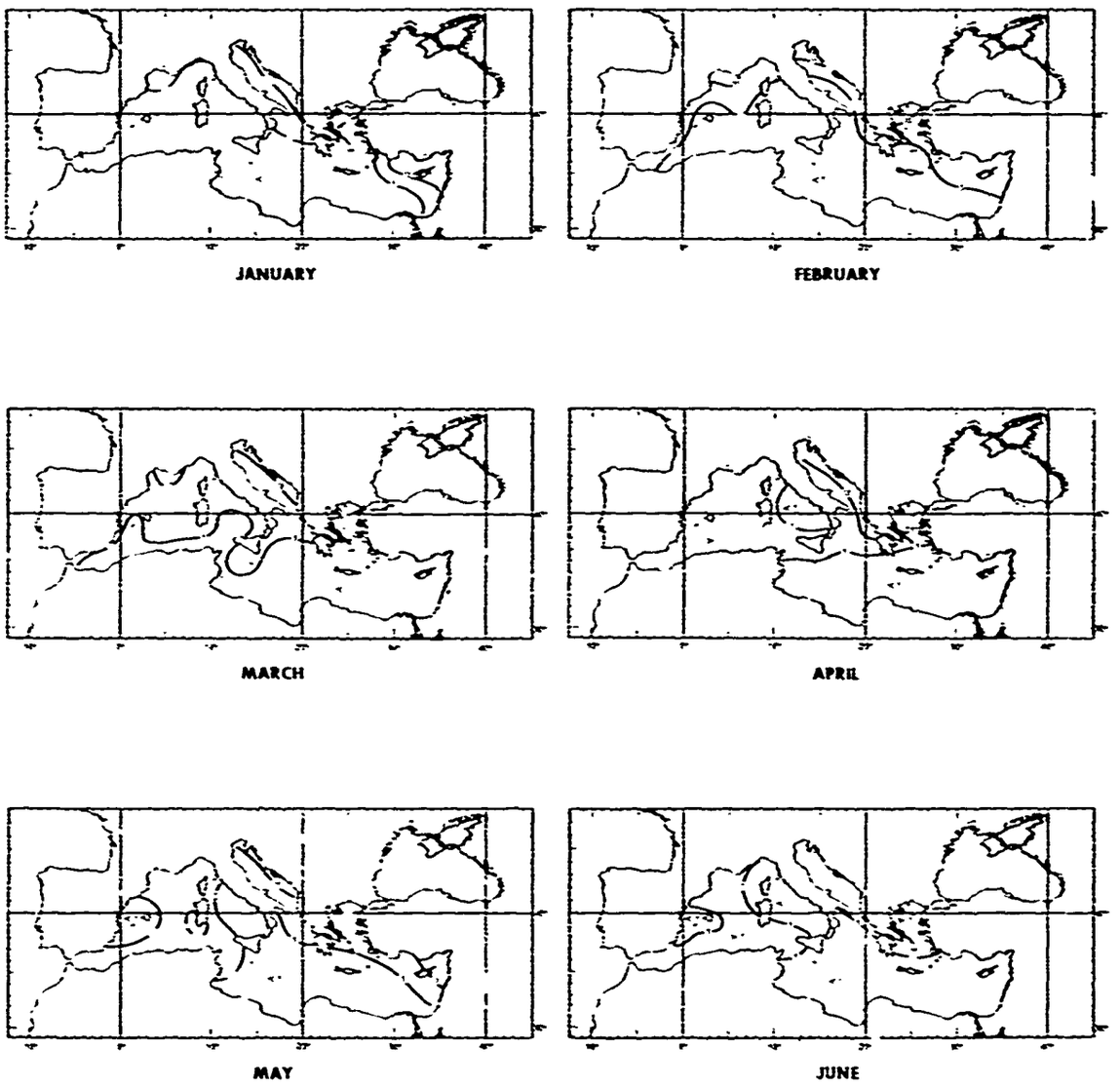

Figure 2.1.5-1. Percentage Frequency of Occurrence of Visibility $\leq$ 5 nm for the Months January through June

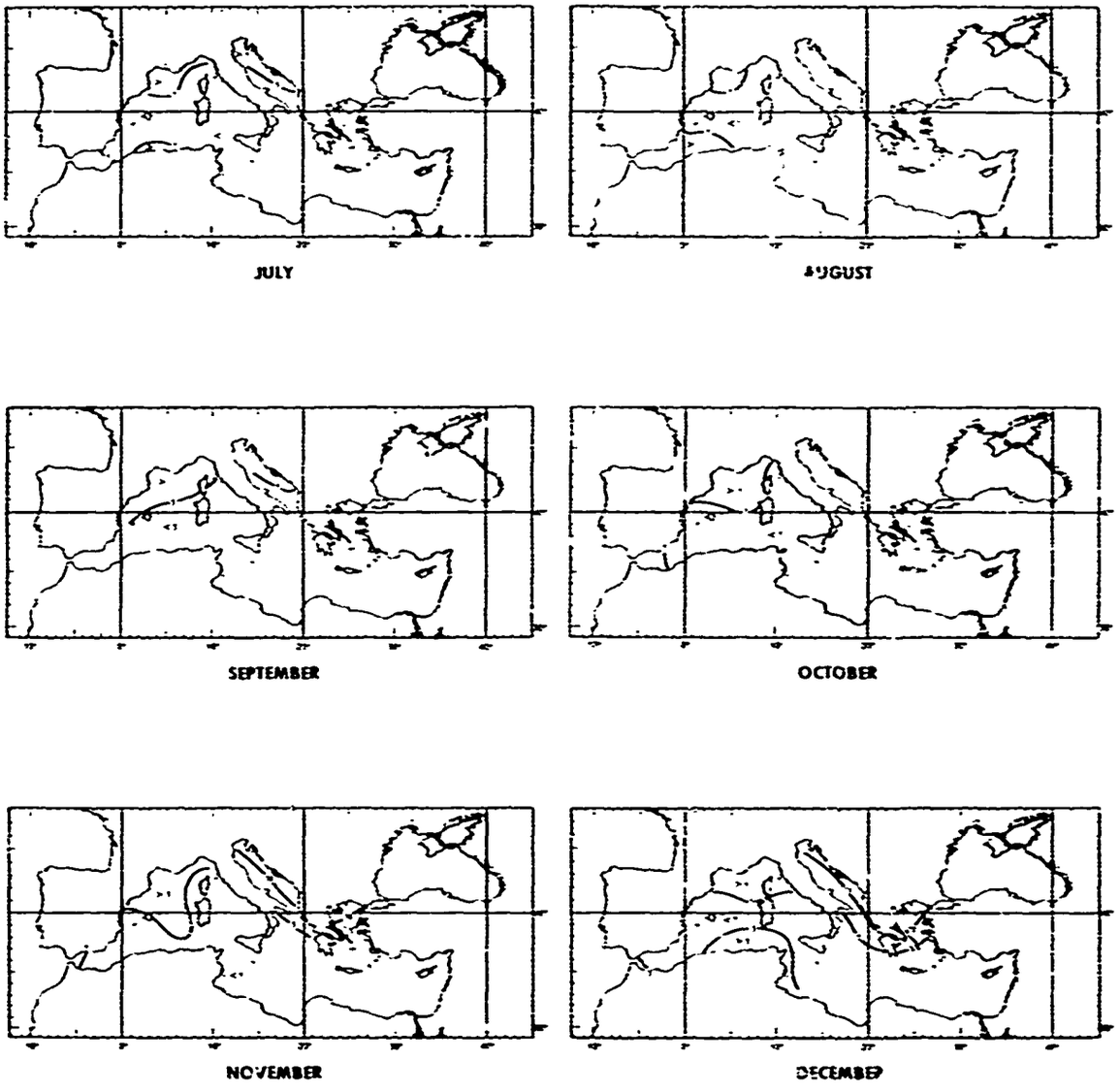

Figure 2.1.5-2. Percentage Frequency of Occurrence of Visibility $\leq$ 5 nm for the Months July through December

2.1.6.1(U) Sea (U). Since seas broadly reflect the direction and strength of the generating wind, they form the basis for methods, such as the Beaufort Wind Scale, for estimating wind speeds. The converse estimation of wave characteristics from wind conditions has long interested wave theoreticians and forecasters. These specialists have developed various graphs, tables, and formulas to represent the relationships. Table 2.1.6-I, based on a combination of several theoretical and empirical principles of wind wave generation, is a recent example. It should be noted, however, that the tabulated values are to be used with caution, since fully developed seas* are believed to be relatively infrequent, particularly at the higher wind speeds.

(U) Figures 2.1.6-1 through 2.1.6-6 show isolines of the cumulative percentage frequency of occurrence of sea heights equal to and higher than five, eight, and 12 feet on a monthly basis.

(U) Seas are roughest in winter, the season of strongest winds associated with maximum cyclonic activity. In February, seas five feet and higher occur about 40 percent of the time through the spine of the Mediterranean. Such seas extend from the Gulf of Lion (with a maximum frequency of 50 percent), through the Strait of Sicily and north of the Gulf of Sirte to the Dodecanese Islands and the coast of Turkey. High seas (equal to and higher than 12 feet) occur more than ten percent of the time through the same waters.

(U) Sea heights are lowest in summer, when wind forces and storm activity reach a minimum. The average frequency of rough and higher seas (equal to and higher than five feet) is about ten percent, except in Aegean waters where, because of strong etesian winds, they average 20 percent. The frequency of high seas (equal to or higher than 12 feet) exceeds five percent only in the Gulf of Lion.

2.1.6.2(U) Swell (U). The distribution of swell is similar to that of seas. In winter, the greatest frequencies of moderate swell (six to 12 feet) and high swell (over 12 feet) are found in the large and deep basins of the Mediterranean that are open to long wind fetches; such heights are rare in summer. Isolines of the cumulative frequency of occurrence of swell heights equal to or greater than 12 feet are shown in figures 2.1.6-7 and 2.1.6-8 by the month.

---

*Fully developed seas are those which have achieved the maximum height to which waves can be generated by a given wind force blowing over sufficient fetch. The fetch is the distance over the sea surface across which the wind blows in essentially the same direction.

TABLE 2.1.6-I. WIND AND WAVE RELATIONSHIPS
FOR FULLY-DEVELOPED SEA

Beaufort number	Wind Speed: knots	mph	meters per second	km per hour	Nautical term	U.S. Weather Bureau term	Hydrographic Office: Term and height of waves, in feet	Code	International: Term and height of waves, in feet	Code	Waves observed at sea
0	under 1	under 1	0.0-0.2	under 1	Calm		Calm, 0	0			Sea like mirror
1	1-3	1-3	0.3-1.5	1-5	Light air	Light	Smooth, less than 1	1	Calm, glassy, 0	0	Ripples with appearance of scales; no foam crests.
2	4-6	4-7	1.6-3.3	6-11	Light breeze		Slight, 1-3	2	Rippled, 0-1	1	Small wavelets; crests of glassy appearance, not breaking
3	7-10	8-12	3.4-5.4	12-19	Gentle breeze	Gentle	Moderate, 3-5	3	Smooth, 1-2	2	Large wavelets; crests begin to break; scattered whitecaps
4	11-16	13-18	5.5-7.9	20-28	Moderate breeze	Moderate			Slight, 2-4	3	Small waves, becoming longer; numerous whitecaps.
5	17-21	19-24	8.0-10.7	29-38	Fresh breeze	Fresh	Rough, 5-8	4	Moderate, 4-8	4	Moderate waves, taking longer form; many whitecaps; some spray.
6	22-27	25-31	10.8-13.8	39-49	Strong breeze				Rough, 8-13	5	Larger waves forming; whitecaps everywhere; more spray.
7	28-33	32-38	13.9-17.1	50-61	Moderate gale	Strong					Sea heaps up; white foam from breaking waves begins to be blown in streaks.
8	34-40	39-46	17.2-20.7	62-74	Fresh gale		Very rough, 8-12	5	Very rough, 13-20	6	Moderately high waves of greater length; edges of crests begin to break into spindrift; foam is blown in well-marked streaks.
9	41-47	47-54	20.8-24.4	75-88	Strong gale	Gale	High, 12-20	6			High waves; sea begins to roll; dense streaks of foam; spray may reduce visibility.
10	48-55	55-63	24.5-28.4	89-102	Whole gale		Very high, 20-40	7	High, 20-30	7	Very high waves with overhanging crests; sea takes white appearance as foam is blown in very dense streaks; rolling is heavy and visibility reduced.
11	56-63	64-72	28.5-32.6	103-117	Storm	Whole gale	Mountainous, 40 and higher	8	Very high, 30-45	8	Exceptionally high waves; sea covered with white foam patches, visibility still more reduced
12	64-71	73-82	32.7-36.9	118-133							
13	72-80	83-92	37.0-41.4	134-149							
14	81-89	93-103	41.5-46.1	150-166							
15	90-99	104-114	46.2-50.9	167-183	Hurricane	Hurricane	Confused	9	Phenomenal, over 45	9	Air filled with foam; sea completely white with driving spray; visibility greatly reduced.
16	100-108	115-125	51.0-55.0	184-201							
17	109-118	126-136	56.1-61.2	202-220							

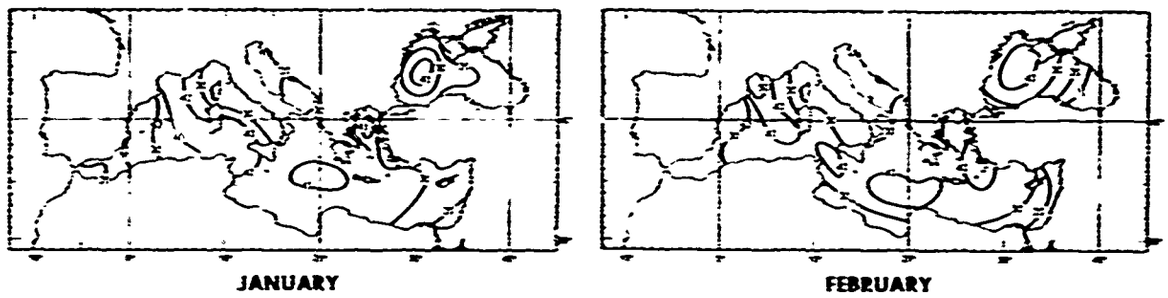

5 Feet

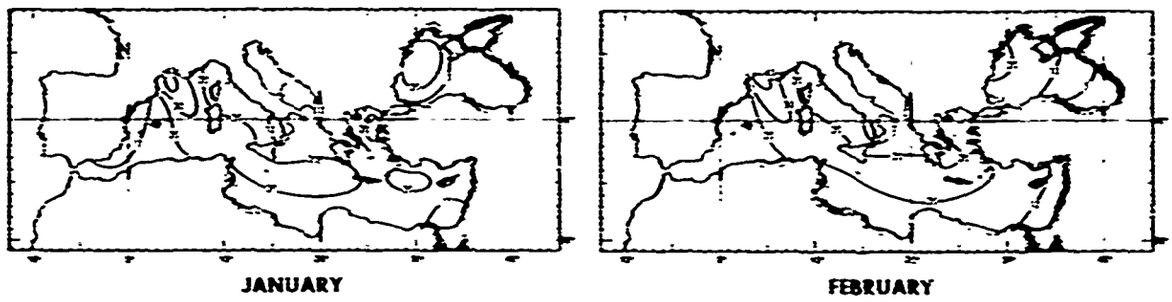

8 Feet

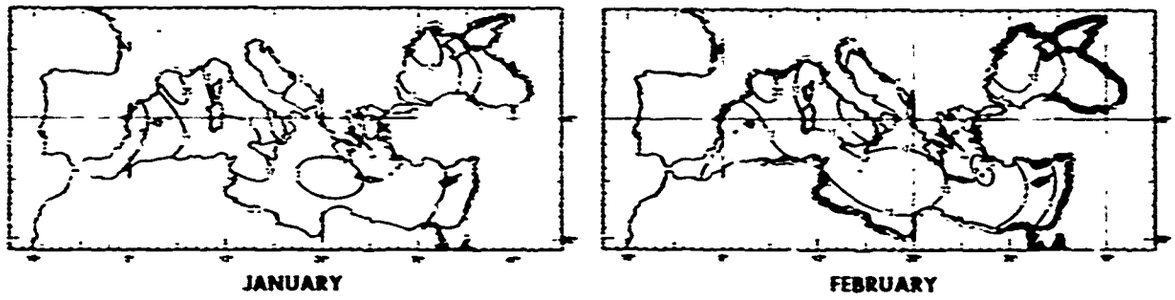

12 Feet

Figure 2.1.6-1. Cumulative Percentage Frequency of Occurrence of Sea Heights Exceeding 5, 8 and 12 feet for the Months of January and February

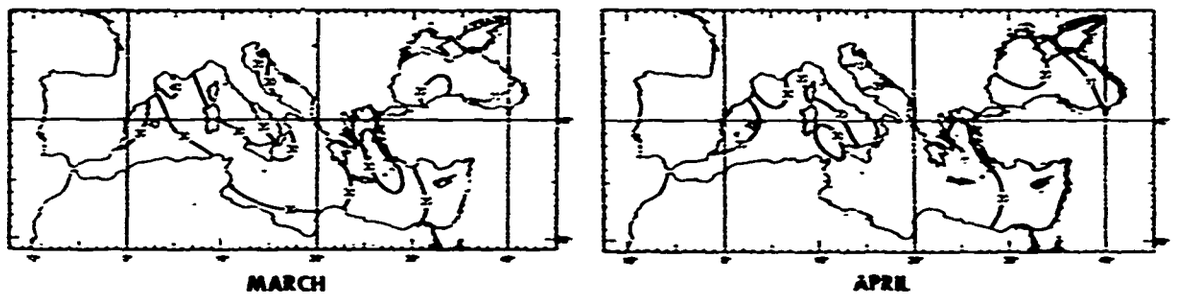

5 Feet

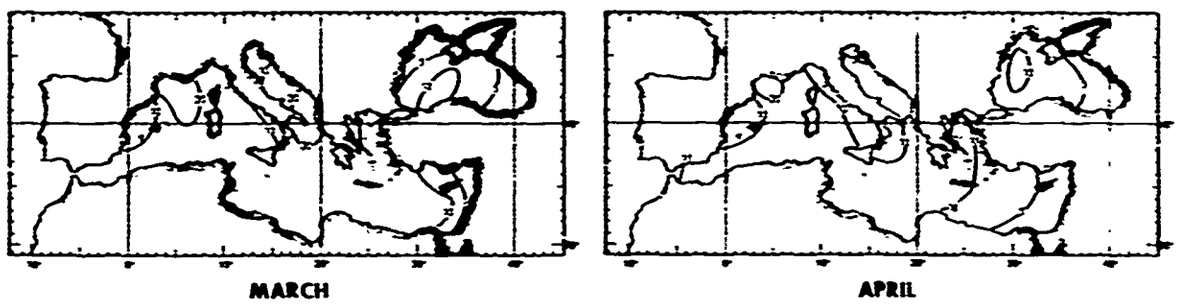

8 Feet

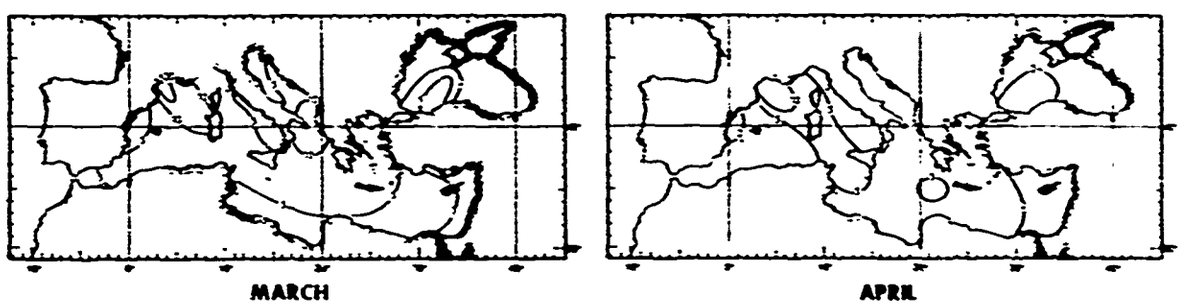

12 Feet

Figure 2.1.6-2. Cumulative Percentage Frequency of Occurrence of Sea Heights Exceeding 5, 8 and 12 feet for the Months of March and April

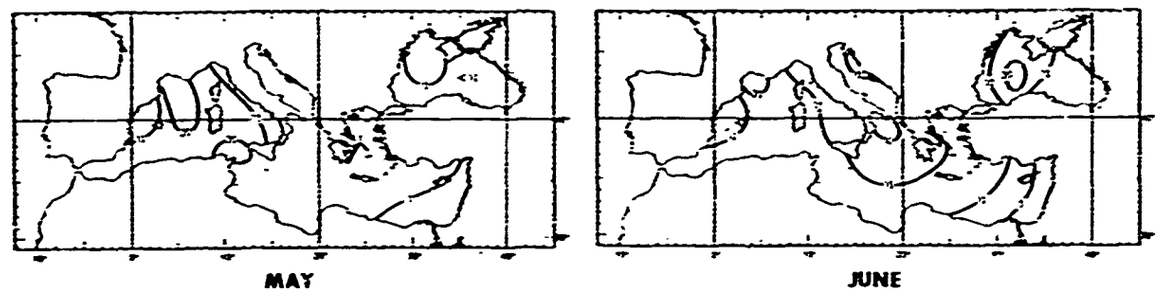

5 Feet

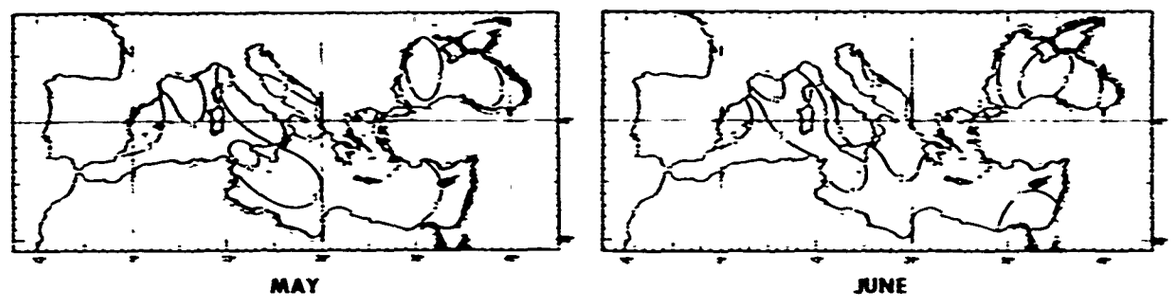

8 Feet

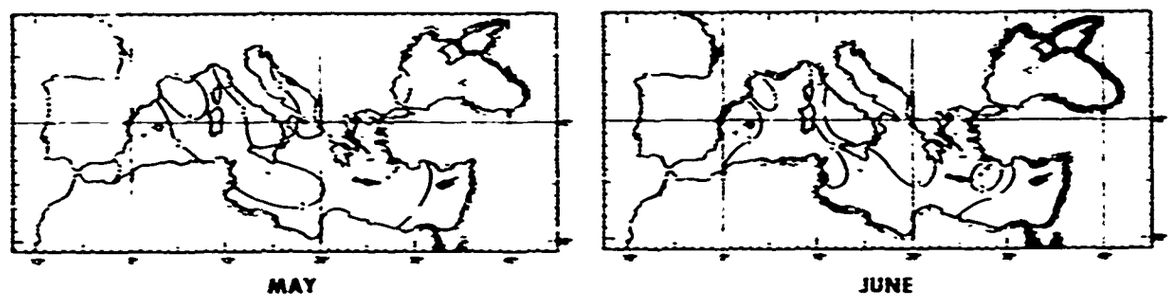

12 Feet

Figure 2.1.6-3. Cumulative Percentage Frequency of Occurrence of Sea Heights Exceeding 5, 8 and 12 feet for the Months of May and June

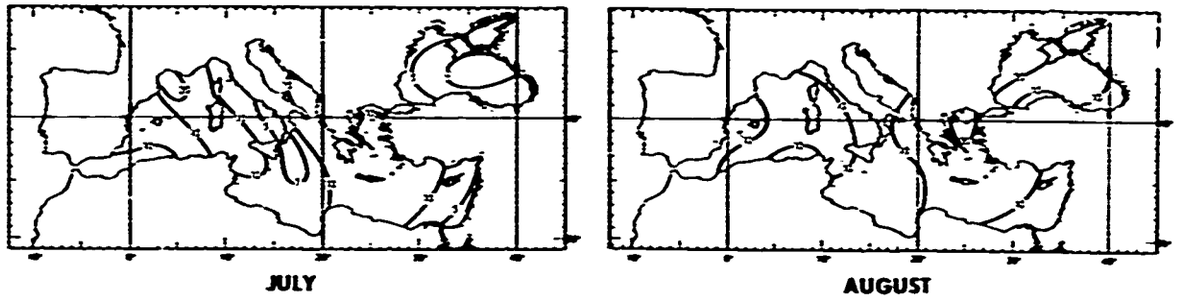

5 Feet

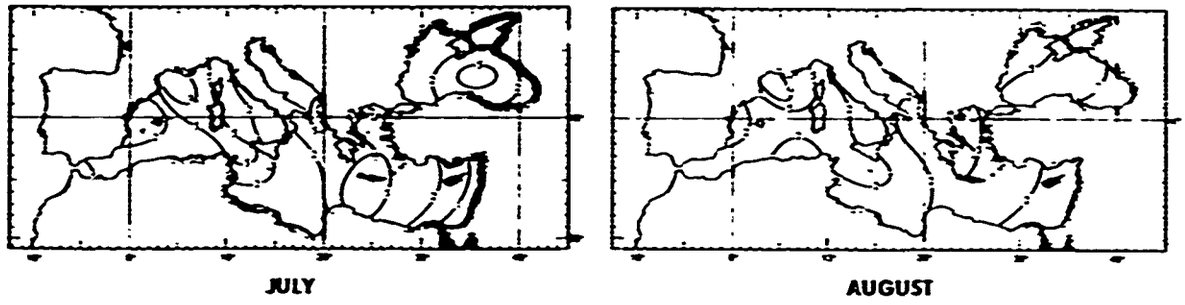

8 Feet

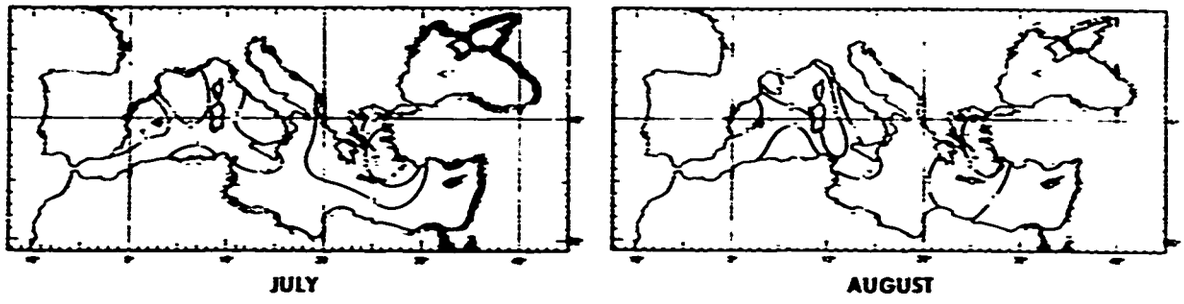

12 Feet

Figure 2.1.6-4. Cumulative Percentage Frequency of Occurrence of Sea Heights Exceeding 5, 8 and 12 feet for the Months of July and August

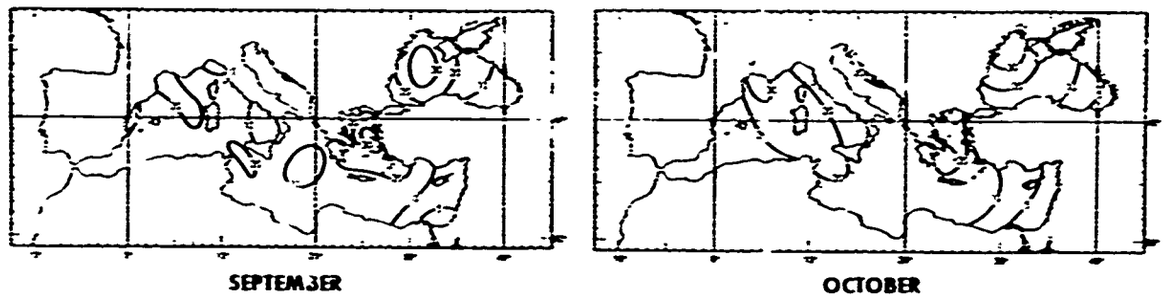

5 Feet

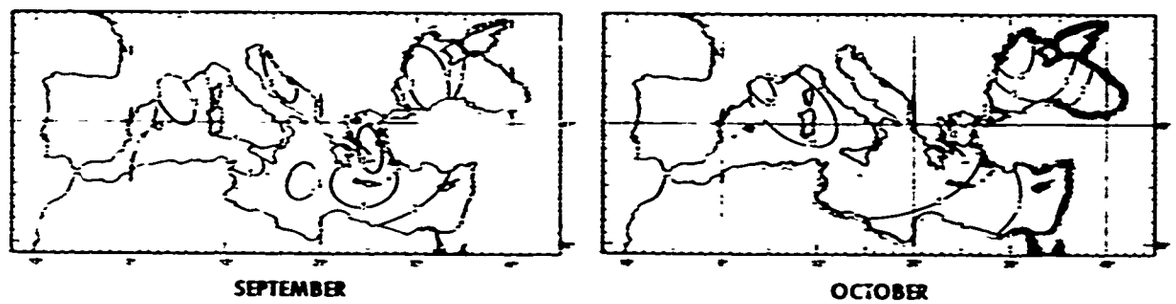

8 Feet

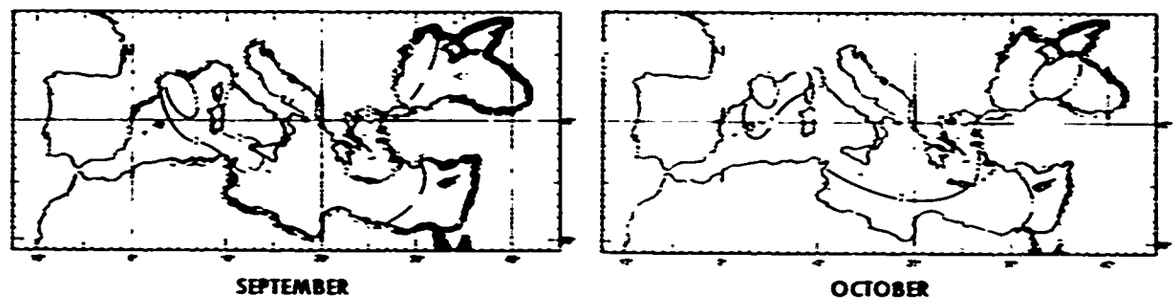

12 Feet

Figure 2.1.6-5. Cumulative Percentage Frequency of Occurrence of Sea Heights Exceeding 5, 8 and 12 feet for the Months of September and October

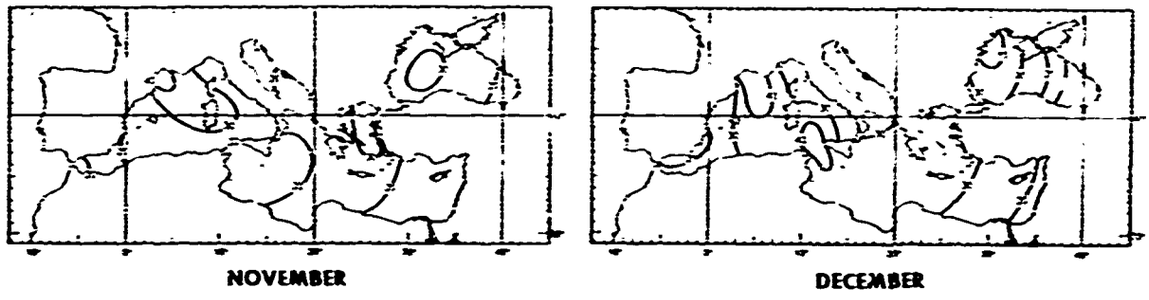

5 Feet

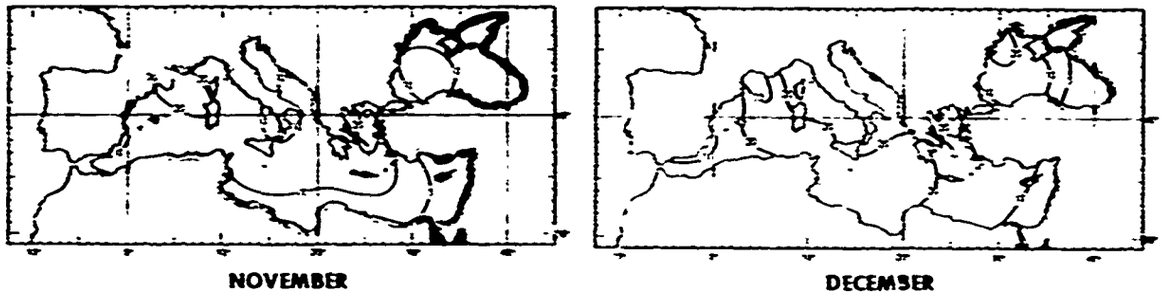

8 Feet

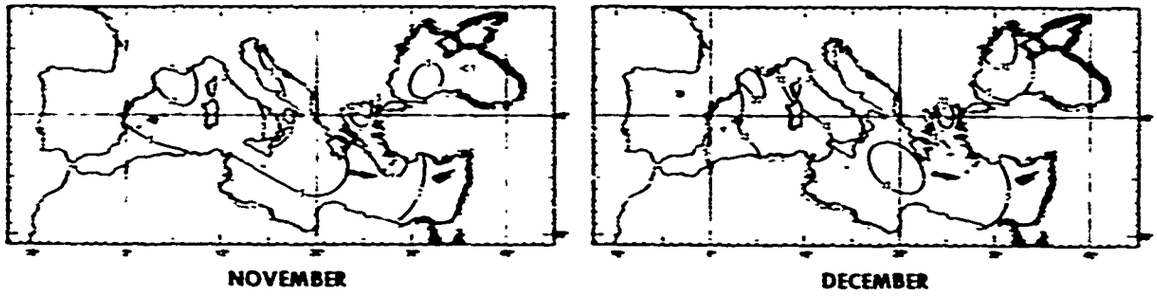

12 Feet

Figure 2.1.6-6. Cumulative Percentage Frequency of Occurrence of Sea Heights Exceeding 5, 8 and 12 feet for the Months of November and December

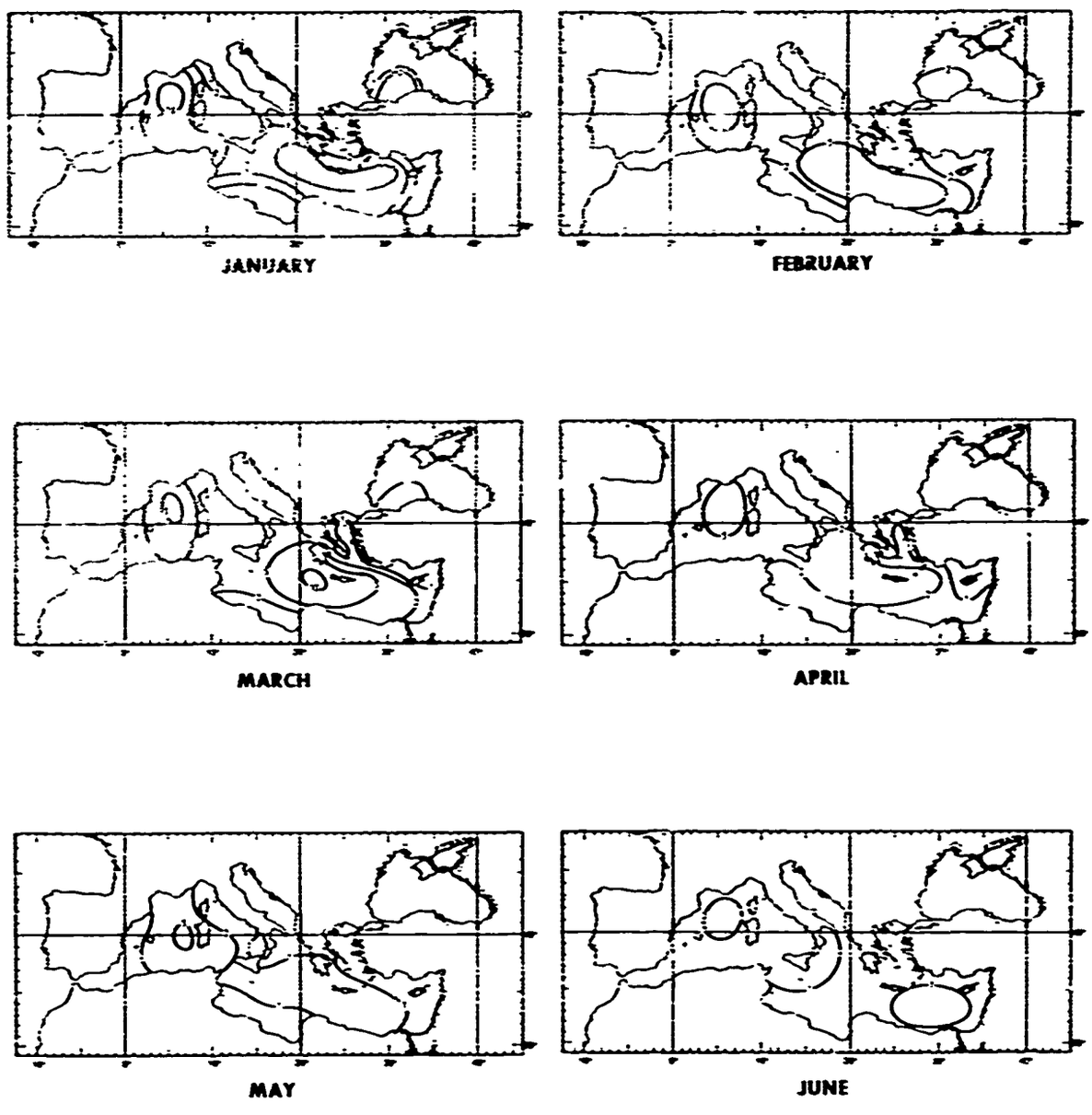

Figure 2.1.6-7. Cumulative Percentage Frequency of Occurrence Swell Exceeding 12 feet for the Months January through June

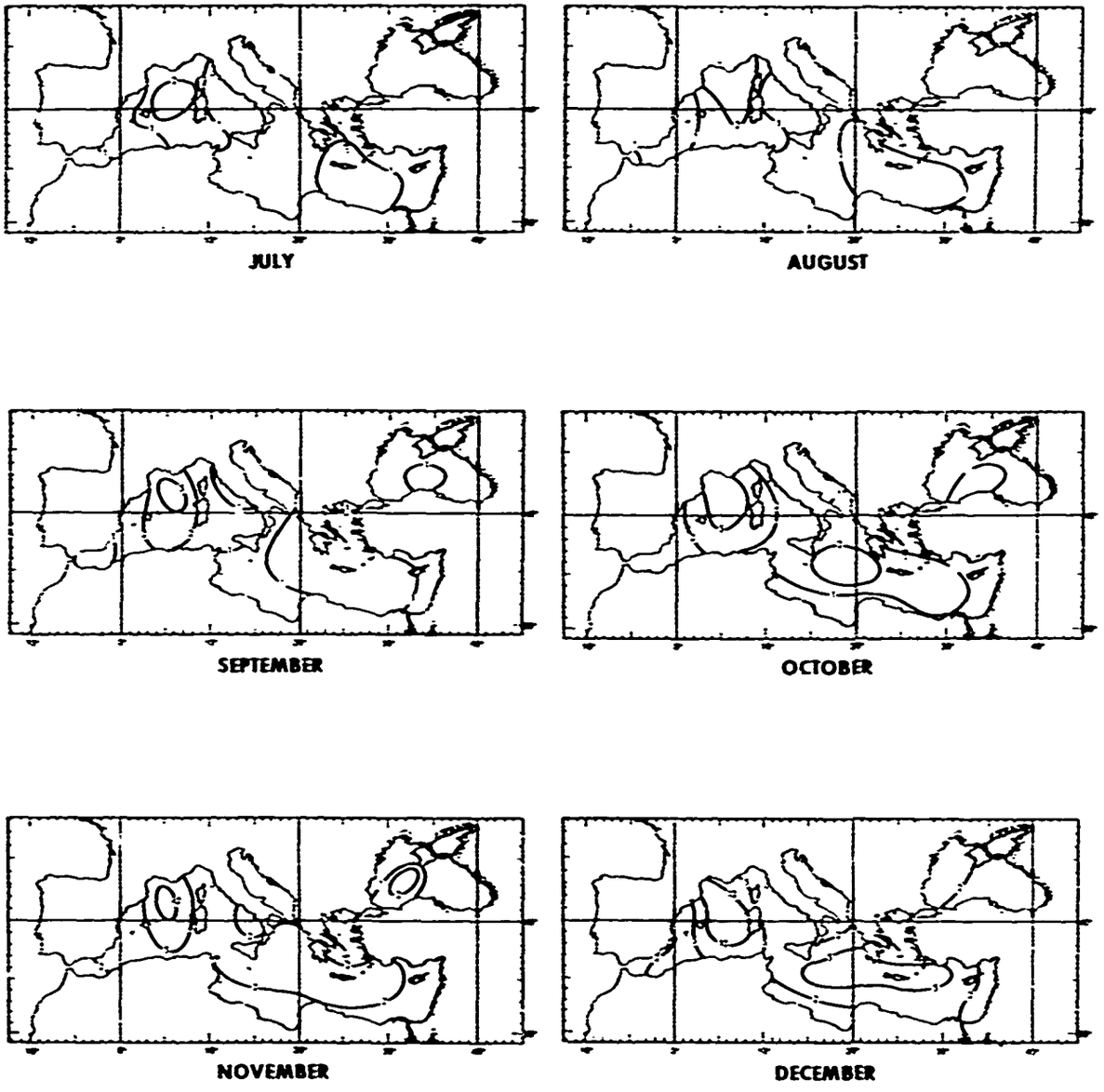

Figure 2.1.4-3. Cumulative Percentage Frequency of Occurrence Swell Exceeding 12 feet for the Months July through December

2.1.6.3(U) Extreme Wave Heights (U). The highest seas to be encountered in the Mediterranean occur off the coasts of Spain and France during winter. In this region, seas occasionally exceed 20 feet and may even attain 40 feet. These severe seas are caused by the strong winds (mistral, tramontana) gererated by deep extratropical cyclones located in north Italian waters.

2.1.6.4(U) Storm Surges (U). During extended periods of strong winds, storm surges, particularly severe when associated with high tides, may occur along shallow coastal regions that are open to long fetches. A rare combination of events of this kind occurred in November 1966 when a surge of six and one-half feet was measured in Venice during a prolonged southeast gale.

2.1.6.5(U) Tides (U). Tides in the Mediterranean are slight but are of some significance in straits and bays during periods of greatest tidal variation. Tidal ranges exceed two feet only in the Strait of Gibraltar (6 feet) and the Gulf of Gabes (5 feet).

REFERENCES

1. Weather Bureau, National Weather Records Center. Wind, sea and swell data tabulated from marine punched card decks. Asheville, North Carolina, unpublished

2. Naval Weather Service Command 1970. Summary of synoptic meteorological observations, Mediterranean marine areas, Vol. 1-9

ADDITIONAL SOURCES

1. Central Intelligence Agency 1960. National intelligence survey, Atlantic Basin, part IX--Mediterranean and Black Seas, section 1, marine climate, Washington, D.C., CONFIDENTIAL

2. Central Intelligence Agency 1963. National intelligence survey, Atlantic Basin, part IX--Mediterranean and Black Seas, section 2, oceanography, Washington, D.C., SECRET

3. Great Britain, Hydrographer of the Navy 1963-1970. Mediterranean pilot, Volumes I-IV, N.P. 45-48, Ninth Edition, London

4. Great Britain, Hydrographic Department 1961. Mediterranean pilot, Vol. V, S.D. No. 49, Fifth Edition, London

5. Kendrew, W.G. 1953. Climates of the continents, The Clarendon Press, Oxford, Fourth Edition

6. Koninklijk Nederlands Meteorologisch Instituut 1972. Marine climatological summaries for the Mediterranean and Southern Indian Ocean, Vol. 4, 1964

7. Royal Netherlands Meteorological Institute 1957. The Mediterranean, oceanographic and meteorological data, 'S-Gravenhage

8. Trewartha, G.T. 1961. The earth's problem climates, The University of Wisconsin Press, Madison

9. University of Chicago, Institute of Meteorology 1944. Climatology of the Mediterranean area by Erwin R. Biel, Misc. Repts. No. 13, Chicago

10. U.S. Naval Oceanographic Office 1963. Oceanographic atlas of the North Atlantic Ocean, section IV, sea and swell, Publication No. 700, Washington, D.C.

11. U.S. Naval Oceanographic Office 1971. Sailing directions (planning guide) for the Mediterranean, Pub. No. 130, First Edition

12. U.S. Naval Oceanographic Office 1962. Operational oceanography of the Eastern Mediterranean Sea for submariners, Special Publication No. 50, Washington, D.C., CONFIDENTIAL

13. U.S. Naval Hydrographic Office 1962. Operational oceanography of the Western Mediterranean for submariners, Special Publication No. 49, Washington, D.C., CONFIDENTIAL

Section 2.2, Physical Oceanography, begins overleaf.

2.2(U) Physical Oceanography (U)

2.2.1(U) Temperature, Salinity, and Water Masses (U). The Mediterranean Sea can be typified by a three-layer water column, each layer of which contains a distinct water mass. The near-surface layer contains low-salinity Atlantic water that enters the Mediterranean through the Strait of Gibraltar and is circulated throughout the Mediterranean by the prevailing surface currents (Lacombe and Tchernia, 1972). This water mass can be found as far east as the coast of Israel and the Aegean Sea (Oren, 1971). The near-surface layer is extremely variable in terms of both temperature and salinity, and is subject to marked seasonal changes caused by surface insolation and evaporation during summer, and by surface cooling and convective mixing during winter.

(U) At depths between about 200 and 1000 meters, most of the Mediterranean Sea is occupied by warm, high-salinity Levantine Intermediate Water (LIW). This water mass is formed in the eastern Mediterranean by vertical thermohaline convection of high-salinity surface waters. According to Wust (1961), the regions east and west of Rhodes are primary sources of LIW during winter. Lesser amounts of LIW also are formed in the Levantine Basin during summer. During both seasons, a core of this high-salinity water mass flows west through the Ionian Sea (at about 33° to 35°N) and then through the Strait of Sicily into the western Mediterranean. LIW is found throughout the Tyrrhenian Sea and Algerian Basin, and flows as a well-defined boundary current along the Algerian continental slope before exiting from the Mediterranean Sea through the Strait of Gibraltar. This LIW current is generally both stronger and less variable during winter. In the Strait of Gibraltar, outflowing LIW forms a distinct undercurrent below a depth of 275 meters that reaches velocities as high as 100 cm/sec (Wust, 1961). A considerable degree of temporal and spatial variability in temperature and salinity occurs in the intermediate layer throughout the Mediterranean Sea, but not nearly as much as occurs in the near-surface layer.

(U) Below depths of 800 to 1000 meters, several basins of the Mediterranean Sea are occupied by distinct bottom water masses that display very little temporal and spatial variability within a given basin. Generally, separate bottom water masses are recognized in the western Mediterranean Sea (Alboran Basin, Algerian Basin, and Tyrrhenian Basin), Adriatic Sea, eastern Mediterranean Sea (Ionian Basin and Levantine Basin), and Sea of Crete. The temperatures and salinities of these four water masses increase to the east, being lowest in the western Mediterranean and highest in the Sea of Crete. Western Mediterranean bottom water is formed at the northern end of the Algerian Basin (Ligurian Sea) by deep convective mixing during winter (MEDOC Group, 1970). Adriatic Sea Bottom Water is formed in a similar fashion

in the northern Adriatic Sea and flows out of the Straits of Otranto into the Ionian Basin where it mixes with resident higher salinity water to form Eastern Mediterranean Bottom Water (Pollack, 1951). Some Eastern Mediterranean Bottom Water also is formed by a flow of deep waters from the north across the sills on either side of Crete (Miller, 1972a). Sea of Crete Bottom Water is formed in situ by convective mixing during winter. However, its extremely high temperature and salinity probably are largely a function of isolation from the remainder of the eastern Mediterranean. Although bottom currents have not been observed in most of the Mediterranean, there is no evidence of stagnancy in any of the major Mediterranean basins, including the Sea of Crete (Miller, 1972a).

(U) Figure 2.2.1-1 shows the T-S indices of major Mediterranean water masses for summer and winter. This figure is a generalized composite of 12 typical T-S diagrams; their locations are shown in figure 2.2.1-2. No attempt has been made to characterize Atlantic Water in figure 2.2.1-1 due to its extreme variability during both seasons. However, the figure does show the marked difference between near-surface conditions in the western and eastern Mediterranean during both seasons. Generally speaking, the concentrations of unmixed LIW (after Wust, 1961) are greater than 55% in the eastern Mediterranean and less than 45% in the western Mediterranean. This is a result of intensive mixing of the LIW core during its passage across the Strait of Sicily. As demonstrated by Wust, LIW concentrations are slightly higher during winter than during summer. Figure 2.2.1-1 also illustrates the temperature and salinity differences between the four major bottom water masses found in the Mediterranean Sea.

(U) The Alboran Sea (figure 2.2.1-3) displays the minimum winter and summer sea surface temperatures and salinities encountered on any of the Mediterranean T-S/sound velocity diagrams. This is due to the large concentration of Atlantic Water in this region. Because of its near-surface location, Atlantic Water is not denoted on the sound velocity profiles in figure 2.2.1-3 or any subsequent figure in this series. It is, however, indicated on the T-S diagrams in figures 2.2.1-3 through 2.2.1-14. The concentrations of unmixed LIW in the Alboran Sea are the minima encountered in the Mediterranean (between 10% and 15%).

(U) The southern Algerian Basin (figure 2.2.1-4) shows distinctly higher temperatures and salinities during both seasons than those found in either the Alboran Sea (figure 2.2.1-3) or the northern Algerian Basin (figure 2.2.1-5). The former difference is due to diminished effects of the Atlantic Water flow and more intense summer insolation, the latter to a latitudinal effect. Similarly, the

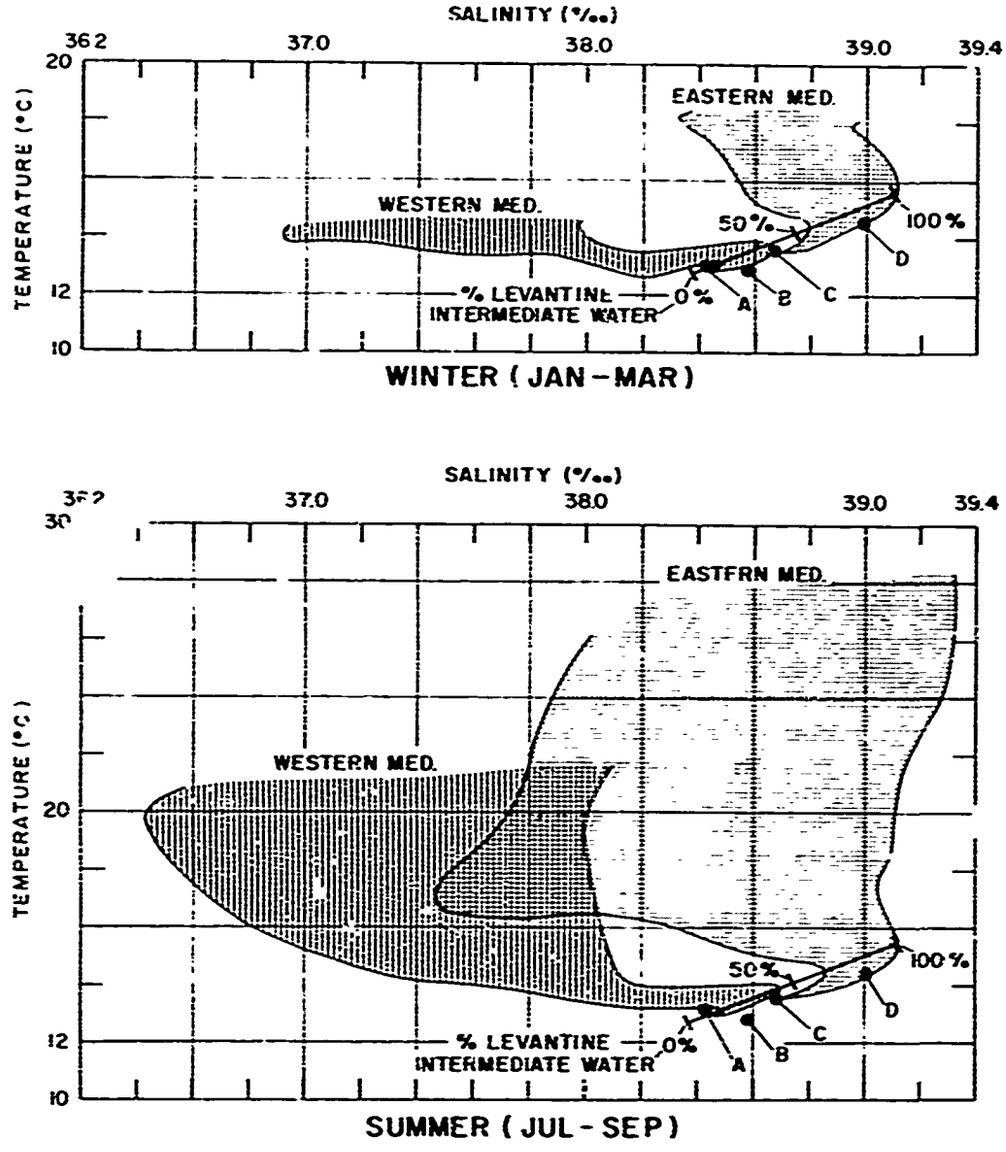

LEGEND

A = WESTERN MEDITERRANEAN BOTTOM WATER
B = ADRIATIC SEA BOTTOM WATER
C = EASTERN MEDITERRANEAN BOTTOM WATER
D = SEA OF CRETE BOTTOM WATER

NOTE:
LEVANTINE INTERMEDIATE WATER T-S CURVE & PERCENTAGES AFTER WUST (1961)

Figure 2.2.1-1. Temperature-Salinity Relations During Winter and Summer

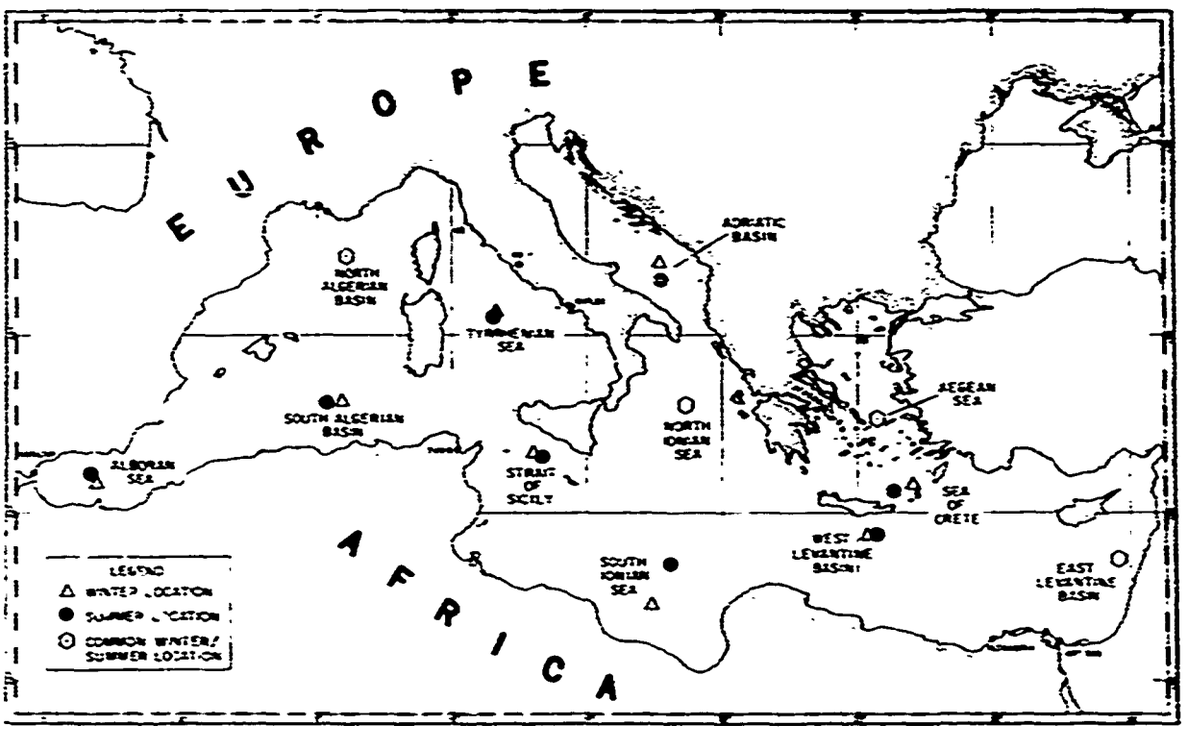

Figure 2.2.1-2. Location of Temperature-Salinity/ Sound Velocity Comparisons

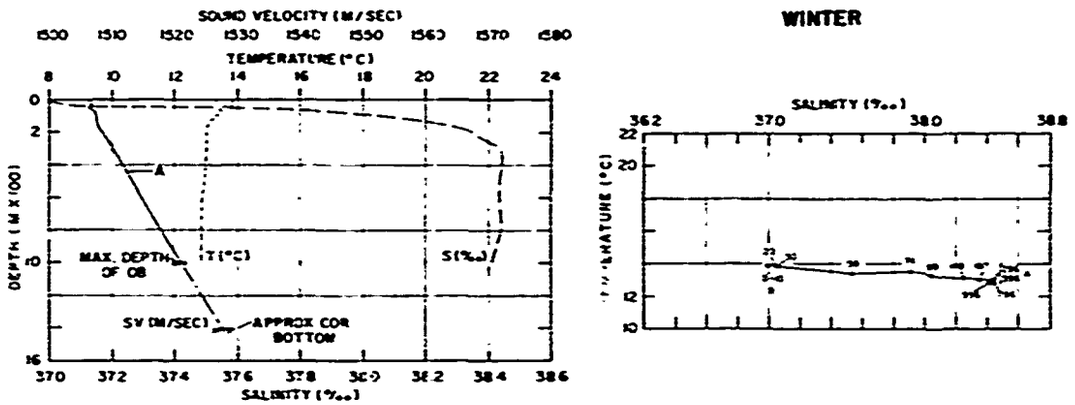

LEGEND A = DEPTH OF LEVANTINE INTERMEDIATE WATER SALINITY MAXIMUM
B = DEPTH OF ATLANTIC WATER SALINITY MINIMUM

SOURCE ATLANTIS CRUISE 263 STA 6309
35°45'N, 3°06'W
4 FEBRUARY 1961

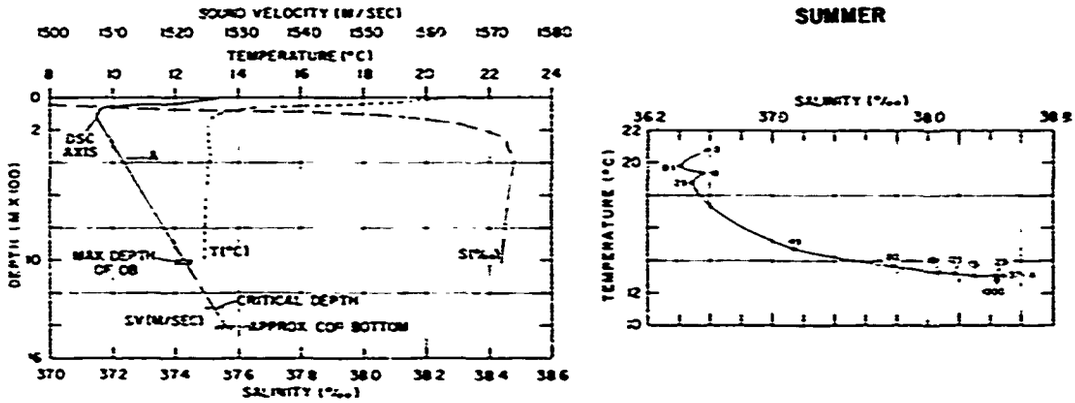

LEGEND A = DEPTH OF LEVANTINE INTERMEDIATE WATER SALINITY MAXIMUM
B = DEPTH OF ATLANTIC WATER SALINITY MINIMUM

NOTE SURFACE SALINITY = 36.58‰

SOURCE ATLANTIS II CRUISE 59 STA 4
36°00'N, 3°19'W
10 JULY 1970

Figure 2.2.1-3. Winter and Summer Temperature, Salinity, Sound Velocity Profiles and Temperature-Salinity Diagrams for Alboran Sea

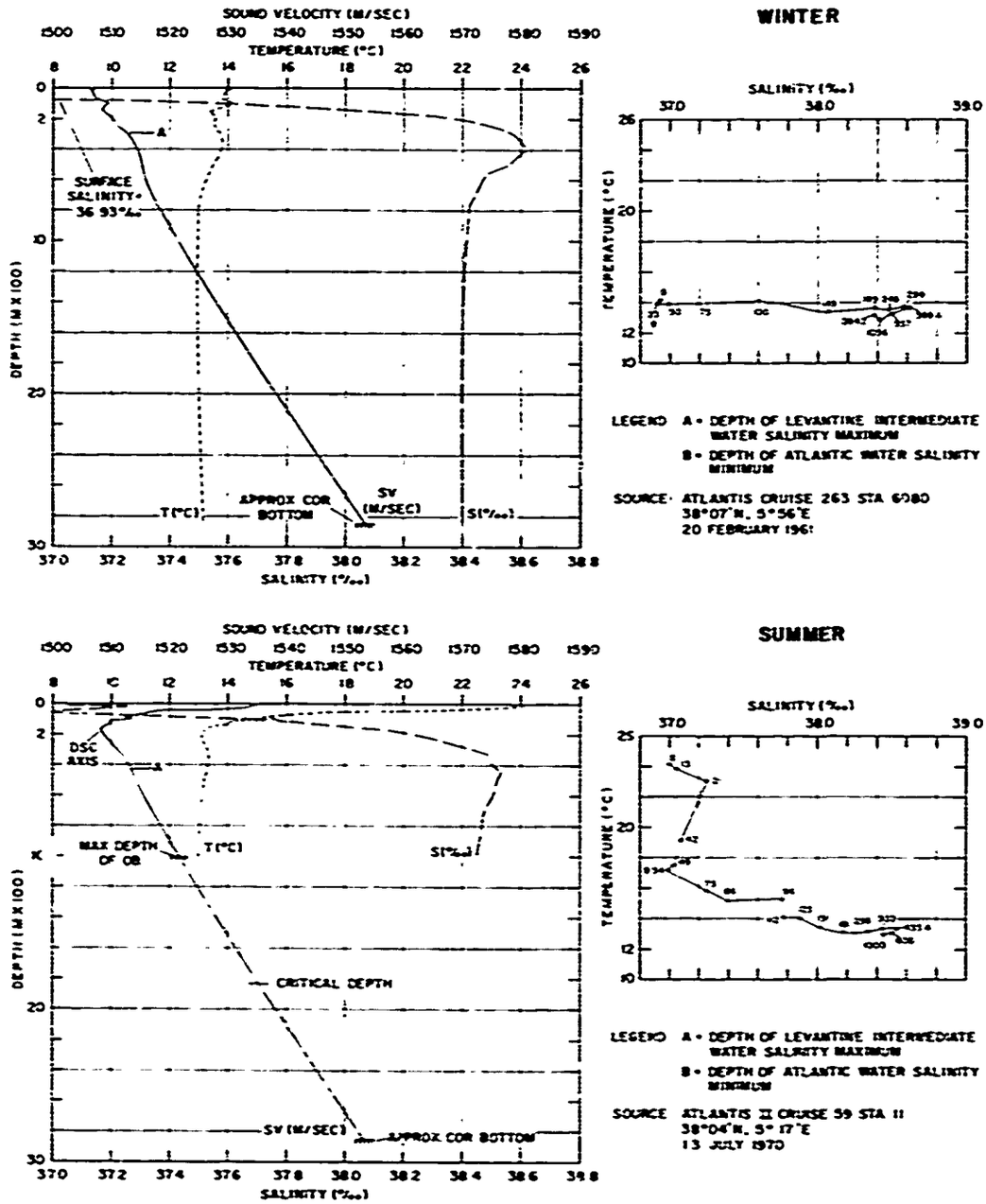

Figure 2.2.1-4. Winter and Summer Temperature, Salinity, Sound Velocity Profiles and Temperature-Salinity Diagrams for Southern Algerian Basin

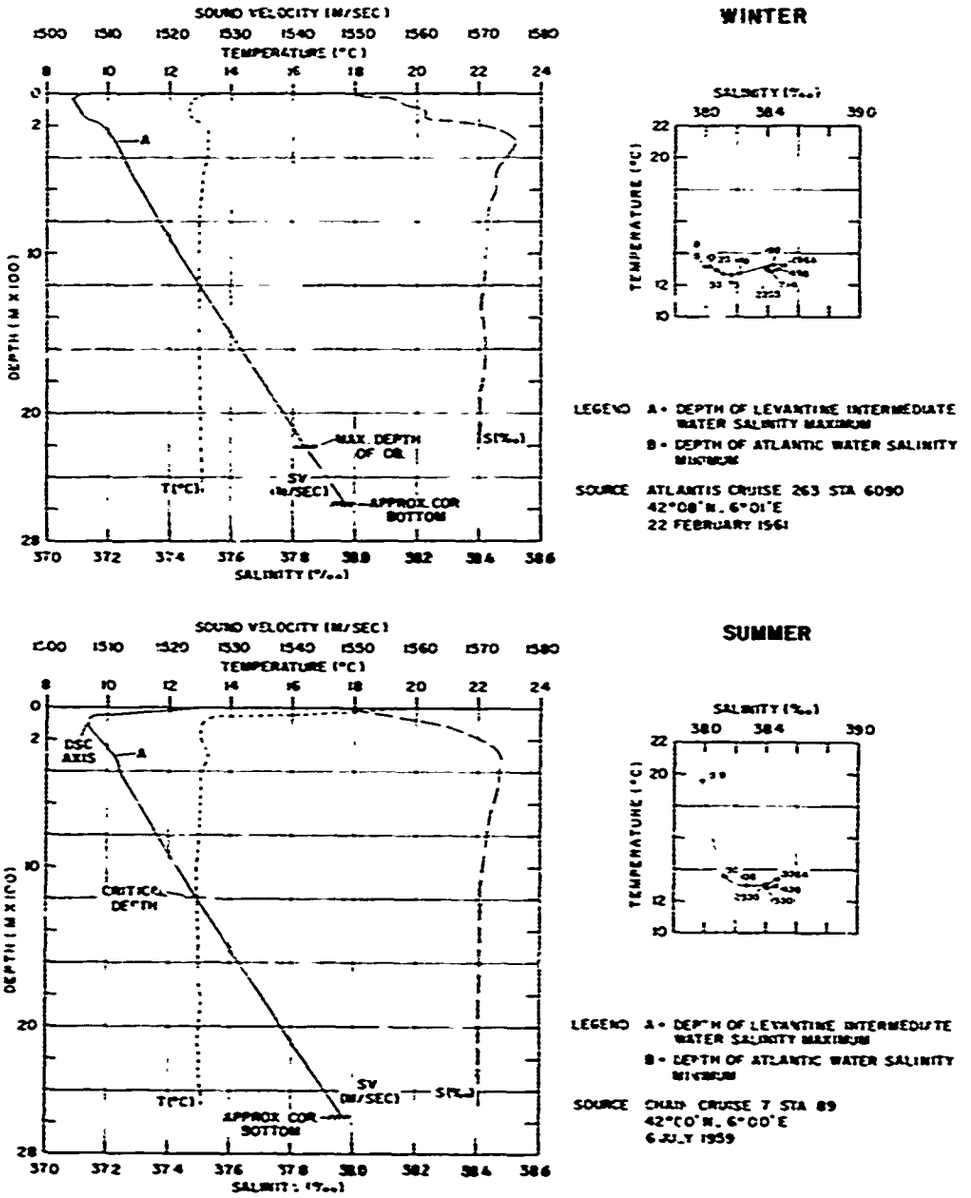

Figure 2.2.1-5. Winter and Summer Temperature, Salinity, Sound Velocity Profiles and Temperature-Salinity Diagrams for Northern Algerian Basin

concentration of LIW is greater in the southern Algerian Basin (25–30%) than in either the Alboran Sea (10–15%) or the northern Algerian Basin (15–20%) due to the preferential flow of LIW along the Algerian continental slope.

(U) During both summer and winter, sea surface temperatures and salinities in the Tyrrhenian Sea (figure 2.2.1-6) are similar to those found in the northern Algerian Basin (figure 2.2.1-5). However, concentrations of unmixed LIW are higher in the Tyrrhenian Sea than anywhere else in the western Mediterranean (about 45% unmixed LIW). This indicates that a substantial part of the LIW flow leaving the Strait of Sicily is deflected north into the Tyrrhenian Sea. According to Miller (1972b), LIW flows out of the Tyrrhenian Sea south of the island of Sardina.

(U) The summer and winter T-S/sound velocity diagrams for the Strait of Sicily (figure 2.2.1-7) lie northwest of the average position of the Malta Front, and therefore more closely resemble western Mediterranean conditions. This front separates the cooler, less saline near-surface waters of the western Mediterranean from the warmer, more saline waters of the eastern Mediterranean and has been extensively described in the region south of Sicily by Johannessen, et al. (1971) and Briscoe, et al. (1972). During both seasons, approximately 55% unmixed LIW is found in the Strait of Sicily.

(U) In the Adriatic Basin (figure 2.2.1-8), the presence of both Atlantic Water and LIW (unmixed concentrations of 45–50%) is apparent during both seasons. At the bottom of the Adriatic Basin (about 1200 meters depth), the temperatures and salinities during summer and winter are considerably less than those found south of the Strait of Otranto in the northern Ionian Sea (figure 2.2.1-9). This is in agreement with a flow of bottom water out of the Adriatic Sea into the Ionian Sea. Both Atlantic Water and LIW are clearly evident in the northern Ionian Sea, as are the evaporative effects of summer insolation. Unmixed LIW concentrations shown in the northern Ionian Sea (about 65%) are greater than those found in either the Adriatic Sea (figure 2.2.1-8) or in the southern Ionian Sea (figure 2.2.1-10). However, even greater unmixed LIW concentrations (70–75%) would be expected in the central Ionian Sea (33° to 35°N) along the preferential flowpath of this high-salinity water mass. Intensive summer evaporation is obvious in the upper 30 meters in the southern Ionian Sea. However, during both winter and summer the sea surface salinities shown in figure 2.2.1-10 are the lowest encountered in the eastern Mediterranean. This is due to a strong flow of Atlantic Water in the Gulf of Sidra and just off the Libyan continental shelf (Lacombe and Tchernia, 1972).

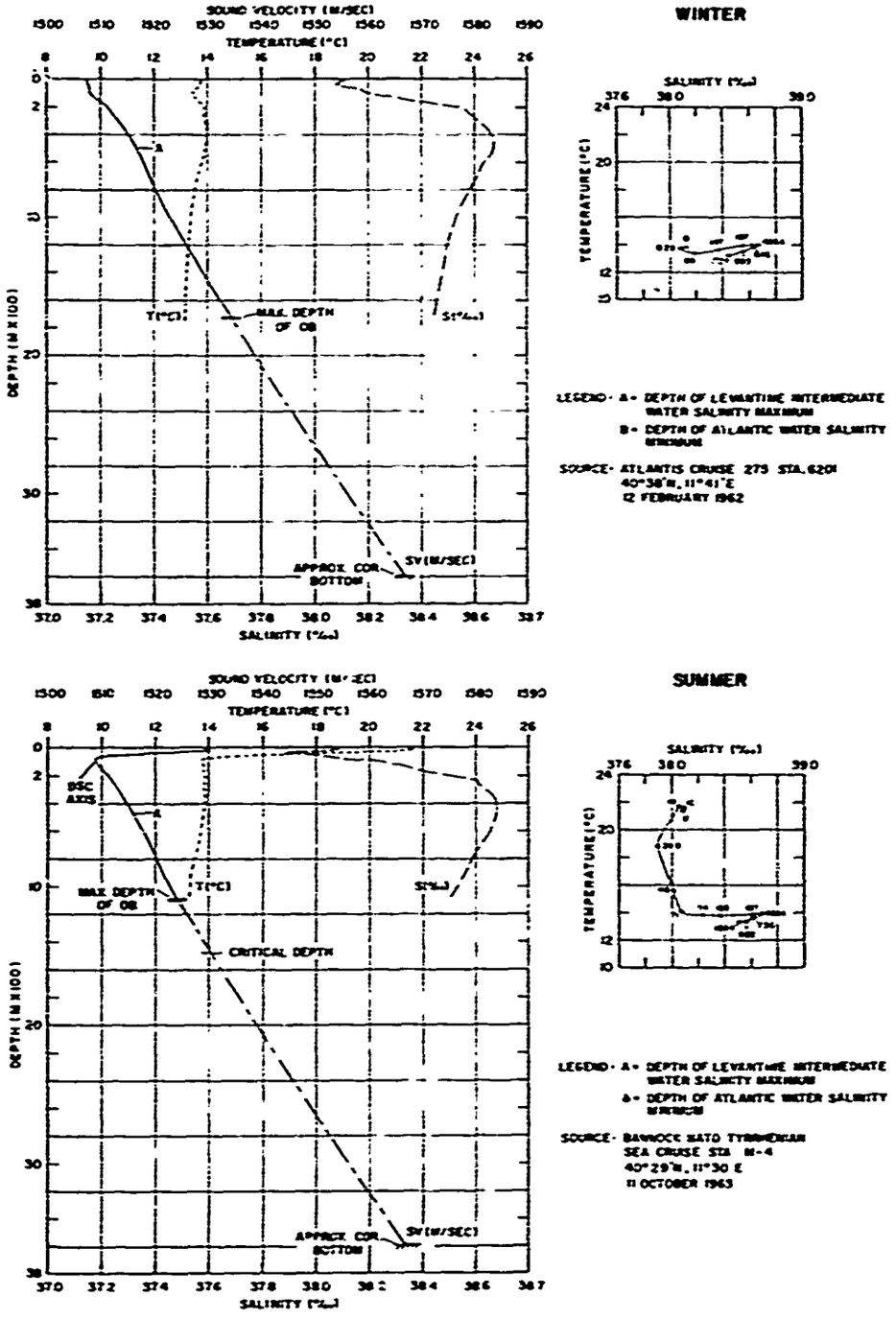

Figure 2.2.1-6. Winter and Summer Temperature, Salinity, Sound Velocity Profiles and Temperature-Salinity Diagrams for Tyrrhenian Sea

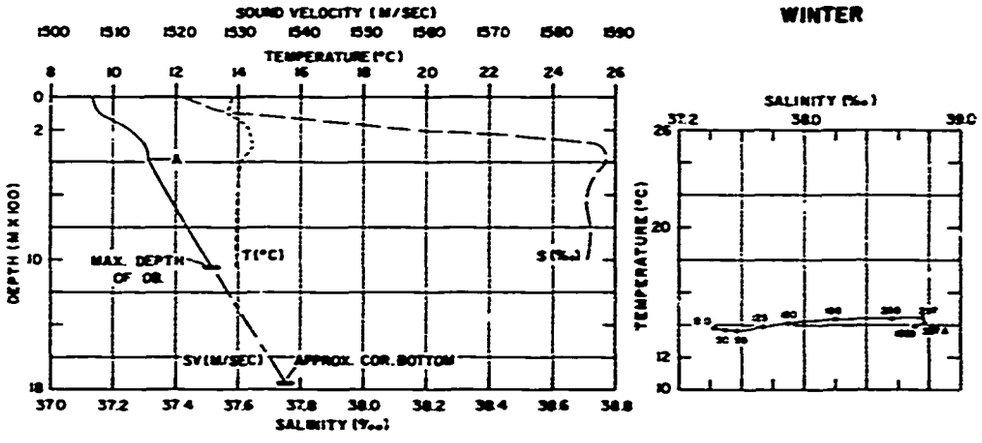

LEGEND: A = DEPTH OF LEVANTINE INTERMEDIATE WATER SALINITY MAXIMUM
B = DEPTH OF ATLANTIC WATER SALINITY MINIMUM

SOURCE: AESD DATA BANK
MARSDEN SQ. 143, 1° SQ. 62
35°38'N, 12°56'E
31 MARCH 1929

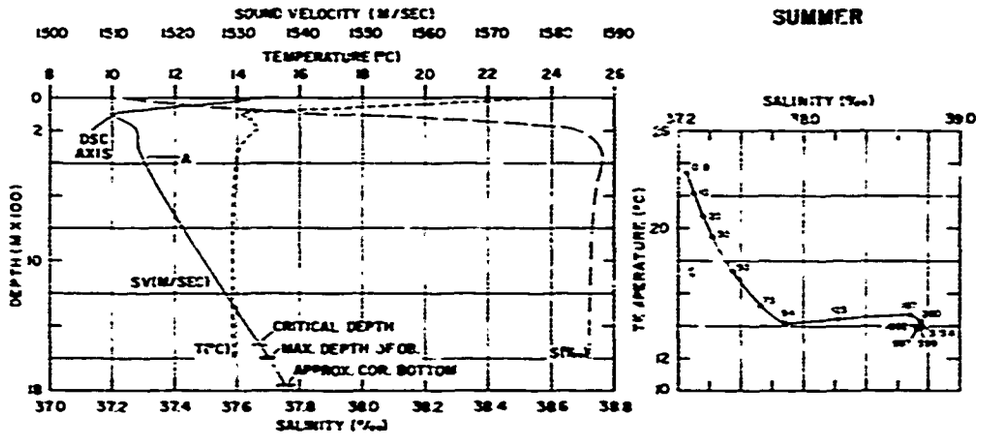

LEGEND: A = DEPTH OF LEVANTINE INTERMEDIATE WATER SALINITY MAXIMUM
B = DEPTH OF ATLANTIC WATER SALINITY MINIMUM

SOURCE: AESD DATA BANK
MARSDEN SQ. 143, 1° SQ. 63
36°30'N, 13°15'E
14 JULY 1958

Figure 2.2.1-7. Winter and Summer Temperature, Salinity, Sound Velocity Profiles and Temperature-Salinity Diagrams for Strait of Sicily

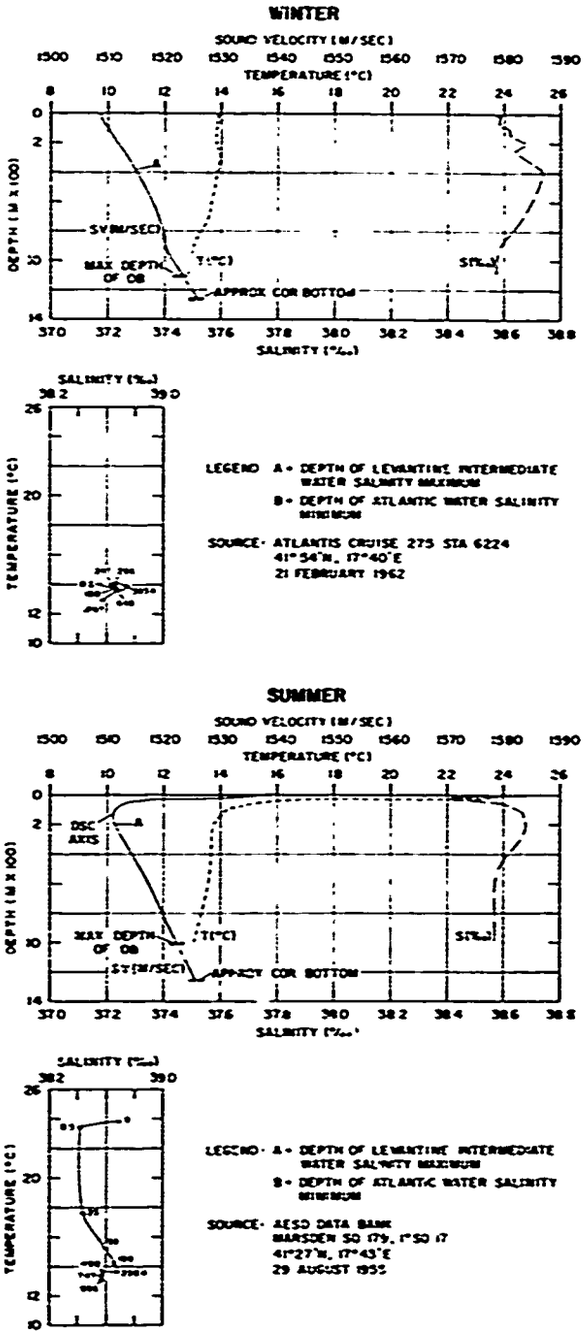

Figure 2.2.1-8. Winter and Summer Temperature, Salinity, Sound Velocity Profiles and Temperature-Salinity Diagrams for Adriatic Basin

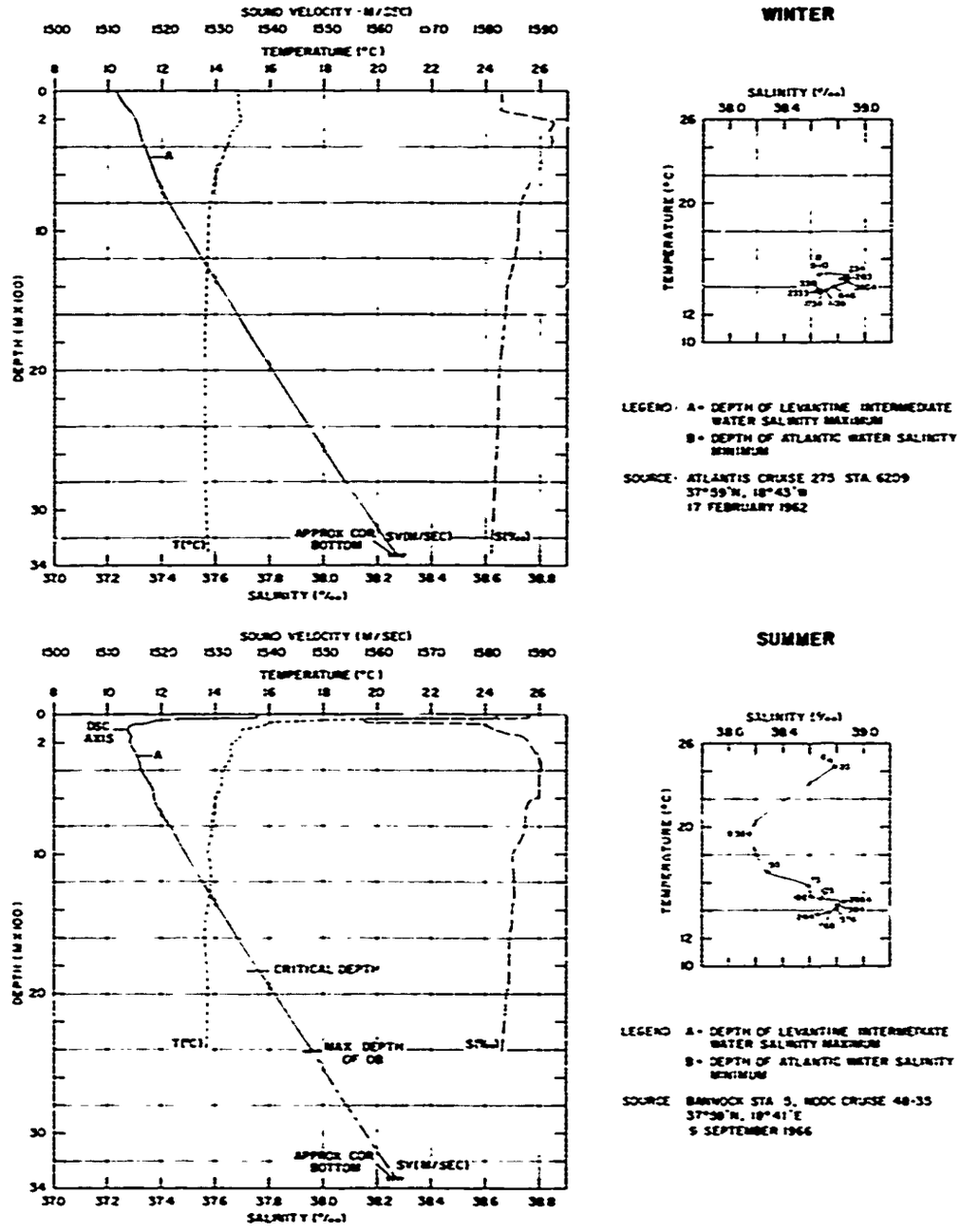

Figure 2.2.1-9. Winter and Summer Temperature, Salinity, Sound Velocity Profiles and Temperature-Salinity Diagrams for Northern Ionian Sea

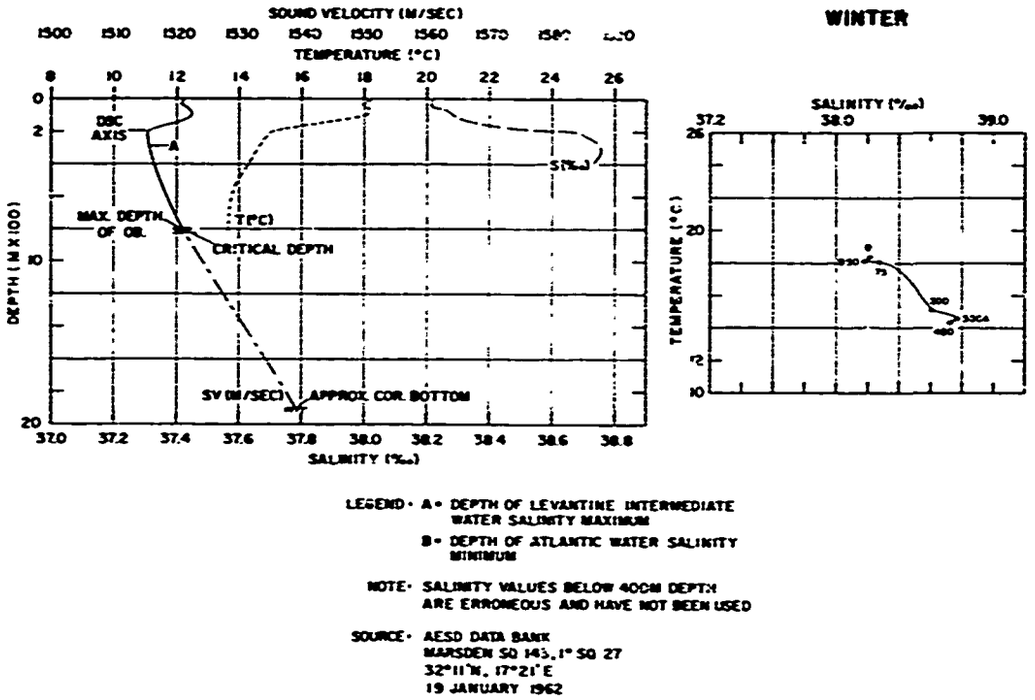

LEGEND: A = DEPTH OF LEVANTINE INTERMEDIATE WATER SALINITY MAXIMUM
B = DEPTH OF ATLANTIC WATER SALINITY MINIMUM

NOTE: SALINITY VALUES BELOW 400M DEPTH ARE ERRONEOUS AND HAVE NOT BEEN USED

SOURCE: AESD DATA BANK
MARSDEN SQ 143, 1° SQ 27
32°11'N, 17°21'E
19 JANUARY 1962

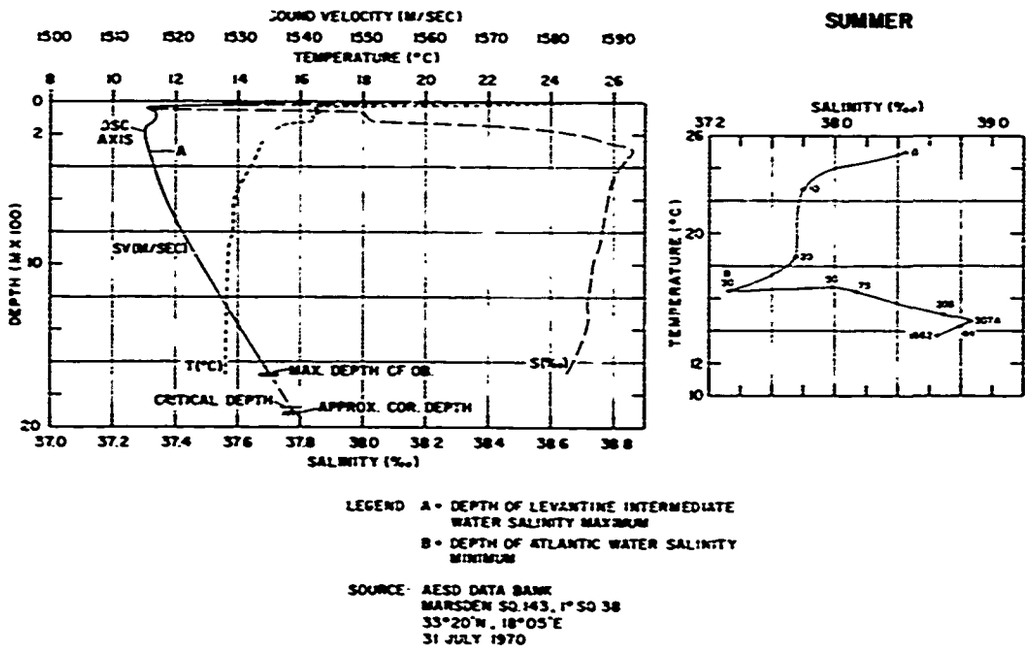

LEGEND: A = DEPTH OF LEVANTINE INTERMEDIATE WATER SALINITY MAXIMUM
B = DEPTH OF ATLANTIC WATER SALINITY MINIMUM

SOURCE: AESD DATA BANK
MARSDEN SQ 143, 1° SQ 38
33°20'N, 18°05'E
31 JULY 1970

Figure 2.2.1-10. Winter and Summer Temperature, Salinity, Sound Velocity Profiles and Temperature-Salinity Diagrams for Southern Ionian Sea

(U) In the Aegean Sea (figure 2.2.1-11), near-surface temperatures and salinities during winter are typical of those found throughout the eastern Mediterranean. However, during summer, near-surface salinities are frequently less than 38.0°/oo due to low-salinity water that enters the Aegean Sea through the Dardanelles from the Black Sea. Nevertheless, Atlantic Water is found in the Aegean Sea during both seasons. The existence of LIW in the Aegean Sea is uncertain. However, Wust (1961), does show LIW in the eastern Aegean Sea during both seasons at a depth of about 100 meters. Farther south in the Sea of Crete (figure 2.2.1-12), LIW is definitely present during winter and summer in unmixed concentrations of greater than 85%. Near-surface temperatures and salinities in the Sea of Crete are higher than those in either the Aegean Sea (figure 2.2.1-11) or in the western Levantine Basin (figure 2.2.1-13) during both seasons. As previously noted, Sea of Crete Bottom Water has extremely high temperatures and salinities. The temperature and salinity minima found at a depth of about 800-1000 meters in figure 2.2.1-12 roughly correspond with sill depths between the Sea of Crete and the Levantine Basin. This substantiates geographic isolation as one factor in the formation of anomalous Sea of Crete Bottom Water.

(U) In the western Levantine Basin (figure 2.2.1-13), sea surface temperatures and salinities are typical for the eastern Mediterranean, and LIW is present in unmixed concentrations of 80-85% during both seasons. In the eastern Levantine Basin (figure 2.2.1-14), sea surface temperatures and salinities for both seasons are the maxima encountered anywhere in the Mediterranean. However, the Atlantic Water salinity minimum is still a pronounced feature. During summer, the LIW salinity maximum has unmixed concentrations of nearly 100%. During winter, the near-surface salinity is greater than that at the LIW core. This indicates that this high-salinity water mass is formed in the eastern Levantine Basin during winter.

(U) In summary; two predominant water masses are circulated throughout the Mediterranean Sea at near-surface and intermediate depths. The near-surface water mass (Atlantic Water) enters the Mediterranean through the Strait of Gibraltar, generally flows from west to east, and becomes warmer and more saline during its residence in the Mediterranean. Conversely, the intermediate water mass (LIW) flows generally to the west after its formation by convective mixing in the Levantine Basin, and becomes cooler and less saline before leaving the Mediterranean through the Strait of Gibraltar. However, below about 100 meters depth, both temperature and salinity are extremely constant and vary only between major physiographic basins. The effects of this three-level ocean on sound velocity structures are discussed in section 3.1.1.

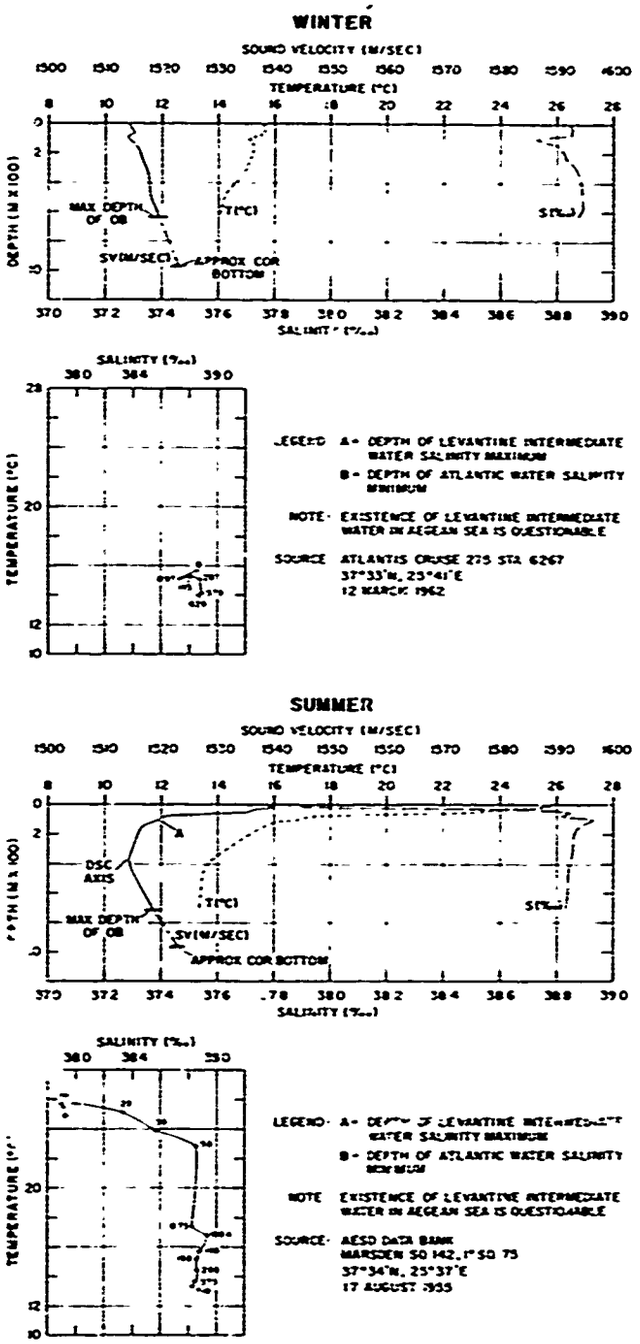

Figure 2.2.i-11. Winter and Summer Temperature, Salinity, Sound Velocity Profiles and Temperature-Salinity Diagrams for Aegean Sea

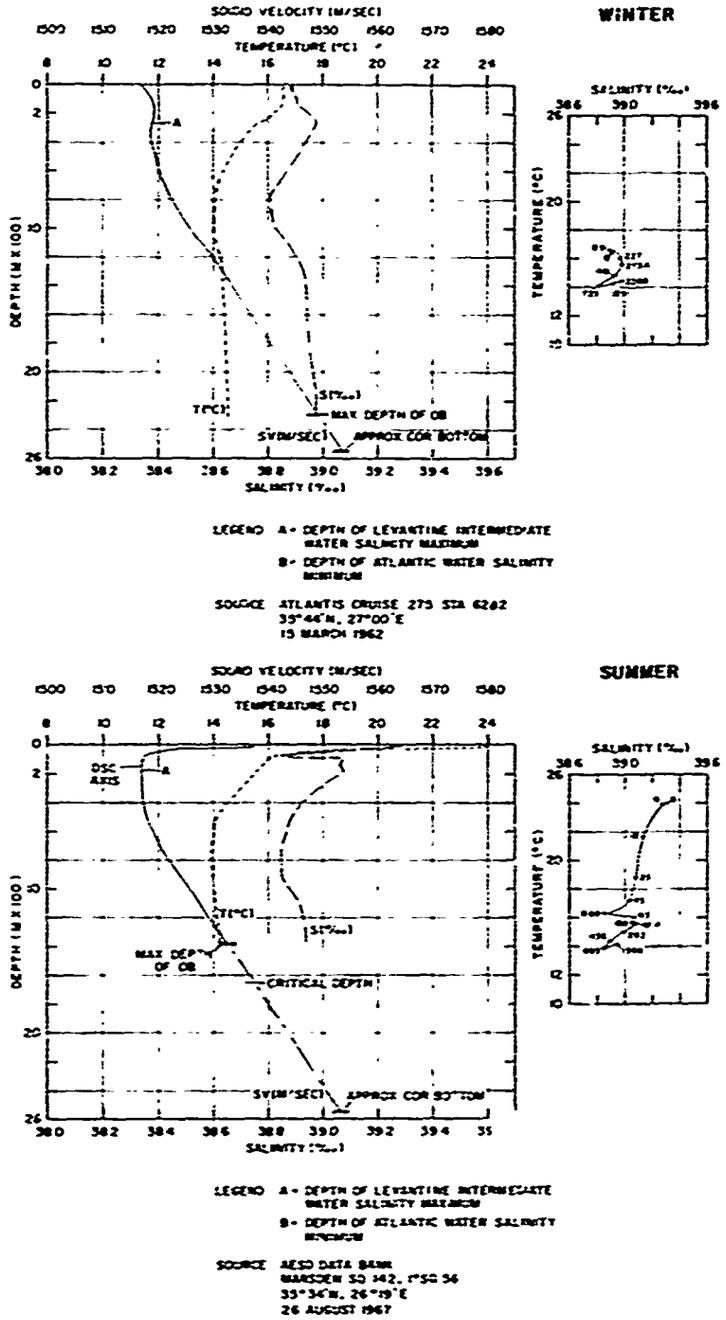

Figure 2.2.1-12. Winter and Summer Temperature, Salinity, Sound Velocity Profiles and Temperature-Salinity Diagrams for Sea of Crete

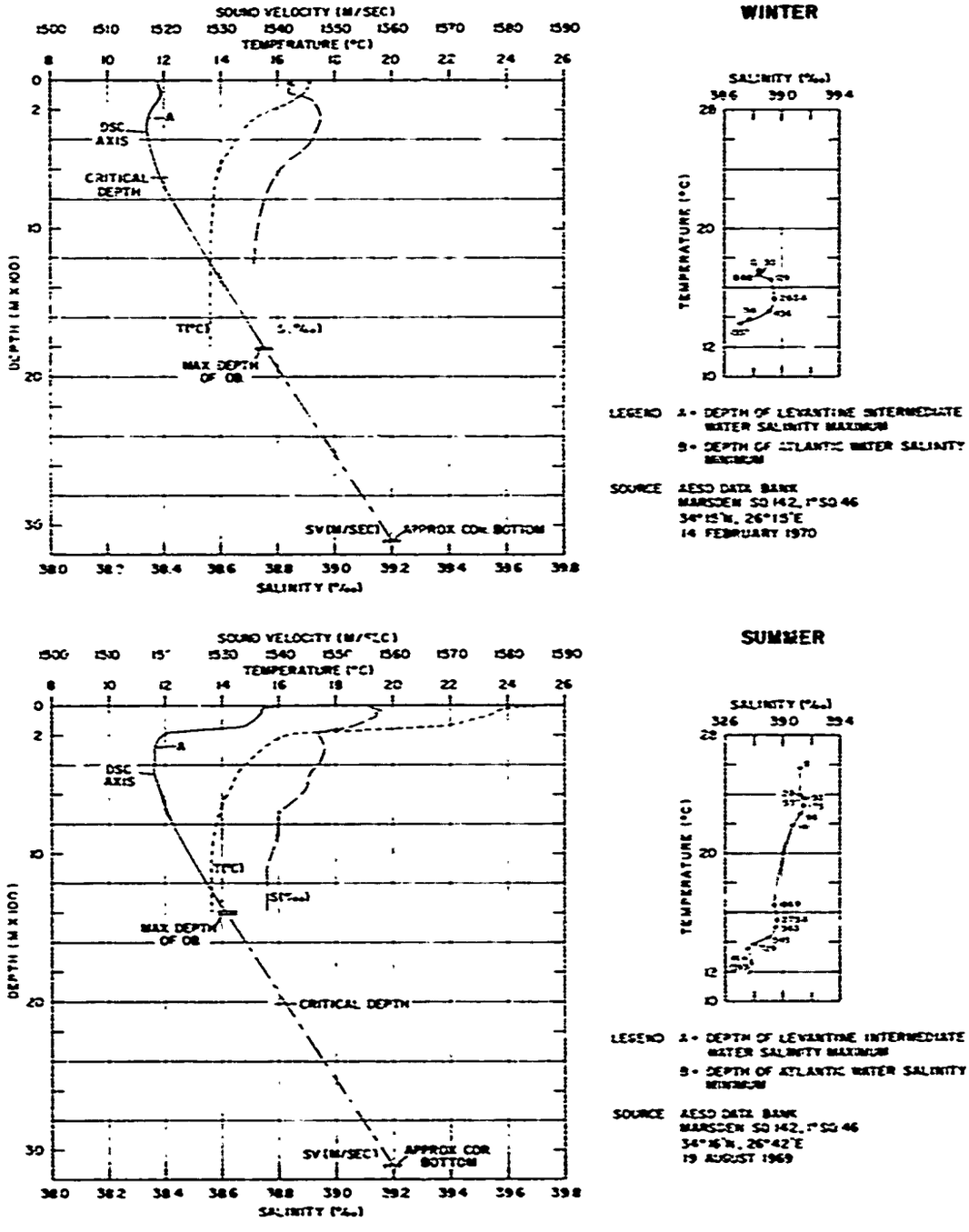

Figure 2.2.1-13. Winter and Summer Temperature, Salinity, Sound Velocity Profiles and Temperature-Salinity Diagrams for Western Levantine Basin

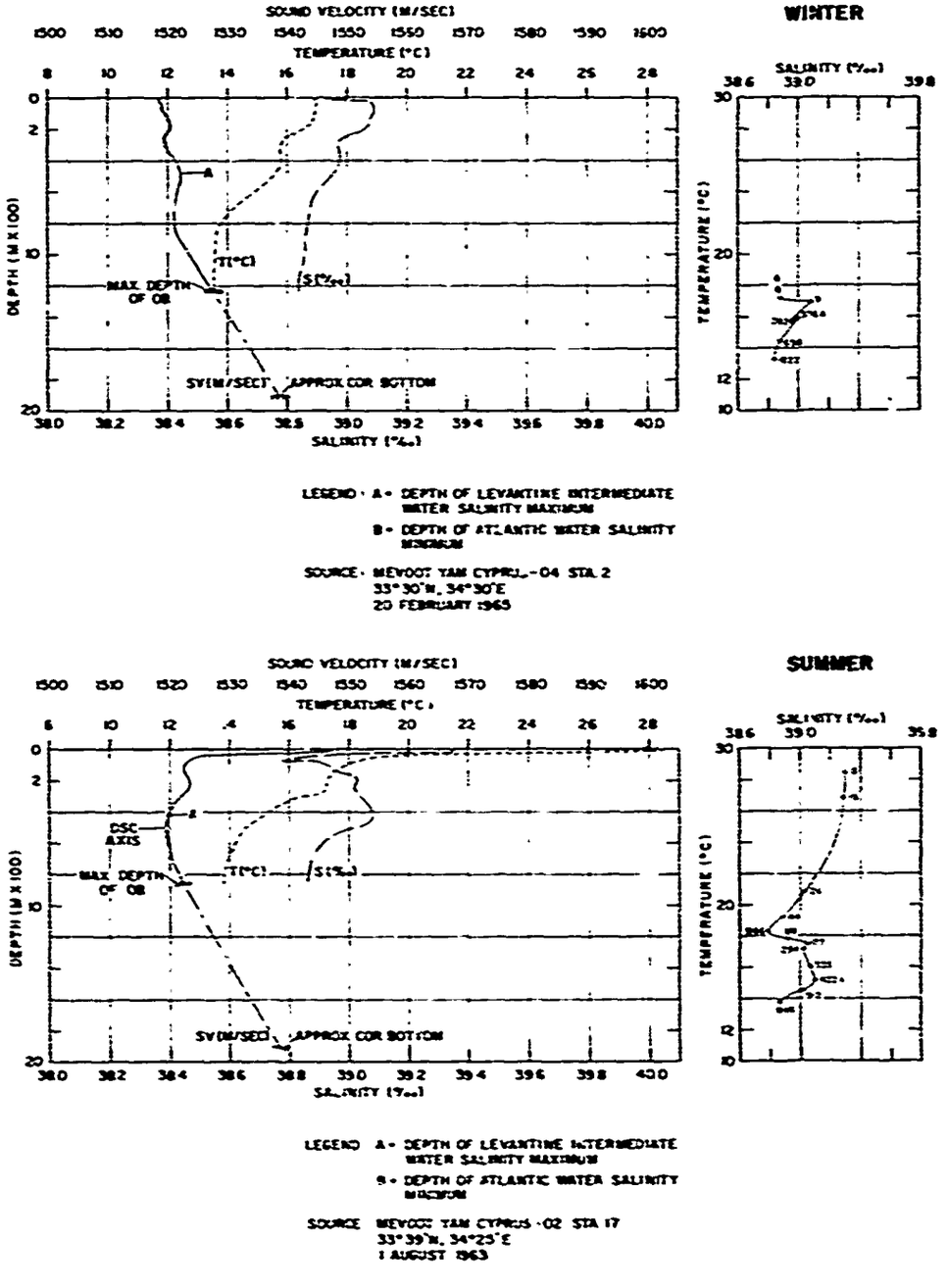

Figure 2.2.1-14. Winter and Summer Temperature, Salinity, Sound Velocity Profiles and Temperature-Salinity Diagrams for Eastern Levantine Basin

REFERENCES

1. Briscoe, M.G., Johannessen, O.M. and Vincenzi, S. 1972. The Maltese oceanic front: a surface description by ship and aircraft, SACLANT ASW Res. Cen., SACLANT Conf. Proc. No. 7, La Spezia, p. 153

2. Johannessen, O.M., de Strodel, F. and Gehin, C. 1971. Observations of an oceanic frontal system east of Malta in May 1971 (MAY FROST), SACLANT ASW Res. Cen. Tech. Memo. No. 169, La Spezia

3. Lacombe, H. and Tchernia, P. 1972. Caracteres hydrologiques et circulation des eaux en Mediterranee. In: The Mediterranean Sea, A Natural Sedimentation Laboratory, ed. Stanley, D.J., Dowden, Hutchinson, and Ross, Inc., Stroudsburg, Pennsylvania, p. 25 (in French)

4. MEDOC Group 1969. Observations of the formation of deep water in the Mediterranean Sea. Nature, , p. 1037

5. Miller, A.R. 1972a. Speculations concerning bottom circulation in the Mediterranean Sea. In: The Mediterranean Sea, A Natural Sedimentation Laboratory, ed. Stanley, D.J., Dowden, Hutchinson, and Ross, Inc., Stroudsburg, Pennsylvania, p. 37

6. Miller, A.R. 1972b. The Levantine Intermediate Water mass from Sardinia to Rhodes. SACLANT ASW Res. Cen., SACLANT Conf. Proc. No. 7, La Spezia, p. 108

7. Oren, O.H. 1971. The Atlantic Water in the Levant Basin and on the Shores of Israel, Cah. Oceanogr., 23(3), p. 291

8. Pollack, M.J. 1951. The sources of deep water in the eastern Mediterranean Sea, J. Mar. Res., 10, p. 128

9. Wust, G. 1961. On the vertical circulation of the Mediterranean Sea, J. Geophys. Res., 66(10)

2.2.2(U) Surface Currents (U). Surface currents throughout the Mediterranean are determined principally by the prevailing winds and surface evaporation. Their mean direction and speed are shown in figures 2.2.2-1 and 2.2.2-2 by the month.

(U) Throughout the year surface water from the Atlantic Ocean moves through the Strait of Gibraltar into the western Mediterranean and is driven generally in a counter-clockwise direction by the prevailing northwesterly winds. Southerly winds that occur for varying periods in winter interrupt this counter-clockwise flow. When the wind from any one quarter has been strong and continuous, drift currents are set up. During gales, current speeds of 4 to 5 knots may occur. Winds from the east can retard, or from the west can augment the inflow of Atlantic surface water, depending on their duration and force. Wind driven currents can affect water masses down to 100 feet but are negligible below this depth; however, wind drift usually is weak because wind speeds in this area range from Beaufort Force 0 to 3. Strong winds from the west in summer and the east in winter can develop appreciable cross-currents.

(U) Rapid evaporation of surface water in the western Mediterranean, particularly in the northern part of the Balearic and Ligurian Seas, produces surface water of high salinity which sinks and is replaced by less saline Atlantic surface water that flows east through the Strait of Gibraltar. The salt balance between the Mediterranean and the Atlantic is maintained by a bottom counter-current of high salinity that flows out of the Mediterranean through the Strait of Gibraltar. Mixing occurs between the surface and bottom currents forming a transition zone which has strong vertical movements and weak, variable currents.

(U) Strong tidal currents superimposed on the surface and subsurface currents reduce the inflow when they set from the Mediterranean into the Atlantic Ocean, and increase the inflow when they set from the Atlantic into the Mediterranean.

(U) The most persistent part of the prevailing surface current in the western basin flows east between Gibraltar and Tunisia where about 50 to 65 percent of all current observations show a set between northeast and southeast, and of these most show a set due east. Transient westerly sets are caused by easterly gales. The most variable currents (in direction) occur in the central parts of the basins. There is a westerly return current along the north slope.

(U) The surface current sets southeastward into the eastern Mediterranean through the Strait of Sicily at speeds ranging from 0.2 to 1.0 knot. In the Malta channel the current is influenced by the wind but generally sets east-southeast at 1.2 knots. Along the south coast of Sicily the southeast setting current is weak except when

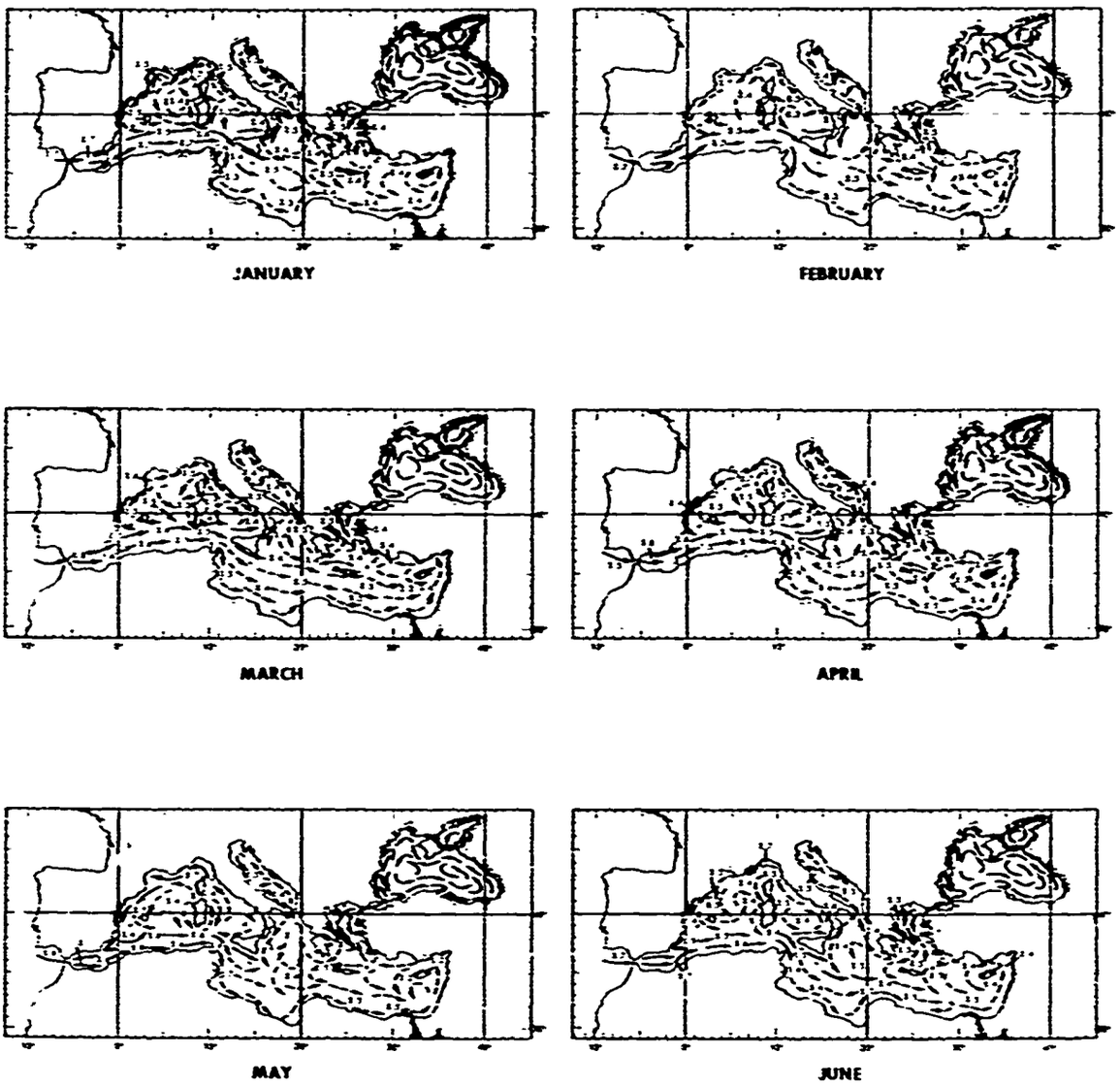

Legend: Solid arrows denote a persistence of 25 percent of the time or greater. Dashed arrows denote a persistence of less than 25 percent of the time.

Figure 2.2.2-1. Mean Surface Current Direction and Speed (in knots) for the Months January through June

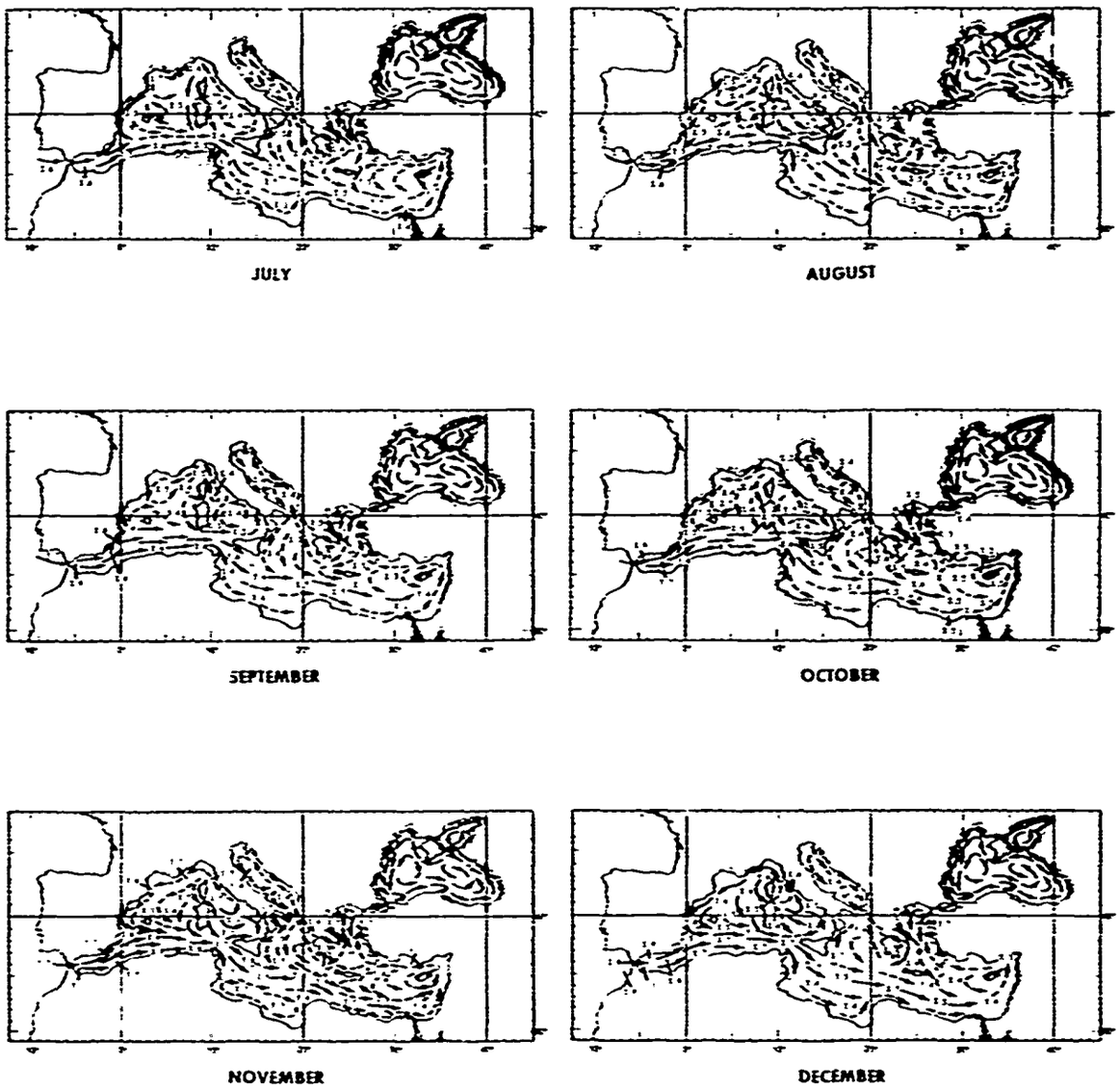

Legend: Solid arrows denote a persistence of 25 percent of the time or greater. Dashed arrows denote a persistence of less than 25 percent of the time.

Figure 2.2.2-2. Mean Surface Current Direction and Speed (in knots) for the Months July through December

accelerated by west to northwest winds. During strong southerly winds a northwest setting current may occur along the south coast of Sicily and during gales it may attain a speed of 2.0 knots. The counter-clockwise circulation of the eastern Mediterranean deflects the 0.1 to 1.0 knot southeast setting currents off Tunisia and Libya toward the coast. Except for a counter current in the Gulf of Sirte, the surface currents set eastward along the coast of eastern Libya and into the Levantine Basin at speeds of 0.4 to 0.8 knot.

(U) In the Levantine Basin the surface currents set east at 0.4 to 1.0 knot paralleling the coast of Egypt. However, off the coast of Libya and Egypt this current may set westward for brief periods under the influence of strong southern winds that occur most frequently in winter. The surface current parallels the coast around the Levantine Basin at speeds of 0.4 to 1.0 knot off Israel and Lebanon, 1.0 to 1.5 knots between Syria and Cyprus and 0.4 to 1.0 knot off Turkey and between Crete and Turkey into the Aegean Sea. Part of this current veers south to southeasterly around the west tip of Cyprus at speeds of 0.2 to 0.6 knot and completes the counter-clockwise movement of the Levantine Basin. North of Crete a portion of the southward flowing Aegean current divides. One branch sets eastward at speeds of 0.2 to 0.7 knot, part rejoining the northward currents in the Dodecanese and part passing around the eastern tip of Crete and setting westward south of the island. The other branch veers westward at speeds of 0.2 to 0.7 knot between the coast of Greece and Crete and continues northwestward along the west coast of Greece toward the Ionian Sea.

(U) The surface current which enters the Ionian Sea from the Aegean Sea also divides. One branch flows northward along the western coast of Greece at speeds of 0.2 to 0.6 knot and joins the counter-clockwise circulation of the Adriatic Sea. The other branch veers southwestward and joins the southeast flowing currents in the Ionian Sea.

(U) This branch completes the counter-clockwise circulation of the eastern Mediterranean Sea. The prevailing circulation pattern of the eastern Mediterranean Sea does not exist as a steady flow. Currents are weak and variable and their degree of variability cannot be predicted.

2.2.3(U) Ocean Fronts (U). Ocean fronts are boundaries between different water masses. Fronts may vary in degree from the extreme changes in physical properties observed across the north wall of the Gulf Stream to the almost negligible physical change observed across transient, near-surface fronts that are produced by convergence in otherwise homogeneous areas. Typically, the surface change across a front consists of an exaggerated horizontal temperature and salinity gradient, plus a shift in surface circulation. Major fronts may exhibit temperature gradients of up to 12°C over a distance of 10 kilometers. No fronts of this nature

occur in the Mediterranean Sea. Even with minor fronts, however, the thermohaline structure may be complex. Other frontal characteristics include considerable horizontal change in temperature and salinity with corresponding density variation, rapid change in sonic layer depth, and the presence of multiple sound channels.

(U) During several cruises covering many of the basins or smaller seas throughout the Mediterranean, a number of thermal fronts or frontal zones have been encountered. In the eastern Mediterranean, 20 frontal zone crossings have been recorded at various locations (Levine and White, 1972). At some of these locations the frontal zone had no surface manifestation, but the front was observable in the seasonal thermocline. One study (Katz, 1972) indicates a frontal zone in the western Mediterranean, at the entrance to the strait southwest of Sardinia. There is also evidence of a frontal crossing northwest of Sicily, at the entrance to the Tyrrhenian Sea. The positions of documented frontal crossings in the Mediterranean are shown in figure 2.2.3-1. It is quite possible that additional fronts in the Mediterranean may be identified in the future, because fronts are possible wherever differing water masses interact as well as wherever shallow sills are located. In theory, fronts should be found in the Mediterranean wherever the relatively cold, fresh surface water of North Atlantic origin comes into contact with the warmer, more saline water inherent to the Mediterranean.

(U) From a practical point of view, only the Maltese front, extending northeastward from the Island of Malta toward the Ionian Sea, is of significance to ASW operations. Documented positions of the Maltese front for winter, spring, and summer are shown in figure 2.2.3-2 (references 1-8). Seasonal variations in frontal location occur as the front migrates eastward from the shallow water of the continental shelf in spring, to deeper water in summer. By winter it is located within the Ionian Sea, in water deeper than 1,500 fathoms. Frontal migration is most likely the result of the influence of large scale meteorological processes (Johannessen et al., 1971). Meandering, i.e., wave-like perturbation of the front, was also observed during several investigations from multiple closely spaced crossings of the front (references 2, 5, 7).

(U) Temperature differences across the front normally range from 1.0° to 1.5°C, with greater differences occasionally observed. Figures 2.2.3-3 and 2.2.3-4 are typical examples of temperature profiles on both sides of the front during spring and summer. In spring, surface heating of the cold water overlying the continental slope may cause surface temperature to the west of the front to be greater than in the normally warm water to the east. This trend is reversed by summer, and surface temperature to the east of the front once again becomes warmer. During summer, the depth to the top of the seasonal thermocline was observed to be greater in the cold water west of the front than in the warm water east of the front (Anderson et al., 1972). The seasonal thermocline extended to a depth of 150 meters in the cold water during

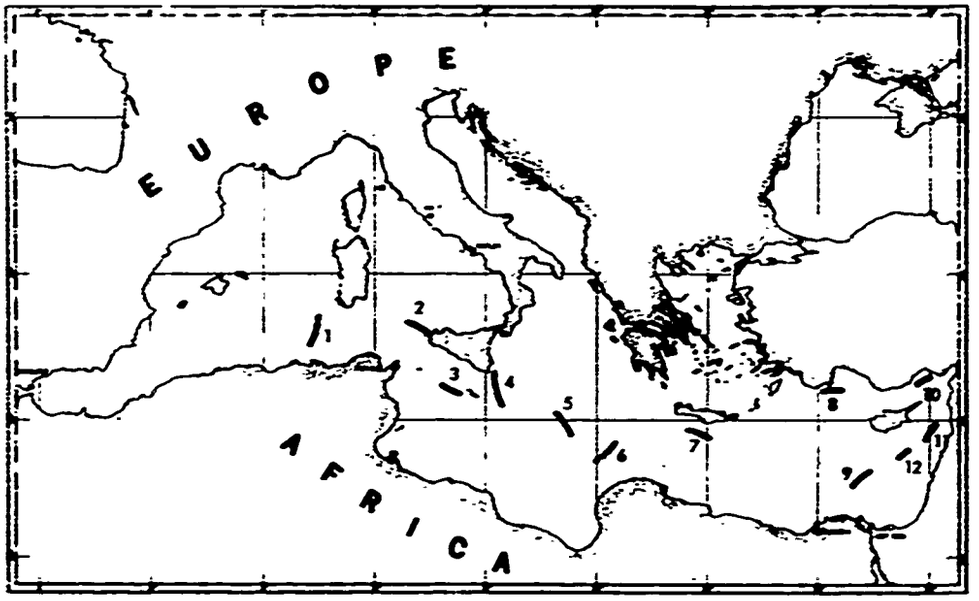

Figure 2.2.3-1. Location of Documented Frontal Crossings in the Mediterranean Sea

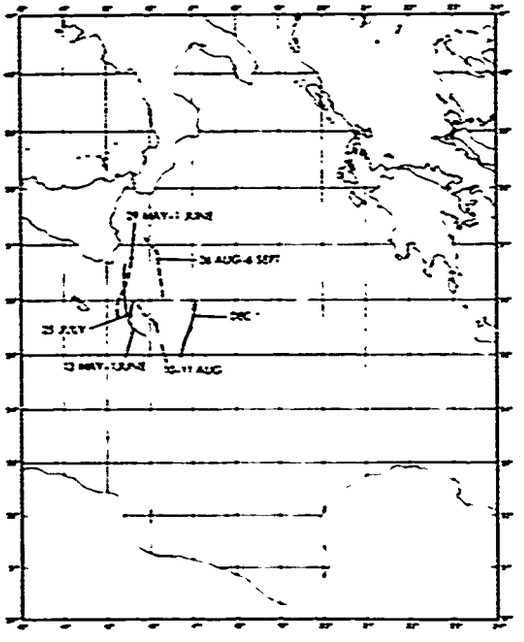

Figure 2.2.3-2. Meandering of Maltese Front

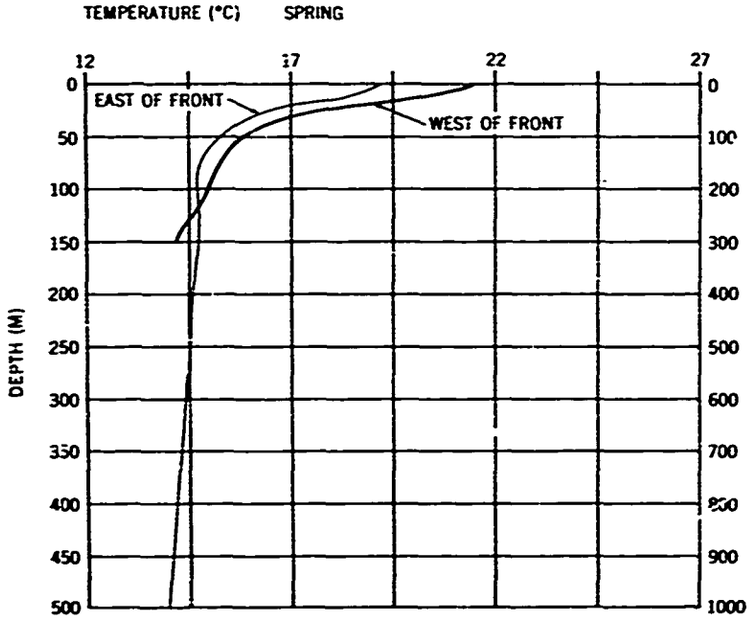

Figure 2.2.3-3. Temperature Differences Across the Maltese Front, Spring

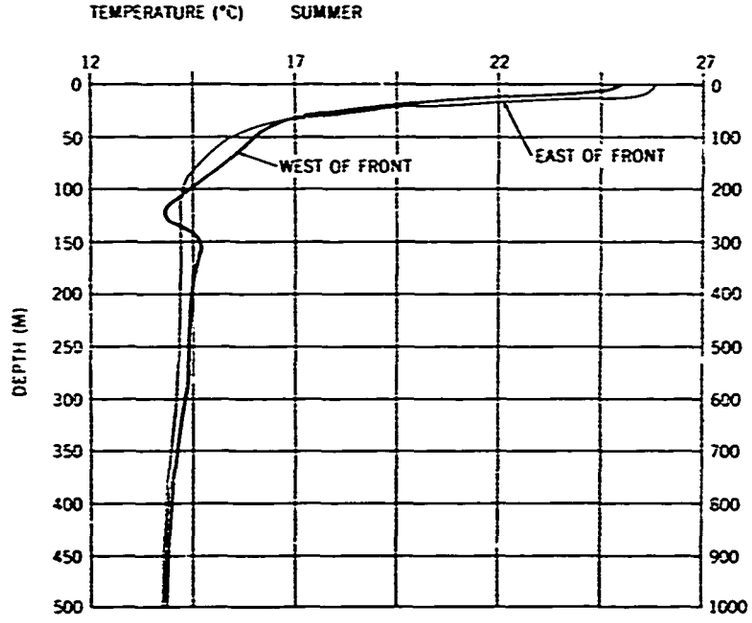

Figure 2.2.3-4. Temperature Differences Across the Maltese Front, Summer

summer and to only 100 meters in the warm water. A well defined temperature inversion (sound channel) has been observed at the base of the thermocline in the warm water (Shonting and Nacini, 1971).

(U) The salinity of the water of Atlantic origin observed west of the Maltese front is less than that of the water of Levantine origin observed to the east of the front (Molcard, 1972). Typical examples of salinity profiles on both sides of the front are shown in figures 2.2.3-5 and 2.2.3-6 for spring and summer. A salinity difference across the front on the order of 0.6°/oo occurs in summer because of evaporation caused by the increased solar heating.

(U) Typical examples of sound speed profiles on either side of the front are shown in figures 2.2.3-7 and 2.2.3-8 for spring and summer.

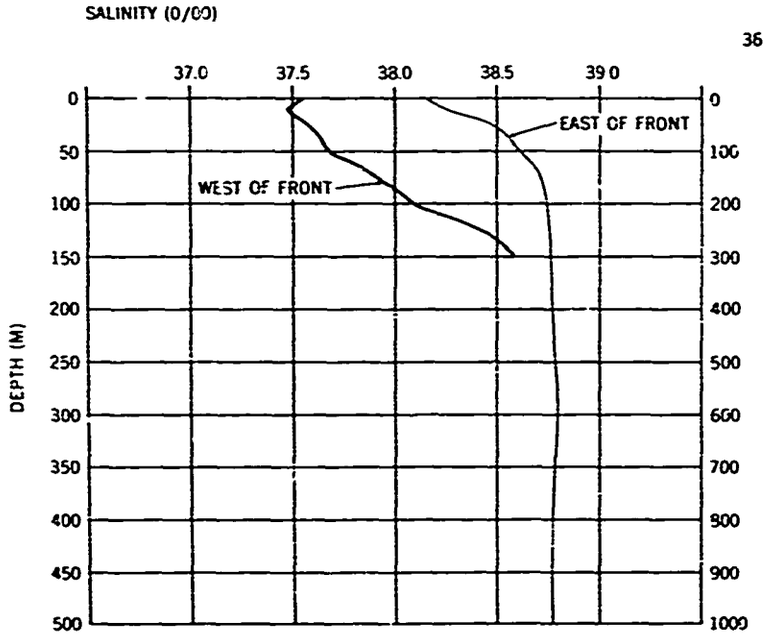

Figure 2.2.3-5. Salinity Differences Across the Maltese Front, Spring

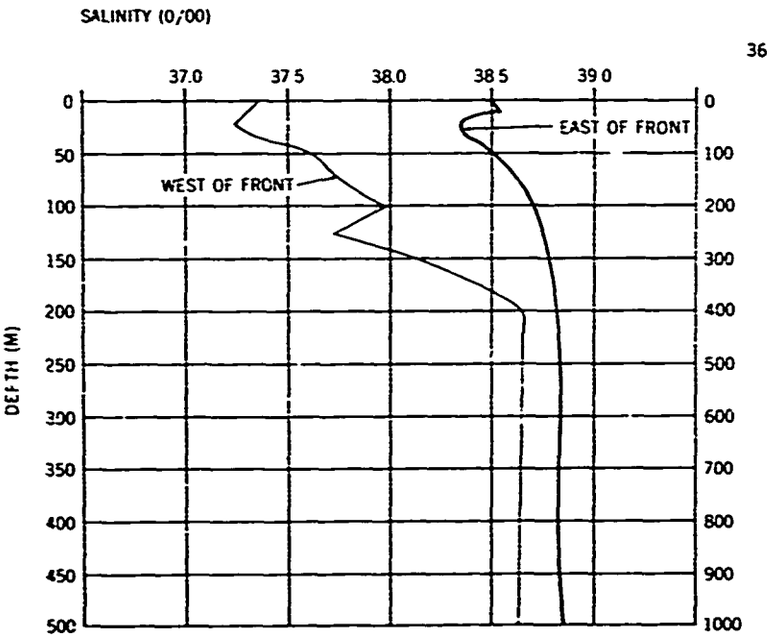

Figure 2.2.3-6. Salinity Differences Across the Maltese Front, Summer

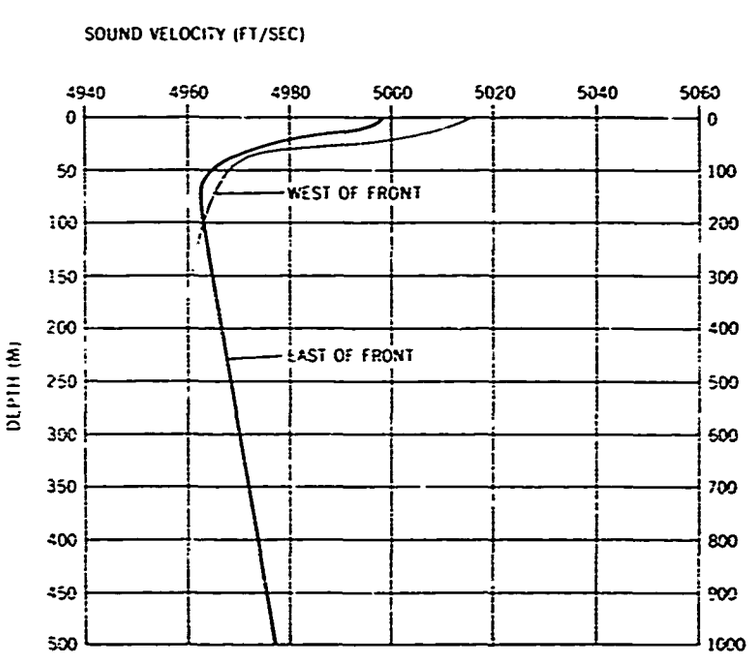

Figure 2.2.3-7. Sound Velocity Differences Across the Maltese Front, Spring

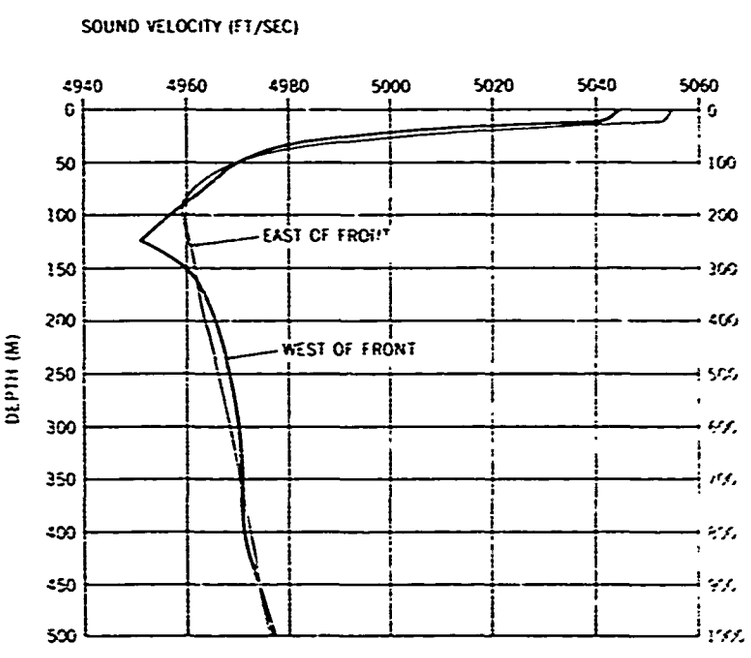

Figure 2.2.3-8. Sound Velocity Differences Across the Maltese Front, Summer

REFERENCES

1. Woods, J.D. and Watson, N.R. 1970. Measurement of thermocline fronts from the air. Underwater Science and Technology, June, p. 90

2. Johannessen, O.M., de Strobel, F. and Gehin, C. 1971. Observations of an oceanic frontal system east of Malta in May 1971 (MAY FROST), SACLANTCEN, Technical Memorandum No. 169, NATO UNCLASSIFIED

3. Molcard, R. MILOCMED 1968: A drogue experiment in the Ionian Sea Part II: A study of large scale diffusion, SACLANTCEN, Technical Memorandum No. 182, October 1972, NATO UNCLASSIFIED

4. Briscoe, M.G., Johannessen, O.M. and Vincenzi, S. 1972. The Maltese oceanic front: A surface description by ship and aircraft, SACLANT Confidential Proc. No. 7, SACLANT ASW Res. Cen., p. 153, La Spezia

5. Levine, E.R. and White, W.B. 1972. Thermal frontal zones in the Eastern Mediterranean Sea. J. Geophys. Res., 77, p. 1081

6. Ozturgut, E. 1972. The theoretical effect of an oceanic front on acoustic propagation, SACLANTCEN, Technical Report No 213, NATO CONFIDENTIAL

7. Anderson, R.W., Fisher, A., Jr. and Hanssen, G.L. Analysis of airborne radiation thermometer and bathythermograph observations in the Ionian Sea during summer 1972. NAVOCEANO Technical Note 7700-9-73

8. Gilcrest, R.A. 1973. Thermal survey of the Ionian Sea front, spring 1972. Survey Report 6150-1-73, U.S. Naval Oceanographic Office, Washington, D.C.

9. Shonting, D.H. and Nacini, E. 1971. A summary of oceanographic data obtained in deep water in the Strait of Sicily in May 1970. (MILOCMED Surv 70), SACLANTCEN Technical Memorandum No. 168

10. Katz, E.J. 1972. The Levantine intermediate water between the Strait of Sicily and the Strait of Gibraltar. Deep Sea Res., 19, p. 507

2.2.5(U) Internal Waves (U). Internal waves, as defined in reference 10, are subsurface waves found between layers of different density or within layers where vertical density gradients are present. They can exist in any stratified fluid and can be caused by flow over an irregular bottom, atmospheric disturbances, tidal forces, and shear flow. In deep water, the height of internal waves may be several hundred feet; however, in the main thermocline they are normally 20-50 feet high. They have an amplitude at all depths except at the bottom, where it is zero, and at the free surface, where it is negligibly small. The distribution of amplitude over depth is influenced by the density distribution, since less energy is required to displace a weak density boundary than a strong one. Because of the large vertical and horizontal displacement of particles, internal waves are important factors in water mixing and transport. In the Mediterranean Sea, internal waves would be expected to be particularly prominent where relatively low density water of Atlantic origin overrides denser water of Levantine origin and where surface water is separated from subsurface water by a seasonal thermocline.

(U) A number of studies have been made for the Strait of Gibraltar where internal waves are generated by water of Atlantic origin flowing (i.e., horizontal shear) over markedly different water of Levantine origin (references 1-5). The onset of an approaching internal wave is indicated by a deepening of isotherms. This is followed by a train (group) of oscillations of varying amplitudes that eventually decay. After the passage of the wave group, the isotherms return to their original depth (references 4, 5). The maximum wave amplitudes in trains that have been observed vary from 23 to 75 meters (references 1, 4, 5). The observed periods of individual waves vary from 18 minutes near the beginning of a wave group to about eight minutes in the decaying tail. Group periods vary from 1.6 to 3.5 hours. Bands of ripples separated by smooth water have been observed to move eastward at the surface and it is postulated that they represent the surface manifestation of the interaction between Atlantic and Levantine water (reference 1). The ripple bands may be discernible on surface radar (references 1, 4). Oscillation of the deep scattering layer may occur in period with the internal waves (reference 1).

(U) Reports of internal waves in other Mediterranean areas are meager. One would normally expect to encounter internal waves where two water masses are in proximity, such as in the Strait of Sicily, but available observations failed to record their presence (reference 6). However, internal waves with characteristics similar to those reported in the Strait of Gibraltar have been observed in the Ionian Sea (references 7, 8).

(U) Internal waves may have considerable effect on sound propagation (reference 9). Where the depth of the thermocline varies sinusoidally, an in-layer source will produce areas of high sound intensity below the thermocline simultaneously with wave crests. In the case where the source is near the surface, passage of an internal wave causes both disappearance

(U)
of the surface duct and variations of the shadow zone (reference 2). Where the source is deep, insonification of the surface area may be affected significantly.

REFERENCES

1. Frasetto, R. 1964. Short period vertical displacements of the upper layers of the Strait of Gibraltar. SACLANTCEN Technical Report No. 30, Parts I and II, NATO UNCLASSIFIED

2. Allan, T.D. 1966. Observed sound velocity and temperature profiles in the Strait of Gibraltar during the passage of an internal wave. SACLANTCEN Technical Report No. 66, NATO UNCLASSIFIED

3. Steyaert, M. 1966. Project Gibraltar: Resultats des observations hydrologiques effectuees a bord du navire belge "Eupen" (Mai-Juin 1961), Sous-Comite Ocean. de L'Organ. du Traite de L'Atl. Nord, Rapp. Tech OTAN No. 31

4. Ziegenbein, J. 1969. Short internal waves in the Strait of Gibraltar. Deep-Sea Res., 16(5), p. 479

5. Ziegenbein, J. 1970. Spatial observations of short internal waves in the Strait of Gibraltar. Deep-Sea Res., 17(5), p. 867

6. Shonting, D.H. and Nacini, E. 1972. A summary of oceanographic data obtained in deep water in the Strait of Sicily in May 1970. (MICROMED SURV 70), Proc. SACLANT Confidential No. 7, NATO UNCLASSIFIED

7. Dahme, A. and Lombardi, A. 1970. Variations of the sound speed and its gradients in the Ionian Sea in May - June 1968. (MILOCMED 68), SACLANTCEN Technical Report No. 173, NATO CONFIDENTIAL

8. Dahme, A. and Dehaen, A. 1972. MILOCMED 68: A drogue experiment in the Ionian Sea, Part I, the temperature time series, SACLANTCEN Technical Report No. 181, NATO UNCLASSIFIED

9. Lee, O.S. 1961. Effect of an internal wave on sound in the ocean. J. Acous, Soc. Amer., 33, p. 677

10. Fairbridge, R.W., 1966. The Encyclopedia of Oceanography, Reinhold Publishing Corp. p. 402

Section 2.3, Geology and Geophysics begins overleaf.

2.3(U) Geology and Geophysics (U)

2.3.1(U) Bathymetry (U). The bathymetry of the Mediterranean Sea is shown in figure 2.3.1-1* by means of 100 fathom contours that are based on an assumed velocity of sound in sea water of 4800 ft/sec. However, a nomogram (figure 2.3.1-2) provides separate depth corrections in four regions of the Mediterranean for variations of vertical sound velocity from the assumed values. The following is a brief summary of the bathymetric features.

(U) The floor of the Strait of Gibraltar is a sill dividing the Mediterranean Sea from the Atlantic Ocean, with a limiting depth of approximately 175 fathoms. The bottom relief is extremely rugged. In the Alboran Sea there is no break to distinguish between the continental shelf and the slope. The basin floor lies at about 700 fathoms, and a maximum depth of about 840 fathoms occurs at the eastern end of the basin, where it narrows to a submarine valley that descends into the deeper Balearic Basin.

(U) The floor of the Balearic Basin is flat to mildly sloping and lies at depths of 1400 to 1500 fathoms. The continental shelf is narrow to nonexistent around most of the basin. The maximum depth of the basin exceeds 1400 fathoms.

(U) The floor of the Tyrrhenian Basin is irregular, but in some places at depths of 1800 fathoms or more it is relatively flat. Numerous peaks and knolls rise from the basin floor and slopes. The Tyrrhenian Basin is separated from the Ionian Basin by a sill with a depth of slightly less than 200 fathoms in the Strait of Sicily and has depths of less than 50 fathoms in the Strait of Messina.

(U) The continental shelf reaches a maximum width of about 300 nm east of Tunisia. There are northwest-southeast trending troughs on the continental shelf between Sicily and Tunisia where depths are about 700 to 860 fathoms.

(U) The Adriatic Sea lies mostly on the continental shelf. The floor of the Adriatic Basin is 600 to 700 fathoms deep and has little local relief. The maximum depth of 765 fathoms is in the Strait of Otranto adjacent to the sill which separates the Adriatic from the Ionian Basin. Limiting depths on the sill are approximately 450 fathoms.

*Figure 2.3.1-1 is inserted in the envelope bound at the back of this volume.

Figure 2.3.1-2a. Depth Correction Regions for Bathymetric Chart

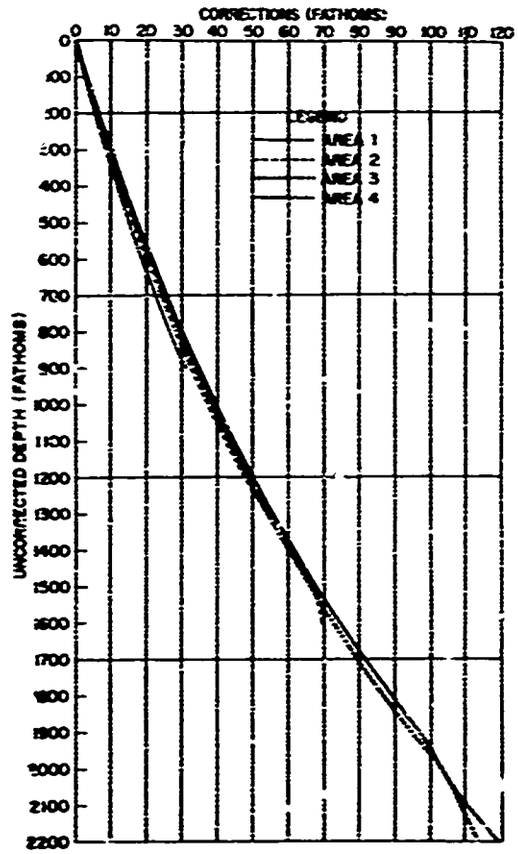

Figure 2.3.1-2b. Depth Correction Nomogram for the Mediterranean Sea Regions Indicated in Figure 2.3.1-2a

(U) The floor of the Ionian Basin has considerable local relief consisting of seamounts, and many large and small elevations, depressions, and valleys.

(U) Most of the Levantine Basin floor is mildly undulating with several relatively flat regions. Several deep depressions lie off Turkey and Rhodes three of which exceed 2000 fathoms.

2.3.2(U) Physiography (U). The physiography of the Mediterranean may be logically divided into western and eastern regions. The western region, west of Sicily, consists of continental margins descending to abyssal plains formed by turbidity flows. The eastern region is much more complex structurally and physiographically, in many respects being typical of the usual oceanic divisions. An example of this is a series of basins paralleling and abutting the Mediterranean Ridge. Tectonic activity in this region has repeatedly deformed abyssal plains of the past similar to those which occur in the western Mediterranean. There are, however, many small abyssal plains in the deepest parts. Most are a few miles across.

(U) A recently revised physiographic province chart is shown in figure 2.3.2-1*. A physiographic relief chart is shown in figure 2.3.2-2*.

2.3.3(U) Bottom-Sediments (U). A great number of bottom samples have been collected from the Mediterranean Sea using a variety of collecting techniques (cores, grabs, dredges). Descriptions of these samples range considerably in sophistication; some descriptions entail detailed laboratory examination while others represent a single word in a ships log. A recent summary of Mediterranean sedimentation has been given in "The Mediterranean Sea - A Natural Sedimentation Laboratory" edited by D.J. Stanley and published by Dowden, Hutchinson and Ross, Inc., 1972. These data, of varying credibility, were plotted, evaluated, and ultimately used to compile the sediment map presented as figure 2.3.3-1*.

(U) Two broad physiographic divisions were used to characterize the Mediterranean: shelf and other shallow water areas, and the deep sea. Based on several thousand observations, four sediment types are represented on the shelf: (1) gravel, pebbles and shells; (2) sand - silt; (3) sand - silt mixed with silty clays; and (4) silty clays. Ordinarily, the 200 meter contour was used to define the seaward limit of the shelf. In several regions, however, this contour was ignored when the deeper water sediments had obvious similarities with the adjacent shelf sediments.

(U) In the deep areas of the Mediterranean, roughly 100 non-uniformly distributed piston cores were used to describe the sediment patterns. The predominant surface sediment type is a fine-grained silty clay consisting predominantly of terrigenous clay or biogenous carbonate, or both. The silt fraction, usually dispersed irregularly through the clays, consists of oceanic plankton shells, continental

*These figures are inserted in the envelope bound at the back of this volume.

mineral grains (quartz, feldspar, mica, etc.), and volcanic ash. The very small dispersed sand fraction contained oceanic plankton shells.

(U) In certain areas, these surface layers of silty clay are underlain by well-stratified sands and silts consisting of volcanic ash and/or mineral grains (quartz, feldspar, etc.). Because the acoustic performance of a low frequency system is sensitive to such layers, their distribution is reflected in the sediment map. In the provinces indicated, these layers generally lie a few meters deep in the sediment, and often just below the surface.

2.3.4(U) Subbottom Structure (U). The subbottom structure in oceanic areas is obtained from the seismic refraction method (for a summary see: The Sea, Vol. 3, pp. 20-48, Edited by M. Hill). There were only six published references available, undoubtedly due to the difficulty in obtaining these data. These publications are represented by numbers on figure 2.3.4-1, corresponding to the reference list.

(U) No effort was made to obtain unpublished data from either research institutions or petroleum companies. Only reversed profile refraction data were used, thus avoiding any ambiguous results. Some of these data were presented as single points while others were given by the refraction lines. For the latter, the structure beneath the profile is shown at the mid-point of the profile.

(U) These refraction data have been presented in the following format.

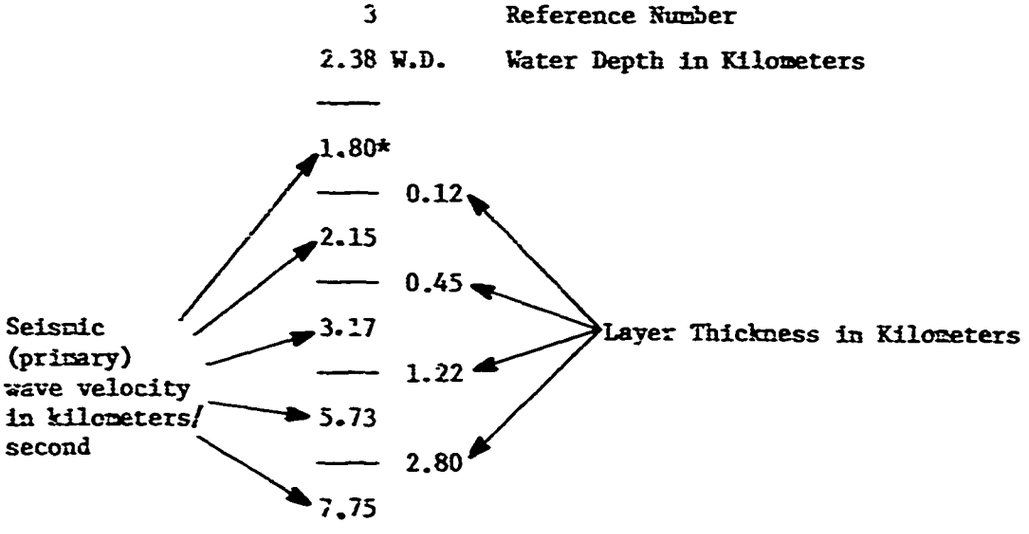

* Represents an assumed velocity

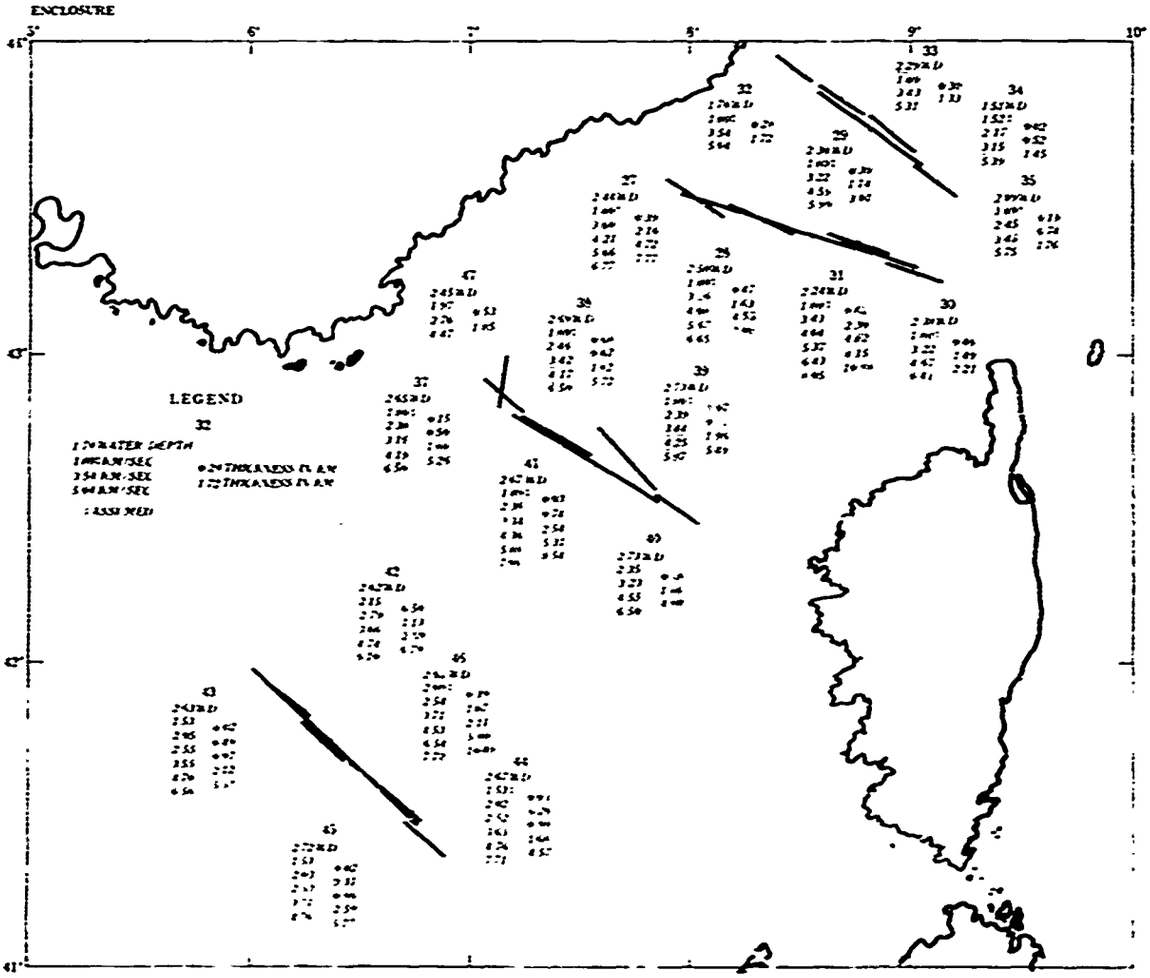

Figure 2.3.4-1b.* Mediterranean Subbottom Structure

*Figure 2.3.4-1a has been inserted in the envelope bound at the back of this volume.

(U) The numbers above the data on the several maps refer to a consecutive listing of refraction stations. This listing was prepared and is retained by the U.S. Naval Oceanographic Office, Code 6120, and contains all information pertinent to the original data. The stations are also described in the references as follows:

Stations	Reference
1-5	Ewing, M. and Ewing, J. (1959)
6-12	Michno (1963)
13-19	Gaskell, T.F., et al., (1959)
20-46	Fahlquist, D.A. and Hersey, J.B. (1969)
47	Leenhardt, O. (1969)
48-49	Wong, H.K., et al., (1970)

REFERENCES

1. Ewing, M. and Ewing, J. 1959. Seismic refraction measurements in the Atlantic Ocean Basins, in the Mediterranean Sea, on the Mid-Atlantic Ridge, and in the Norwegian Sea. Bull. G.S.A., Vol. 70, p. 291

2. Michno 1963. Seismic investigations of sediments of the Tyrrhenian and Ionian Seas. Okeanologiia, Vol. 3, p. 853

3. Gaskell, T.P., Hill, M.N. and Swallow, J.C. 1959. Seismic measurements made by H.M.S. CHALLENGER in the Atlantic, Pacific, and Indian Oceans and in the Mediterranean Sea, 1950-1953. Philosophical Transactions of the Royal Society, Vol. 251, Series A.988, p. 23

4. Fahlquist, D.A. and Hersey, J.B. 1969. Seismic refraction measurements in the Western Mediterranean Sea. Bull. de l'Institut Oceanographique, Vol. 67, No. 1386

5. Leenhardt, O. 1969. Depouillement d'un profil sismique par la methode de refraction tire au large de la cote varoise. C.R. Soc. Geol. Fr., Vol. 4, p. 157

6. Wong, H.K., Zarudzki, E.F.K., Knott, S.T. and Hays, E.E. 1970. Newly discovered group of diapiric structures in Western Mediterranean. Bull. A.A.P.G., Vol. 54, No. 11, p. 2200

2.4(U) Biological Factors (U)

2.4.1(U) Marine Animal Targets (U). Potential submarine-like sonar contacts in the Mediterranean include several types of cetaceans (whales and porpoises) and certain schooling fishes. Sperm whales are widely distributed in the Mediterranean, occurring throughout the year. They are most common in the western basin. Fin whales enter the western part of the Mediterranean Sea in autumn, some individuals remaining until spring. Characteristics of whales and other large animals occurring in this area are presented in table 2.4.1-I. The seasonal distribution of marine mammals is shown in figures 2.4.1-1 through 2.4.1-4.

(U) Large fishes, such as tuna, may produce strong sonar echoes. Smaller fishes that occur in large dense schools also constitute good acoustic targets. The principal schooling fishes in this area are members of the sardine, anchovy, mackerel, and jack families. The combination of a fish school and accompanying predators, such as tuna or porpoises, may present a confusing target to the sonarman.

(U) In general, schooling fishes are most abundant in coastal waters where they feed and spawn. Large schools of sardines and mackerel appear off the coasts of Spain and Algeria in spring and move eastward to the waters of Tunisia and Italy by early summer. Concentrations of spawning sardines occur during autumn and winter off the coasts of France and Yugoslavia. Sardines are abundant during autumn in the far eastern part of the Mediterranean. Mackerel and sardines migrate from the Aegean Sea into the Sea of Marmara during early summer. Many of the mackerel continue into the Black Sea, becoming abundant in the northern part during summer. Large schools of anchovies occupy the Sea of Azov during spring and summer but depart through Kerchenskiy Proliv in early autumn. Figure 2.4.1-5 shows the distribution, relative abundance, and months of greatest abundance of schooling fishes in the area.

(U) Fishes large enough to produce individual echoes include the bluefin tuna (thunnus thynnus), and the ocean sunfish (mola mola). The tuna schools migrate eastward from Gibraltar to the Ionian Sea in spring and return to the western basin of the Mediterranean Sea in summer. The bluefin tuna attains a length of 7 to 10 feet in these waters. The ocean sunfish has been reported from the western Mediterranean Sea and the Adriatic Sea. This oddly shaped fish, nearly circular in side view, occasionally is encountered in small groups up to about 12 individuals basking in the sun at the sea surface. Large specimens may reach a length of 8 to 10 feet.

TABLE 2.4.1-I. CHARACTERISTICS OF CERTAIN LARGE MARINE ANIMALS

NAME (COMMON AND SCIENTIFIC)	SIZE (FEET)	GROUPING HABITS	GENERAL OCCURRENCE	SWIMMING CHARACTERISTICS *	
				SPEED (KNOTS)	SURFACING AND DIVING BEHAVIOR
Whalebone Whales ** Fin (Balaenoptera physalus)	50 to 80	Singly or in pairs, may gather in schools of several to 50 or more	Coastal and offshore waters of Mediterranean	8 normal, 15 to 20 maximum	Takes 3 to 15 breaths before diving 8 to 15 minutes; maximum dive 30 minutes***
Sei (Balaenoptera borealis)	40 to 55	do	do	24 in spurts of less than ½ mile	Takes a few breaths before diving 5 to 10 minutes***
Humpback (Megaptera novaeangliae)	35 to 55	Small groups of 4 to 8, sometimes to 20	do	4.5 average, 2.5 to 15 range	1 to 18 shallow dives before deep dives of 15 to 20 minutes***
Minke (Balaenoptera acutorostrata)	20 to 30	Small groups or schools of 10 or more	Mediterranean coastal waters and occasionally in Black Sea	5 average; 16 maximum	Takes 5 to 8 breaths before a prolonged dive***
Toothed Whales and Porpoises:** Sperm whale (Physeter catodon)	30 to 60	Singly or in small groups; schools of 40 to 50	Coastal and offshore waters of Mediterranean	3 to 4 average, 10 to 12 maximum, 20 in spurts	Blows 30 to 60 times for 10 to 11 minutes; dives to 500 fathoms or more for 40 to 75 minutes
Bottlenose whale (Hyperodon ampullatus)	20 to 30	Groups of 4 to 12	do	na	Normally surfaces every 10 to 20 minutes; may remain submerged 60 minutes or more
Goose-beaked whale (Ziphius cavirostris)	to 28	Schools of 30 to 40; travel in close formation	do	na	Spouts on surface for about 10 minutes; dives for up to ½ hour or more
Pilot whale (Globicephala melaena)	15 to 25	Large groups up to 2,000 or more	do	To 20 or more	na
False killer whale (Pseudorca crassidens)	12 to 18	Schools of 10 to 300	do	na	na
Grampus, Risso's dolphin (Grampidelphis griseus)	10 to 13	Singly or in small groups less than 12	Coastal and offshore waters of western Mediterranean and the Adriatic	na	na
Bottlenose porpoise (Tursiops truncatus)	10 to 12	Singly or in schools to 100 or more	Black Sea and coastal and offshore waters of Mediterranean	10 to 12 normal, 20 in spurts	Normally surfaces every 15 to 30 seconds; maximum dive about 10 minutes
Common dolphin (Dolphinus delphis)	6 to 8	Schools to several hundred	Black Sea and coastal waters of Mediterranean	25 maximum	na
Harbor porpoise (Phocoena phocoena)	4 to 6	Small Groups or schools to 100 or more	do	10 to 15 normal, 20 in spurts	Surfaces 3 to 4 times a minute
SEALS: Monk seal (Monachus monachus)	to 7	Small herds, usually less than 20	Mediterranean coastal waters; rare in Black Sea	na	na
SHARKS Basking (Cetorhinus maximus)	35 to 40	Singly or in pairs; occasionally in small schools	Coastal and offshore waters of Mediterranean, chiefly western part	Sluggish	Usually at surface, may submerge to 200 fathoms

na Data not available.

* Swimming characteristics will vary if the animal is disturbed.

** All whales are presumed to produce swimming noises, probably by the beating action of their flukes at the surface; subsurface fluke beats have been reported to be relatively noiseless.

*** Whalebone whales rarely submerge deeper than 50 fathoms.

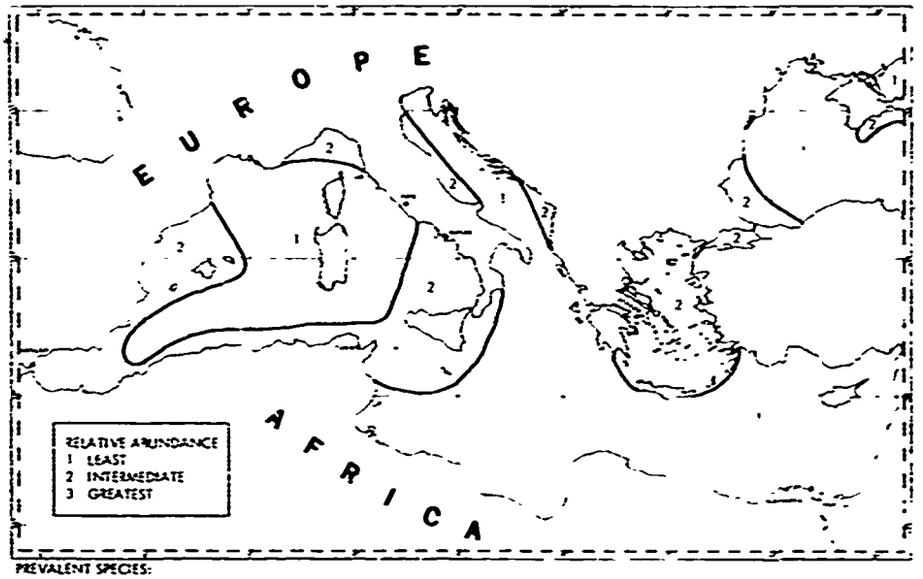

Figure 2.4.1-1. Distribution of Marine Mammals, Winter

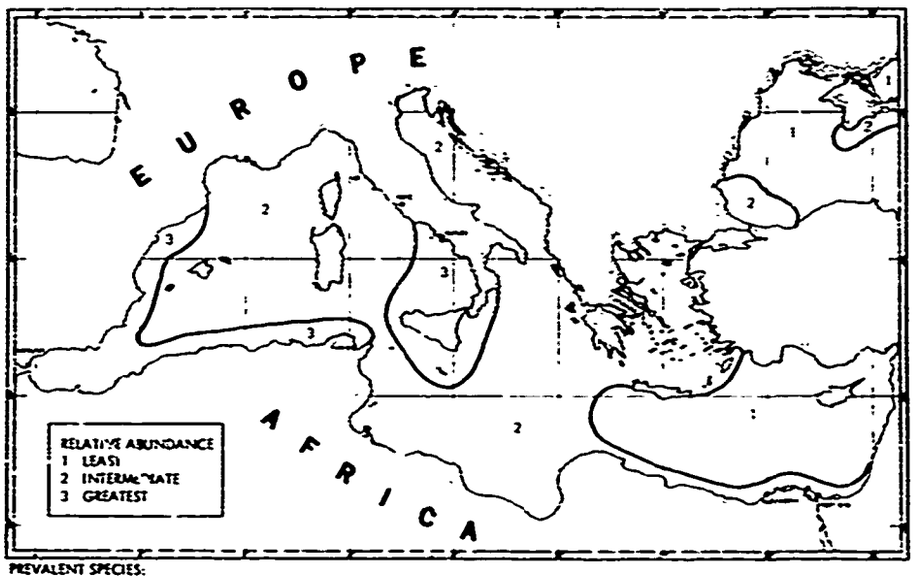

Figure 2.4.1-2. Distribution of Marine Mammals, Spring

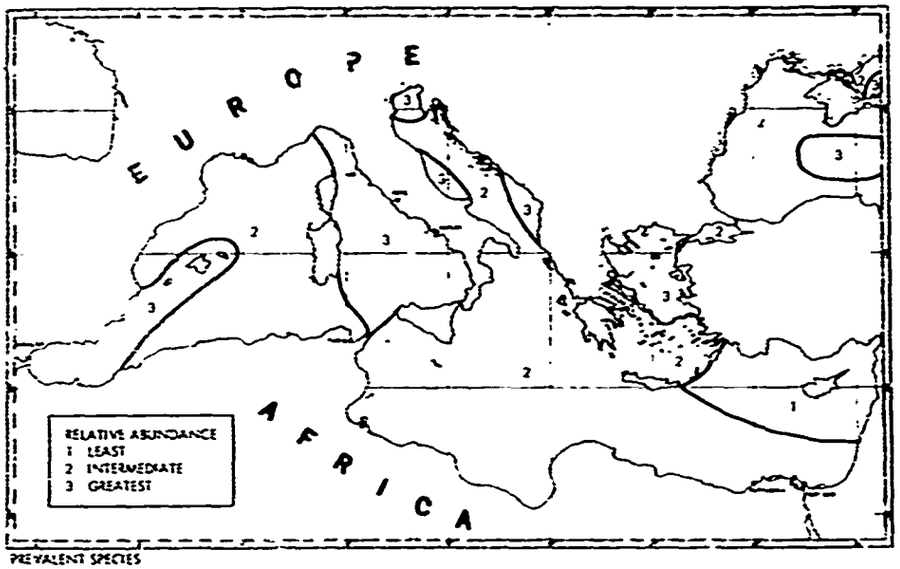

Figure 2.4.1-3. Distribution of Marine Mammals, Summer

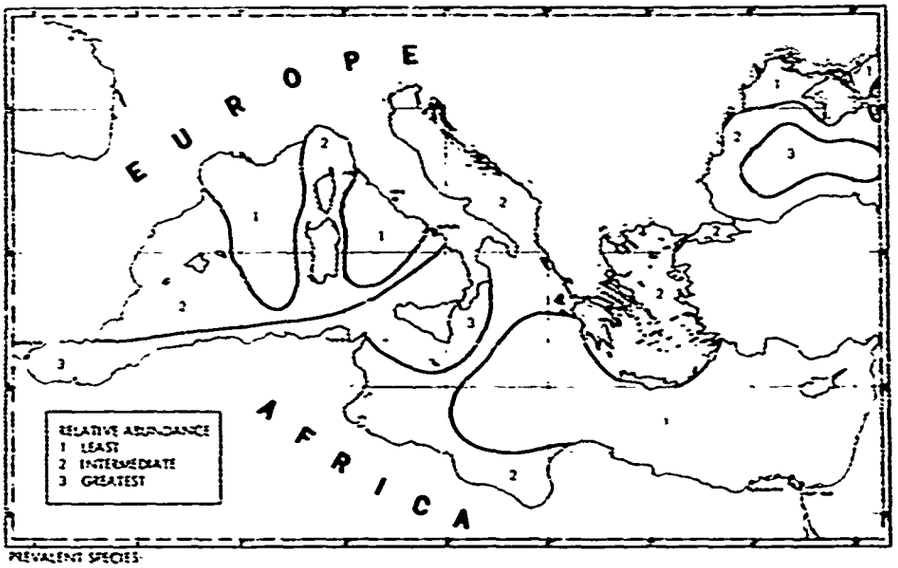

Figure 2.4.1-4. Distribution of Marine Mammals, Autumn

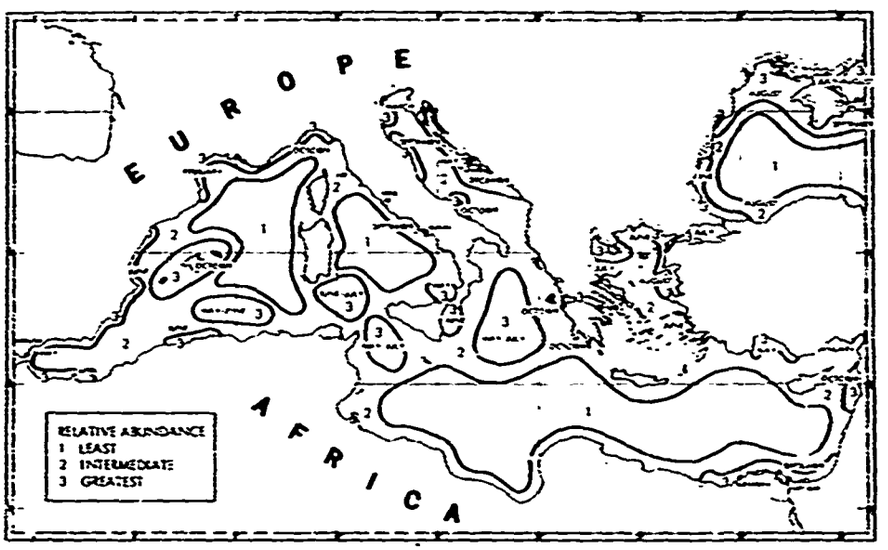

Figure 2.4.1-5. Distribution, Relative Abundance, and Months of Greatest Abundance of Certain Schooling Fish (Principally Herring, Sardine, Anchovy, and Mackerel)

2.4.2(U) Soniferous Marine Animals (U)

2.4.2.1(U) Mammals (U). Whales and porpoises are capable of emitting a variety of sounds. The baleen (whalebone) whales produce tones that are relatively low-pitched, from about 15 to 8,000 Hz. The ultrasonic clicks of some porpoises may exceed 200 kHz. The acoustic characteristics of cetaceans occurring in this area are summarized in table 2.4.2-I.

2.4.2.2(U) Fish (U). Many of the common fishes of this region are known to be sound producers; others are considered capable of sound production because of their close relationship to North Atlantic species that are known to be soniferous. The principal frequencies of most fish sounds in this region lie between 50 and 800 Hz. An exception is the triggerfish, which produces a metallic scratching sound with considerable energy in the 2,400 to 4,800 Hz band. Characteristics of representative soniferous fishes are presented in table 2.4.2-II.

(U) Sound-producing fishes are concentrated in coastal waters and are more abundant in certain partially enclosed bodies of water such as the Gulf of Lion, Gulf of Gabes, and the Aegean and Black Seas.

(U) In winter, there is an offshore movement to deeper water; fish noise is greatest along the African coast and minimal in the northern part of the Mediterranean Sea and in the Black Sea. Croaker and gurnard noise increases in the northern part of the area in spring and continues at a high level until early autumn.

(U) The seasonal distribution and abundance of the principal soniferous fishes are shown in figures 2.4.2-1 through 2.4.2-4.

2.4.2.3(U) Crustaceans (U). The snapping or pistol shrimp is a small crustacean that individually produces a loud snapping sound, but in a large colony produces a continuous crackling noise. Shrimp noise ranges in frequency from less than 1 kHz to 50 kHz, with principal components between 2 and 20 kHz. Shrimp crackle dominates water noise above 2 kHz and exerts a strong masking effect on signals. At 1000 Hz, noise over shrimp beds can reach levels equivalent to sea state 4. In regions where the characteristics of shrimp noise have been studied, no significant seasonal variations have been noted. However, slight diurnal variations have been reported, the nighttime level being somewhat higher than the daytime level.

(U) Another soniferous crustacean of this area is the spiny lobster or langouste. This animal makes a rasping or rattling sound by rubbing its long antennae against a ridged area of its shell. Frequencies range from 40 Hz to about 9 kHz, with greatest intensities at 600 Hz, 800 Hz,

TABLE 2.4.2-I. ACOUSTIC CHARACTERISTICS OF MEDITERRANEAN CETACEANS

Species	Frequency Range (Hz)	Principal Frequencies (Hz)	Source Level (dB//1uPa)	Description of Sound
Fin Whale	15 - 34	20	170 - 180	Pure tone pulses of about 1 sec duration repeated at a rate of several per minute
Sei Whale	20 - 200	40	55 - 60	Sporadic moans 0.5 to 2.5 sec in duration
Minke Whale	60 - 130	60 - 120	160 - 165	Sounds of 0.2 to 0.3 sec, sweeping downward in frequency
Humpback Whale	200 - 8000	200 - 1600	154 - 172	Variety of grunts, moans and sustained tones that may rise or fall in frequency
Sperm Whale	200 - 32,000	3000 - 5000	165.5 - 175.3	Powerful clicks emitted at rates varying from 1/sec
Pilot Whale	1000 - 8000	2000 - 4000	na	Squeals and whistles, narrowband or sweeping up or down several kHz
	8000 - 20,000	8000	na	Short, broadband pulses of a few msec duration at rates of 10-50/sec
Bottlenose Whale	3000 - 16,000	3000 - 5000 7000 - 9000 12,000 - 14,000	na	Whistles and chirps of 115-850 msec, single frequency or sweeps through various frequencies
	500 - 26,000	8000 - 12,000	weak	Clicks of 2-17 msec at rates up to 82/sec
False Killer Whale	3000 - 12,000	4000 - 8000	na	Narrowband whistles of 0.5-1.0 sec
Bottlenose Porpoise	2000 - 20,000	7000 - 15,000	na	Various whistles of 1 sec or less
	100 - 200,000	30,000 - 60,000	70	Clicks of 50-250 msec at rates of 40-500/sec
Common Dolphin	2000 - 40,000	8000 - 16,000 2000 - 32,000	na	Various whistles of 1 sec of less
	100 - 150,000		140	Clicks of 50-250 msec at rates of 5-250/sec
Harbor Porpoise	1000 - 20,000	1000 - 3000	25 - 30	Clicks of 0.5-5.0 msec at rates up to 1000/sec resulting in modulated whistles

TABLE 2.4.2-II. BIOACOUSTIC CHARACTERISTICS OF FISH

Fish	Abundance Distribution Habitat	Frequency Range (Hz)	Peak Energy at (Hz)	Peak Pressure (dB re μPa)	Description of Sound
Croakers	Present throughout most of the area. Common in waters less than 45 fathoms deep. Usually spawns in late Spring (April through June); prefers smooth or soft bottoms.	30 to 6300	30 to 1200 peak point at 400	126 1 meter	Drum sounds, moans, and grumbling produced by species in area. Most sound produced during evening hours and breeding periods.
Gurnards	Present mainly in deep waters of the area; usually near smooth or sandy bottoms.	50 to 1700	400	120 1 meter	Clucking, double drum sounds produced by species in area. Most sound produced during periods of danger and breeding.
Grunts	Present to common in water depths less than 25 fathoms occur near smooth bottoms and near reefs.	100 to 1600	200	107 1 meter	Rasping, amplified by air bladders.
Toadfishes	Common, usually in shallow waters inhabiting sand and mud bottoms among weeds. Often seek shelter under rocks or debris.	50 to 800 140 to 3850	60; 240 to 300; 140 to 350	146 1 meter	Loud boat-whistle blast or honk preceeded by a grunt or growl. Maximum noise during spawning period which usually occur during December.
Damselfishes	Common throughout year in shallow waters of area; usually in rough bottom habitats; sometimes in schools.	50 to 1500	below 500	116 1 meter	Clicks, rasps, and drumming. Most sound produced during breeding.
Herringlike fishes	Common in most of area throughout year, with greatest abundance during March through September. Pelagic schools.	0 to 2000; 1200 to 5000	800; 2000 to 3500	10 to 15 dB above ambient sea noise	Veering noises; chirping sounds produced by sardines in area. Some species also produce weak internal squeaks and knocks.

TABLE 2.4.2-II. BIOACOUSTIC CHARACTERISTICS OF FISH (Continued)

Fish	Abundance Distribution Habitat	Frequency Range (Hz)	Peak Energy at (Hz)	Peak Pressure (dB re μPa)	Description of Sound
Mackerels, jacks, bonitos	Pelagic schooling fishes of similar size. First two types most common in area during March through September. Bonito present all year, with most abundance during April through June.	0 to 4000	below 1000	106 1 meter	Thumps, pops, crackles as the school turns; also produce weak internal rasps.
Tunas	Pelagic schools migrate through the area from west to east during April through June, from east to west during September through November.	400 to 5000	500 to 700 1500 to 2000	25 above average sea noise	Knocks produced as schools swim or turn.
Bluefishes	Found in large concentrations near the coast during January through June.	20 to 220	Under 180	Not available	Weak clicks, thumps, and knocks.
Groupers	Occur mostly among rock and coral bottoms near shore	0 to 400	Below 150	127 1 meter	Grunts, knocks, booms. Occasional single, 4-beat, and 6-beat, but usually 5-beat bursts of sound when disturbed. Each of the five "drum beats" consists of five sound pulses with rapidly dropping pitch.
Triggerfish	Sluggish fish of reef or rocky regions, sometimes living among weeds. Seasonal fluctuation is insignificant.	75 to 9600	700 to 1800 2400 to 4800 depending on species	126 1 meter	Metallic scratching; humming and drumming sounds.
Hake	Strong swimmers of all water levels from bottom to surface occuring from tide line to depths of 200 fathoms or more. Most abundant in shoal waters during July through September when spawning; general movement to deeper water in November and December	80 to 575	300	Not available	Single weak knock; hoots; raps.

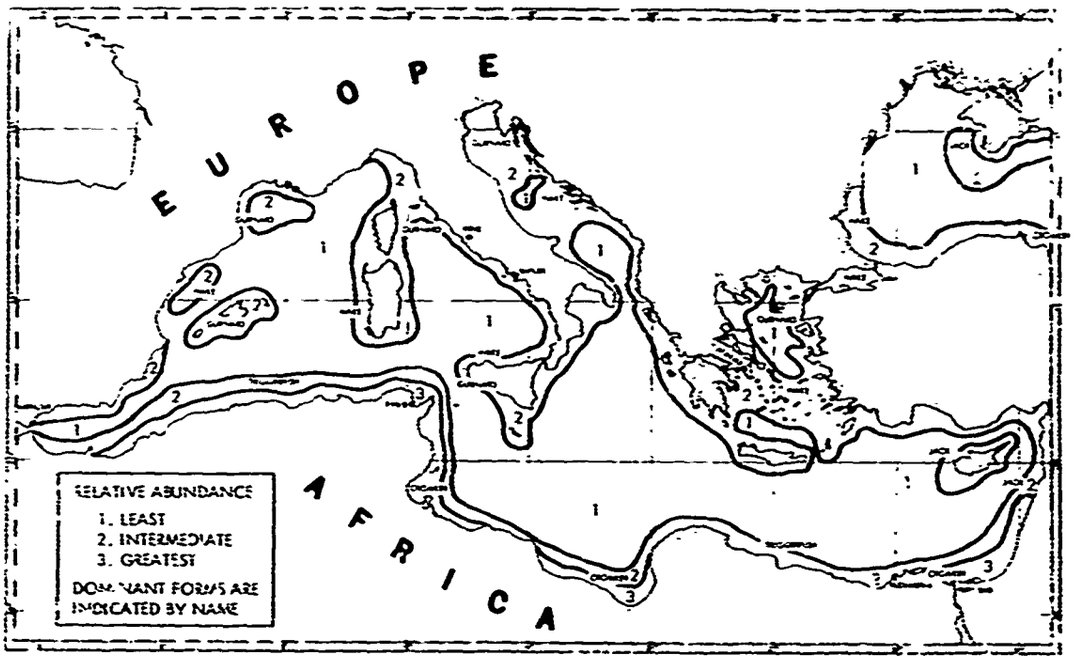

Figure 2.4.2-1. Distribution of Sound Producing Fish, Winter

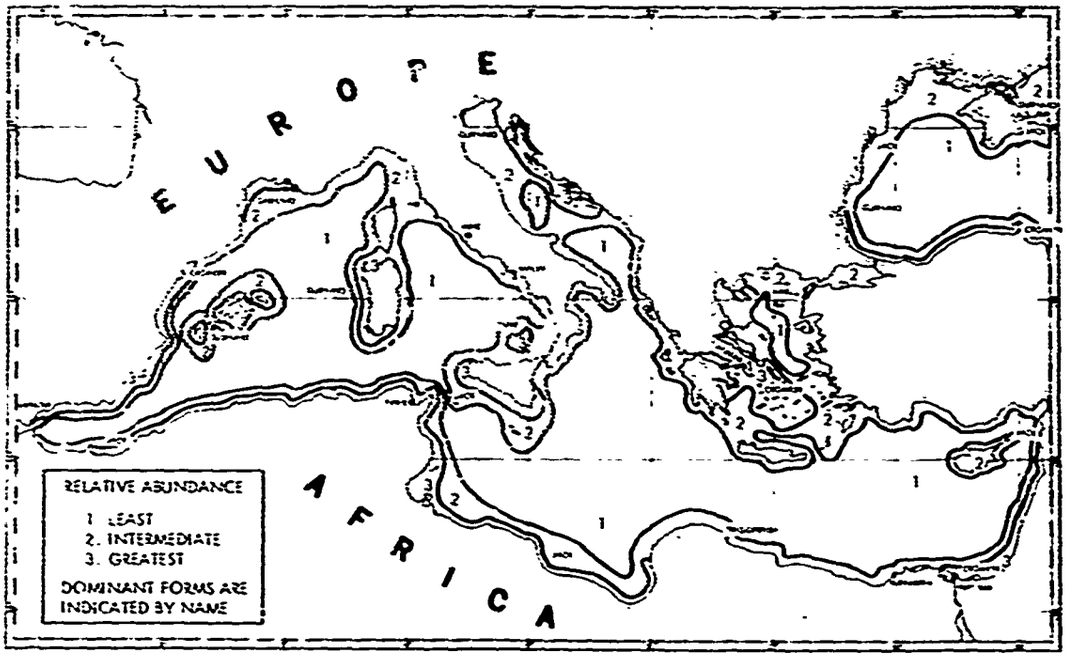

Figure 2.4.2-2. Distribution of Sound Producing Fish, Spring

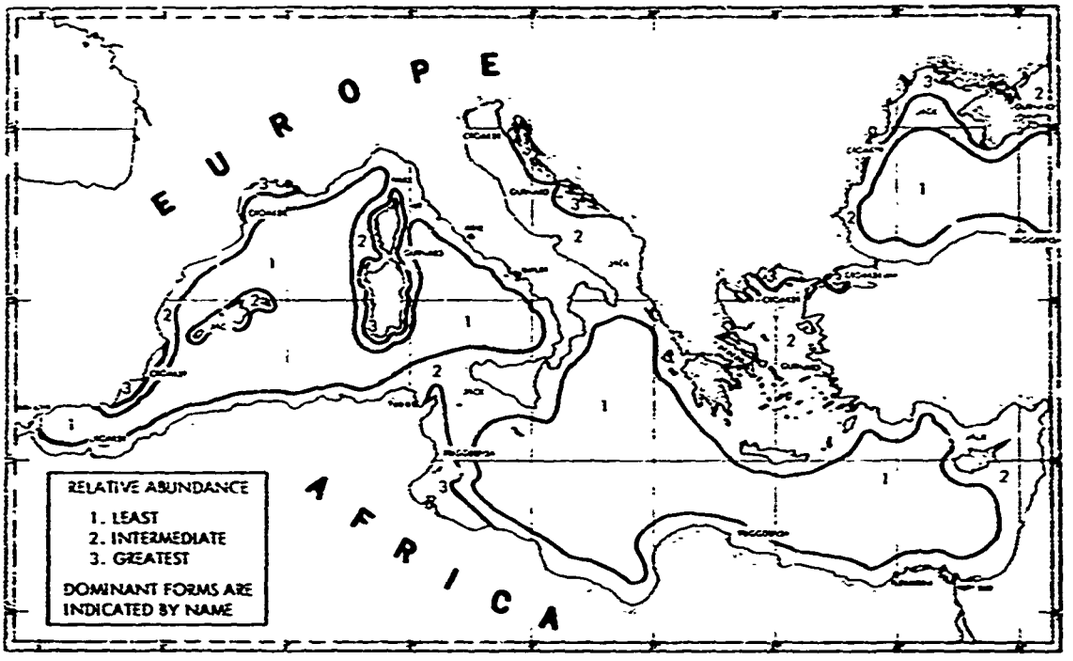

Figure 2.4.2-3. Distribution of Sound Producing Fish, Summer

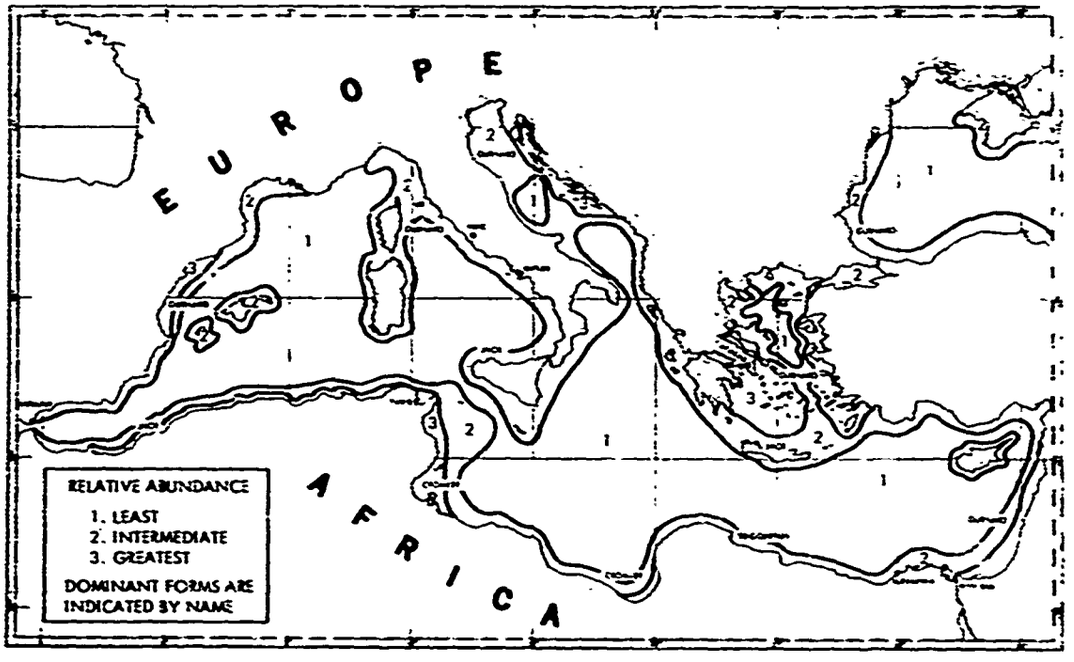

Figure 2.4.2-4. Distribution of Sound Producing Fish, Autumn

and 2.5 to 4.7 kHz. Spiny lobsters tend to increase their production of sound when gathered together in groups. Thus, the combined output of many lobsters may result in a significant increase in the overall ambient noise level in certain localities.

(U) The characteristics of snapping shrimp and spiny lobsters are presented in table 2.4.2-III. The characteristics of squids, which are also noise-producers, are also presented in this table.

(U) Figure 2.4.2-5 shows the distribution of snapping shrimp in the Mediterranean, based on literature records and limiting environmental factors. Published reports indicate that snapping shrimp are abundant off the coasts of Algeria, Italy, and Yugoslavia. Favorable habitats, characterized by rocky or coral bottom in depths between 5 and 30 fathoms, exist around most of the Mediterranean islands, along much of the North African coast, and off the western Black Sea coast.

(U) The spiny lobster also frequents rocky or coral bottoms, but its depth limit is greater than that of the snapping shrimp. Specimens have been taken from more than 100 fathoms in the Mediterranean, along the coasts of France and Yugoslavia, about the Greek islands, and along the rocky parts of the African coast.

2.4.3(U) Bioluminescence (U). Bioluminescence, usually referred to as phosphorescence by mariners, has been observed throughout most of the Mediterranean. Under the proper environmental conditions, microscopic and larger protozoans, crustaceans, and jellyfishes responsible for bioluminescence increase in abundance to such an extent that the light they emit gives the sea a luminous appearance. Bioluminescence may be weak and evident only at the tops of breaking waves, or it may be bright and long lasting, resulting in displays that are observable for great distances. The latter type of bioluminescence usually is seen in warmer waters and has been termed "sea fire" or "milky sea".

(U) The characteristics of a luminous display depend primarily on the kinds of organisms present, their size, and their relative abundance. Most colors of the visible spectrum have been seen in displays at one time or another, but yellow, white, or shades of blue are seen most frequently. Displays are classified according to three basic types:

- Sheet Type - a diffuse, shimmering light, often making the sea surface appear milky. This type of display usually is produced by masses of tiny, light-emitting organisms called dinoflagellates. Displays may cover large areas of the sea surface, at times causing a uniform glow from horizon to

TABLE 2.4.2-III (U)

BIOACOUSTIC CHARACTERISTICS OF INVERTEBRATES (U)

Invertebrates	Abundance Distribution Habitat	Frequency Range (Hz)	Peak Energy at (Hz)	Peak Pressure (dB re 1μPa)	Description of Sound
Snapping Shrimp	Present in the area where habitat conditons are favorable. Prefer coral or rocky bottom offering concealment. Usually at depths less than 30 fathoms.	Below 2000 to above 15,000	4000 to 8000	155 at one meter (single snap)	Continuous crackling noises over beds similar to frying fat. Shrimp crackles dominate water noise above 2000 Hz. Noise level slightly higher at night with peak just before sunrise and after sunset
Spiny Lobster	Common, widely distributed. Usually inhabit rough bottoms such as reefs to depths of 100 fathoms, but mainly in much shallower water.	40 to 12,000	600 (rattle) 800; 2500 to 4700 (rasp)	97 at one meter	Slow, low-pitched rattles, sharp rasp or creaking noise. Most sound production at night.
Squid	Occur in deeper offshore waters during the day and migrate to shallower near-shore waters at night.	0 to 4500	1000 to 2000	108 at one meter	Emit popping and squirting sounds as they swim.

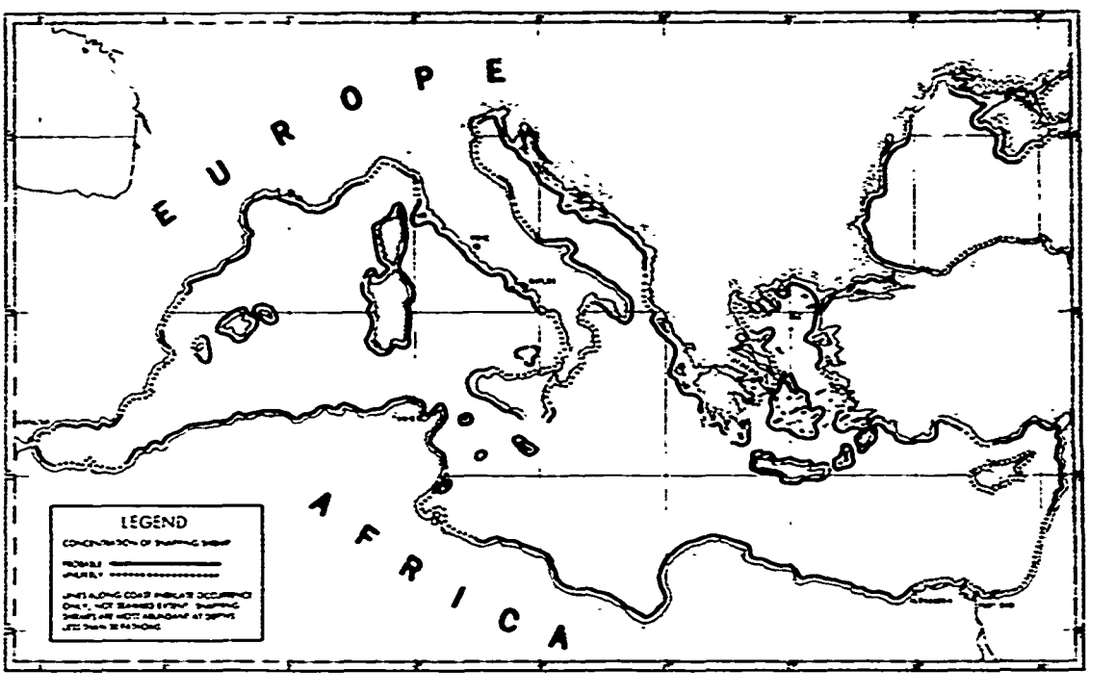

Figure 2.4.2-5. Distribution of Snapping Shrimp

horizon, or they may appear as irregular patches or wide ribbons of light in an otherwise dark sea.

- Spark Type - innumerable flickering pinpoints of light, particularly conspicuous in the wake of a ship, along the hull line, or in agitated waters. Crustaceans, such as copepods and euphausiids, cause this type of display. They luminesce in response to external stimuli, such as objects moving through the water or the action of the wind on the surface of the sea.

- Glowing-Ball Type - appearing as distinct and separate flashes or blobs of light of various diameters, commonly having a disc or globular shape, and originating either at or below the surface of the sea. The organisms responsible for this type of display include jellyfishes, ctenophores, and tunicates. Glowing-ball displays are more common in warm waters and are much more varied in appearance and color than the other types.

(U) Bioluminescent displays frequently consist of a combination of two basic types; occasionally, all three types may be seen at the same time.

(U) In addition to the three basic types of bioluminescence, certain other displays have been reported, such as expanding or contracting patches of light, wheels of light rotating on or just below the surface of the sea ("phosphorescent wheels") and large milky bubbles that seem to rise to the surface and burst. Innumerable variations of the above phenomena have been observed. The puzzling phenomenon of "phosphorescent wheels" has not been noted in this area.

(U) All marine organisms responsible for light displays are planktonic, i.e., they drift passively with the ocean currents. The abundance and distribution of these organisms in a specific region depend upon the various environmental factors that affect the organisms as they are carried into or through a region.

(U) Large concentrations of bioluminescent organisms (and thus bioluminescence displays) occur more frequently in coastal waters of the Mediterranean, including those of the various islands, than in the open sea. Marine organisms responsible for displays are abundant in the western Mediterranean and gradually become less abundant toward the eastern part of the sea. However, the north and central parts of the

Adriatic are exceptions, because they contain a much richer concentration of bioluminescent organisms than do other parts of the Mediterranean. Also bioluminescent forms are much more abundant in the Sea of Marmara, the Black Sea, and the Sea of Azov than in the Mediterranean, with the exception of the north and central Adriatic.

(U) Figures 2.4.3-1 through 2.4.3-4 present the seasonal distribution and abundance of luminescent organisms based upon recorded data and estimates. Organisms capable of producing bioluminescence are least abundant during winter (January through March). However, concentrations of jellyfishes and euphausiids in the Gulf of Corinth make this body of water the most likely site of glowing-ball and spark-type luminescence during this season.

(U) In spring (April through June) an increase in plankton increases the potential for sheet-type luminescence. High concentrations of jellyfishes are responsible for extensive areas of glowing-ball type luminescence off the western Italian coast and the Gulf of Corinth.

(U) Maximum bioluminescence potential exists during summer (July through September). Plankton organisms capable of spark-type luminescence probably are concentrated at depths of 30.5 to 182.9 meters (100 to 600 feet).

(U) During autumn (October through December) the summer abundance of bioluminescent organisms may continue somewhat throughout most of the area. However, the number of organisms and frequency of displays is expected to decrease as the season progresses.

(U) Submarine movement can be detected if bow waves and wakes become bioluminescent. The wake is particularly noticeable, appearing as a long luminescent streak or band in a dark sea. Periscope wakes and torpedo tracks also may appear luminescent. Figure 2.4.3-5 indicates bioluminescent wake lengths and initial brightest distances for different types of bioluminescence versus ship and ordnance speed. Submerged submarines have been visually observed to depths of over 80 meters (269 feet) when outlined by bioluminescence. Starlight scopes or electronic image intensifiers increase the depth of observation. Depths to which bioluminescence can be observed are listed in table 2.4.3-I. The values presented in figure 2.4.3-5 and table 2.4.3-I are based on theoretical computations.

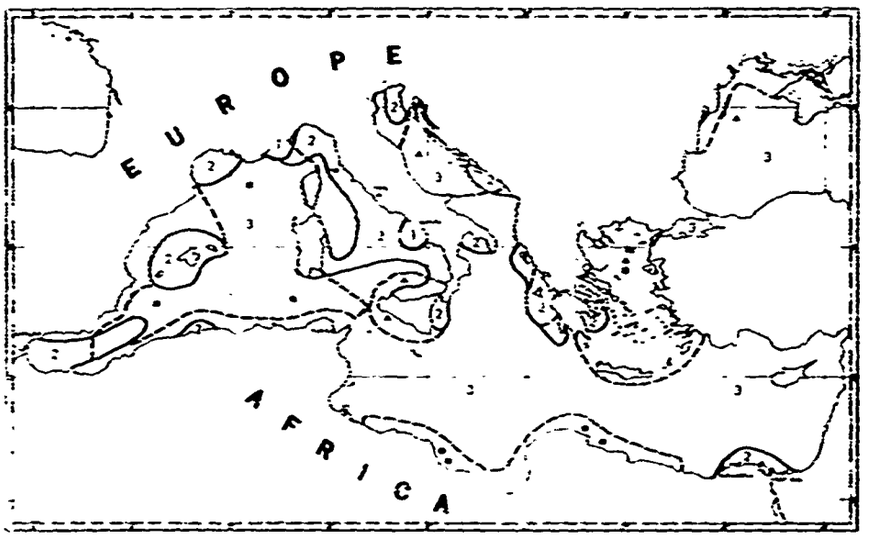

Figure 2.4.3-1. Distribution and Abundance of Bioluminescent Organisms, Winter (January-March)

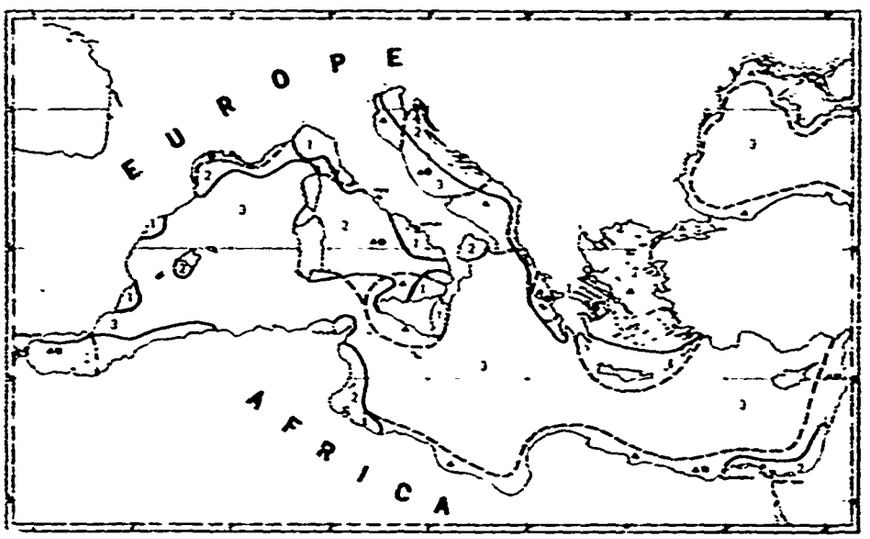

Figure 2.4.3-2. Distribution and Abundance of Bioluminescent Organisms, Spring (April-June)

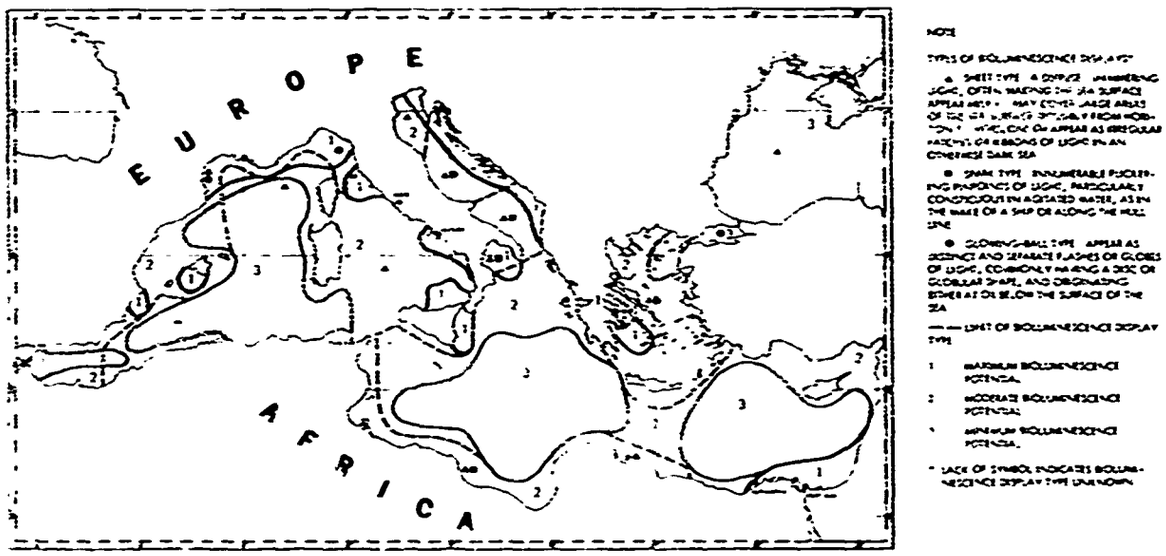

Figure 2.4.3-3. Distribution and Abundance of Bioluminescent Organisms, Summer (July-September)

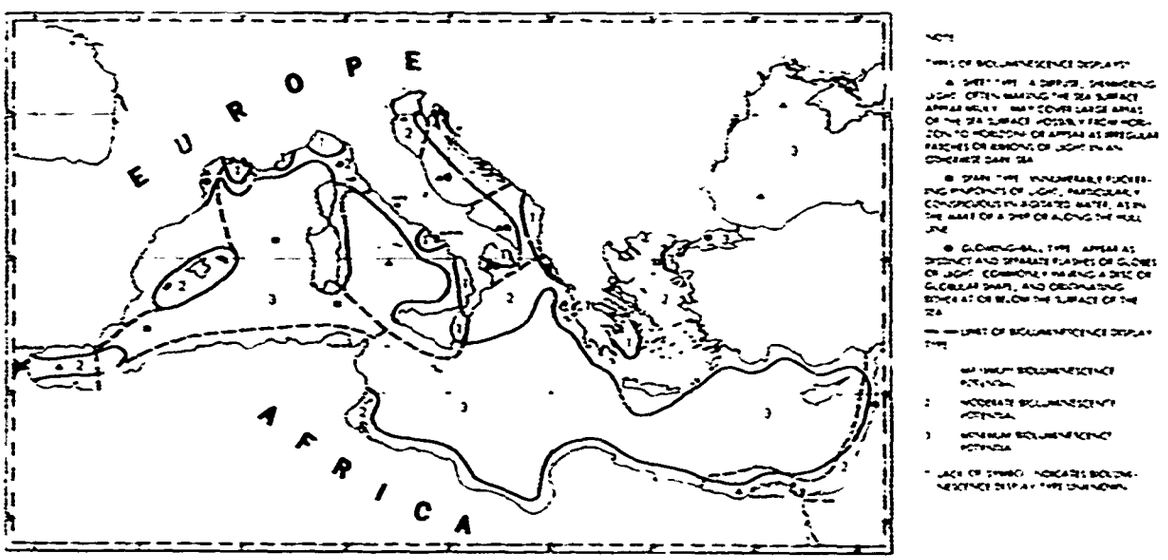

Figure 2.4.3-4. Distribution and Abundance of Bioluminescent Organisms, Autumn (October-December)

BIOLUMINESCENCE CHARACTERISTICS

(A) WAKE LUMINESCENCE USUALLY MILKY OR GREENISH WHITE CONTINUOUS GLOW WITHOUT ISOLATED SPOTS OR FLASHES OF LIGHT. OCCASIONAL LARGE PATCHES OF WHITE LUMINESCENCE. WATER OFTEN CALM IN ROUGH SEA. WATER MAY APPEAR OILY VISCOUS AND DISCOLORED USUALLY VARIOUS SHADES OF RED, YELLOW OR BROWN.

(B) WAKE LUMINESCENCE USUALLY GREEN OR BLUE. SMALL BRIGHT FLASHES (SCINTILLATION) WITHOUT LARGE SPOTS OR FLASHES OF LIGHT. WATER MAY BE DISCOLORED VARIOUS SHADES OF RED. INDIVIDUAL FLASHES MAY BE SURROUNDED BY CLOUDLIKE LUMINESCENCE.

(C) WAKE LUMINESCENCE USUALLY GREEN OR BLUE. NUMEROUS ISOLATED SPOTS OR FLASHES OF LIGHT. LIGHT MAY FLARE BRIGHTLY AND FADE OR PULSATE. LUMINESCENT SPOTS USUALLY OVAL OR ROUND. WATER OFTEN FILLED WITH GELATINOUS PLANKTON.

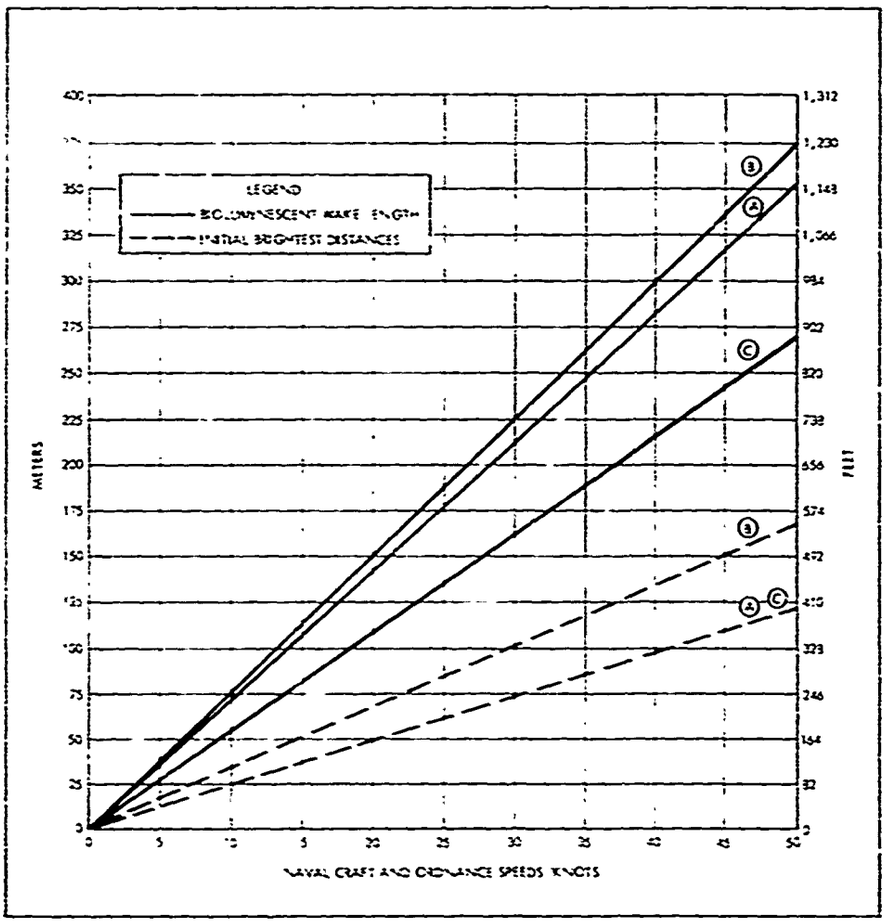

MAXIMAL LUMINESCENT WAKE AND INITIAL BRIGHTEST DISTANCES WERE BASED ON FLASH AND GLOW TIMES OF LUMINESCENT PLANKTON. LUMINESCENT WAKES HAVE BEEN REPORTED LONGER THAN THOSE ABOVE, ONE EXTENDED OVER 1,200 METERS 3,937 FEET. THE MAXIMAL LENGTH GIVEN WAS AN AVERAGE MAXIMUM

Figure 2.4.3-5(C). Bioluminescent Wake Lengths and Initial Brightest Distances (U)

TABLE 2.4.3-I(C). MAXIMUM DEPTH IN METERS (FEET) AT WHICH BIOLUMINESCENTLY ILLUMINATED SUBMARINE MAY BE DETECTED FROM OVERHEAD[a] (U)

	Coastal Water*		Oceanic Water**	
Light Conditions	Unaided Eye	Starlight Scope	Unaided Eye	Starlight Scope
Dark Day	2.3 (7.6)	2.8 (9.2)	5 (16.4)	5 (16.4)
Twilight	10.0 (32.8)	13.5 (44.2)	21 (68.9)	28 (91.9)
Deep Twilight	16.8 (54.7)	24.0 (72.2)	35 (114.8)	50 (164.0)
Full Moon	24.0 (78.7)	35.0 (114.8)	51 (167.3)	73 (239.5)
Quarter Moon	31.5 (103.2)	42.8 (140.4)	65 (213.3)	89 (292.0)
Starlight	36.0 (118.1)	49.8 (163.4)	75 (246.1)	103 (337.9)
Overcast Night	39.3 (129.0)	57.0 (187.0)	82 (269)	121 (397.0)

a Adapted from R.H. Brown, NRL Report 1065, June 2, 1970, Preliminary Analysis of the Detection of Objects by Bioluminescence, Table 3, p. 16

* Secchi disc visible to a depth of about 16 meters (53 feet)

** Secchi disc visible to a depth of about 34 meters (112 feet)

REFERENCES

1. Brunelli, G. 1937. Mammiferes marins (Premier Rapport) (Marine Mammals - First Report), Commission Internationale pour l'Exploration Scientifique de la Mer Mediterranee, Rapports et Proces-Verbaux des Reunions, Nouvelle Serie, Vol. 10, p. 225

2. California University, Division of War Research 1945. Underwater noise caused by snapping shrimp. Contract NObs 2074 (formerly OEMsr-30). [Washington]: U.S. Navy Bureau of Ships

3. Dullea, R.K. and Fisch, N.P. 1971. Volume-scattering measurements in the Mediterranean Sea (U). Navy Underwater Systems Center, Newport, R.I., TM No. TA11.014-71

4. Fish, M.P. 1954. The character and significance of sound production among fishes of the Western North Atlantic. Bulletin of the Bingham Oceanographic Collection, Vol. 14, art. 3

5. Jesperson, P. 1923. On the quantity of macroplankton in the Mediterranean Sea and the Atlantic. Report on the Danish Oceanographic Expeditions 1908-10 to the Mediterranean and adjacent seas. Vol. 3, Miscellaneous Papers, paper 3

6. Jorgenson, E. 1920. Mediterranean Ceratia. Report on the Danish Oceanographical Expeditions 1908-10 to the Mediterranean and adjacent seas. Vol. 2, Biology, paper J.1

7. Morozova-Vodianitskaia, N.V. 1957. Phytoplankton in the Black Sea and its quantitative growth. (Fitoplankton v Chernom more i ego kolichestvennce Razvite), Trudy Sevastopol'skoi Biologicheskoe Stantsii, Vol. 9, p. 3. (Translated by M. A. Slessers, U.S.H.O. Trans. 80, 1960)

8. Moulton, J.M. 1957. Sound production in the spiny lobster, panulirus argus (Latreille). Biological Bulletin, Vol. 113, No. 2, p. 286

9. Nadezhin, V.M. 1950. Conditions determining the density of population of some fish and dolphins in the Black Sea. (Usloviia kontsentratsii nekotorykh ryb i del'finov v Chernom more), Rybnoe Khoziaistvo, Vol. 26, No. 1, p. 31. (Translated by M. A. Slessers, U.S.H.O. Translated by M. A. Slessers, U.S.H.O. Trans. 29, 1958)

10. Norman, J.R. and Fraser, F.C. 1949. Field book of giant fishes. New York: Putnam

11. Priol, E. 1923. Remarques sur les especes de grondins les plus communes des cotes de France. (Remarks on the most common species of gurnards of the French coasts), Revue des Travaux de l'Office Scientifique et Technique des Peches maritimes, p. 23-30

12. Tarasov, N.I. 1943. Biology of the sea on the Navy (Biologiia moria i flot). Moscow: Naval Publishing House of the Peoples Commissariat of the USSR Navy. (Translated by F.R. Preveden, ONI Translation No. A-496, 1952)

13. Tarasov, N.I. 1956. Luminescence of the sea (Svecheniye morya). Moscow: Akademiya Nauk SSSR, Institut Okeanologii, Izdatel'stvo Akademii Nauk SSSR. (Translated by M. A. Slessers, U.S.H.O. Trans. 5 1957)

14. Tomilin, A.G. 1957. Mammals of the USSR and adjacent countries. (Zveri SSSR i prilezhashchikh stran), Vol. IX, Cetacea, Moscow. Translated from Russian by Israel Program for Scientific Translations, Jerusalem, 1967

15. Tuzet, O. 1947. Le plancton du Golfe du Lion et de l'etang de Thau. The plankton of the Gulf of Lion and the Inlet of Thau. Bulletin du Museum d'Histoire Naturelle de Marseille, Vol. 7, Nos. 2-3, p. 91-95

2.5(C) Shipping Density (U)

(U) Shipping in the Mediterranean is extremely heavy as compared to most other parts of the world, with the possible exception of certain coastlines. It is estimated that on any given day there are over 1000 ships of over 1,000 tons displacement underway. This count does not include large numbers of smaller commercial and recreational boats, which could be of significance in terms of noise production near the French and Italian coasts. This shipping is spread throughout the Mediterranean, but has its greatest concentration on the shipping lane from Gibraltar, along the Algerian coast, through the Strait of Sicily and on to the eastern Mediterranean. Historically, and perhaps in the future, the ship density on the shipping lane depends on whether or not the Suez Canal is open. The lane from Gibraltar to Suez is about 1800 miles long and is estimated to contain 330 ships with the canal open and about 150 ships with it closed. Of the order of 100 to 120 ships per day pass through the Strait of Gibraltar which, on an evenly spaced basis, is one every 12 to 15 minutes.

(U) As a result of all this traffic, the noise level in the Mediterranean is significantly higher at the low frequencies (1000 Hz and below) than almost anywhere else in the oceans. Furthermore, the bulk of the ship traffic is sufficiently local that, since most distances between ports are very short, it can change significantly over a very short period of time. Some general characteristics of shipping in the Mediterranean, including noise data, are given in table 2.5-I.

(C) TABLE 2.5-I (U)

GENERAL STATISTICS ON SHIPPING IN THE MEDITERRANEAN SEA (KELLER AND WEINSTEIN, 1971) (U)

Total Number of Ships in the Mediterranean, 1 June 1967	1070
Average Number of Transits through Gibraltar, (1963-1965)	157 ships/day
Average Ships Tonnage (Gibraltar)	5000 tons
Average Ships Length (Gibraltar)	500 ft.
Average Draft (Gibraltar)	28 ft.
Average Draft (Lloyd's Register)	16 ft.
Average Ship Speed (Gibraltar)	15 knots
Average Spectral Noise Level of a 15 knot Ship of 500 ft. Length at 80 Hz	157 dB//1μPa @ 1 yd
320 Hz	150 dB//1μPa @ 1 yd
1000 Hz	137 dB//1μPa @ 1 yd

(C) Although it is evident that shipping is more dense in the Mediterranean than in most other ocean areas, no reliable data on Mediterranean shipping density are available. A major effort was made in 1967 to obtain a complete picture of all ship positions in the Mediterranean on a single date, to coincide with a NATO worldwide analysis of shipping. While this effort was successful, the subsequent closing of the Suez Canal has caused modifications to the traffic patterns and shipping density in the Mediterranean.

(U) The estimated number of ships in each one-degree square, obtained from the 1967 effort, is shown in figure 2.5-1, adapted from Keller and Weinstein (1971). No data are presented in the figure for the Adriatic and Aegean basins. Other blank areas indicate absence of shipping at the time of the observation.

(C) No comparable effort has been made since the closing of the Suez Canal. Keller and Weinstein (1971) have estimated the shipping density for a day in June 1968, to reflect the change created by the blocking of Suez. Data regarding the number of ships transiting the Suez Canal were applied to the 1967 observations to arrive at this 1968 estimate. The estimated density with the canal blocked is shown in figure 2.5-2.

(U) The shipping data presently used in the Fleet ASW prediction models (with the Suez Canal closed) are based on the NATO study, as well as on data from the World Meteorological Organization (WMO) and from Automated Marine International (AMI). These data are presented in figures 2.5-3 through 2.5-8 by the month (Wolff, 1974). The figures show, for a particular month, the average number of ships that would be expected in each one-degree square, if a series of "snapshots" of the Mediterranean were taken during the month in question. Note the increase in the average shipping density over the 1967 data. This is reflected in an increase in measured ambient noise during this period (cf section 3.3.2).

(U) Except for the track, described earlier, from Gibraltar to the eastern Mediterranean, shipping in the Mediterranean does not follow well-defined, narrow lanes (Solomon, 1974). In the western part, between Gibraltar and Sicily, traffic flows both in the north-south and east-west directions, and the shipping distribution outside the southern track is relatively random. East of Sicily, the east-west traffic follows two broad and poorly-defined tracks. These are a northern route, leading toward the Aegean and Turkey, and a southern route, leading toward Alexandria and the Levantine coast.

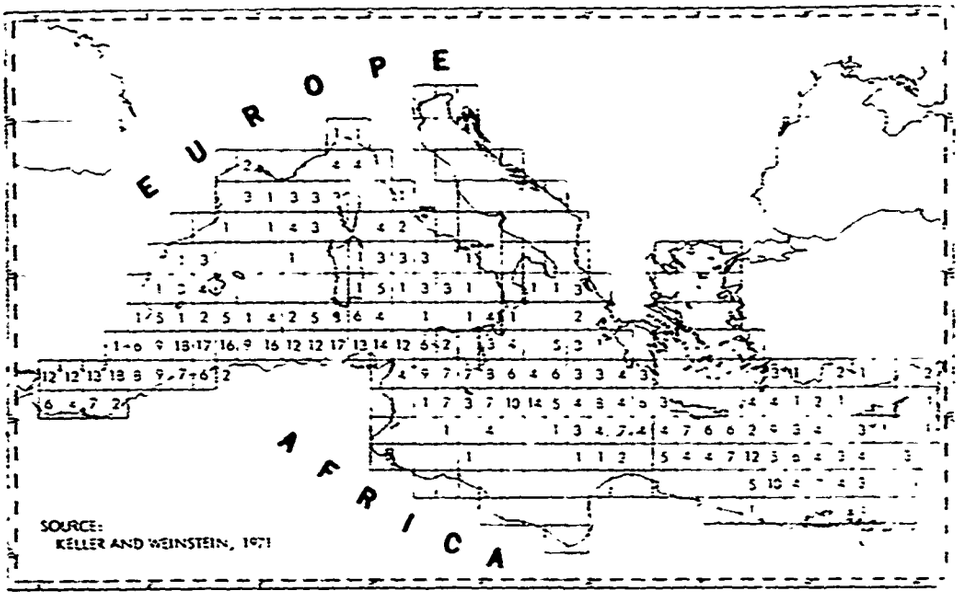

Figure 2.5-1(C). Shipping Density, June 1967, OEG Estimate (Before Closing of Suez Canal) (U)

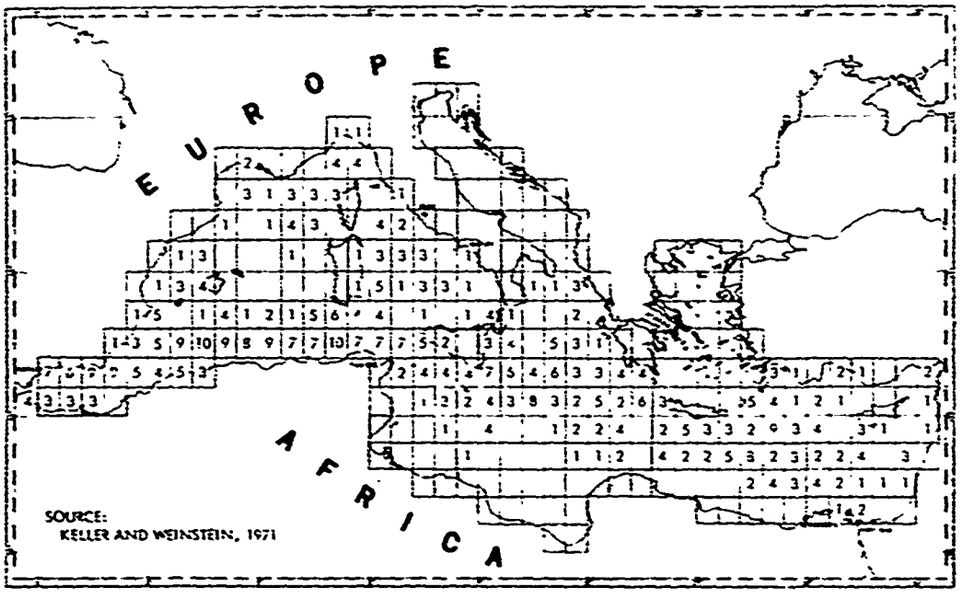

Figure 2.5-2(C). Best Estimate of Shipping Density for a Day in June 1968 (Suez Closed) (U)

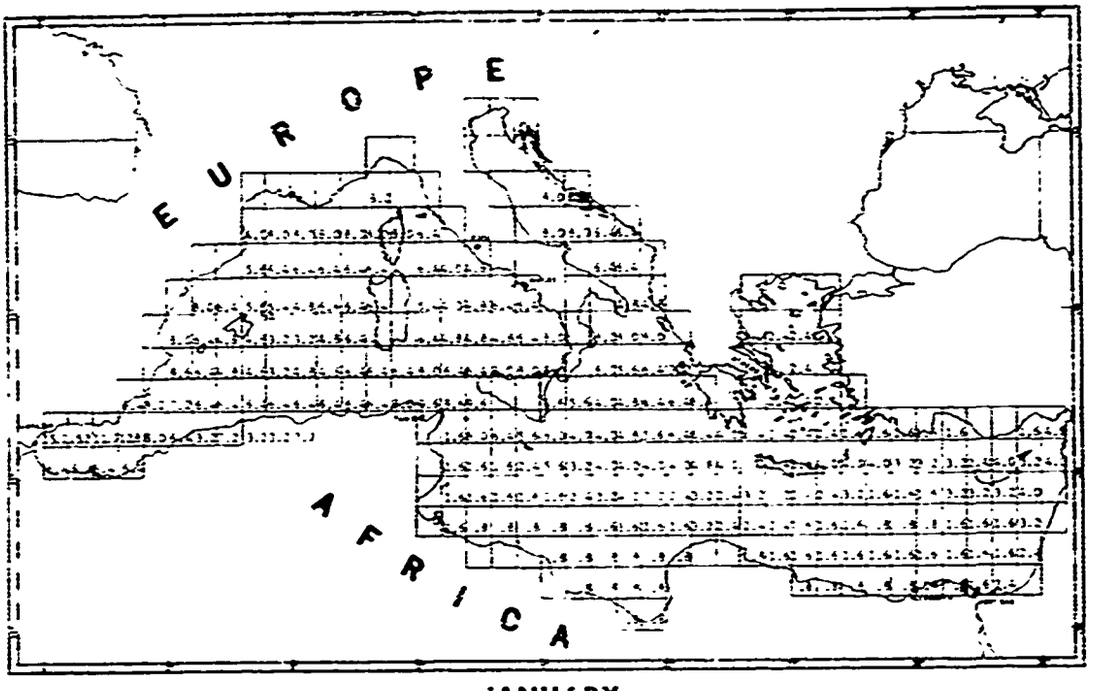

JANUARY

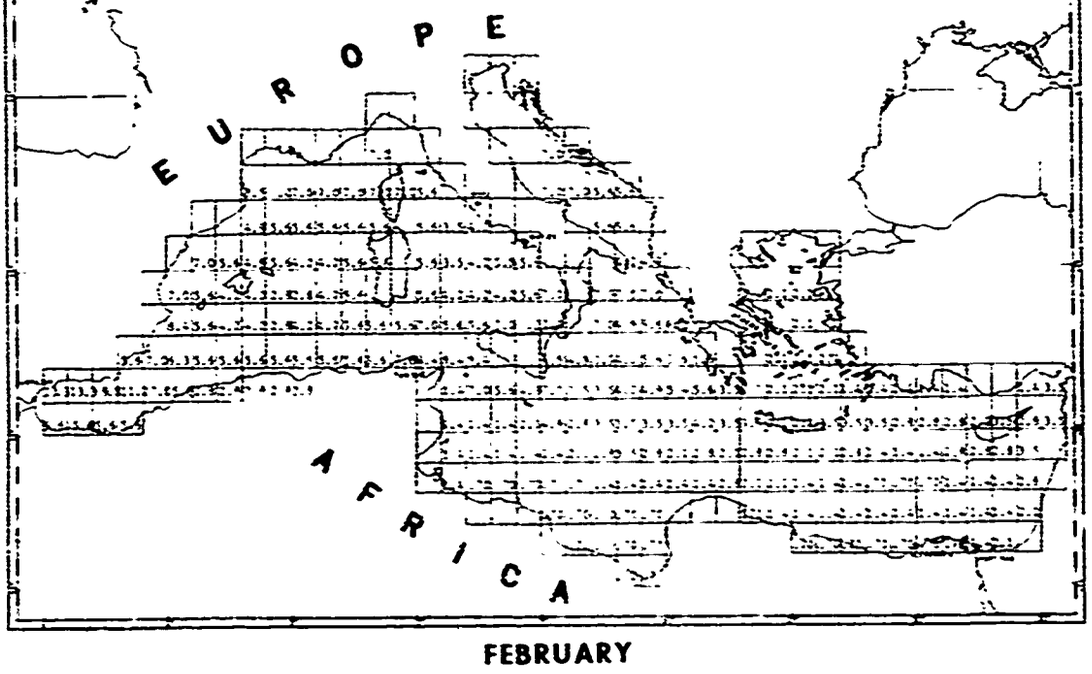

FEBRUARY

Figure 2.5-3. Average Shipping Density, January and February (Canal Closed)

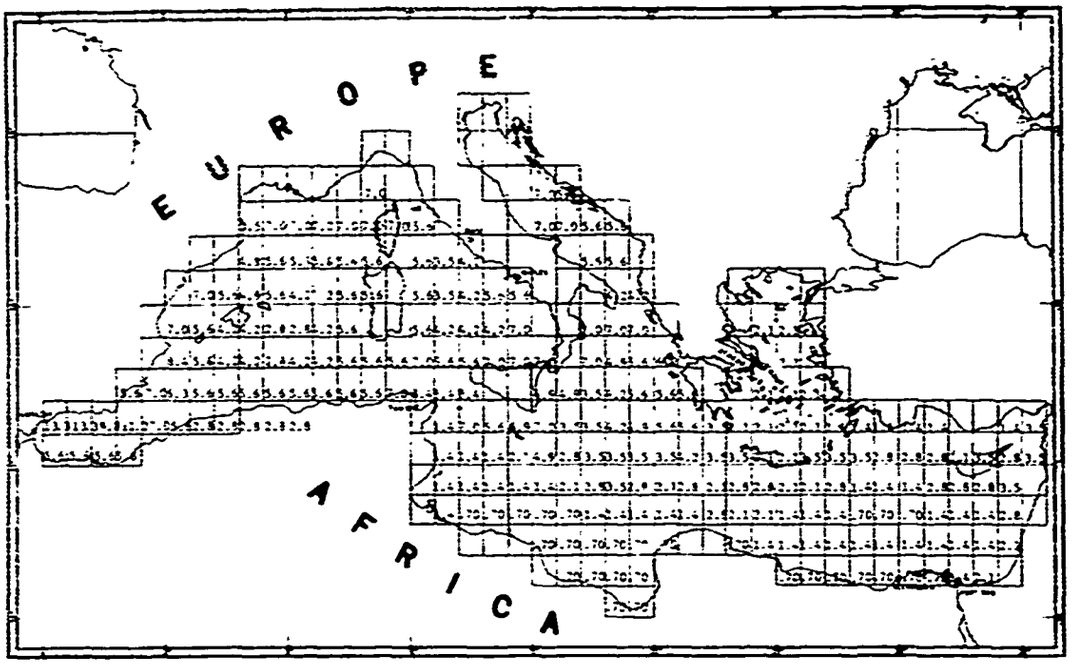

MARCH

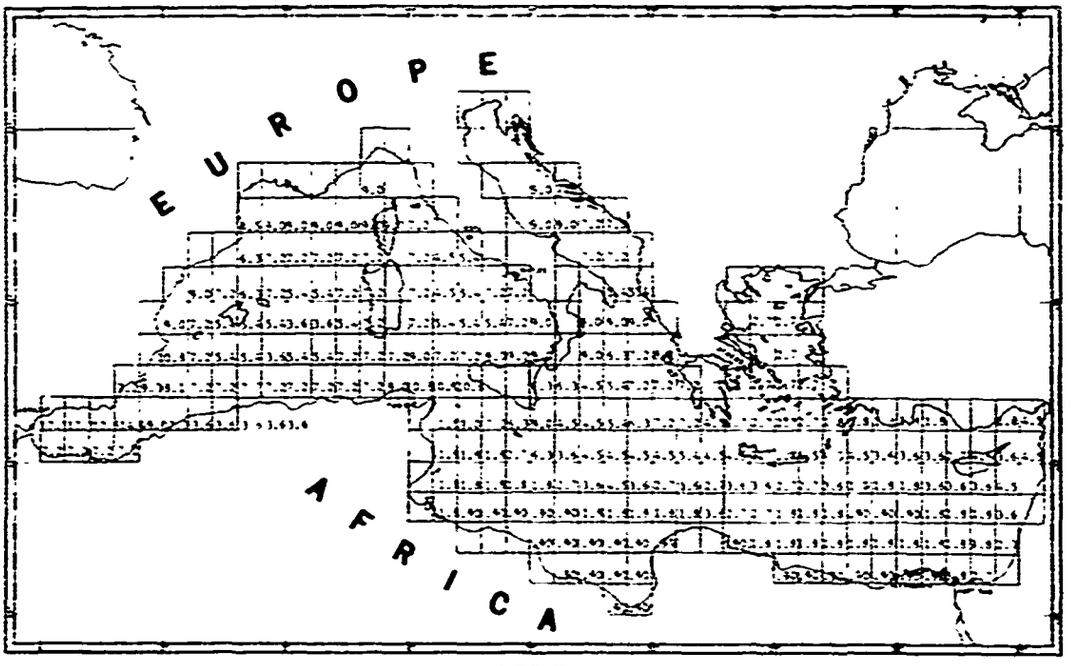

APRIL

Figure 2.5-4. Average Shipping Density, March and April (Canal Closed)

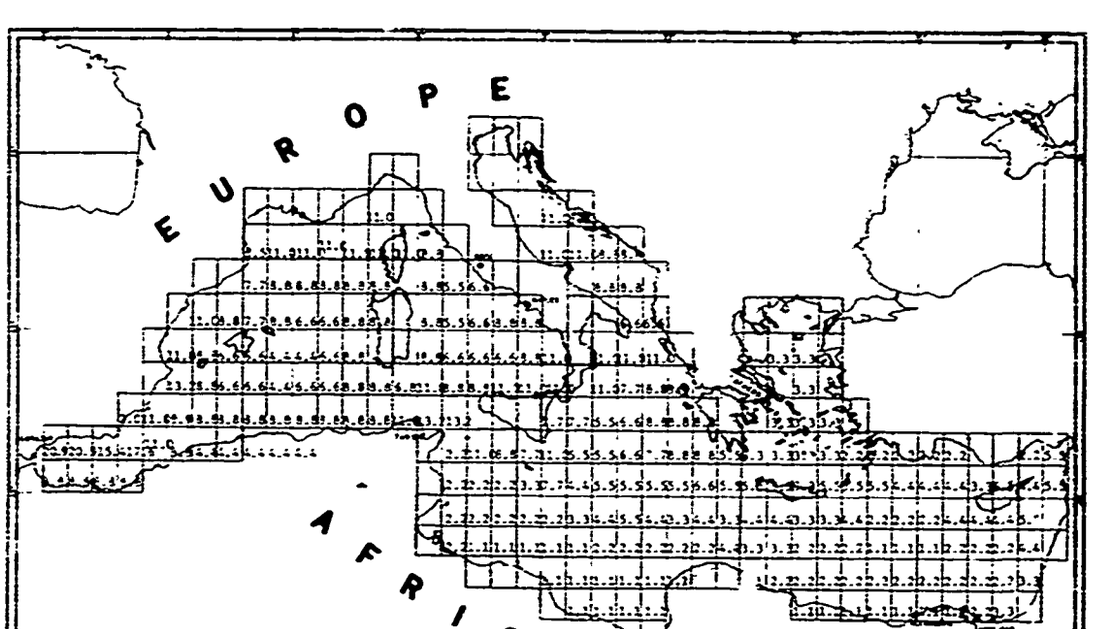

MAY

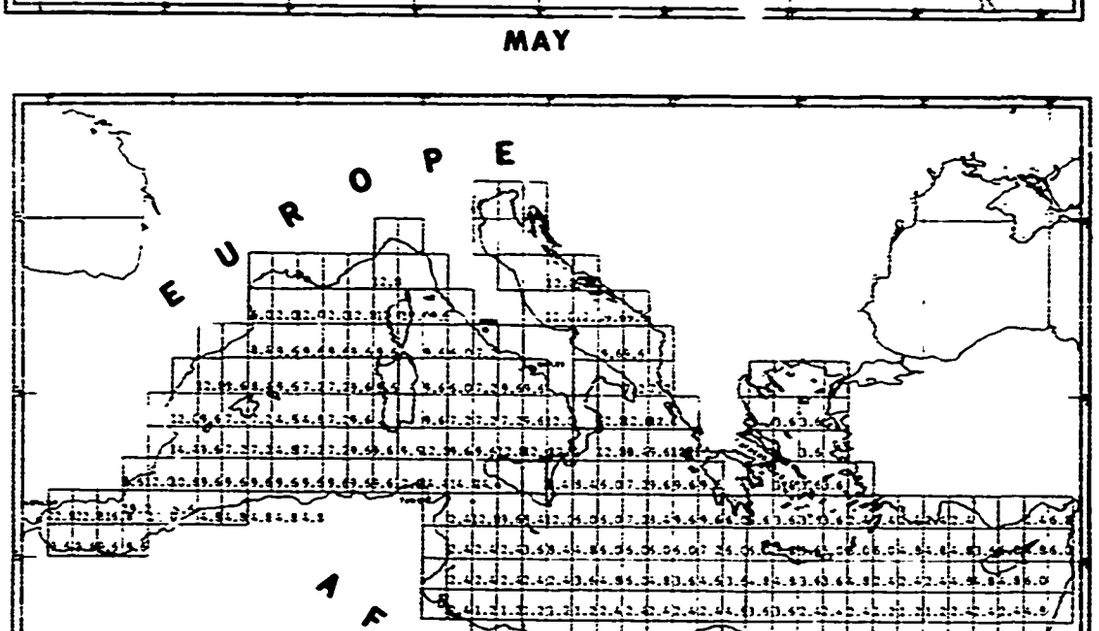

JUNE

Figure 2.5-5. Average Shipping Density, May and June (Canal Closed)

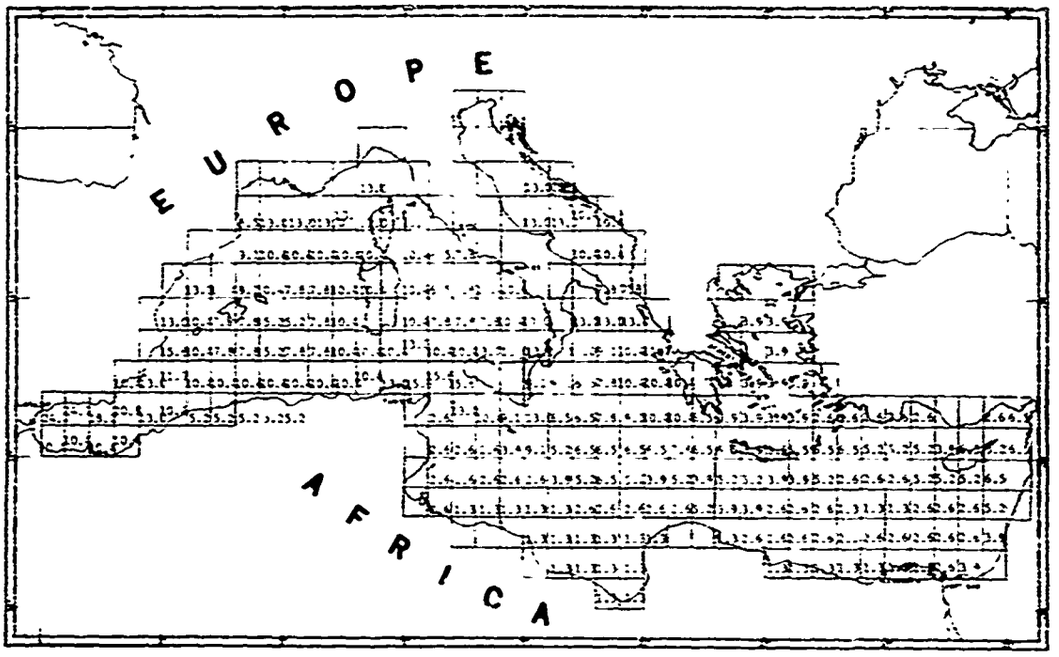

JULY

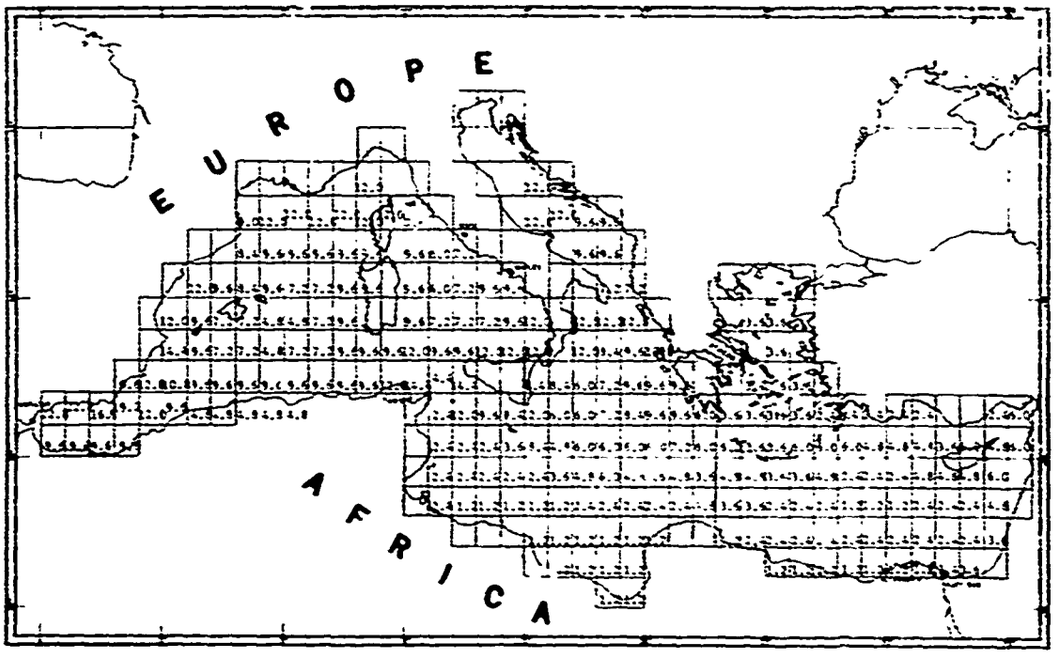

AUGUST

Figure 2.5-6. Average Shipping Density, July and August (Canal Closed)

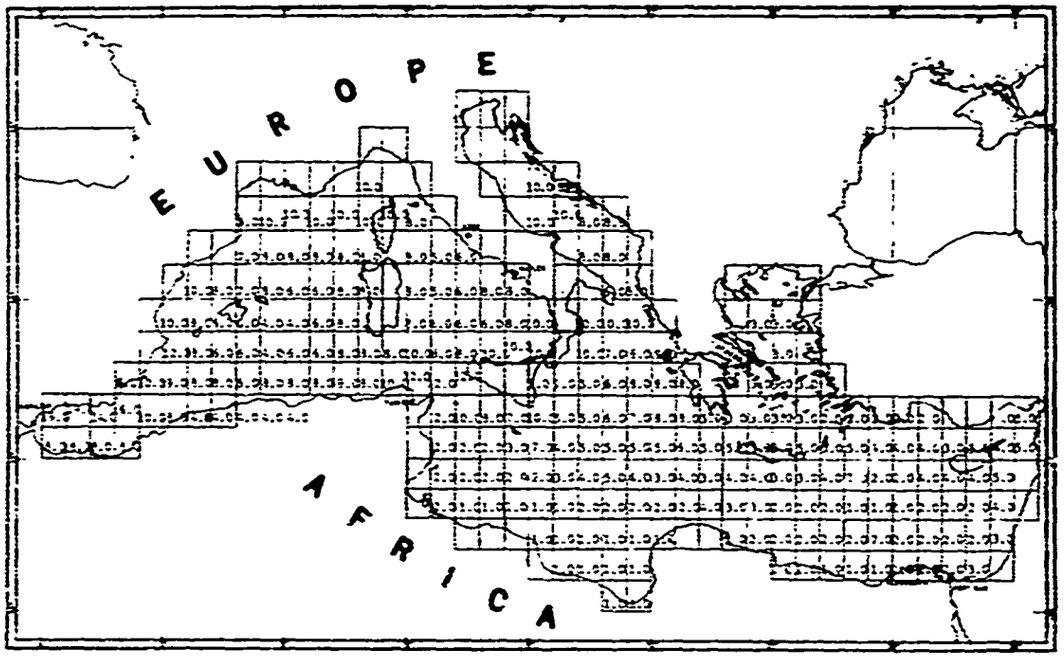

SEPTEMBER

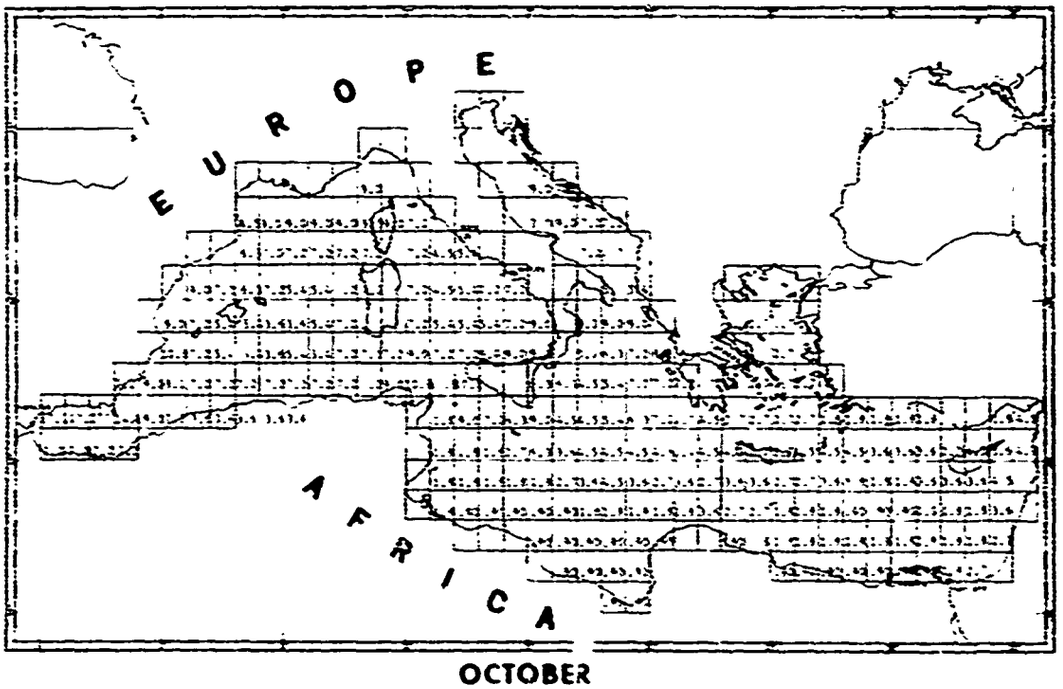

OCTOBER

Figure 2.5-7. Average Shipping Density, September and October (Canal Closed)

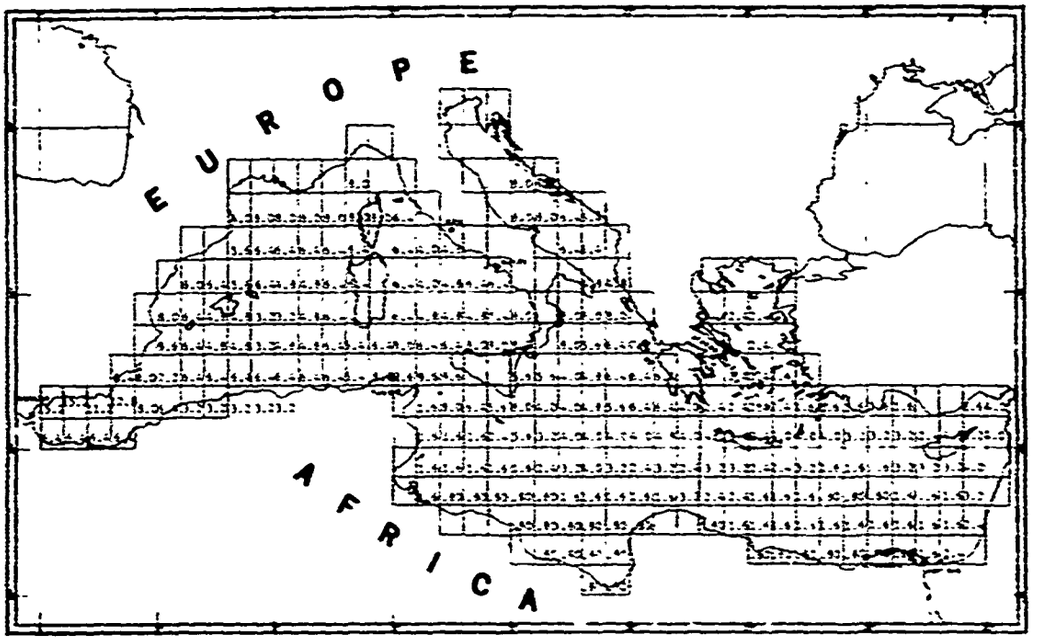

NOVEMBER

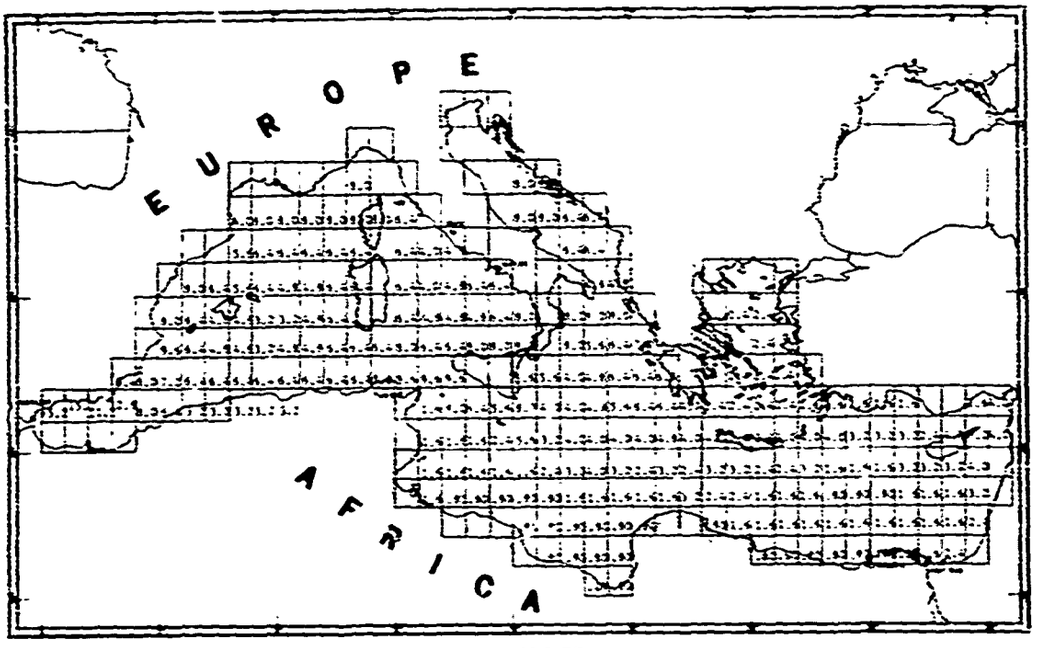

DECEMBER

Figure 2.5-8. Average Shipping Density, November and December (Canal Closed)

REFERENCES

1. Keller, E.A. and Weinstein, M.S. 1971. Prime factors affecting ASW surveillance in the Mediterranean (U). Raff Associates, Inc., Report No. 71-5, SECRET

2. Solomon, L. 1974. Private communication. Planning Systems, Inc.

3. Wolff, P. 1974. Ocean Data Systems, Inc., unpublished data

3.0(C) MEDITERRANEAN SEA ACOUSTICS (U)

(U) This section describes the acoustic characteristics of the Mediterranean. The influence of the environmental factors of section 2.0 upon the acoustics is discussed where applicable. The major topics addressed in this section consist of the following:

- Sound velocity structure (3.1)
- Sound transmission (3.2)
- Ambient noise (3.3)

For ready reference, the terms used in the discussion are defined in table 3.0-I and figure 3.0-1.

3.1(C) Sound Velocity Structure (U)

(U) In the following sub-sections, the generalized sound velocity structure of the Mediterranean Sea is described in terms of representative sound velocity profiles for Mediterranean ASW prediction areas; sound velocity cross-sections; average a real contours of the depth of the deep sound channel (DSC) axis, the axial velocity and critical depth; regions of depth excess and depth difference; and average a real contours of sonic layer depth (SLD). These quantities are defined in table 3.1-I. Because of a delay in seeing effects of the weather on the velocity structure in December and June, the four standard seasons of winter (January through March), spring (April through June), summer (July through September) and autumn (October through December) were used in these analyses as contrasted to the definition of seasons in section 2. However, due to the high variability during the transition seasons (spring and autumn) most of these analyses are depicted only for the two extreme seasons of winter and summer. The data base used in all analyses was the Acoustic Environmental Support Detachment (AESD) data bank, which includes Nansen cast, salinity-temperature-depth (STD) and sound velocity/salinity-temperature-depth (SV/STD) data processed by the National Oceanographic Data Center (NODC) as of September, 1972. These data were supplemented by additional data of several types that are listed in the LRAPP Mediterranean Data Catalog (Tracor, 1974).

(C) All sound velocities used in the above analyses are based on the equation of Wilson (1960), although it is not the most accurate equation for Mediterranean Sea sound velocity calculations. According to Anderson (1971), sound velocities derived from Wilson's equation are consistently higher than measured sound velocities in the Mediterranean Sea, particularly at depths greater than 1000 m. In this same paper, Anderson has developed a second-degree polynomial equation that more accurately represents measured sound velocities in the Mediterranean (referred to as the NUC equation in following discussions). Table 3.1-I compares values calculated using the Wilson and NUC equations in the four major Mediterranean basins.

TABLE 3.0-I (U)

GLOSSARY (U)

Sound velocity profile - The variation of sound velocity with depth.

Surface layer - This is the layer of water just below the sea surface in which the velocity of sound is susceptible to changes produced by heating, cooling and wave action (wind). It may contain a layer of isothermal water that is formed by convection and wind action. In this case, there is a positive sound velocity gradient due to pressure. Under prolonged calm and sunny conditions, this mixed layer disappears and is replaced with water in which the temperature decreases with depth. In this case, the sound velocity gradient is negative.

Seasonal thermocline - This is the layer of water beneath the surface layer in which the temperature, and hence the sound velocity, decreases with depth but varies with the seasons.

Main thermocline - This is the layer of water beneath the seasonal thermocline in which the temperature, and hence the sound velocity, decreases with depth but is affected only slightly by seasonal changes.

Deep isothermal layer - This is the layer of water beneath the main thermocline and extending to the bottom which has a nearly constant temperature (13°C) and in which the velocity of sound increases with depth due to the pressure effect. In winter in certain regions, the isothermal layer can extend all the way to the surface.

Sound channel axis - Between the negative velocity gradient of the main thermocline and the positive gradient of the deep isothermal layer, a velocity minimum exists. Sound traveling above or below this velocity minimum tends to be bent toward it by refraction, so that it becomes trapped in a channel, called the deep sound channel, and the location of the velocity minimum is called the axis of the sound channel.

Critical depth - This is the depth at which the sound velocity in the deep isothermal layer (deep positive gradient) becomes equal to the near surface sound velocity.

Depth excess - Depth excess is the difference between the bottom depth and critical depth when the bottom is deeper than the critical depth.

Depth difference - Depth difference is the difference between critical depth and bottom depth when the bottom is shoaler than critical depth.

Surface layer depth - This is the depth of the surface layer (depth to the seasonal thermocline) and exists only when the sound velocity gradient is positive in the surface layer.

Surface duct - For a positive gradient in the surface layer, sound traveling in the layer is bent upwards toward the surface velocity minimum and tends to become trapped in the surface layer, thus forming a duct or channel.

Convergence zone - For a source in the surface layer and a velocity structure as shown in figure 3.0-1, the ray, labeled (1) and called the split ray, is partially trapped in the surface duct and partially refracted by the deep positive gradient back to the surface. This ray becomes horizontal at the critical depth and is called the limiting ray. Rays with slightly steeper depression angles are also refracted back to the surface and intercept it at closer ranges. As the depression angle increases further, the corresponding rays intercept the surface at increasing ranges, thus resweeping the area insonified by the rays with smaller depression angles. This phenomenon of focusing is called a convergence zone. For some depression angle, a ray will become grazing to the bottom. A full convergence zone is formed only when the bottom is deep enough for the bottom grazing ray to intercept the surface at or beyond the split ray, 1.

Caustic - When representing sound propagation in terms of rays, a surface that defines the envelope formed by the intersections of adjacent rays is called a caustic. At a caustic, a focusing of the rays occurs, bringing together all the rays emitted within some solid angle from the source, and creating an abnormally high intensity. Ray theory is inadequate for calculating the intensity at a caustic, because ray theory predicts an infinite energy density when the cross-section of a ray bundle becomes zero. A convergence zone is a caustic that occurs at or near the surface.

RSR - This is a propagation path involving refraction at depth and a surface reflection.

RR - This is a propagation path formed by pure refraction, with no surface or bottom interaction.

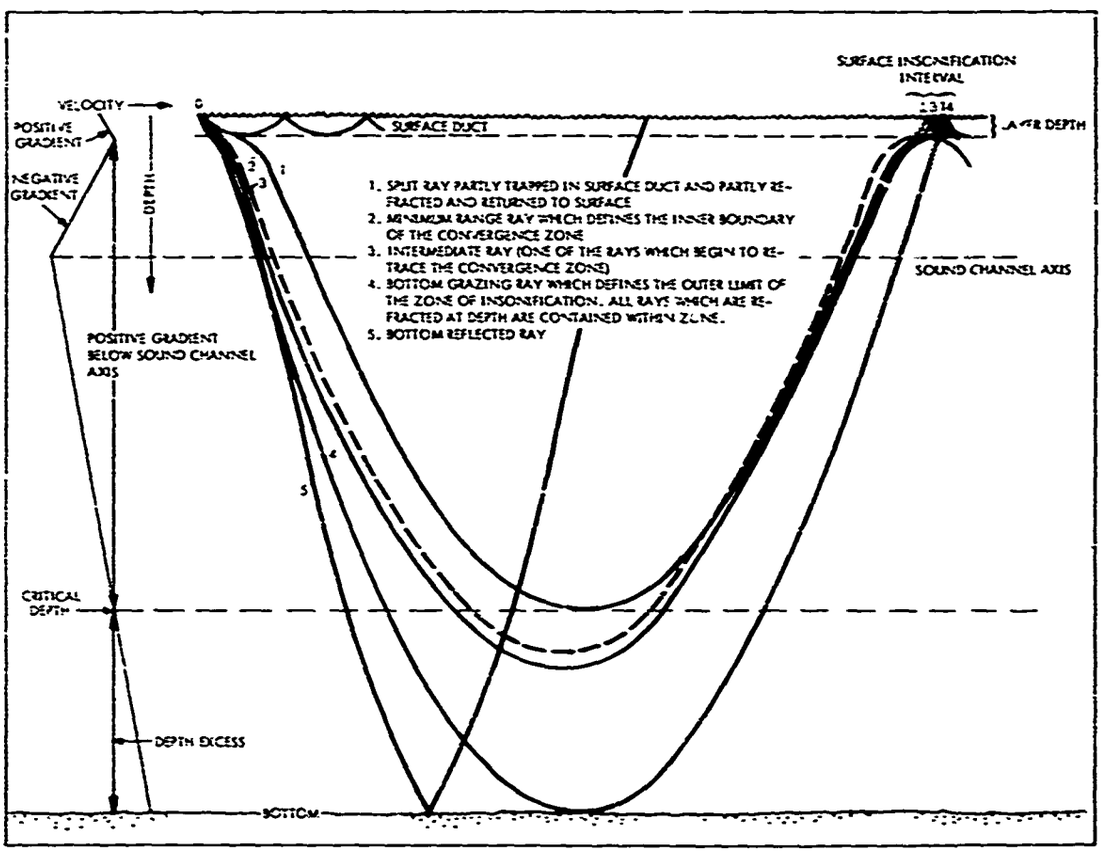

Figure 3.0-1. Sound Transmission Modes

TABLE 3.1-I (C)

COMPARISON OF WILSON AND NUC SOUND VELOCITIES
FOR MAJOR MEDITERRANEAN BASINS (U)

ALGERIAN BASIN

Depth (m)	Wilson	NUC	Difference (m/sec)
1000	1521.5	1520.6	0.9
1500	1529.9	1528.8	1.1
2000	1538.5	1537.2	1.3
2500	1547.1	1545.8	1.3

TYRRHENIAN BASIN

Depth (m)	Wilson	NUC	Difference (m/sec)
1000	1523.1	1521.9	1.2
1500	1530.8	1529.6	1.2
2000	1539.0	1537.7	1.3
2500	1547.5	1546.0	1.5

IONIAN BASIN

Depth (m)	Wilson	NUC	Difference (m/sec)
1000	1524.3	1523.4	0.9
1500	1532.5	1531.4	1.1
2000	1540.9	1539.6	1.3
2500	1549.4	1547.9	1.5
3000	1558.1	1556.3	1.8
4000	1575.7	1573.6	2.1

LEVANTINE BASIN

Depth (m)	Wilson	NUC	Difference (m/sec)
1000	1524.2	1523.1	1.1
1500	1532.4	1531.3	1.1
2000	1540.9	1539.6	1.3
2500	1549.6	1548.1	1.5
3000	1558.3	1556.7	1.6
4000	1576.1	1574.4	1.7

NOTES:

- Sound velocities in m/sec
- Wilson values from AESD 5° square averages
- NUC values taken from Anderson (1971)

(C) Despite the inadequacies of Wilson's equation, this equation is the basis for all of the sound velocity profiles contained in the AESD data bank, and was therefore retained. Supplemental measured sound velocity data (such as that from exercises and programs like MGS, IMP, IOMED, TASSRAP and DECKPLATE) were used only to a maximum depth of 500 m. Beyond 500 m depth, temporal and spatial sound velocity variability generally masks differences between calculated and measured sound velocities. One of the principal problems in using the Wilson rather than the NUC equation occurs in the calculation of critical depths. Critical depths based on deep sound velocity gradients calculated from Wilson's equation can be up to 100 m shoaler than those based on the NUC equation or measured gradients. This maximum error generally falls within the standard deviation of average critical depths for both winter and summer (see section 3.1.4). However, since Wilson's equation gives erroneous deep sound velocity gradients, use of this equation might lead to significant errors in acoustic propagation loss calculations.

(U) As previously discussed in section 2.3.1, two major water masses are circulated throughout the Mediterranean Sea; Atlantic Water in the near-surface layers and LIW at depths between about 200 and 1000 m. The characteristics of these two circulation patterns lead to much higher temperatures and salinities in the eastern Mediterranean Sea. Figure 3.1.1 shows the spatial variability of sound velocity between major Mediterranean basins during the extreme seasons of summer and winter, based on selected sound velocity profiles presented in section 2.2.1. The higher sound velocities during both seasons in the Ionian Sea, Levantine Basin, and Sea of Crete are a direct result of higher temperatures and salinities found east of the Strait of Sicily. The three distinct deep sound velocity gradients shown in figure 3.1-1 in the western Mediterranean, eastern Mediterranean, and Sea of Crete correspond to the discrete bottom water masses encountered in these same regions (see figure 2.2.1-1). In addition, the deep sound velocity gradient in the Tyrrhenian Sea is distinct from that in the Algerian Basin due to the somewhat higher temperatures and salinities encountered in the Tyrrhenian Basin.

(U) Atlantic Water does not markedly affect sound velocity structures in most of the Mediterranean, since it is imbedded in the seasonal thermocline during summer, and is markedly modified by surface cooling during winter. However, in the region just east of the Strait of Gibraltar, Atlantic Water is responsible for the formation of a deep sound channel (DSC) during winter. This feature generally is not found in the western Mediterranean Sea during winter due to extreme surface cooling effects (see further discussion in sections 3.1.2 and 3.1.3). In addition, Atlantic Water can cause the formation of secondary sound channels above the DSC axis, particularly in the western Mediterranean and in regions of strong Atlantic Water flow.

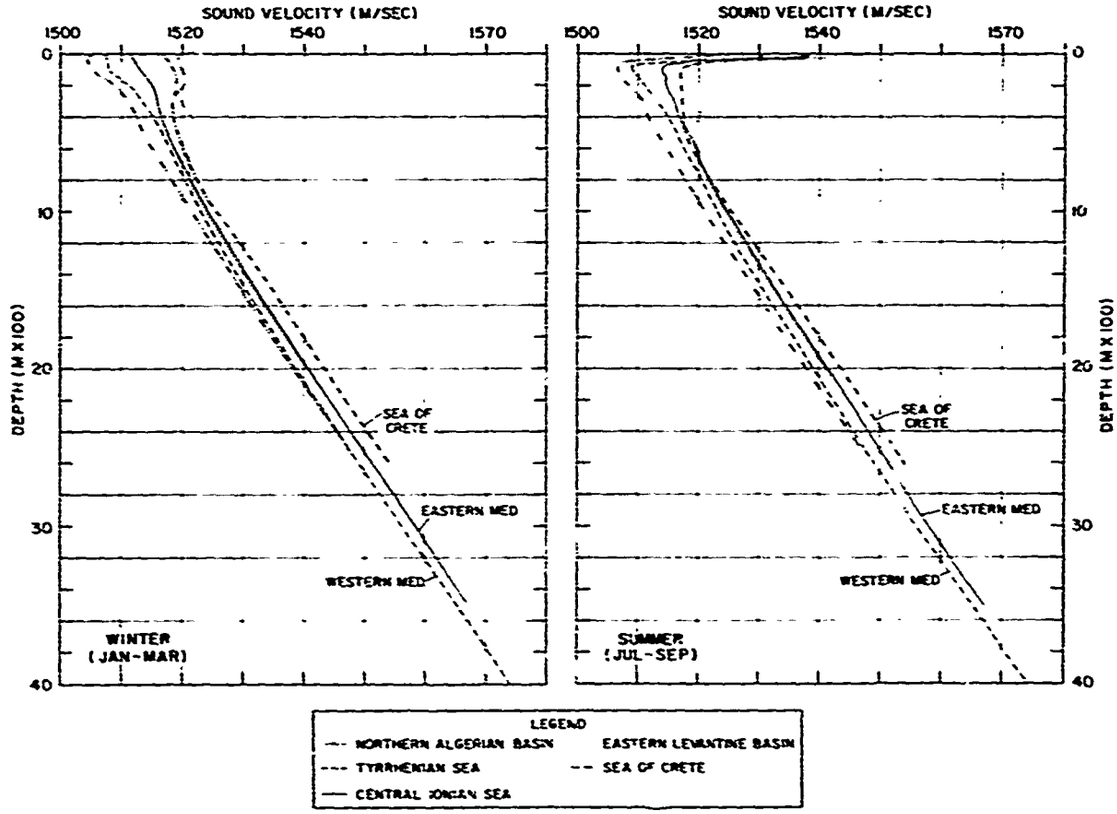

Figure 3.1-1. Spatial Variability of Sound Velocity During Winter and Summer

(U) LIW has a somewhat greater effect on sound velocity structures, particularly in the Levantine Basin and Sea of Crete (see figures 2.2.1-12, -13, and -14). In these regions the DSC axis, when present, occurs either at or immediately below the depth of the LIW high-salinity core. In these cases, high-salinity LIW can induce the formation of secondary sound channels above the depth of the DSC axis (see figure 2.2.1-14). Throughout the remainder of the Mediterranean, LIW can cause the DSC axis. However, throughout the western Mediterranean and the northern parts of the eastern Mediterranean Sea, the depth of the DSC axis generally corresponds to the maximum depth of summer warming and is independent of LIW effects.

3.1.1(C) Sound Velocity Profiles for ASW Prediction Areas (U). Figure 1.0-1 shows the location of Mediterranean ASW prediction areas and is directly based on NAVOCEANO Chart NA8 p. 2401. This chart depicts various physiographic areas and assigns to them bottom loss categories, mean depths and mean deeps. However, the ASW prediction areas outlined in figure 1.0-1 are not based on any sound velocity analyses, but rather only on generalized patterns of sea surface temperature. Figure 3.1.1-1 shows the locations of regions with distinct representative sound velocity profiles. The boundaries of these regions have been drawn to agree with those shown in figure 1.0-1, with the following general exceptions: many of the ASW prediction areas have been broken into two or three separate sound velocity regions (e.g., area 173 has been split into regions 173A, 173B, and 173C); three sound velocity regions have been formed by combining two ASW prediction areas each (i.e., 140-141, 152-153, and 154-155); and the northernmost sections of ASW prediction areas 142, 144, and 146 have been combined to form a sound velocity region typical for the Ligurian Sea (i.e., region 144C). Representative seasonal sound velocity profiles for each of the regions shown in figure 3.1.1-1 are presented as figures A1-1 through A1-59 in Appendix 1. In many of these regions, sound velocity profiles were not available for one or more seasons. All sound velocity profiles have been extended either to the mean deep bottom depth (as given on NAVOCEANO Chart NA8 p 2401) or to an appropriate regional bottom depth. In either case, bottom depths were corrected using the tables of Matthews (1939).

(C) Most of the sound velocity profiles shown in Appendix 1 (figures A1-1 through A1-59) are "representative" or "model" profiles for Mediterranean Sea two-degree squares as selected by the AESD sound speed profile retrieval system (Audet and Vega, 1974). Therefore, these profiles are more or less typical of seasonal oceanographic conditions in given two-degree squares. Since two-degree squares only roughly approximate Mediterranean ASW prediction areas, and since the boundaries of these

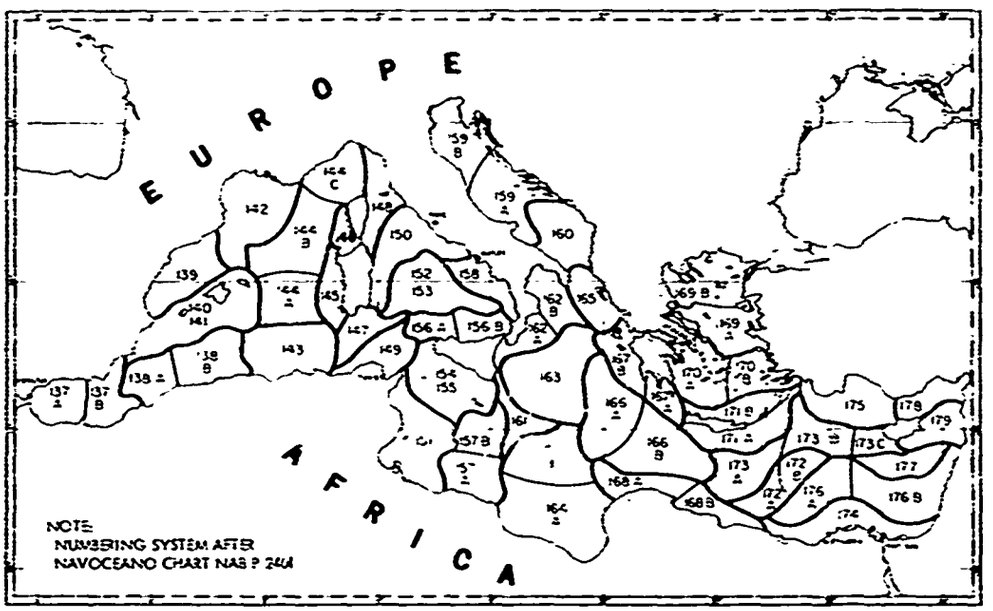

Figure 3.1.1-1(C). Regions with Distinct Representative Sound Velocity Profiles (U)

areas (figure 1.C-1) were purposefully maintained to the maximum degree possible in circumscribing the regions depicted in figure 3.1.1-1, a seasonal profile in any given sound velocity region may not differ markedly from a profile for the same season in an immediately adjacent region. However, the overall annual variation in sound velocity within a given region (i.e., the composite of the four seasonal profiles) is always significantly different from that observed in adjacent regions.

3.1.2(C) Sound Velocity Cross-sections (U). Figure 3.1.2-1 shows the locations of five pairs of sound velocity cross-sections constructed to represent conditions during the extreme seasons of winter and summer, plus a single summer cross-section along the major axis of the Strait of Sicily. These 11 cross-sections are shown in figures 3.1.2-2 through 3.1.2-12. Each cross-section consists of a series of sound velocity profiles plotted at their position of observation, plus a generalized profile of bottom topography. The depth of the DSC axis and the critical depth are identified on each cross-section. The values of axial depth, sound velocity at the DSC axis, and critical depth shown in the cross-sections may differ from those given in sections 3.1.3 and 3.1.4, since the latter represent average values. Many of the sound velocity profiles have been extended below the maximum depth of observation using nearby historical deep sound velocity gradients. Since there is a horizontal offset between the bottom of each sound velocity profile and its position of observation, many profiles extend into the apparent bottom. Most profiles have been extrapolated to the actual corrected bottom depth at the position of observation.

(C) Figures 3.1.2-2 and 3.1.2-3 show the vertical sound velocity structure for winter and summer along a line extending from the Strait of Gibraltar across the southern Algerian Basin and through the Strait of Sardinia into the Tyrrhenian Sea. In response to intensive surface cooling during winter (figure 3.1.2-2), positive sound velocity gradients are found throughout most of the southern Algerian Basin and Tyrrhenian Sea. This creates a situation where the bottom does not limit sound propagation (i.e., where the entire water column responds like a surface duct). Exceptions to this situation are found in two regions: between the Strait of Gibraltar and about 3°W, and between about 0° and 5°E. However in both regions, depth excess is adequate for convergence zone propagation. During summer (figure 3.1.2-3), a continuous DSC axis is found throughout the western Mediterranean. The depth of the DSC axis varies between about 50 and 200 m, and is generally shoaler in the Tyrrhenian Sea. The sound velocity at the DSC axis varies between 1507 and 1509 m/sec, and is generally less in the Alboran Sea. Critical depth along this cross-section varies between about 1150 and 1850 m and is greatest at about 5°E.

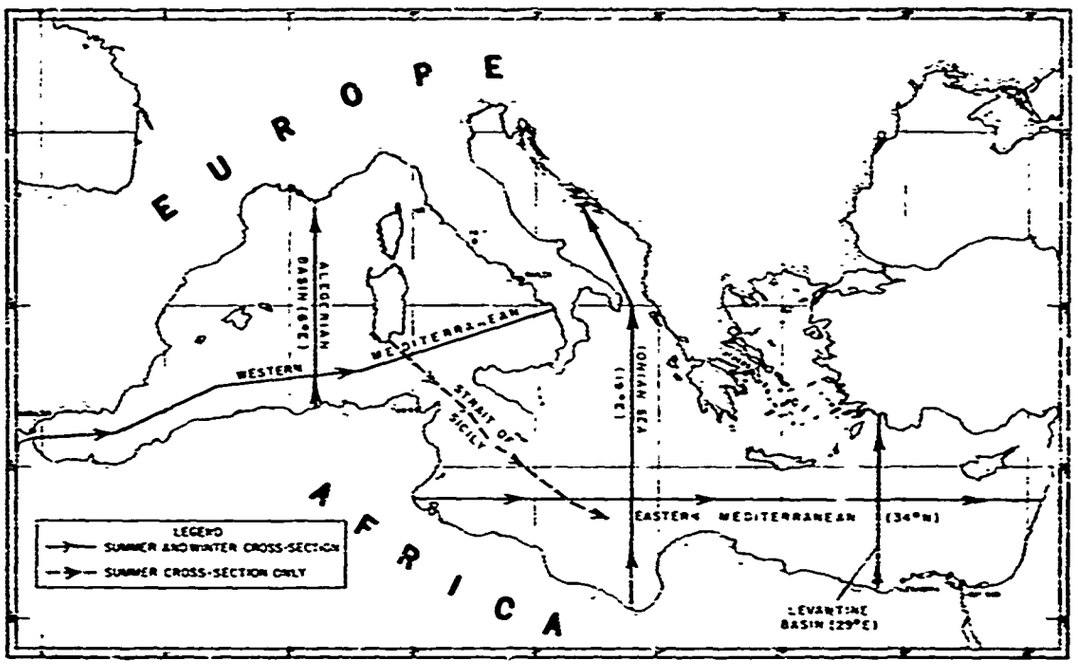

Figure 3.1.2-1. Location of Sound Velocity Cross-sections

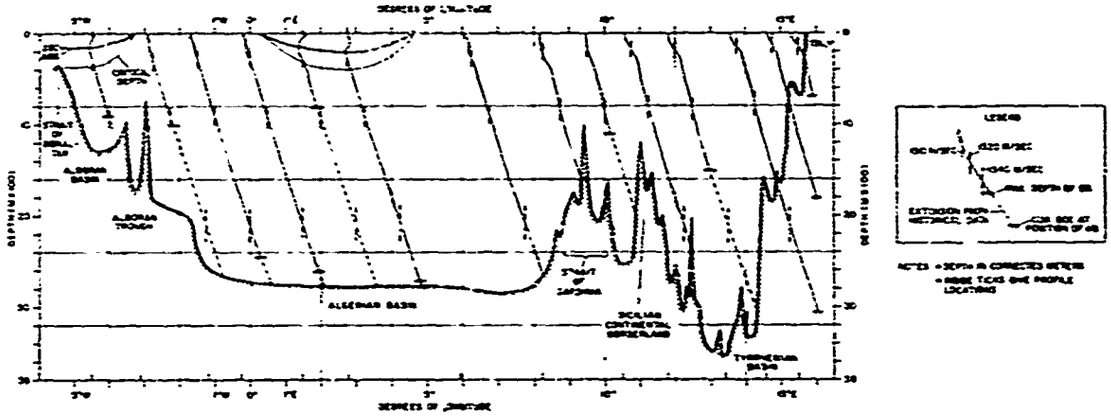

Figure 3.1.2-2. West-East Sound Velocity Cross-section in Western Mediterranean for Winter, January-March

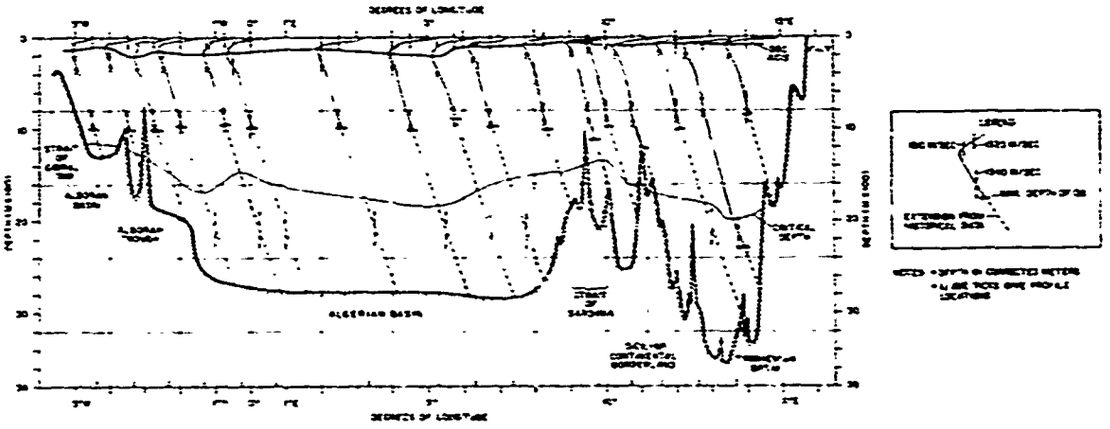

Figure 3.1.2-3. West-East Sound Velocity Cross-section in Western Mediterranean for Summer, July-September

However, depth excess probably is adequate for convergence zone transmission throughout most of the southern Algerian and Tyrrhenian Basins during summer. Sonic layers occur only sporadically during summer in the western Mediterranean and do not permit reliable surface duct propagation. During summer, spurious secondary sound channels above the depth of the DSC axis are encountered throughout much of the southern Algerian Basin. These features are caused by inflowing Atlantic Water and may be locally significant in detecting a shallow target.

(C) Figures 3.1.2-4 and 3.1.2-5 depict winter and summer sound velocity cross-sections along 6°E between Algeria and southern France. During winter (figure 3.1.2-4), positive sound velocity gradients are found along this entire cross-section, creating a situation where the sound channel is at the surface and the bottom does not limit sound propagation. During summer (figure 3.1.2-5), surface insolation creates a DSC at about 100 m depth. Sound velocities at the DSC axis vary from about 1509 m/sec in the south to less than 1507 m/sec at the northern end of the Algerian Basin. Critical depth shoals to the north and allows ample depth excess for convergence zone propagation. During summer, a surface duct is absent over most of this track.

(C) Figure 3.1.2-6 shows a summer sound velocity cross-section along the major axis of the Strait of Sicily that extends from the southern tip of Sardinia into the Ionian Sea. Sound velocity structures in the Strait of Sicily are extremely variable due to intensive mixing in the near-surface layer and to a pronounced northwest setting flow of LIW at intermediate depths. At a range of about 350 nm from the southern tip of Sardinia, surface sound velocities increase to greater than 1540 m/sec. This range may demark the position of the Malta Front. Both the sound velocity at the DSC axis and the axial depth are less along the first 300 nm of figure 3.1.2-6 (i.e., northwest of the suspected position of the Malta Front). This front separates the cooler, less saline waters of the western Mediterranean from the warmer, more saline waters of the Ionian Sea. The shallow topography of the Strait of Sicily precludes convergence zone transmission during summer. Surface ducts are extremely sporadic during summer in the Strait of Sicily, eliminating this mode of sound propagation.

(C) Figures 3.1.2-7 and 3.1.2-8 depict winter and summer sound velocity cross-sections along 34°N in the eastern Mediterranean Sea. During winter (figure 3.1.2-7), no persistent DSC axis exists along 34°N. In the Gulf of Gabes, between about 19° and 23°E, and again between about 28° and 32°E, positive sound velocity gradients extend from the sea surface to the bottom creating a situation where the entire water column acts like a surface duct and bottom topography does not limit sound propagation. However, transient DSC structures might occur during any given winter (see figures 3.1.3-1 through 3.1.3-3, below), depending on wind and

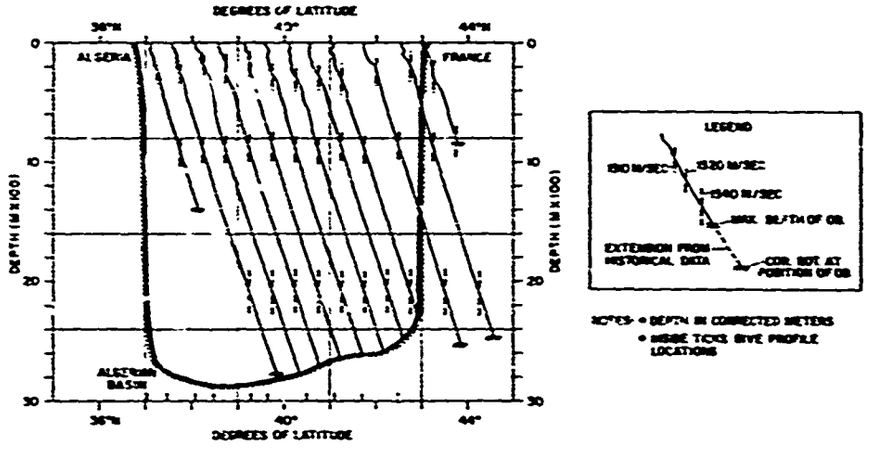

Figure 3.1.2-4. South-North Sound Velocity Cross-section in Algerian Basin (6°E) for Winter, January-March

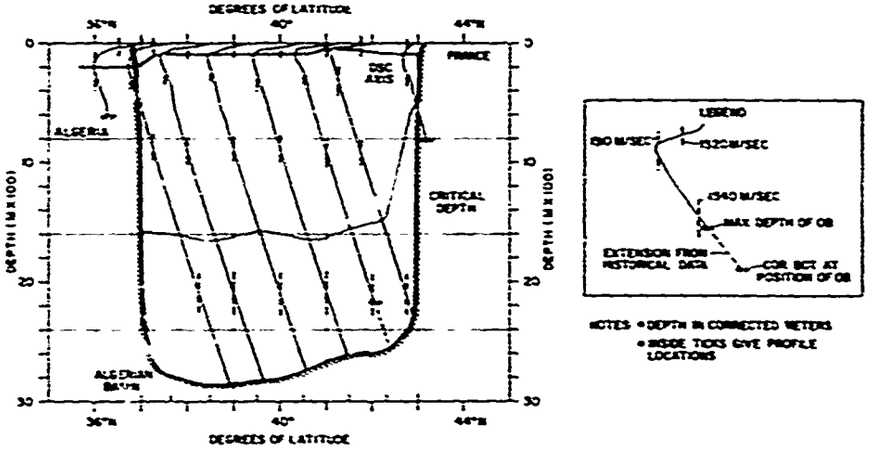

Figure 3.1.2-5. South-North Sound Velocity Cross-section in Algerian Basin (6°E) for Summer, July-September

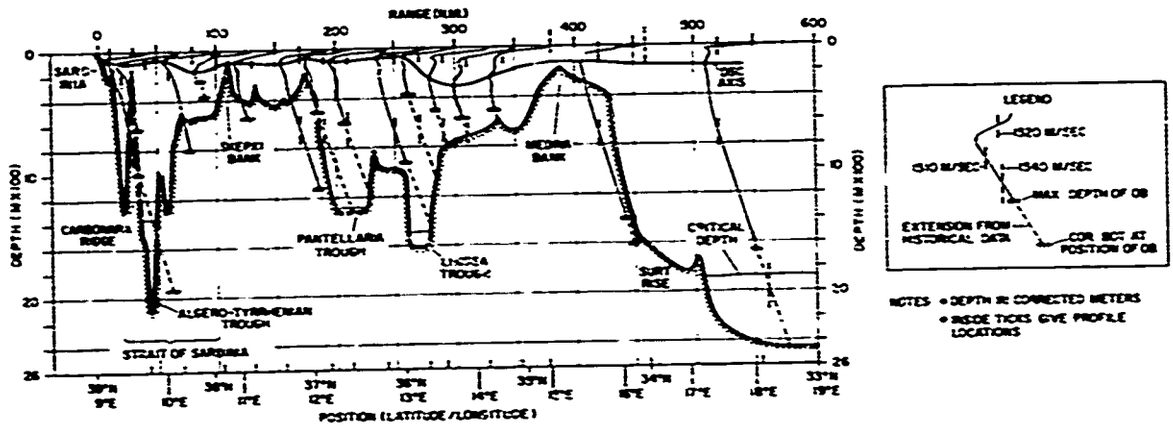

Figure 3.1.2-6. Sound Velocity Cross-section Along Major Axis of the Strait of Sicily for Summer, July-September

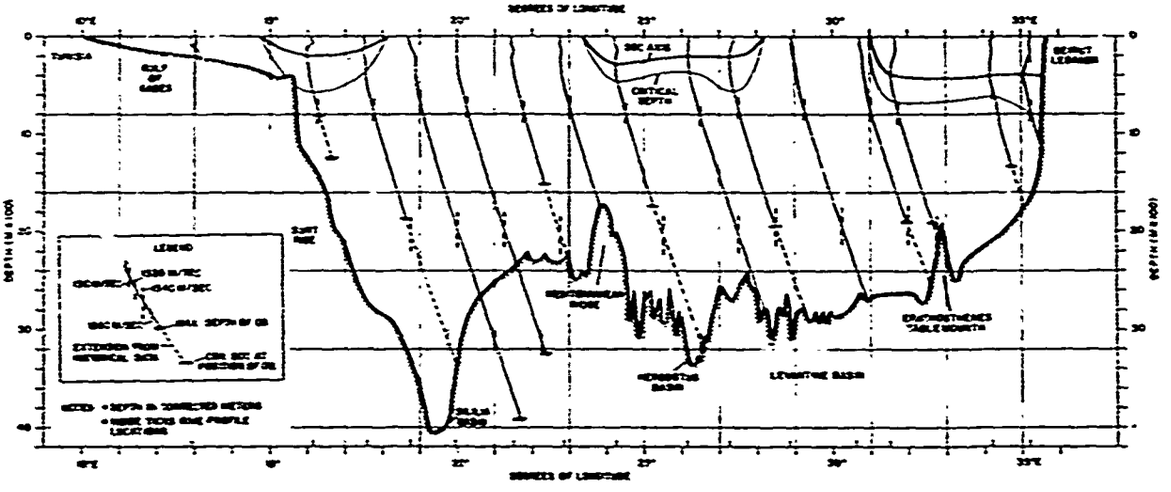

Figure 3.1.2-7. West-East Sound Velocity Cross-section in Eastern Mediterranean (34°N) for Winter, January-March

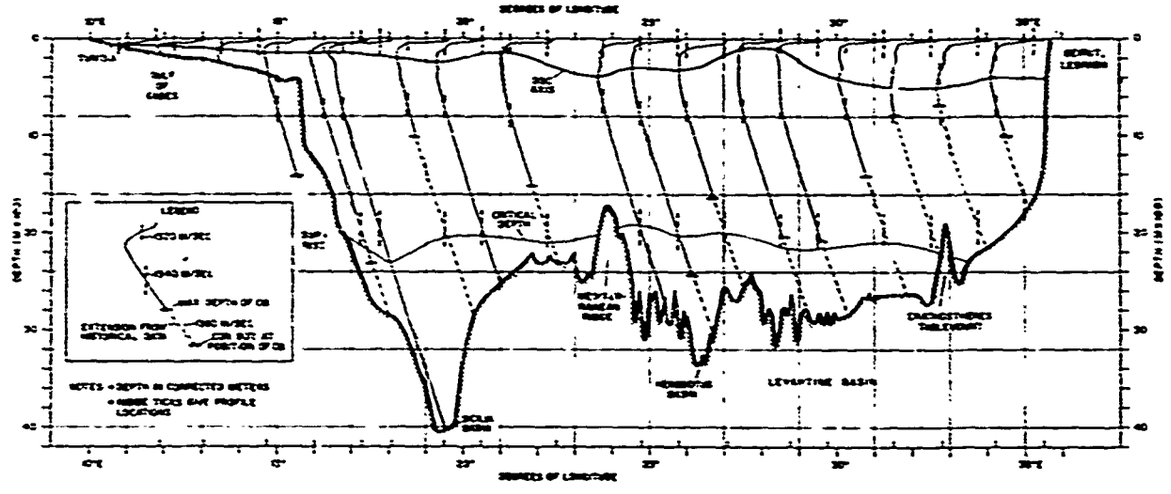

Figure 3.1.2-8. West-East Sound Velocity Cross-section in Eastern Mediterranean (34°N) for Summer, July-September

weather conditions. Water depth is more than adequate for RSR propagation throughout most of the eastern Mediterranean during winter. During summer (figure 3.1.2-8), a DSC axis is found at depths that vary between about 100 m in the Gulf of Gabes to about 500 m in the eastern Levantine Basin. The sound velocity at the DSC axis increases to the east from less than 1515 m/sec in the Gulf of Gabes to about 1519 m/sec near Eratosthenes Tablemount. In the Ionian Sea (Sicilian Basin), depth excess is adequate for convergence zone propagation during summer. However, the shoaler bottom topography of the Levantine Basin limits depth excess to generally less than 1000 m. An extremely shallow sonic layer (less than 20 m deep) can be found in the eastern Mediterranean during summer. However, this feature is too sporadic and ill defined to produce a reliable surface duct. During summer, secondary sound channels above the depth of the DSC axis are found east of about 30°E. These channels could permit short-range detection of a target at the depth of the channel.

(C) Figures 3.1.2-9 and 3.1.2-10 present winter and summer sound velocity cross-sections along 19°E that extend north from the Gulf of Sidra across the Strait of Otranto into the Adriatic Sea. During winter (figure 3.1.2-9), DSC structures are present only in the Gulf of Sidra and the Strait of Otranto. The former are caused by warmer near-surface conditions off the Libyan coast, and the latter by mixing. Over the remainder of the cross-section, surface cooling causes semi-permanent positive sound velocity gradients that extend from the sea surface to the bottom. During summer (figure 3.1.2-10), a DSC is found at depths that vary from about 250 m in the south to about 50 m in the Adriatic Sea. Sound velocities at the DSC axis generally decrease to the north from about 1514 m/sec in the Gulf of Sidra to about 1511 m/sec in the Straits of Otranto. However, north of about 40°N, the sound velocity at the DSC axis is less than 1509 m/sec due to the lower temperatures and salinities in the Adriatic Sea. Over the Sicilian Basin, depth excess is adequate for convergence zone propagation during summer. In addition, a shallow, sporadic sonic layer is present throughout most of the Ionian Sea that could permit some surface duct propagation.

(C) Figures 3.1.2-11 and 3.1.2-12 illustrate the vertical sound velocity structure along 29°E in the Levantine Basin during winter and summer. During winter (figure 3.1.2-11), positive sound velocity gradients occur over the crest of the Mediterranean Ridge. Such features are not apparent in the average DSC statistics for winter (figures 3.1.3-1 and 3.1.3-2, below), indicating that they may be transient in nature. Surface duct and RSR propagation are ensured along 29°E during winter. During summer (figure 3.1.2-12), the depth of the DSC axis generally shoals between the coast of Egypt and the crest of the Mediterranean Ridge, but then deepens to about 350 m over the Rhodes Basin. The sound velocity at the DSC axis approaches a maximum of

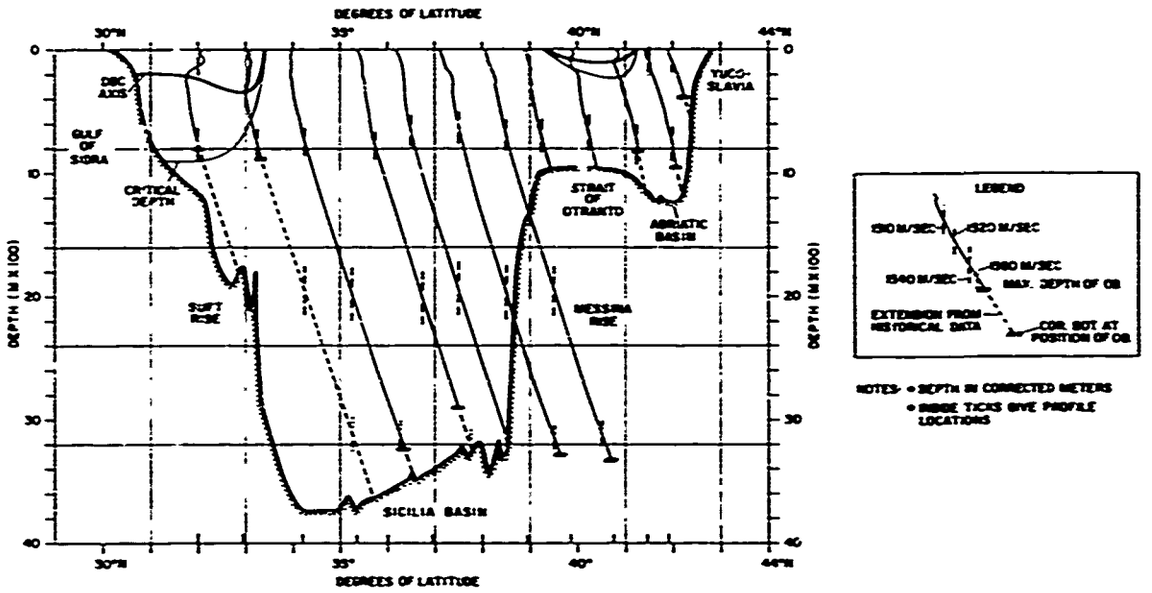

Figure 3.1.2-9. South-North Sound Velocity Cross-section in Ionian Sea (19°E) and Adriatic Sea for Winter, January-March

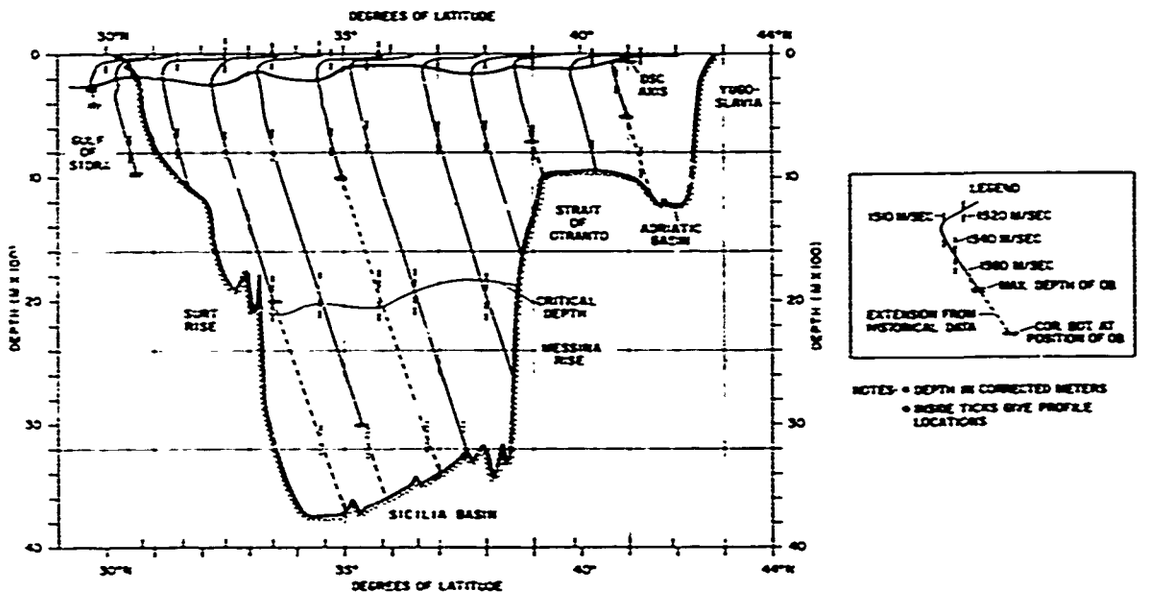

Figure 3.1.2-10. South-North Sound Velocity Cross-section in Ionian Sea (19°E) and Adriatic Sea for Summer, July-September

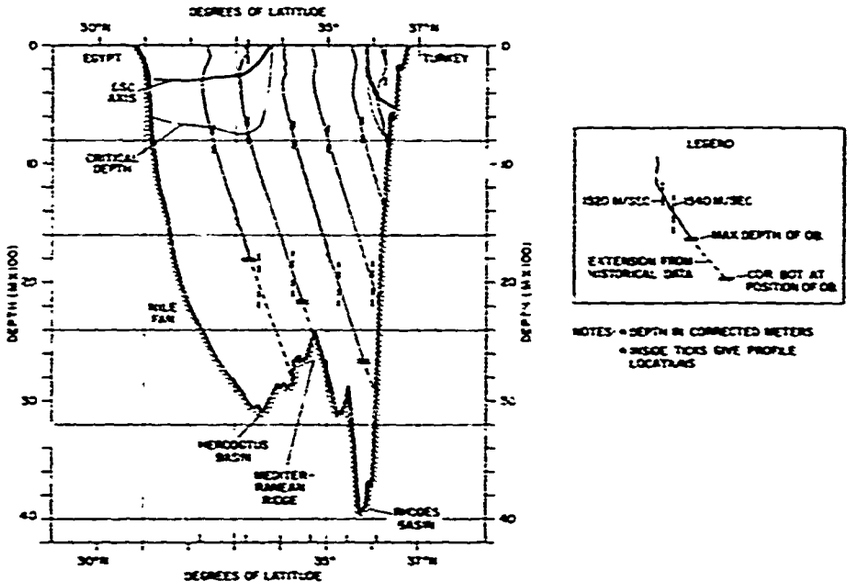

Figure 3.1.2-11. South-North Sound Velocity Cross-section in Levantine Basin (29°E) for Winter, January-March

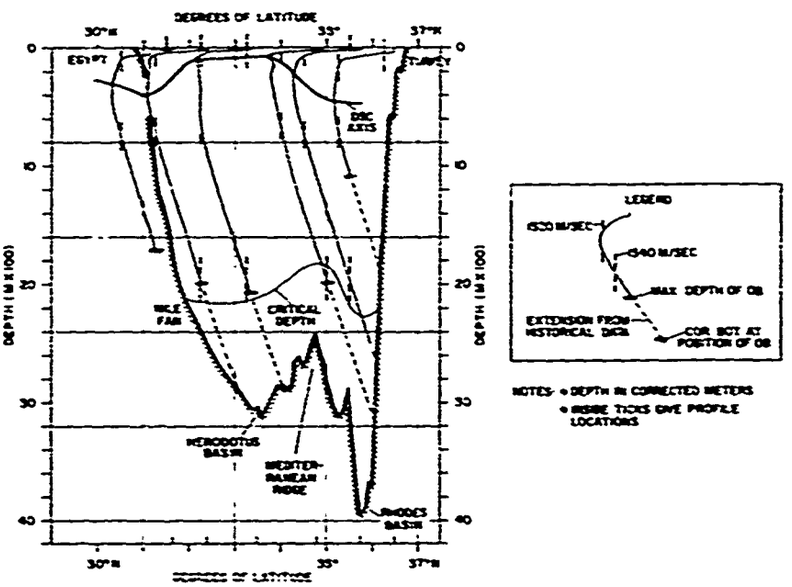

Figure 3.1.2-12. South-North Sound Velocity Cross-section in Levantine Basin (29°E) for Summer, July-September

1518 m/sec at about 33°N, probably in response to the presence of a core of high salinity LIW. Depth excess is adequate for the formation of convergence zones along 29° E during summer. An ill-defined surface duct is present along most of this track, but is not strong enough for reliable propagation.

(U) The sound velocity cross-sections shown in figures 3.1.2-2 through 3.1.2-12 portray generalized vertical structures only for the two extreme seasons of winter and summer. During the transition seasons of spring and autumn, the upper 500 m of the water column is subject to short-period changes associated with rapid warming and cooling. Similar short-period changes could also occur during winter and summer in some regions, causing significant changes in acoustic propagation conditions. For this reason, the propagation patterns presented in these figures should be considered representative only for the areas depicted. In addition, many of the sound velocity structures in the Mediterranean are sensitive to the near-surface environment, and can be drastically altered by anomalous weather conditions.

3.1.3(U) Deep Sound Channel Axis (U). In the Mediterranean Sea, the depth and sound velocity of the DSC axis vary with season (Fenner, 1968) in response to surface cooling and insolation. However, during the transition seasons of spring and autumn, average values of both parameters have relatively large standard deviations. Therefore, presentations of average DSC axial depth and sound velocity are shown for only the two extreme seasons of winter and summer, along with their respective standard deviations (figures 3.1.3-1 through 3.1.3-8). During spring and autumn, the average depth of the DSC axis generally lies midway between the average values for winter and summer (Fenner, 1968).

(U) Figures 3.1.3-1 and 3.1.3-2 display the average depth of the DSC axis and its standard deviation during winter. Figures 3.1.3-3 and 3.1.3-4 present similar statistics for the sound velocity at the DSC axis. As previously noted, no DSC is evident in most of the western Mediterranean and in the northern portions of the eastern Mediterranean during winter. In these regions, surface cooling, induced by strong northwesterly winds, destroys the seasonal thermocline present during spring, summer, and autumn. This in turn causes the formation of an essentially positive sound velocity gradient that extends from the ocean surface to the ocean bottom. However, localized warming can cause the formation of transient winter DSC structures, particularly during the month of January. A DSC is present throughout winter in the Alboran Sea and in an isolated region off the eastern Algerian coast, probably due to the effects of relatively warm Atlantic Water near the surface. In the southern portions of the eastern Mediterranean, (i.e., the southern

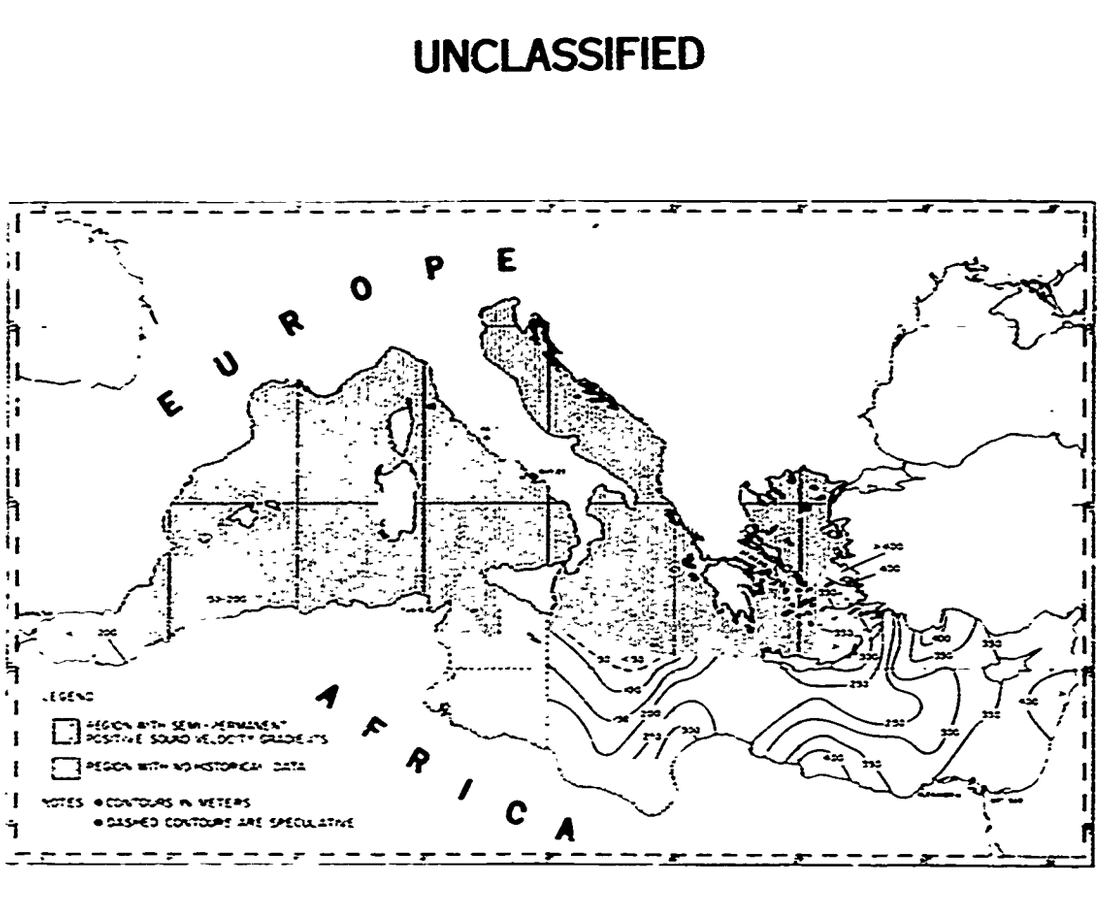

Figure 3.1.3-1. Average Depth of Deep Sound Channel Axis for Winter, January-March

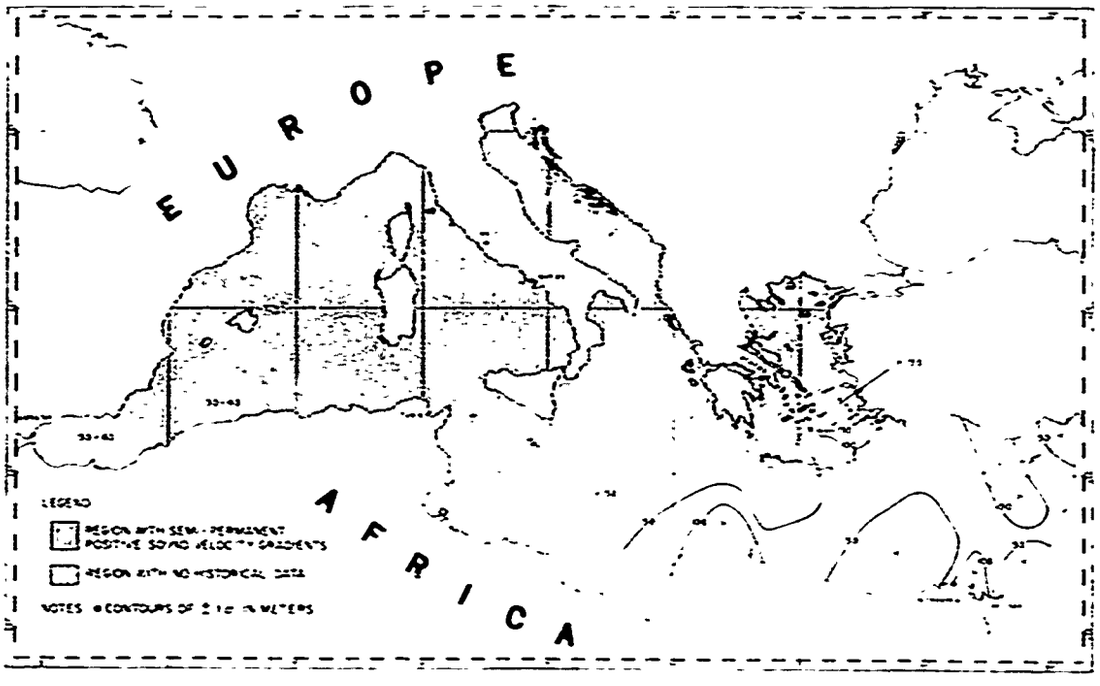

Figure 3.1.3-2. Standard Deviation of Average Deep Sound Channel Axis Depth for Winter, January-March

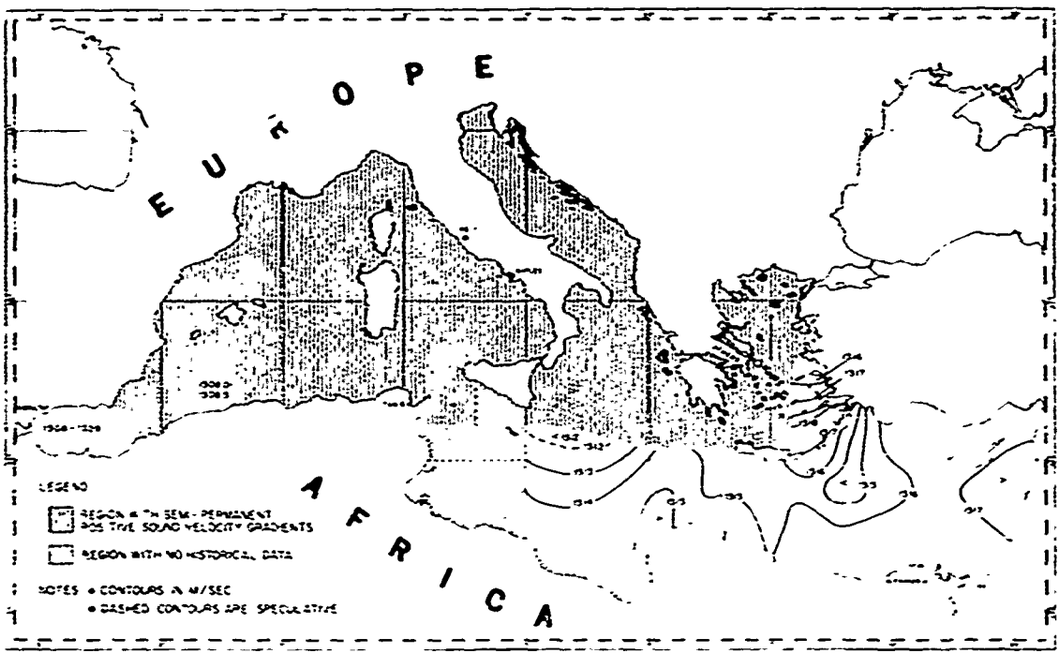

Figure 3.1.3-3. Average Sound Velocity at Deep Sound Channel Axis for Winter, January-March

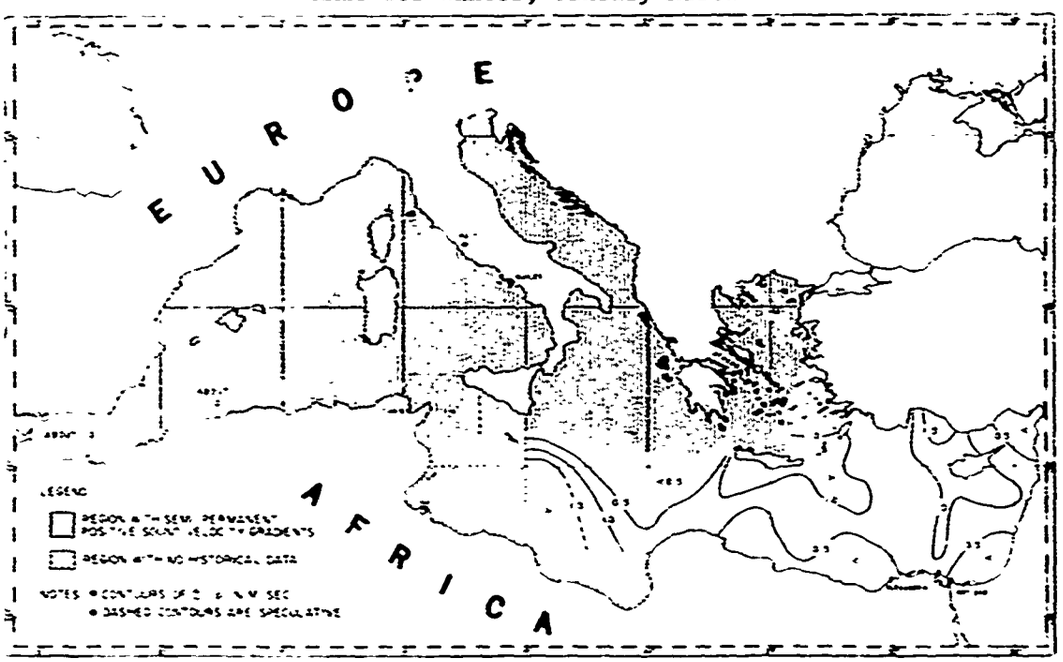

Figure 3.1.3-4. Standard Deviation of Average Deep Sound Channel Axis Sound Velocity for Winter, January-March

Ionian Sea, the Levantine Basin, and the southeastern Aegean Sea), a DSC also is present throughout winter. However, such a structure can be destroyed by extreme near-surface mixing. Examples of the absence of a DSC in the southern Ionian Sea and Levantine Basin were given in figures 3.1.2-7, 3.1.2-9, and 3.1.2-11.

(U) During winter, the average depth of the DSC axis generally increases to the east from less than 50 m in the region near Malta to a depth of greater than 400 m at the eastern end of the Mediterranean. However, average DSC axial depths greater than 400 m also are found in isolated pockets off the Libyan coast, east of Rhodes, and in the southeastern Aegean Sea. The average sound velocity at the DSC axis varies from less than 1512 to greater than 1517 m/sec in a manner similar to that observed for average axial depth. The isopleth patterns of both parameters suggest a general flow to the east emanating from the region between Rhodes and Cyprus. According to Wust (1961), high-salinity LIW is formed in this same region during winter. The average DSC axial depth during winter displays standard deviations that vary from greater than 150 m to less than 50 m, but generally lie between 50 and 100 m over most of the Levantine Basin. Standard deviations in the average sound velocity at the DSC axis vary from greater than 1.5 to less than 0.5 m/sec, but generally lie between 0.5 and 1.0 m/sec over most of the Levantine Basin.

(U) Figures 3.1.3-5 and 3.1.3-6 show the average depth of the DSC axis and its standard deviation for summer. Figures 3.1.3-7 and 3.1.3-8 present similar statistics for the sound velocity at the DSC axis. During summer, a DSC is present throughout the Mediterranean except in the Gulf of Gabes and in the northern half of the Adriatic Sea. Both these regions are too shallow for the formation of a DSC during summer. The average depth of the DSC axis generally increases to the east from less than 100 m along the southern coast of France to greater than 400 m off the coast of Israel. However, the average depth of the DSC axis also is less than 100 m in the northwestern Aegean Sea. This anomaly may be related to low-salinity water flowing out of the Black Sea through the Dardanelles. The average sound velocity at the DSC axis also increases to the east from less than 1507 m/sec north of the Balearic Islands to greater than 1517 m/sec at the eastern end of the Mediterranean Sea. However, in the Aegean Sea, average values of less than 1512 m/sec are found off the coast of Greece while average values of more than 1518 m/sec are found off the coast of Turkey, creating a strong northwest to southeast gradient. Another strong gradient occurs across the Strait of Sicily, where the average sound velocity at the DSC axis changes by about 6 m/sec over a distance of about 150 nm. This gradient is caused both by the Malta Front and by mixing of LIW at intermediate depths. Isopleth patterns of the average depth and sound velocity at the DSC axis suggest a flow from the Levantine Basin through the Strait of Sicily into the southern Algerian Basin similar to the pattern followed by high-salinity LIW.

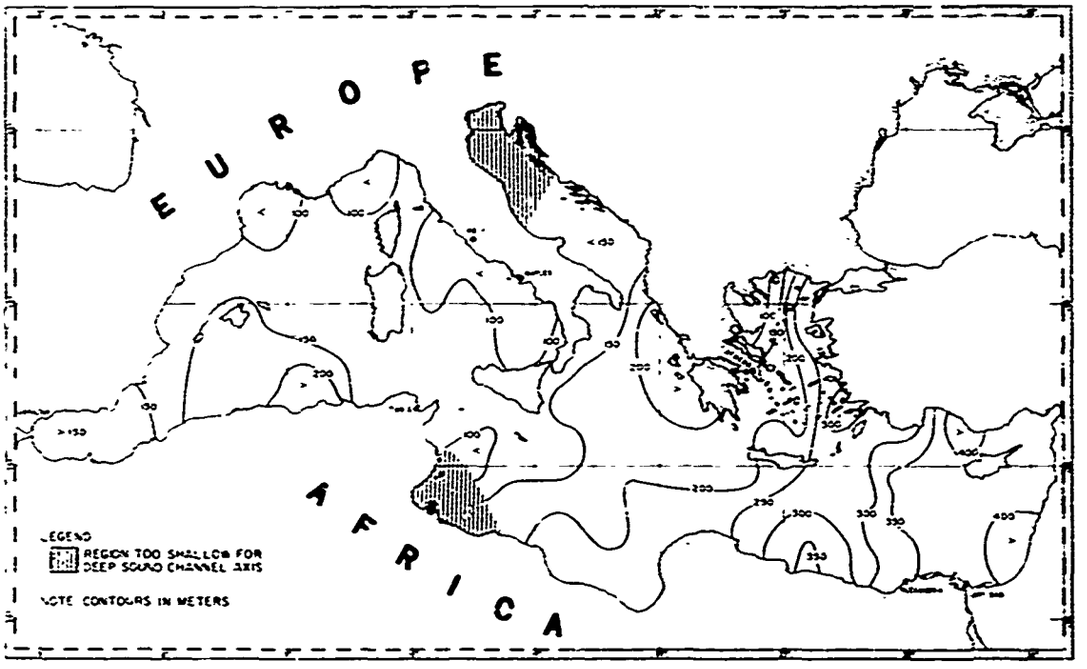

Figure 3.1.3-5. Average Depth of Deep Sound Channel Axis for Summer, July-September

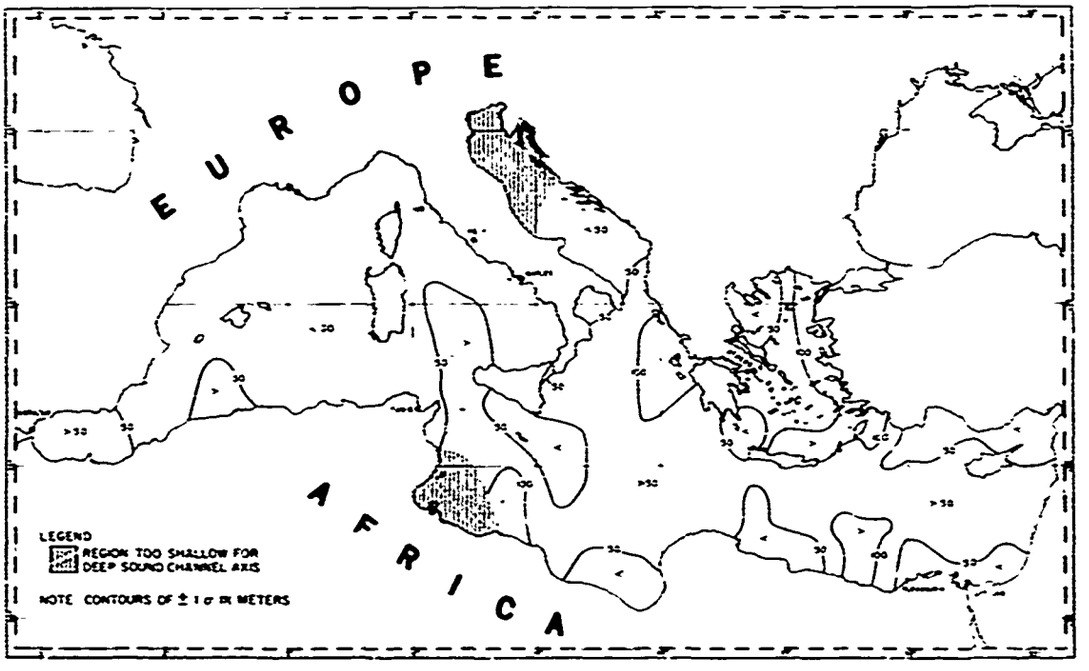

Figure 3.1.3-6. Standard Deviation of Average Deep Sound Channel Axis Depth for Summer, July-September

Figure 3.1.3-7. Average Sound Velocity of Deep Sound Channel Axis for Summer, July-September

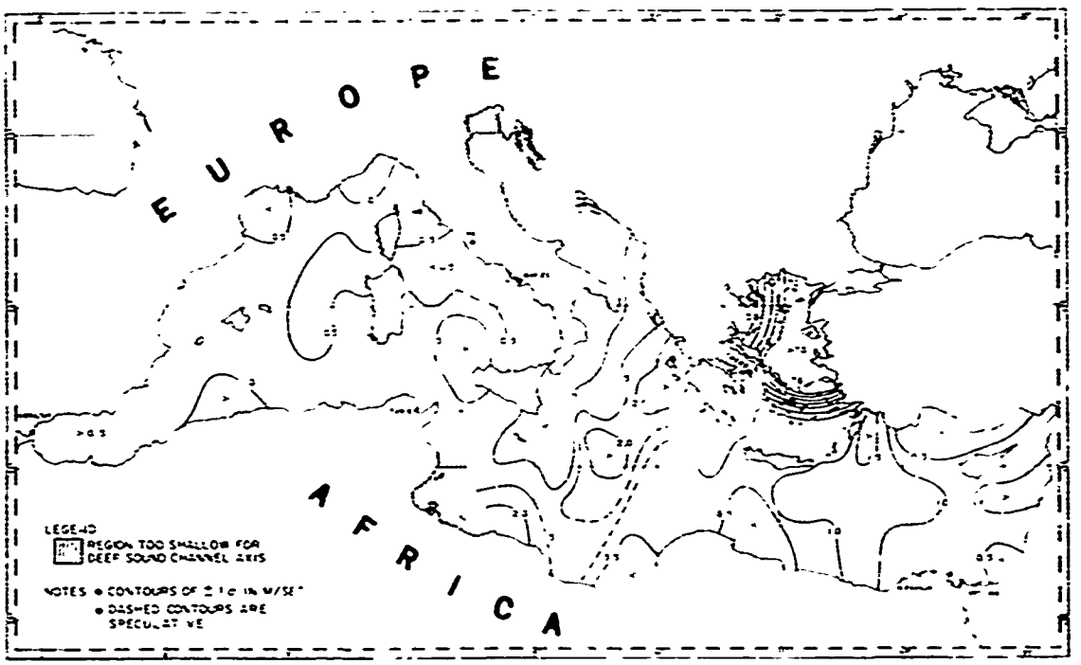

Figure 3.1.3-8. Standard Deviation of Average Deep Sound Channel Axis Sound Velocity for Summer, July-September

(U) Summer standard deviations in the average depth of the DSC axis generally lie between 50 and 100 m, and are somewhat less in the Algerian Basin. Standard deviations in the average axial sound velocity are much greater than those of average DSC axial depth, and vary from more than 7.0 m/sec in the eastern Aegean Sea to less than 0.5 m/sec in both the Gulf of Sidra and most of the western Mediterranean. Since axial sound velocities are more sensitive to water masses than are axial depths, the large standard deviations apparent in the axial sound velocities probably reflect either water mass movements or actual changes in water mass types.

3.1.4(U) Critical Depth (U). By definition, critical depth is based on both the maximum sound velocity in the near-surface layer and the deep sound velocity gradient. Since sound velocities in the near-surface layer are subject to extreme temporal variability (diurnal, monthly, and seasonal), critical depths also show significant temporal variability and associated large standard deviations. Figures 3.1.4-1 through 3.1.4-5 show annual critical depth curves complete with monthly standard deviations for the Alboran Sea, central Algerian Basin, Tyrrhenian Sea, central Ionian Sea, and central Levantine Basin, respectively. Except for the Alboran Sea, these curves show a near-normal distribution of average critical depth with time, but also show significant monthly standard deviations. The near-normal distributions of average critical depth versus time probably are caused by the regularity of the annual heating-cooling cycle in major Mediterranean basins. Near-normal data distributions are particularly evident in the central Algerian Basin (figure 3.1.4-2) and the central Ionian Sea (figure 3.1.4-4). Both of these regions are relatively far from the influence of a land mass. In the landlocked Alboran Sea, however (figure 3.1.4-1), average critical depths observed during May are less than those during April, and average critical depths during September appear to be less than those for October. This is a reversal of the trends usually observed during spring and autumn. In all five regions, average critical depths and their standard deviations are quite variable during the transition seasons of spring and autumn. In addition, existing oceanographic data have poor temporal and spatial distributions during the two transition seasons. Therefore, contour charts of average critical depth were constructed only for the extreme seasons of winter and summer.

(U) Figures 3.1.4-6 and 3.1.4-7 depict the average critical depth and its standard deviation for winter. In the hatched regions in these two figures, there is no DSC structure and critical depth is at the surface. Figures 3.1.4-8 and 3.1.4-9 show the same parameters for summer. Since both critical depth and the bottom are highly variable in the Mediterranean, the various isopleths in figures 3.1.4-6 through 3.1.4-9 are shown in regions where the bottom is shoaler than critical depth

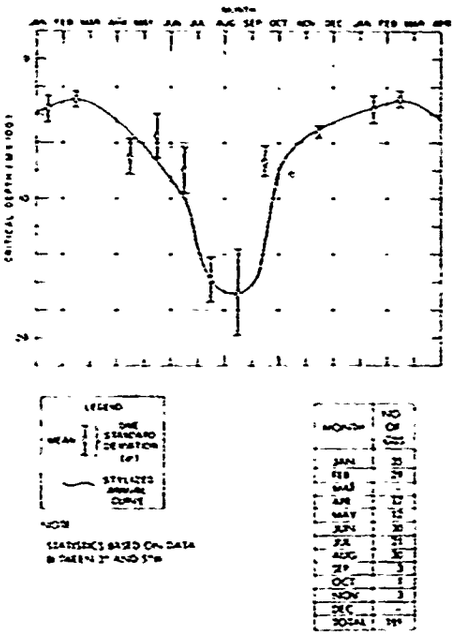

Figure 3.1.4-1. Annual Critical Depth Curve for Alboran Sea

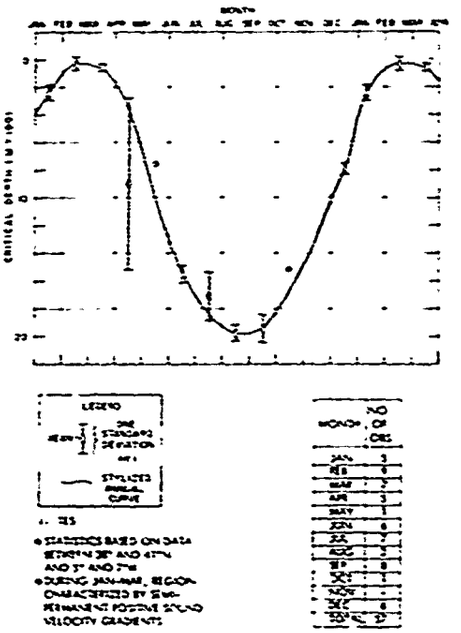

Figure 3.1.4-2. Annual Critical Depth Curve for Central Algerian Basin

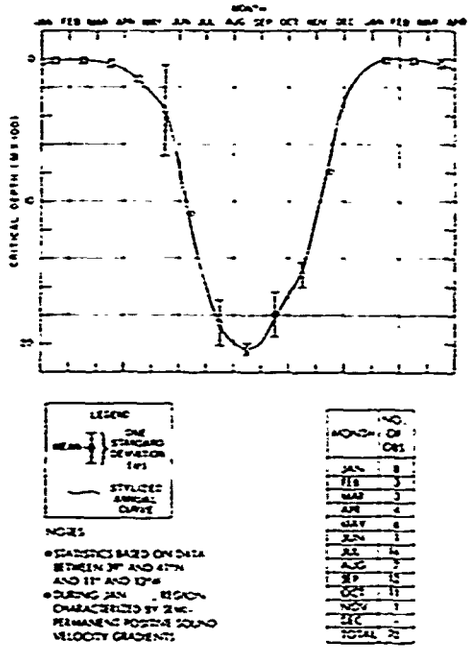

Figure 3.1.4-3. Annual Critical Depth Curve for Tyrrhenian Sea

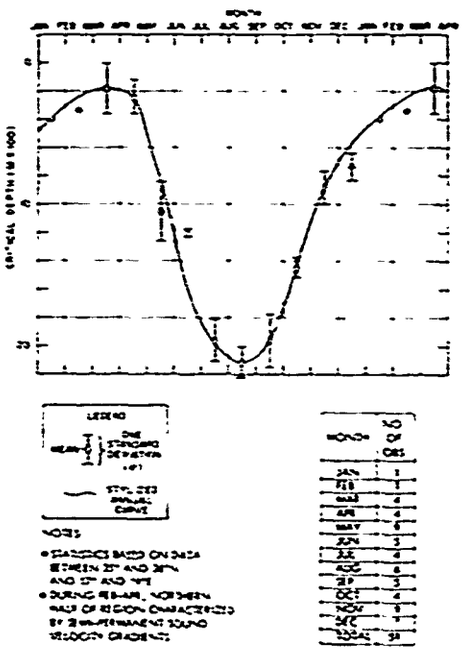

Figure 3.1.4-4. Annual Critical Depth Curve for Central Ionian Sea

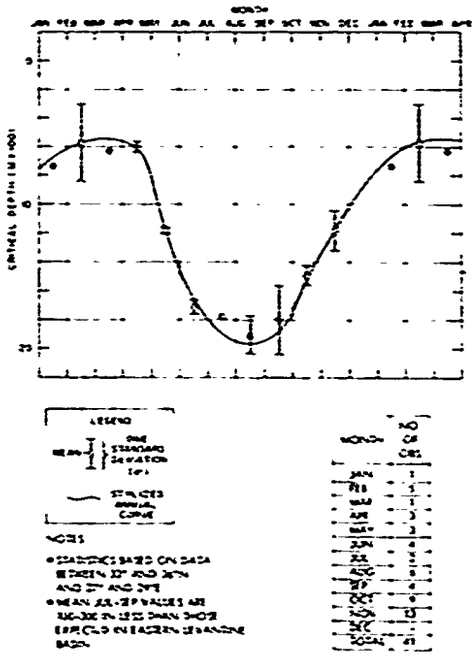

Figure 3.1.4-5. Annual Critical Depth Curve for Central Levantine Basin

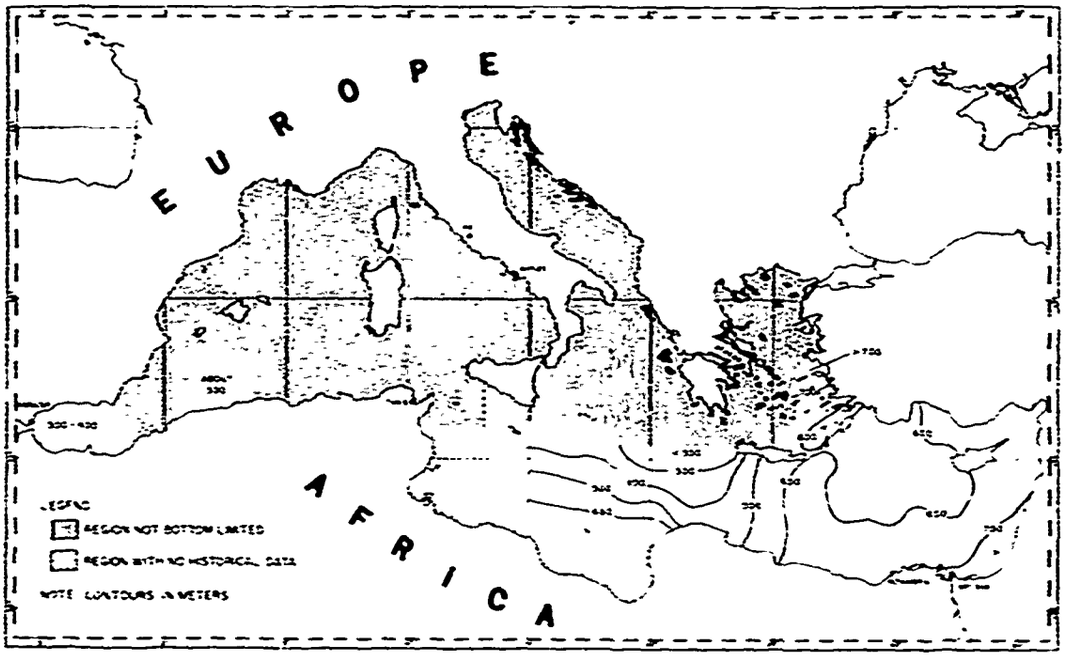

Figure 3.1.4-6. Average Critical Depth for Winter, January-March

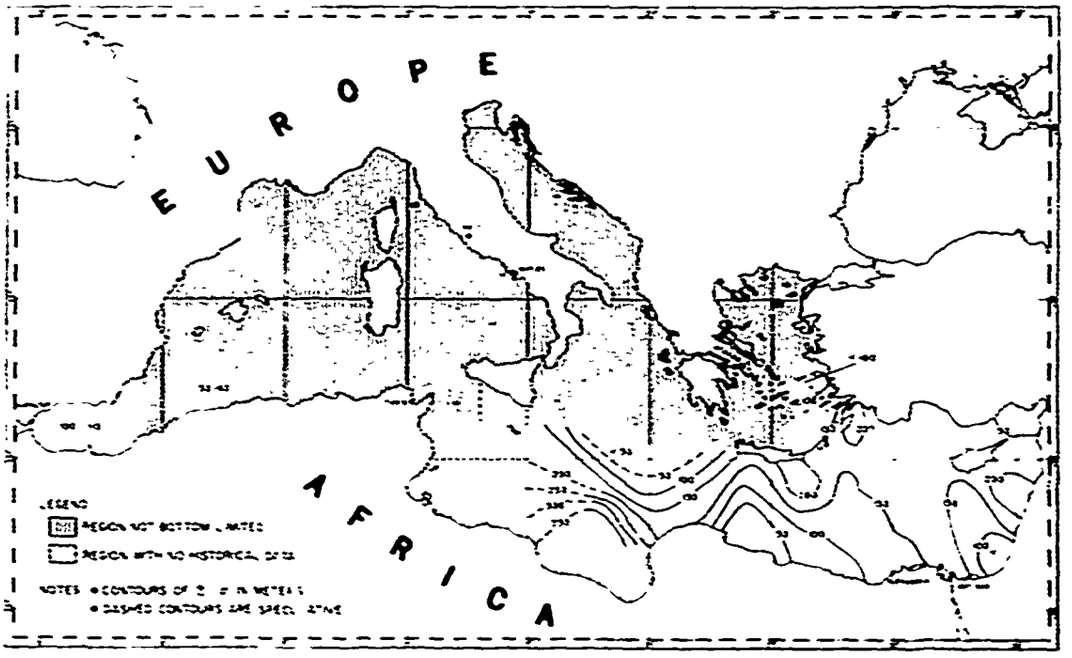

Figure 3.1.4-7. Standard Deviation of Average Critical Depth for Winter, January-March

Figure 3.1.4-8. Average Critical Depth for Summer, July-September

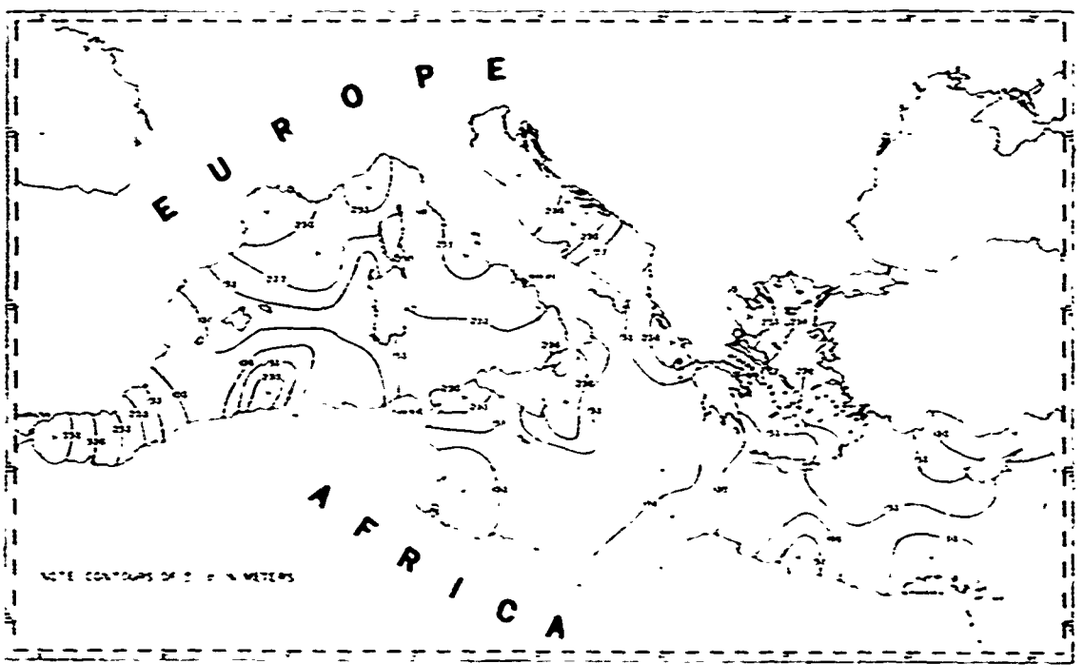

Figure 3.1.4-9. Standard Deviation of Average Critical Depth for Summer, July-September

(i.e., regions of depth difference) as well as in depth excess regions. Depth difference and depth excess regions for winter and summer are identified in figures 3.1.4-10 and 3.1.4-11 respectively.*

(U) During winter (figure 3.1.4-6), surface cooling produces semi-permanent positive sound velocity gradients throughout most of the western Mediterranean and in northern portions of the eastern Mediterranean. In these regions, critical depth is at the sea surface and propagation is not bottom limited. However, warmer near-surface conditions in the southern Ionian Sea, Levantine Basin, and southeastern Aegean Sea lead to the formation of a DSC and result in average critical depths that vary from less than 400 m south of Peloponnesus to greater than 700 m at the eastern end of the Mediterranean Sea. An isolated region with average critical depths greater than 700 m also occurs off the Turkish coast in the southeastern Aegean Sea. In the Alboran Sea and in an isolated pocket off the coast of eastern Algeria, relatively warm Atlantic Water leads to a DSC structure and average critical depths between 300 and 400 m during winter. Standard deviations in average critical depth during winter (figure 3.1.4-7) vary between only about 100 and 200 m in the Levantine Basin, but between about 50 and 350 m in the southern Ionian Sea. In the Alboran Sea, standard deviations are about 100 m. The large variation in standard deviations in the southern Ionian Sea is partially caused by the Malta Front, but also is a result of rapid changes in near-surface cooling throughout this region (also see figure 3.1.4-4).

(U) During summer (figure 3.1.4-8), critical depths vary from less than 1500 m in the Gulf of Lion to greater than 2300 m in the region east of Cyprus. Critical depths less than 1600 m are found in the northern ends of the Algerian Basin and Adriatic Sea and in the northeastern part of the Aegean Sea off the Dardanelles. Critical depths greater than 2000 m are found in the Gulf of Gabes, Gulf of Sidra, off the Libyan coast, and throughout most of the eastern Levantine Basin. In the Alboran Sea, critical depths are somewhat greater than 1600 m. Standard deviations in average summer critical depth (figure 3.1.4-9) vary from generally less than 100 m in the eastern Levantine Basin to greater than 350 m in the western Alboran Sea. Regions with standard deviations greater than 250 m occur in the Ligurian Sea, the Tyrrhenian Sea, and the northwestern Aegean Sea. Generally, standard deviations in average summer critical depth are greater in the western than in the eastern Mediterranean Sea. This is due partially to more uniform surface insolation in the eastern Mediterranean. The extremely high standard deviations in the western Alboran Sea (greater than 350 m) probably are caused by local variability in surface insolation and fluctuations in the Atlantic Water inflow (also see figure 3.1.4-1). However, standard deviations in summer average

*These figures are inserted in the envelope bound at the back of this volume.

critical depth also reflect the monthly distribution of data. Generally speaking, regions with high percentages of August (mid-summer) data have lower standard deviations than regions with preponderant percentages of July and/or September data. In the western Mediterranean Sea, a high percentage of the historical observations were collected during the month of July, whereas in the eastern Mediterranean Sea, a majority were collected during August.

3.1.5(C) Depth Excess and Depth Difference (U). Figures 3.1.4-10 and 3.1.4-11 depict regions shoaler and deeper than average critical depth for winter and summer, respectively. Regions shoaler than average critical depth are regions of depth difference. Regions where the ocean bottom exceeds critical depth are regions of depth excess. As a general rule, more than 400 m of depth excess are required for reliable convergence zone propagation from a near-surface source. Somewhat more depth excess may be required for meaningful long-range RSR propagation.

(C) During winter (figure 3.1.4-10), the majority of the Mediterranean Sea has greater than 1000 m of depth excess. Exceptions are found in the Alboran Sea, in the Strait of Sicily, and along the continental margin in the eastern Mediterranean Sea. However, in most of the western Mediterranean and northern portions of the eastern Mediterranean (i.e., northern Ionian Sea, Adriatic Sea, and most of the Aegean Sea) a positive sound velocity gradient occurs between surface and bottom, permitting uninterrupted RSR propagation with little bottom interaction.

(C) During summer (figure 3.1.4-11), warmer near-surface conditions result in considerable regions of depth difference throughout the Mediterranean Sea. These regions include the Alboran Sea, the Balearic Plateau, the Strait of Sardinia, much of the Tyrrhenian Sea, the Strait of Sicily, the entire Adriatic and Aegean Seas, portions of the northern Ionian Sea, most of the eastern Levantine Basin, and a substantial portion of the Mediterranean Ridge between about 22° and 25°E. In these areas, convergence zone propagation is severely limited or interrupted by the bottom.

(C) Elsewhere in the Mediterranean, however, large regions with 400 to 1000 m of depth excess occur in the Algerian Basin, Tyrrhenian Sea, Ionian Sea, and western Levantine Basin. During summer, RSR propagation between the major basins of the Mediterranean generally is impeded by regions of shallow topography. Within the four major deep water basins, however, RSR propagation can be used reliably everywhere.

3.1.6(U) Sonic Layer Depth (U). Sonic Layer Depth (SLD) in the Mediterranean Sea is a function of surface heating, which tends to reduce the SLD, and

vertical mixing due to surface cooling and/or wave action, which drives the SLD deeper. In winter surface cooling and strong northwesterly winds (tramontana, bora, mistral) destroy the seasonal thermocline, thereby forming an essentially isothermal and isohaline layer to the sea floor. Absence of a near surface sonic maximum (SLD) during this period creates a situation where the entire water column acts as a surface duct.

(U) The advent of surface heating coupled with decreasing winds in spring permits the seasonal thermocline to reform. As surface heating increases, a sound speed minimum occurs at the base of the newly formed thermocline, thus causing an in-layer sound channel which persists until overwhelmed in the autumn as the thermocline deepens. Continued surface heating causes surface sound speed values to increase rapidly until they become greater than values at the 300 m level. The transition from deep to shallow SLD normally occurs between mid-April and mid-May. SLD remains at or near the surface until winter cooling and increasing winds eliminate the seasonal thermocline.

(U) Seasonal SLD charts are shown in figures 3.1.6-1 through 3.1.6-4, as computed from expendable bathythermograph (XBT) data averaged over one-degree rectangles. The winter chart (figure 3.1.6-1) shows the effect of cool, dry winds from continental Europe. Water temperature exceeds air temperature by as much as 10°C, causing the near surface layer to be dense and unstable (Lacombe and Tehernia, 1971). Thus vertical mixing occurs, forming a deep, homogeneous surface layer with SLD deeper than 300 m in the northern part of the Western Mediterranean and in the Adriatic Sea. Relatively shallow SLD occurs in the southern half of the Strait of Gibraltar owing to the influx of Atlantic waters. Presence of a meridional atmospheric pressure gradient over the eastern Mediterranean directs water of Atlantic origin northward toward the Adriatic Sea rather than toward the Levantine Basin (Oren, 1971). The resultant shift in circulation combined with relatively mild weather (reduced convective and wind mixing) results in SLD deepening to only moderate depths in the Levantine Basin.

(U) The effect of increased surface heating, decreased winds, and river runoff is evident in the SLD analysis for spring (figure 3.1.6-2). Shallow layer depths are found in shallow areas, where Atlantic water moves eastward along the African coast, and in the Levantine Basin. Deep layer depths persist where Mediterranean Deep Water was manufactured during the previous winter, but even here the trend toward summer conditions is shown by the variability of the analysis.

(U) By summer, the atmospheric pressure system has become zonal (east-west) and Atlantic water is once again transported into the Levantine Basin (Oren, 1971). SLD rarely exceeds 30 meters throughout the entire area (figure 3.1.6-3). The tendency for transient surface warming (afternoon effect) during periods of maximum insolation is well established.

Figure 3.1.6-1. Mean Sonic Layer Depth, Winter

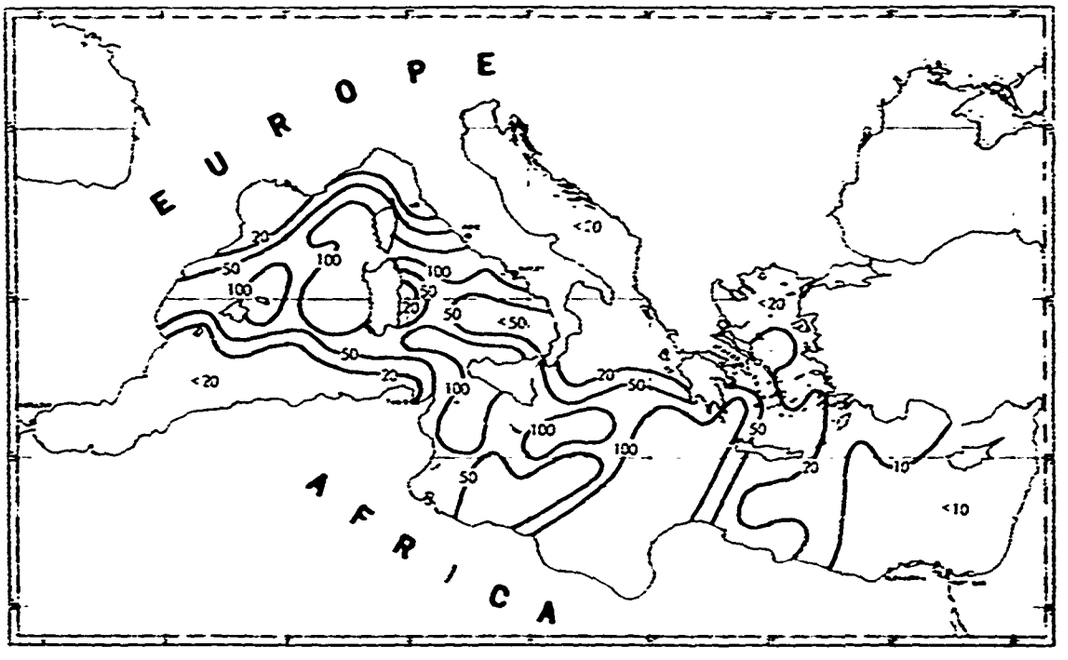

Figure 3.1.6-2. Mean Sonic Layer Depth, Spring

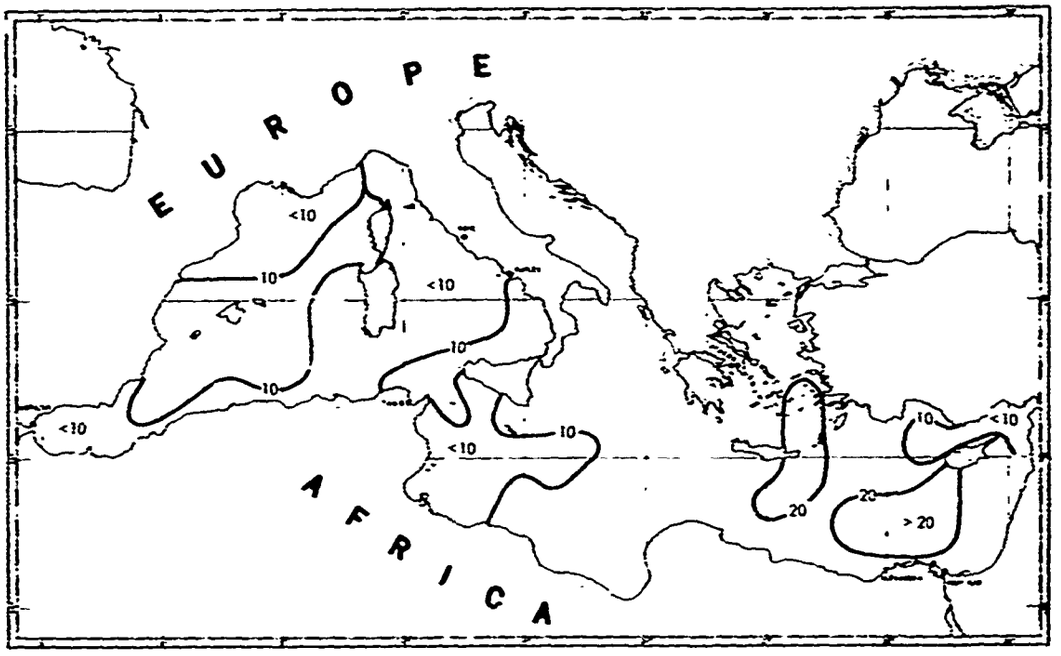

Figure 3.1.6-3. Mean Sonic Layer Depth, Summer

Figure 3.1.6-4. Mean Sonic Layer Depth, Autumn

(U) Increased surface cooling and wind mixing erode the thermocline during autumn. Although SLD generally ranges from 20 to 50 meters (figure 3.1.6-4), local variation will occur because of variance in meteorological conditions.

(U) The annual march of SLD in the Western Mediterranean, Ionian Sea, and Levantine Basin is shown in figures 3.1.6-5 through 3.1.6-7. Mean monthly SLD is indicated by the solid line, 95 percent limits by the broken lines. Number of observations, frequency of zero SLD, and frequency of SLD at or greater than 300 m is given below each figure. Despite minor differences in the data, several factors are evident:

a. Maximum SLD occurs in February or March and minimum SLD in June or July.

b. Variability is greatest in April and least in June or July.

c. Zero SLD occurs most frequently in May but never exceeds 40 percent of the observations.

d. The frequency of SLD at or greater than 300 meters is greater than 75 percent in the western Mediterranean during winter in contrast to less than 50 percent in the Levantine Basin.

REFERENCES

1. Anderson, E.R. 1971. Comparison of Mediterranean Sea sound-velocimeter measurements with sound speeds calculated from Wilson's equation (U). NUC Tech. Pub. no. 217, San Diego, California, (CONFIDENTIAL)

2. Audet, J.J., Jr. and Vega, G.G. 1974. AESD sound speed profile retrieval system (RSVP). AESD Tech. Note no. 74-03, Washington, D.C., (in press)

3. Fenner, D.F. 1968. Environmental data requirements and surveillance parameters for the Mediterranean Sea (U). USOC Requirements Document, NAVOCEANO, Washington, D.C., (SECRET-NOFORN-LIMDIS)

4. Lacombe, H. and Tchernia, P. 1972. Caracteres hydrologiques et circulation des eaux en Mediterranean. In: The Mediterranean Sea, A Natural Sedimentation Laboratory, ed. Stanley, D.J., Dowden, Hutchinson, and Ross, Inc., Stroudsburg, Pennsylvania, p. 25, (in French)

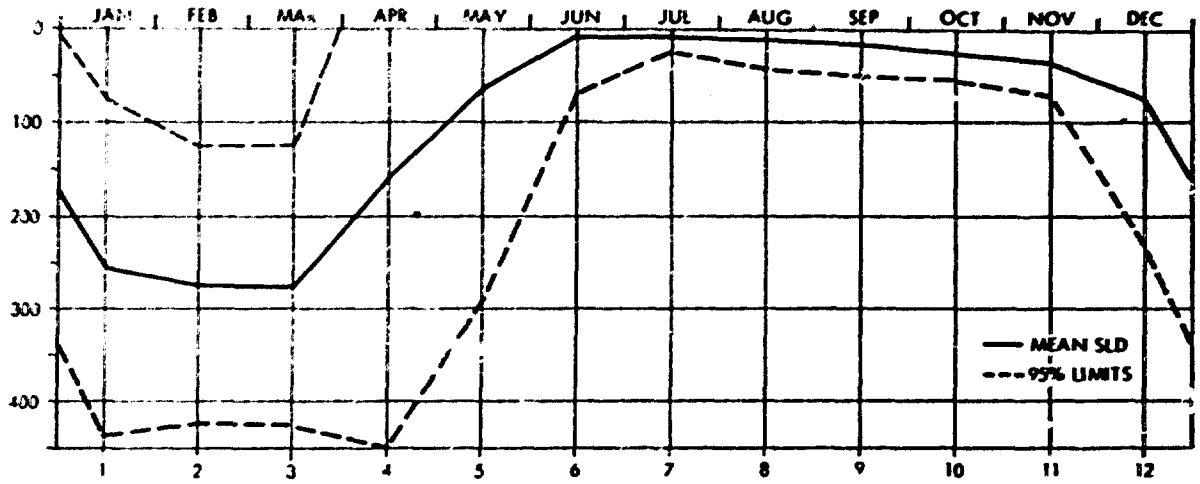

NUM Obs	240	215	314	263	327	326	478	515	397	287	405	384
% ZERO SLD	0	1.8	1.9	22.4	29.7	23.9	18.2	22.1	12.1	11.1	4.4	1.1
% SLD ≥ 300M	77.5	87.0	86.6	50.2	16.8	0.9	0.	0.2	0.3	0.	0.	9.8

Figure 3.1.6-5. Monthly SLD Data, Western Mediterranean

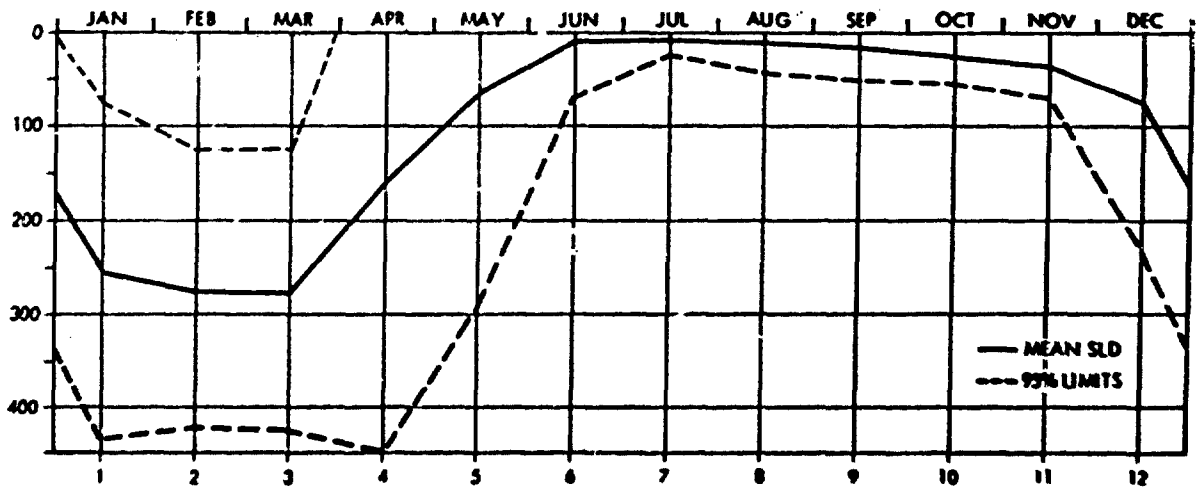

NUM Obs	180	173	144	327	452	320	283	493	377	277	548	215
% ZERO SLD	0	0	0.7	12.5	35.4	18.8	13.4	13.4	6.6	5.4	2.7	1.4
% SLD ≥ 300M	45.0	60.1	65.3	51.4	3.3	0.	0.	0.	0.	0.	0.2	1.4

Figure 3.1.6-6. Monthly SLD Data, Ionian Sea

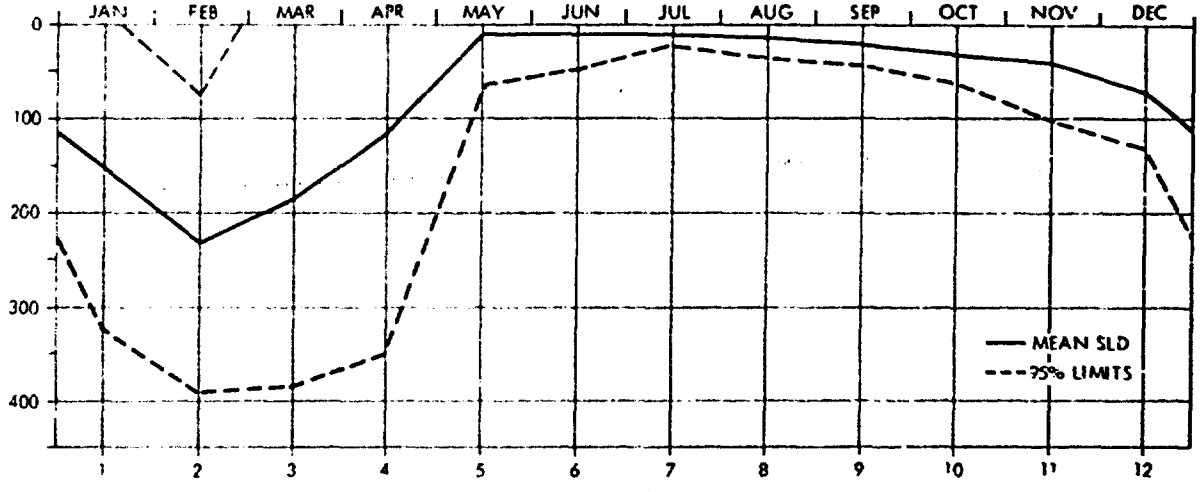

NUM Obs	86	59	136	110	105	275	72	82	656	510	297	135
% ZERO SLD	0	0	0.7	13.6	39.0	18.9	12.5	13.4	4.6	2.4	3.0	2.2
% SLD ≥ 300M	16.3	47.5	32.4	23.6	1.0	0	0	0	0	0	0	0.7

Figure 3.1.6-7. Monthly SLD Data, Levantine Basin

5. Matthews, D.J. 1939. Tables of the velocity of sound in pure water and sea water for use in echo-sounding and sound-ranging, British Admiralty Hydrographic Dept., London

6. Oren, O.H. 1971. The Atlantic Water in the Levant Basin and on the Shores of Israel. Cah. Oceanogr., 23(3), p. 291

7. Tracor, Inc. 1974. Mediterranean data catalog (U). Rockville, Maryland, (CONFIDENTIAL)

8. Wilson, W.D. 1960. Equation for the speed of sound in seawater. J. Acous. Soc. Am., p. 1357

9. Wust, G. 1961. On the vertical circulation of the Mediterranean Sea. J. Geophys. Res., 66(10)

3.2(U) Sound Transmission (U)

3.2.1(U) General (U). In considering the transmission of sound from a source to a receiver, one is interested primarily in the paths over which the sound travels and the propagation loss over these paths. Propagation loss is a measure of the change in sound level as a function of range from the source. It is usually expressed in dB relative to the source level at 1 yd. Propagation loss is the combined effect of losses produced by attenuation (conversion of sound energy into heat), by reflections from the surface and bottom, by scattering from inhomogenieties in the water medium, and by spreading.

(U) The interpretation of a propagation loss measurement is a complex process of combining sound levels arriving at a field point over all physically possible paths from the source to that point. These paths can be combinations of reflections from the surface and bottom with refracted trajectories in between, i.e. they include a variety of propagation modes. The nature of the refracted trajectories depends on the complex sound velocity structure discussed in section 3.1. It is, therefore, not generally possible to assess propagation loss without the benefit of automated models.

(U) A subject of continuing interest is the combination of propagation loss data and modeling results to develop ground rules for interpreting environmental parameters that can be measured by the operational Fleet. These rules can then be used in situ to modify computer generated predictions whenever the environment deviates from the historical or synoptic environmental data used in the predictions supplied to Fleet units. This process, however, becomes manually unmanageable rather quickly, and even the handling of the simpler situations has not been developed to a high degree.

(U) In this section, sound transmission in the Mediterranean Sea is characterized as far as the number, consistency, and extent of the measurements allow. Section 3.2.2 contains a summary of attenuation measurements, for which the results obviously apply to any propagation mode. Section 3.2.3 contains a discussion of the present understanding of the bottom reflection process and the manner in which its effects are summarized. In section 3.2.4, volume scattering and bottom backscattering effects are summarized. In section 3.2.5, the variability of surface duct (and cross-layer) propagation is described. In section 3.2.6, a few summary results of convergence zone propagation are given. And finally, in section 3.2.7, long range low frequency propagation loss measurements are summarized.

3.2.2(U) Attenuation (U). The attenuation of sound in sea water has been investigated extensively, both theoretically and experimentally. A summary of the measurements for the Mediterranean Sea (Leroy, 1967) is shown in figure 3.2.2-1. The curve in the figure can be expressed empirically as

$$\alpha = \frac{0.155 f_r f^2}{f_r^2 + f^2} + 0.006 f^2$$

where α is the attenuation in dB/km, f is the frequency in kHz and $f_r = 1.7$ kHz.

REFERENCES

1. Leroy, C.C. 1967. Sound propagation in the Mediterranean Sea. Albers. V. Underwater Acoustics, Vol. 2, Plenum Press, New York

2. Marsh, H.W. 1963. Attenuation of explosive sounds in sea water. J. Acoust. Soc. Am. 35, 11, p. 1837

3. Schulkin, M. and Marsh, H.W. 1962. Sound absorption in sea water. J. Acoust. Soc. Am. 34, 6, p. 864

4. Sheehy, M.J. and Halley, R. 1957. Measurement of the attenuation of low-frequency underwater sound. J. Acoust. Soc. Am., 29, 4, p. 464.

5. Thorp, W.H. 1965. Deep ocean sound attenuation in the sub-and low kilocycle-per-second region. J. Acoust. Soc. Am., 38, 4, p. 648

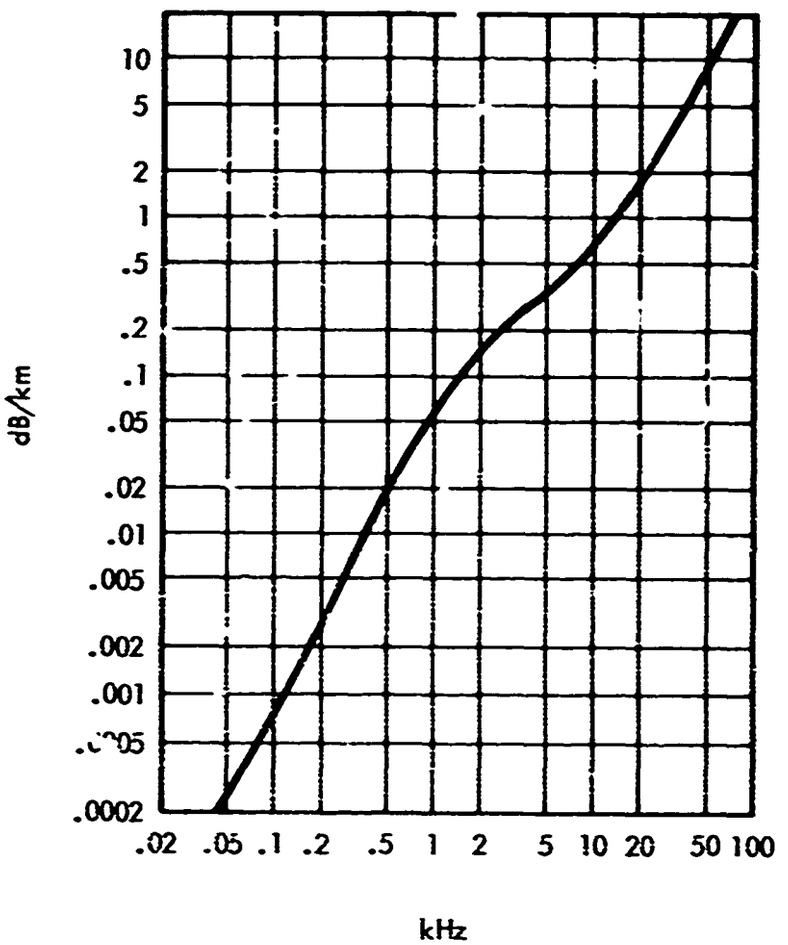

Figure 3.2.2-1. Summary of Attenuation Measurements Below 100 kHz

3.2.3(C) Botton Reflection Loss (U)

3.2.3.1(U) Introduction (U). Botton reflection loss is defined as the residual propagation loss after spreading and absorption losses have been accounted for, when a sound signal travels from source to receiver via a botton reflected path. The reflection angle is called the grazing angle. Evidently, knowledge of the magnitude of the bottom reflection loss as a function of grazing angle for any given geographic location is of vital importance in the prediction or evaluation of sonar performance for those acoustic sensors which may employ a botton bounce mode of operation.

3.2.3.2(U) Development of Standard Bottom Reflection Loss Curves (U). The extensive variability which has been observed in botton reflection loss versus grazing angle at various geographic locations and the natural assumption that the magnitude of the botton reflection loss must be heavily dependent on the quality of the botton has led to attempts to correlate bottom reflection loss characteristics with the associated physiographic provinces. To this end, the bottom reflection loss versus grazing angle curves from more than 1300 acoustic stations of MGS and ASW/USW surveys in diverse ocean areas were analyzed by NAVOCEANO and correlated with their corresponding physiographic province, initially for a frequency of 3.5 kHz, 100 Hz bandwidth, but later extended to also include 1/3 octave band results at frequencies of 0.01, 0.05, 1.0, 2.0 and 3.5 kHz. The data for these analyses were extracted from broadband recordings of SUS signals recorded on a shallow hydrophone. Grazing angles ranged between 3 and 90 degrees.

(C) The end result of this effort produced a grouping of the data into 9 distinct categories of botton reflection loss versus grazing angle, each of which was fitted with a fourth degree polynomial using 0.1 degree averaging of the grazing angle. These curves are shown in figure 3.2.3-1. These nine curves have since been designated as the Navy Interim Standard Bottom Loss Curves for the Frequency Range 1.0 to 3.5 kHz. The results of these analyses are reported in Reference 3 (Christensen, Frank and Kaufman, 1974).

(U) The numeric designator of each of these nine curves is also the numeric designator to be used for labeling the corresponding botton loss province for which the curve represents the average bottom loss characteristics. The curves are therefore commonly referred to as "Botton Loss Province Curves".

(C) For frequencies below 1.0 kHz, FNWC developed the Botton Loss Curve (0.5 kHz), and the Botton Loss Curve (0.1 kHz), shown in figure 3.2.3-2. These curves are currently the Navy Standard for these frequencies. The results are based on the 1963 MGS stations and were reported in 1970 by Bassett and Wolff (reference 2). The numeric

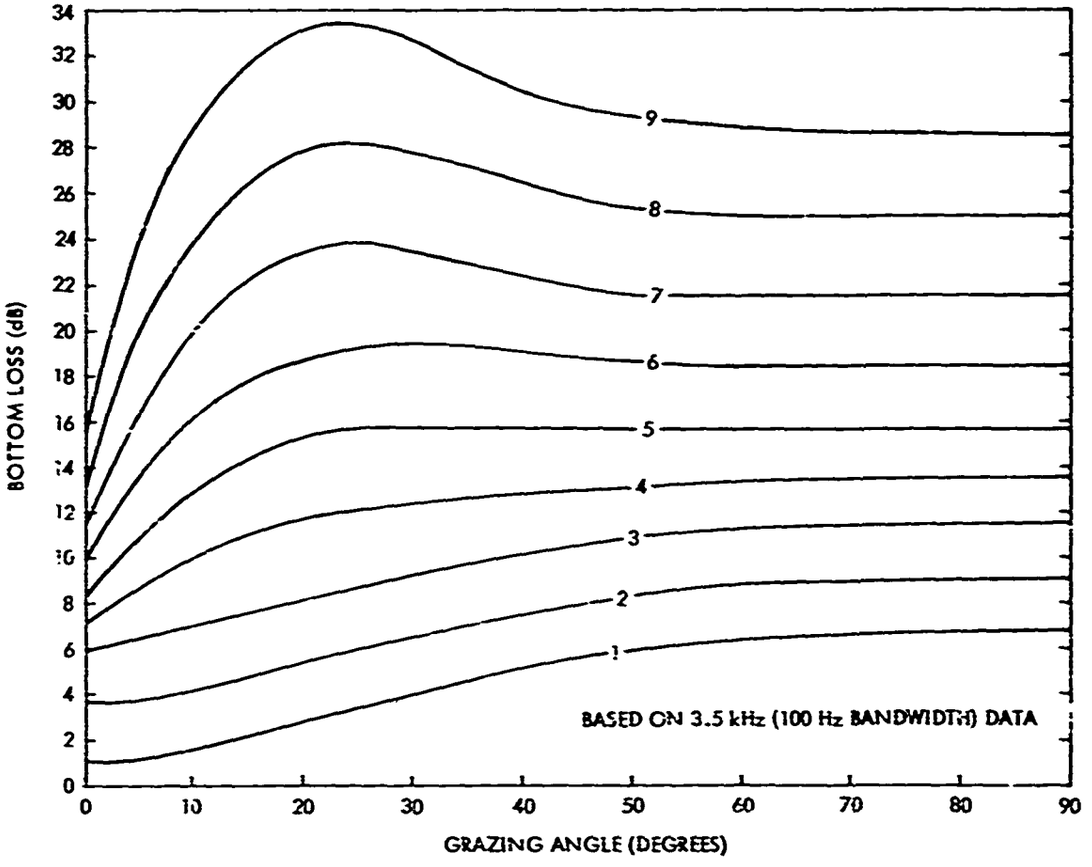

Figure 3.2.3-1(C). Navy Interim Standard Bottom Loss Curves for the Frequency Range 1.0 to 3.5 kHz (U)

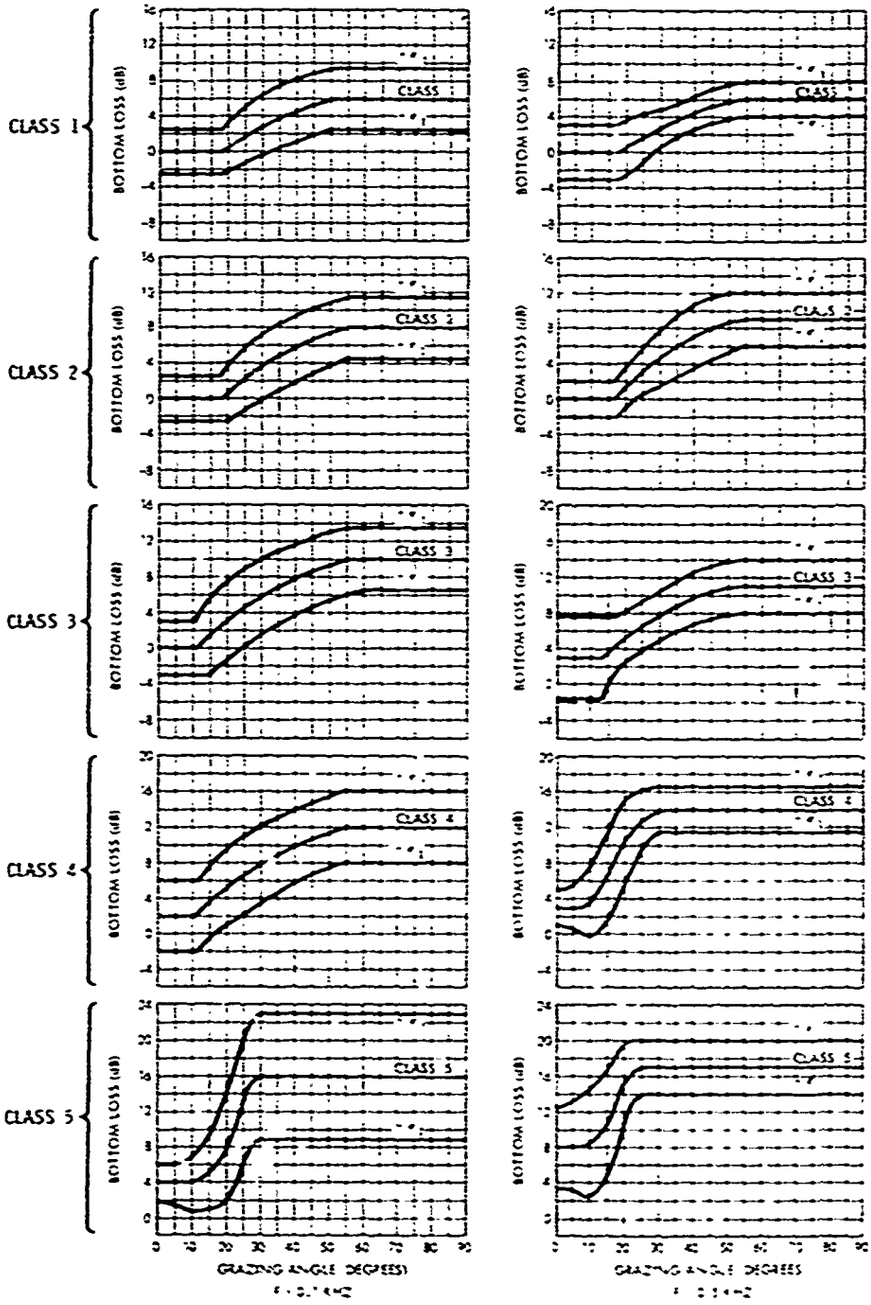

Figure 3.2.3-2(C). Bottom Loss Curves for the Frequencies 0.1 kHz and 0.5 kHz (U)

designators of these curves, like those of figure 3.2.3-1, also correspond to those of the Bottom Loss Province to be associated with it, except that Bottom Loss Provinces 4 through 9 are all characterized by the fifth classification curve of figure 3.2.3-2.

(C) There is evidence, based on Fleet experience, that observed bottom reflection losses may be less than those which are given by figure 3.2.3-2. Additional analyses at these lower frequencies are now being carried out by NAVOCEANO.

3.2.3.3(C) Development of the Bottom Loss Province Chart (U). For the Mediterranean area, bottom reflection loss measurements have been reported for more than 125 sites since 1960. The locations of these sites are shown in figure 3.2.3-3. A description of the various measurements is given in the Data Catalog (MC Report 103, 1974). These data were used in the development or validation of the nine bottom reflection loss curves discussed in the previous section and then in the production of the Bottom Loss Province Chart for North Atlantic Region 8, which includes the Mediterranean Sea.

(U) All of the stations comprising the MGS and ASW/USW data base were plotted (identified by their assigned bottom loss classification designator) on the appropriate Standard Navy Ocean Area Chart. This chart was overlaid by a physiographic province chart developed for the same area and contours were drawn, maintaining a judicious awareness of the physiographic province boundaries to delineate areas having the same bottom loss classification. Physiographic provinces containing groupings of stations representing different bottom loss classifications were contoured to show the areal distribution within the province of each different classification. Likewise, physiographic province boundaries were overridden when a continuum of stations having the same bottom loss classification spanned the boundary between adjacent provinces. The resulting bottom loss province chart for the Mediterranean is shown in figure 3.2.3-4. This chart was a primary input in the development of the Standard ASW Prediction Area Chart (figure 1.0-1, p. 3) which is shown in figure 3.2.3-4 in color.

3.2.3.4(U) Use of the Standard Bottom Reflection Loss Curves and Bottom Reflection Loss Province Charts (U). Data have been reported by Chapman and Keil (8) and Hanrahan (7) in 1971 from which a table can be constructed which correlates bottom loss province category with a qualitative evaluation of the observed performance of the AN/SQS-26 (AXR and CX) sonar for both the search and track modes in the Mediterranean Sea and the Atlantic and Pacific Oceans. The results are given in table 3.2.3-I. Note that the performance in the Mediterranean is one category better than for the same province in the Atlantic and Pacific. This is due primarily to the fact that the Mediterranean is shallower and hence there is less transmission loss along the propagation path.

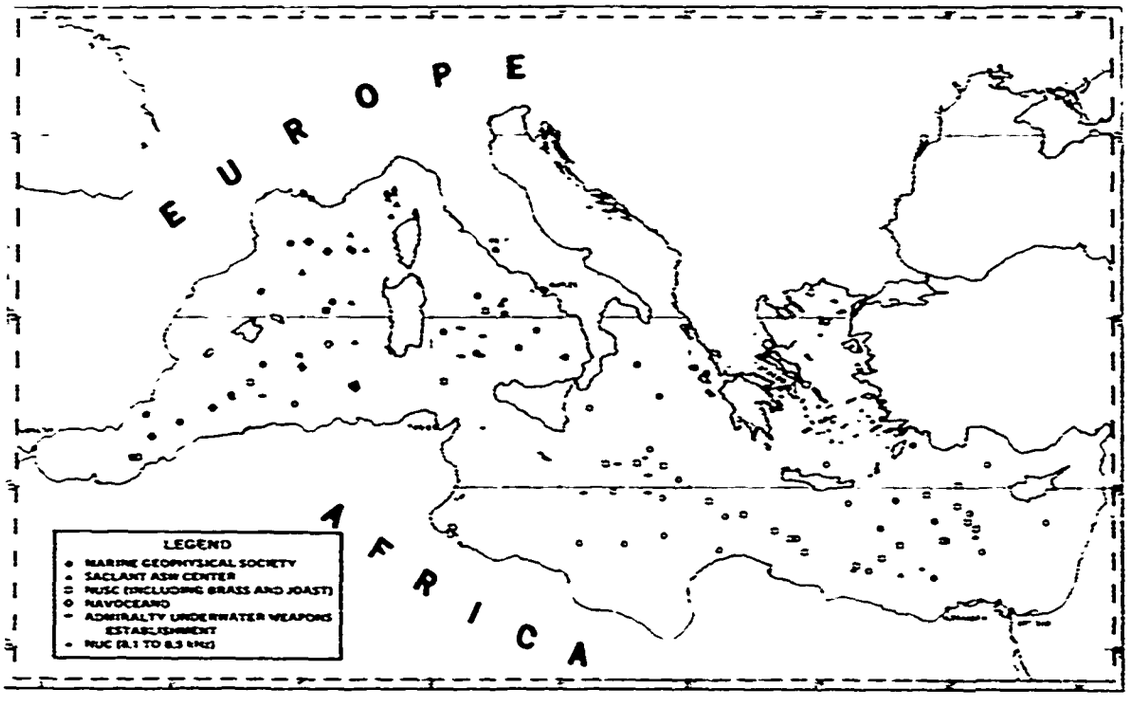

Figure 3.2.3-3. Major Bottom Loss Measurements Stations in the Mediterranean

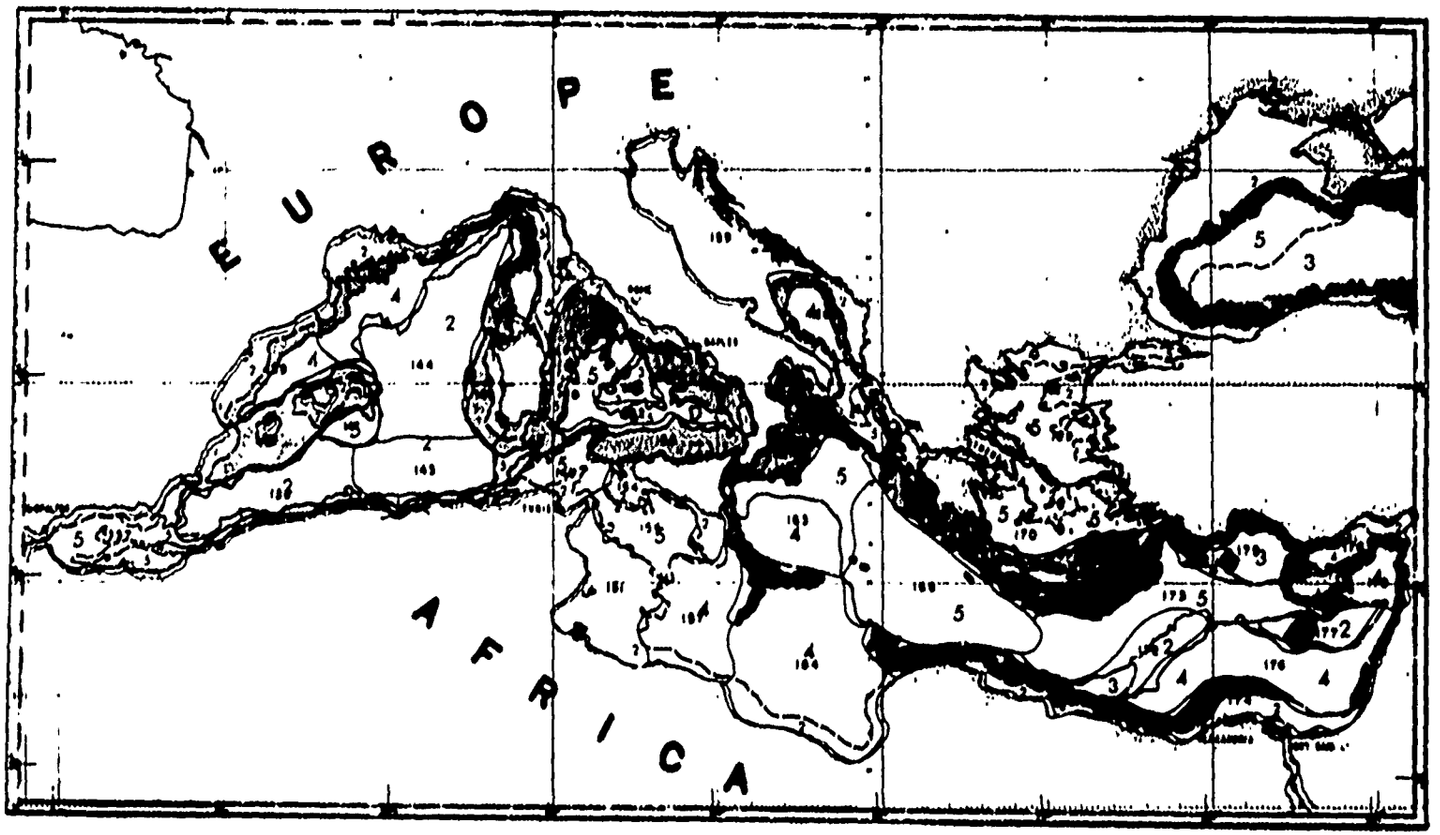

Figure 3.2.3-4(C). Bottom Loss Province Chart for the Mediterranean Sea (U)

CONFIDENTIAL

TABLE 3.2.3-I (U)

EXPECTED BOTTOM BOUNCE PERFORMANCE OF THE AN/SQS-26 (AXR AND CX) SONARS (CHAPMAN & KIEL, 1971; HANRAHAN, 1971) (U)

Bottom Loss Province Category	Mediterranean		Atlantic and Pacific	
	Search Mode	Track Mode	Search Mode	Track Mode
1	Excellent	Excellent	Excellent	Excellent
2	Excellent	Excellent	Good	Excellent
3	Good	Excellent	Fair	Good
4	Fair	Good	Marginal	Fair
5	Marginal	Fair	Unusable	Marginal
6	Unusable	Marginal	Unusable	Unusable
7-9	Unusable	Unusable	Unusable	Unusable

(C) The Navy Interim Standard Bottom Loss Curves for 1.0 to 3.5 kHz (figure 3.2.3-1) have been incorporated into the Fast Asymptotic Coherent Transmission (FACT) model and are used for computing SHARPS II and ASRAPS III outputs above 1.0 kHz. They are also employed by NAVOCEANO in the classification of acoustic stations collected by on-going surveys, with the results being incorporated into updates of the Bottom Loss Province Charts. As mentioned above and shown in figure 3.2.3-4, the Bottom Loss Province Charts are a primary input to the development of the Standard ASW Prediction Charts.

(C) It should be borne in mind that both the Bottom Loss Province Charts and the ASW Prediction Charts were developed for the specific frequency range 1.0 to 3.5 kHz. When frequencies below this range are being considered, both bottom loss province boundaries and classifications tend to degrade. Efforts are currently underway at NAVOCEANO to investigate the feasibility of developing Bottom Loss Province Charts for these lower frequencies.

REFERENCES

1. Acoustic Station Results: MGS Program 1965-67, 1967. Mediterranean Task Area 6; Vol. 2 (U). Texas Instruments, Inc., Special Publication 95-6-2, CONFIDENTIAL

2. Bassett, C.G, Wolff, P.M. 1970. Fleet numerical weather central bottom loss values (U). FNWC Tech Note 58, CONFIDENTIAL

3. Chapman, R.C., Keil, J.G. 1971. Operating doctrine for the AN/SQS-26 system. NUSC Pub. No. NL-4053, CONFIDENTIAL

4. Christensen, R.E., Frank, J, and Kaufman, O. 1974. Navy Interim Standard bottom loss curves at frequencies from 1.0 to 3.5 kHz (U). NAVOCEANO Technical Report 232, CONFIDENTIAL

5. Davis, E.E., O'Neill, C.J. 1973. Bottom reflection loss measurements made from aircraft in the western Mediterranean Sea (U). NAVOCEANO Technical Note 6130-09-73, CONFIDENTIAL

6. Hanrahan, J.J. 1971. AN/SQS-26(AXR) and AN/SQS-35 detection trials in the Mediterranean Sea, 3-16 August 1970 - Results of Phase II, JOAST (Joint Oceanographic Acoustic and System Tests) (U). NUSC Report 4105, CONFIDENTIAL

7. Hanrahan, J.J., Bell, T.G, and Podeszwa, E.M. 1967. Methods for estinating the performance of the AN/SQS-26 (XN-2) sonar (U). USL Report No. 843, CONFIDENTIAL

8. Hanrahan, J.J., Podeszwa, E.M., Rembetski, F.E., and Fries, T.O. 1973. Bottom bounce echo-ranging trials of the AN/SQS-26(AXR) in the eastern Mediterranean, September 1971 (U). NUSC Technical Report 4555, CONFIDENTIAL

9. Hastrup, O.F., Lallement, B. 1969. Acoustic reflectivity measurements in the Mediterranean Sea (U). SACLANT NATO Technical Report 152, CONFIDENTIAL

10. Hastrup. O.F. 1972. The reflection of sonar and explosive pulses from the sea floor (U). SACLANT NATO Technical Report 216, CONFIDENTIAL.

11. Keir, D. Integrated Mediterranean Program (IMP-70). NUC (via personal communication from T. Sullivan, Code 6130, NAVOCEANO)

12. Podeszwa, E.M. 1971. Acoustic province charts based on Marine Geophysical survey bottom loss data (U). NUSC Report 4045, CONFIDENTIAL

13. Reynolds, T.N., Pryce, A.W. 1961. Acoustic propagation in the Atlantic and Mediterranean - Autumn 1960 (U). A.U.W.E. Tech. Note 32/61, CONFIDENTIAL

14. Texas Instruments, Incorporated, 1967. Reverberation (U). SP-95-6-4, Volume 4, Area 6, U.S. Naval Oceanographic Office, Suitland, Maryland, CONFIDENTIAL

15. Weaver, H.R., Geary, J.E., et. al. 1968. The bottom reflection active sonar system (BRASS) program, part II (U). USL Report No. 866-II, CONFIDENTIAL

3.2.4(C) Reverberation in the Mediterranean Sea (U)

3.2.4.1(U) Volume Scattering (U). There are two measures of volume reverberation. One is the scattering strength S_v of the cubic yard of water in decibels. The second is the scattering strength S_c of a column of water extending from the water surface to the bottom and having a cross-section of one square yard. S_c is also in decibels.

(U) Volume reverberation is primarily a biological phenomenon which varies from day to night and from season to season, as well as with geographic location, sonar frequency, and depth. In order to examine variations with time, location, and frequency, the depth variations are eliminated by using the column strength, S_c. In the Mediterranean, S_c's at any given location and time are similar for frequencies from 6 kHz to 10 kHz and from 12 kHz to 20 kHz. Thus, table 3.2.4-I gives values of S_c for summer, day and night, and winter, day and night, for 3.5, 5, 6 to 10, and 12 to 20 kHz. Measurements have not been made in each province. Rather, values for provinces with no data have been predicted from the values in adjacent provinces on the basis of oceanographic information. Provinces for which no values are given are in relatively shallow water where no measurements have been made. Winter has been considered to be from November through March and summer from May through September.

(U) When knowledge of the depth dependent characteristics of volume scattering is required, S_v values must be utilized. Few measurements of S_v have been made in the Mediterranean. Table 3.2.4-II gives scattering layer depths and the maximum S_v in the layer for almost every known measurement. Values cannot be predicted accurately in provinces other than those in which measurements have been made.

3.2.4.2(C) Bottom Backscatter (U). The location of 44 bottom backscattering stations for the Mediterranean Sea at a frequency of 3.5 kHz and having grazing angles 30° to 65° are shown in figure 3.2.4-1. The 3.5 kHz bottom backscattering data were grouped into four groups (A, B, C, and D) having similar backscattering strength versus grazing angle characteristics. Table 3.2.4-III shows the mean values (dB) and standard deviations (dB) for 5° intervals for each of the four groups and for all 44 stations. In addition, fourth order polynomial fit values (dB) at 5° increments and the standard deviation (dB) are given. These data are shown also in figure 3.2.4-2.

(U) The chart (figure 3.2.4-1) shows the backscattering group of each station. Since the data are highly variable in some areas, the following prediction procedure is recommended:

a. For locations near a station or in an area having similar scattering characteristics (A-B, B-C, or C-D), choose the appropriate group - Mean value.

TABLE 3.2.4-I (SUMMER) (C). SCATTERING STRENGTH S_c, IN dB FOR THE MEDITERRANEAN ASW PREDICTION AREAS (U)

Province	Day 3.5 kHz	Night 3.5 kHz	Day 5.0 kHz	Night 5.0 kHz	Day 6-10 kHz	Night 6-10 kHz	Day 12-20 kHz	Night 12-20 kHz
137	-60	-51	-52	-44	-55	-51	-50	-46
138	-60	-49	-49	-45	-50	-50	-50	-48
139	-58	-57	-48	-50	-50	-51	-51	-49
140	-60	-49	-49	-45	-50	-52	-50	-48
141	-60	-49	-49	-45	-50	-50	-50	-48
142	-58	-57	-48	-50	-50	-52	-53	-49
143	-60	-49	-49	-45	-50	-50	-50	-48
144	-58	-57	-48	-50	-50	-52	-53	-49
145	-58	-57	-48	-50	-50	-52	-53	-49
146	-58	-57	-48	-50	-50	-52	-53	-49
147	-	-	-	-	-	-	-	-
148	-65	-57	-54	-48	-54	-51	-50	-49
149	-	-	-	-	-	-	-	-
150	-65	-57	-54	-48	-54	-51	-50	-49
151	-	-	-	-	-	-	-	-
152	-65	-57	-54	-48	-54	-51	-50	-49
153	-65	-57	-54	-48	-54	-51	-50	-49
154	-	-	-	-	-	-	-	-
155	-	-	-	-	-	-	-	-
156	-65	-57	-54	-48	-54	-51	-50	-49
157	-	-	-	-	-	-	-	-
158	-65	-57	-54	-48	-54	-51	-50	-49
159	-	-	-	-	-	-	-	-
160	-	-	-	-	-	-	-	-
161	-61	-57	-51	-46	-50	-54	-48	-49
162	-66	-53	-55	-42	-55	-49	-48	-49
163	-64	-55	-54	-44	-53	-52	-48	-49
164	-61	-57	-51	-46	-50	-54	-48	-49
165	-66	-48	-55	-41	-55	-45	-48	-46
166	-65	-58	-55	-48	-54	-53	-52	-49
167	-66	-49	-55	-44	-54	-49	-52	-49
168	-64	-59	-55	-49	-54	-52	-53	-50
169	-	-	-	-	-	-	-	-
170	-	-	-	-	-	-	-	-
171	-63	-57	-55	-48	-53	-51	-51	-50
172	-68	-57	-59	-48	-57	-51	-51	-50
173	-68	-57	-59	-48	-57	-51	-51	-50
174	-74	-57	-63	-48	-60	-60	-51	-50
175	-74	-57	-63	-48	-57	-60	-51	-50
176	-74	-57	-63	-48	-57	-60	-51	-50
177	-74	-57	-63	-48	-57	-60	-51	-50
178	-74	-57	-63	-48	-57	-60	-51	-50
179	-74	-57	-63	-48	-57	-60	-51	-50

TABLE 3.2.4-I (WINTER) (C). SCATTERING STRENGTH S_c, IN dB FOR THE MEDITERRANEAN ASW PREDICTION AREAS (U)

Province	Day 3.5 kHz	Night 3.5 kHz	Day 5.0 kHz	Night 5.0 kHz	Day 6-10 kHz	Night 6-10 kHz	Day 12-20 kHz	Night 12-20 kHz
137	-53	-53	-47	-47	-49	-46	-47	-47
138	-53	-53	-47	-47	-49	-46	-47	-47
139	-57	-56	-49	-49	-50	-49	-50	-50
140	-53	-53	-	-47	-49	-46	-47	-47
141	-53	-53	-47	-47	-49	-46	-47	-47
142	-57	-56	-49	-49	-50	-49	-50	-50
143	-53	-53	-47	-47	-49	-46	-47	-47
144	-57	-56	-49	-49	-50	-49	-50	-50
145	-57	-56	-49	-49	-50	-49	-50	-50
146	-57	-56	-49	-49	-50	-49	-50	-50
147	-	-	-	-	-	-	-	-
148	-58	-53	-49	-46	-50	-48	-50	-49
149	-	-	-	-	-	-	-	-
150	-58	-53	-49	-46	-50	-48	-50	-49
151	-	-	-	-	-	-	-	-
152	-56	-53	-49	-46	-50	-46	-50	-49
153	-58	-53	-49	-46	-50	-46	-50	-49
154	-	-	-	-	-	-	-	-
155	-	-	-	-	-	-	-	-
156	-58	-53	-49	-46	-50	-46	-50	-49
157	-	-	-	-	-	-	-	-
158	-58	-53	-49	-46	-50	-46	-50	-49
159	-	-	-	-	-	-	-	-
160	-	-	-	-	-	-	-	-
161	-60	-58	-50	-49	-53	-50	-53	-51
162	-60	-58	-50	-49	-53	-50	-53	-51
163	-60	-58	-50	-49	-53	50	-53	-51
164	-60	-58	-50	-49	-53	-50	-53	-51
165	-60	-58	-50	-49	-53	-50	-53	-51
166	-59	-55	-51	-50	-56	-50	-56	-51
167	-60	-56	-50	-49	-54	-50	-54	-50
168	-58	-55	-51	-50	-54	-50	-54	-50
169	-	-	-	-	-	-	-	-
170	-	-	-	-	-	-		-
171	-58	-56	-51	-50	-53	-50	-53	-51
172	-58	-57	-51	-50	-52	-52	-52	-52
173	58	-57	-51	-50	-52	-52	-52	-52
174	-58	-57	-51	-50	-51	-54	-51	-53
175	-58	-57	-51	-50	-51	-54	-51	-53
176	-58	-57	-51	-50	-51	-54	-51	-53
177	-58	-57	-51	-50	-51	-54	-51	-53
178	-58	-57	-51	-50	-51	-54	-51	-53
179	-58	-57	-51	-50	-51	-54	-51	-53

TABLE 3.2.4-II(C). SCATTERING LAYER DEPTHS AND MAXIMUM SCATTERING STRENGTH PER CUBIC YARD (S_V) WITHIN THE LAYER. (U)
(DEPTH IN YARDS X 10^{-2}, S_V IN dB/YD^3)

WINTER

Province	3.5 kHz				5 kHz				6 to 10 kHz				12 to 20 kHz			
	Day		Night		Day		Night		Day		Night		Day		Night	
	Depth	Max S_v	Depth	Max S_v	Depth	Max S_v	Depth	Max S_v	Depth	Max S_v	Depth	Max S_v	Depth	Max S_v	Depth	Max S_v
138			0-3 8-11	-77			0-3 8-11	-71			0-9	-67			0-4	-71
142													2-6	-72	0-3 6-7.5	-74
144	8-12	-80	0-1 8-12	-80	3-12	-74	9-10	-75	3-10	-75	9-10	-73	3-9	-73	0-5	-74
158	5-12	-84	0-4	-80	5-12	-74	0-6	-71	4-11	-76	0-6	-70	0-7	-76	0-4	-71
163	5-11	-83	0-2 8-10	-82	4-12	-76	0-5 5	-73	4-10	-76	-03	-10	0-2 4-8	-78	0-3	-74
173	4-10	-82	0-5	-83	5-11	-78	0-2 5-11	-76	4-9	-77	0-3	-71	3-8	-76	0-2	-72

SUMMER

Province	3.5 kHz				5 kHz				6 to 10 kHz				12 to 20 kHz			
	Day		Night		Day		Night		Day		Night		Day		Night	
	Depth	Max S_v	Depth	Max S_v	Depth	Max S_v	Depth	Max S_v	Depth	Max S_v	Depth	Max S_v	Depth	Max S_v	Depth	Max S_v
138													3.5-5	-70	0-1.5	-64
140			0-1.5	-69											0-1.5	-60
141			0-1	-70											0-3	-66
142													3-5	-72	0-4	-72
144			0-1	-69									0-1 3-5	-72	0-1	-70
156			0-2	-67												
163			0-1.5	-67												
166			0-1.5	-72												
173			0-1.5	-64												

TABLE 3.2.4-III(C). 3.5 kHz BOTTOM BACKSCATTERING STRENGTH IN dB VERSUS GRAZING ANGLE (U)

3.5 kHz BOTTOM BACKSCATTERING STRENGTH IN dB VERSUS GRAZING ANGLE (U).

X	30°		35°		40°		45°		50°		55°		60°		65°	
	X̄	σ	X̄	σ	X̄	σ	X̄	σ	X̄	σ	X̄	σ	X̄	σ	X̄	σ
A (Mean)	-29.8	1.9	-28.8	2.2	-27.7	1.3	-26.2	1.9	-25.8	0.9	-27.8	2.2	-25.7	0.8	-26.1	5.2
A (fit) σ=2.3	-30.2		-28.4		-27.4		-27.0		-26.9		-26.9		-26.7		-26.0	
B (Mean)	-38.1	1.7	-36.0	1.5	-34.5	1.3	-33.1	1.4	-32.4	1.4	-28.4	1.8	-24.4	3.4	-	-
B (fit) σ=1.7	-38.2		-36.1		-34.3		-33.0		-32.3		-28.9		-25.5		-19.4	
C (Mean)	-41.8	2.4	-40.4	2.1	-38.7	2.1	-37.1	2.3	-34.7	3.2	-31.5	2.5	-27.5	3.4	-24.4	5.0
C (fit) σ=2.4	-42.2		-40.6		-38.8		-37.1		-35.1		-32.4		-28.1		-22.4	
D (Mean)	-47.3	3.6	-46.2	3.8	-45.6	3.7	-43.1	2.3	-40.4	3.1	-36.2	2.7	-29.0	4.3	-29.8	3.9
D (fit) σ=3.3	-47.3		-46.7		-45.4		-43.4		-40.5		-36.6		-31.4		-24.9	
All points (Mean)	-40.6	4.7	-39.6	5.0	-38.0	5.6	-36.7	4.9	-34.7	4.5	-32.1	3.6	-27.1	3.7	-21.6	4.8
All points (fit) σ=4.7	-40.6		-39.5		-38.1		-36.6		-34.7		-32.0		-28.4		-23.6	

A - 3 stations
B -11 stations
C -21 stations
D - 9 stations
Total -44 stations

X(MEAS) = Mean bottom backscattering strength in dB, standard deviations (dB) = σ

X(FIT) = Bottom backscattering strength in dB from 4th order polynomical fitting of data, standard deviation (dB) = σ

Figure 3.2.4-1(C). 44 Bottom Backscattering Stations:
A, B, C, D Are Groups For 3.5 kHz (U)

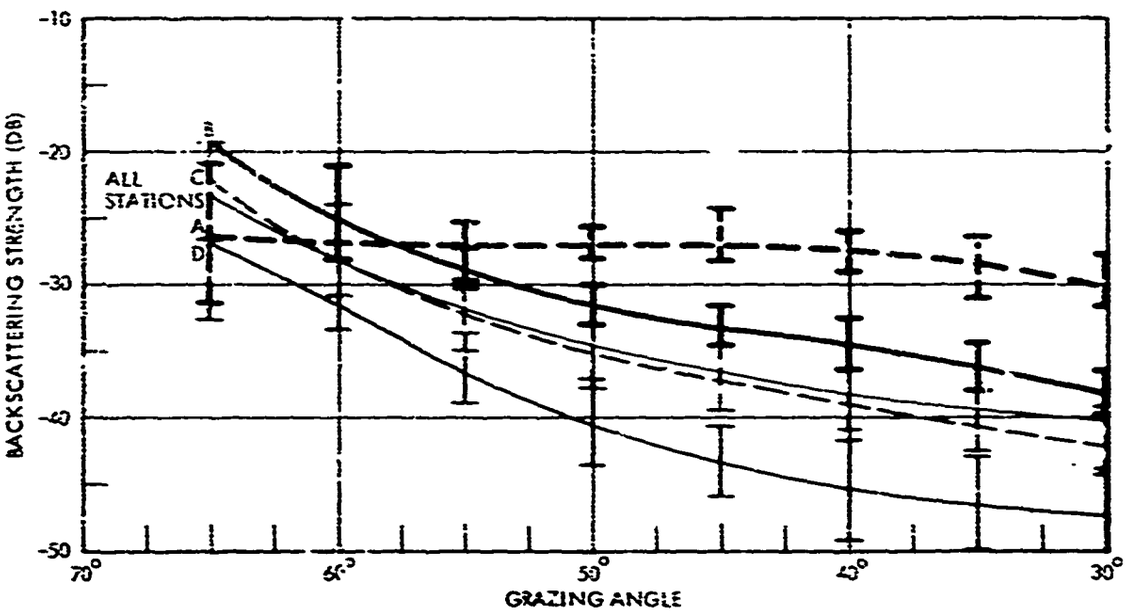

Figure 3.2.4-2(C). 44 Bottom Backscattering Stations:
A, B, C, D Are Groups For 3.5 kHz (U)

b. For a location not close to a station and located in an area of highly variable scattering (e.g., more than 2 groups), use the 44 station group - All points - Mean value.

REFERENCES

1. Dullea, R.K. and Fisch, N.P. 1971. Volume scattering measurements in the Mediterranean Sea (U). Navy Underwater Systems Center, Newport, R.I., TM No. TA11.014-71, CONFIDENTIAL

2. Texas Instruments, Incorporated 1967. Marine geophysical survey program 1965-1967, North Atlantic Ocean, Norwegian Sea and Mediterranean Sea, Area 6, vol. 4 - reverberation. Dallas, Texas, CONFIDENTIAL

3.2.5(U) Surface Channel Propagation (U). Sonic layer depth was discussed in section 3.1.6. From figure 3.1.6-3 it can be seen that during summer the average layer depth varies between 10 and 20 meters, with a probability of having no layer at all of approximately 20% in the western Mediterranean and 10 to 13% in the Ionian Sea and Levantine Sea. The layer is therefore too thin and unstable for reliable surface channel propagation. This situation begins to improve in autumn but, as can be seen from figure 3.1.6-4, layer depths remain generally less than 50 m. In winter, figure 3.1.6-1, layer depths ranging from 100 m in the southern waters to completely isothermal water in the northern western Mediterranean can be found and surface duct propagation is at its maximum reliability. This condition deteriorates in the spring and, because of surface warming, negative gradients often exist. The maximum probability for zero layer depth exists in May, at 30% in the western Mediterranean, 35% in the Ionian Sea and 39% in the Levantine Sea.

(U) The existence of the strong negative gradient in the summer makes cross-layer detection marginal for frequencies in the kHz region. This situation again improves in winter, when the cross-layer situation does not arise in a practical sense.

(U) Propagation loss in the surface duct and for the cross-layer case has been discussed extensively elsewhere (see e.g. Reynolds, 1960). For this reason, as well as because of its high variability, it will not be discussed here.

3.2.6(U) Convergence Zone Propagation (U). From its definition (table 3.0-I) it is evident that reliable convergence zone propagation depends on the water depth being sufficient to ensure that depth excess requirements are met. This has been discussed in sections 3.1.4 and 3.1.5 and is summarized in figures 3.1.4-10 and 3.1.4-11 (in the jacket). When convergence occurs, there are several quantities associated with it that are of interest.

(U) The zone start range at the surface is determined by the surface water temperature (Leibiger, 1972), as shown in table 3.2.6-I. In the spring starting ranges vary between 10 and 35 kyd, while in summer they vary between 30 and 45 kyd through most of the Mediterranean. The range decreases with depth at approximately 6 yds/ft above the thermocline and 2 yds/ft below the thermocline (Kaufman and Axenfeld, 1964).

(U) Propagation loss is about 80 dB to the first zone and 105 to 110 dB to the second. This loss increases by about 10 dB from the surface to just below the thermocline.

TABLE 3.2.6-I(U). CONVERGENCE ZONE START RANGE AS A FUNCTION OF SURFACE TEMPERATURE (U)

Temp	R(kyd)
58°F	16
59	18.5
60	21.4
65	30.8
70	36
75	41.3
80	44.9
85	47.6

3.2.7(C) Long Range Low Frequency Propagation (U). From the discussion in section 3.1.3, it is evident that the deep sound channel is very shallow in the Mediterranean as compared to the open ocean, where it is usually found at 2000 to 4000 meters depth. This accessibility of the DSC axis with such sensors as towed arrays makes it of extreme practical importance to ASW in the Mediterranean Sea. Additionally, because the channel axis is so shallow (at the surface in much of the western Mediterranean in winter) low frequency propagation should show little seasonal variation. For a source at the summer DSC axis depth, there will be RR type propagation, while for a source at the same depth in winter, there will be RSR type propagation.

(C) A significant number of long range low frequency propagation loss measurements have been made in the Mediterranean since 1967 (Hays and Murphy, 1969), (Marshall, 1973), (Martin and Koenigs, 1973), (MC Report 015, 1973), (Schumacher, et al., 1971), (McCloskey and Gottwald, 1972) and (Weston and Horrigan, 1964). The locations of the receivers for these measurements are shown in figure 3.2.7-1. Interest has been largely centered around a shallow (nominal 60' depth) and a deep (nominal 300' depth) target with the receiver near the DSC axis. For summer conditions this corresponds roughly to the target being above the channel (or in the surface layer) or in the sound channel.

(C) Again, it is difficult to summarize these measurements without applying a significant modeling effort. It is of interest, however, to observe their general consistency. A collection of the measured data is presented in figure 3.2.7-2 for the deep source and in figure 3.2.7-3 for the shallow source. The plotted data are composed of the data obtained by Hayes (1969), IOMEDEX (Marshall, 1973), (Martin and Koenigs, 1973) and (MC Report 015, 1973), TASSRAP (McCloskey and Gottwald, 1972) and Schumacher (1971). The points were measured at frequencies ranging from 35 to 130 Hz, in all four major basins, during fall and summer, for receiver depths ranging from 110 to 615 meters, and for both SUS and CW sources. The lower short-dash line in each figure corresponds to inverse square (20 x log (range)) propagation loss. The upper long-dash line in figure 3.2.7-2 represents (arbitrarily) propagation loss given by 33 + 10 log (range).

(C) The upper long-dash line in figure 3.2.7-3 represents (arbitrarily) a propagation loss 6 dB higher than in figure 3.2.7-2 (or 39 + 10 log (range)). Inasmuch as the water medium is dynamic or constantly changing, it is significant that the total spread of all of the measurements is comparable to the spread often encountered in a single measurement as a function of range.

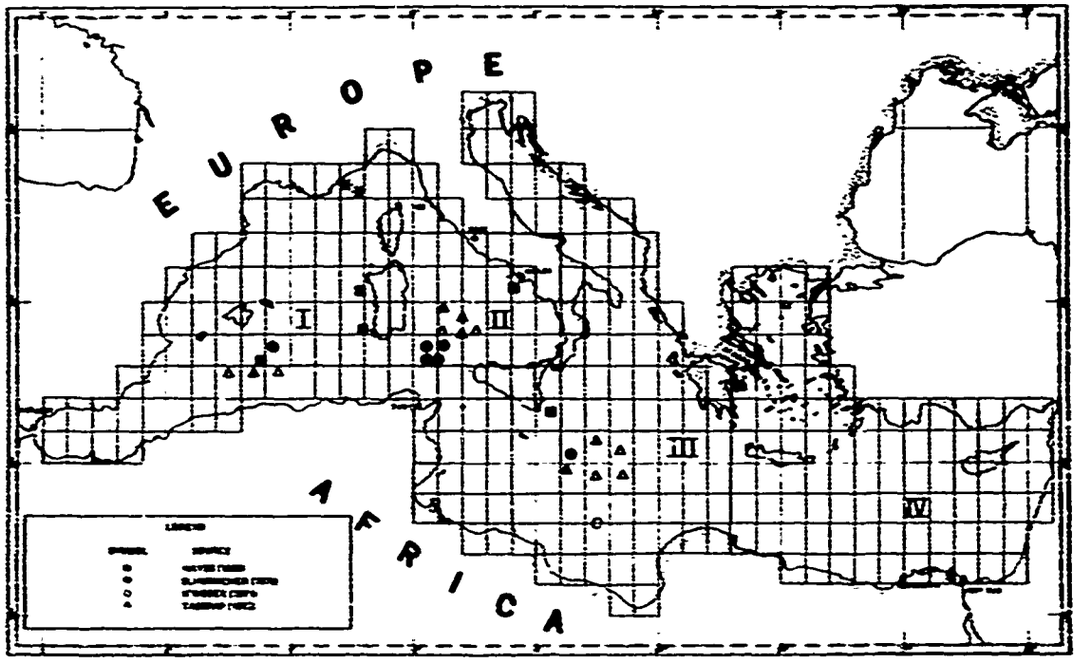

Figure 3.2.7-1(C). Location of Receivers in Low Frequency Propagation Loss Experiments (U)

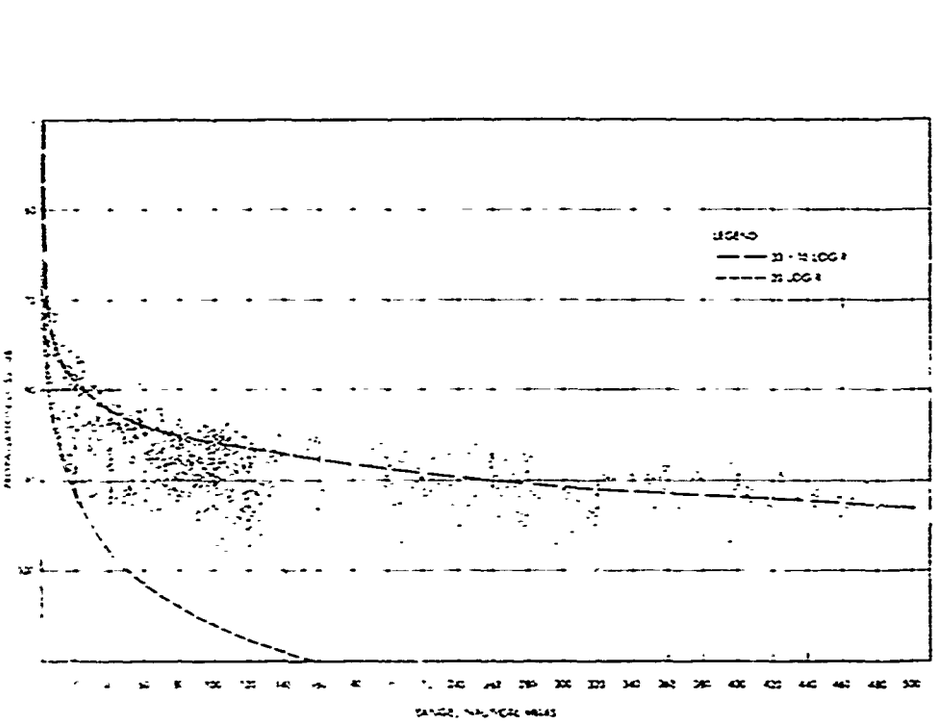

Figure 3.2.7-2(C). Long Range, Low Frequency (35 Hz to 130 Hz) Propagation Loss, All Mediterranean Basins, Summer and Fall, Source and Receiver Deep (U)

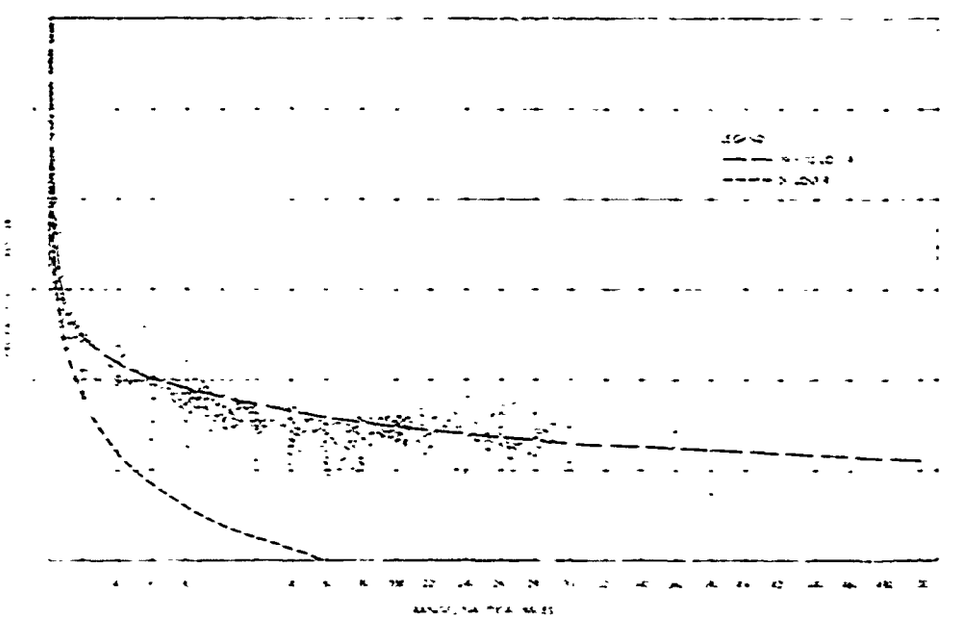

Figure 3.2.7-3(C). Long Range, Low Frequency (35 Hz to 130 Hz) Propagation Loss, All Mediterranean Basins, Summer and Fall, Source Shallow, Receiver Deep (U)

REFERENCES

1. Albers, V.M. 1966. Underwater acoustics handbook II. Ordnance Research Lab., Penn. State Univ. Press

2. Albers, V.M. 1967. Underwater acoustics, volume 2. Ordnance Research Lab., Penn. State Univ., Plenum Press

3. Allan, T.D., et al. 1972. Comparison of measurements and ray-tracing predictions of total propagation loss for the western Ligurian Sea in February 1970 (JOAST) (U). SACLANT, ASW Res. Cen. Tech. Rep. No. 215, La Spezia, NATO CONFIDENTIAL

4. Baxter, L., II and Brockhurst, R. 1967. Some deep-water sound transmission paths south of Cyprus, part II: Diffraction effects. Woods Hole Oceanogr. Inst. Ref. No. 67-40, Woods Hole, Mass.

5. Baxter, L., II, Brockhurst, R., and Hays, E.E. 1964. Some deep-water sound transmission paths south of Cyprus. J. Acous. Soc. Am. 36, p. 2124

6. Beckerle, J.C. Fluctuations in long-range transmission of sound between a fixed source and fixed receivers

7. Bradley, D.L. and Urick, R.J. 1968. A compilation of acoustic transmission loss measurements in shallow water. Naval Ordnance Lab. Rept. No. NOLTR-68-180, CONFIDENTIAL. DDC No. AD-395-179L

8. Buvik, L.M. and Gerrebout, J. 1971. Experimental studies on sound propagation in the Strait of Gibraltar in the presence of internal waves (U). SACLANT ASW Res. Cen. Tech. Rep. No. 184, La Spezia, NATO CONFIDENTIAL

9. Cole, B.F., et al. 1971. IMP-JOAST performance modeling (U). Proc. 8th Navy Symp. Mil. Oceanogr., 2, p. 507, CONFIDENTIAL

10. Davidson, R.O., Ess, R.H., and Leibiger, G.A. 1961. A theoretical analysis of deep-path sound propagation losses in the Norwegian and Mediterranean Seas (U). Vitro Labs, Rep. No. 2206-17-0, West Orange, N.J., CONFIDENTIAL

11. Dyer, I. 1970. Statistics of sound propagation in the ocean. Bolt Beranek and Newman Inc., Cambridge, Massachusetts, JASA, Vol. 48, No. 1

12. Gerrebout, J. 1972. Sound propagation in the Levantine Basin of the Mediterranean Sea during the warming season (U). SACLANT ASW Res. Cen. Tech. Rep. No. 212, La Spezia, NATO CONFIDENTIAL

13. Hays, E.E., Murphy, E.L. 1969. Mediterranean sound transmission (U). Woods Hole Oceanogr Inst. Ref. No. 69-69, Woods Hole, Mass., CONFIDENTIAL

14. Hersey, J.B. 1961. A progress report on environmental studies in the Mediterranean Sea. J. Acous. Soc. Am. 11, 4, p. 753 (a collection of papers)

15. Johannessen, O.M. and Mellberg, L.E. 1972. Layered oceanic microstructure, its effects on sound propagation. SACLANT ASW Research Cen., SACLANTCEN Tech. Rept. No. 206

16. Kaufman, O., and Axenfeld, S. 1964. Convergence zone transmission in the Mediterranean and Black Seas (U). NAVOCEANO Tech. Rep. No. 162, Washington, D.C., CONFIDENTIAL

17. Lallement, B., and Mari, S. 1968. Sound fields from various source depths with emphasis on RAP propagation (U). SACLANT ASW Res. Cen. Tech. Rep. No. 156, La Spezia, CONFIDENTIAL

18. Lauer, R.B., and van der Veen, S.R. 1973. JOAST Mediterranean convergence zone signal correlation studies. Rept. No. NUSC-4413, CONFIDENTIAL. DDC. No. AD-525-923

19. Leibiger, G.A. 1972. Nomograms for convergence zone range prediction. Rept. No. NUSC-TR-4261, CONFIDENTIAL. DDC. No. AD-521-161

20. Leroy, C.C. 1967. Sound propagation in the Mediterranean Sea. SACLANT ASW Res. Cen. Tech. Rep. No. 103, La Spezia

21. Leroy, C.C. 1967. Sound propagation in the western Mediterranean, in Underwater Acoustics. (V.N. Albers, ed.), Vol. 2, Chap. 11, Plenum Press, N.Y.

22. Leroy, C.C. 1965. Sound attenuation between 200 and 10 kHz measured along single paths (U). SACLANT ASW Res. Cen. Tech. Rept. 43, La Spezia

23. Leroy, C.C. 1969. A basic guide to sonar propagation in the Mediterranean and adjacent basins (U). SACLANT ASW Res. Cen. Tech. Rept. No. 154, La Spezia, NATO CONFIDENTIAL

24. Marshall, S.W. 1973. Ambient noise and signal-to-noise profiles in IOMEDEX (U). NRL Rep. No. 2638, Washington, D.C., CONFIDENTIAL

25. Martin, R.L., and Koenigs, P.D. 1973. Analysis of propagation loss and signal-to-noise ratios from IOMEDEX (U). Naval Underwater Systems Center, NUSC Tech. Rept. 4483, CONFIDENTIAL

26. Maury Center for Ocean Science 1973. IOMEDEX, summary report (U). Long Range Acoustic Propagation Project, MC Report 015

27. Neal, G.W. 1972. The effect of thermal fronts on acoustic propagation - a preliminary analysis. Admiralty Underwater Weapons Establishment Rept. No. AUWE-TN-453/72, CONFIDENTIAL. DDC No. AD-521-564

28. Officer, C.B. 1958. Introduction to the theory of sound transmission. The Rice Inst. & Woods Hole Oceanographic Inst., McGraw Hill Book Co.

29. Ozturgut, E. 1972. The theoretical effect of an oceanic front on acoustic propagation (U). SACLANT ASW Res. Cen. Tech. Rept. No. 213, La Spezia, NATO CONFIDENTIAL

30. Reynold, T.N., and Pryce, A.W. 1960. Acoustic propagation in the Atlantic and Mediterranean, autumn 1960. Admiralty Underwater Weapons Establishment Tech. Note 32/61, Portlant, England, CONFIDENTIAL

31. Schumacher, W.R., Thorp, W.H., and Friedel, F.C. 1971. Low-frequency propagation loss experiment in the Mediterranean Sea (U). Proc. 8th Navy Symp. Mil. Oceanogr., 2, p. 464, CONFIDENTIAL

32. Shonting, D.H., and Nacini, E. 1970. Acoustic ray diagrams based on oceanographic data from the Strait of Sicily in May 1970, (MEDMILOC 70) (U). SACLANT ASW Res. Cen. Tech. Memo. No. 176, La Spezia, NATO RESTRICTED

33. McCloskey, T.J., LCDR, and Gottwald, J.T. 1972. Mediterranean TASSRAP exercise final report (U). Maury Center Report 007, SECRET-NOFORN

34. Texas Instruments, Incorporated 1967. Marine Geophysical Survey Program 1965-1967, North Atlantic Ocean, Norwegian Sea and Mediterranean Sea, Area 6, vol. 2, acoustic station results. Dallas, Texas, CONFIDENTIAL

35. Tolstoy, V., and Clay, C.S. 1966. Ocean acoustics: theory and experiment in underwater sound. Hudson Laboratories, Columbia Univ. McGraw Hill Book Co.

36. Urick, R.J. 1967. Principles of underwater sound for engineers. U.S. Naval Ordnance Lab., Silver Spring, Md., McGraw Hill Book Co.

37. Voorheis, A.D., and Baxter, L. 1961. Mediterranean Sea sound transmission measurements (U). Navy J. Underw. Acoustics, 11(4), p. 770, CONFIDENTIAL

38. Weston, D.E., and Horigan, A.A. 1964. Acoustic propagation measurements in two deep-water areas (U). Admiralty Res. Lab. Rept. No. L/R53, Teddington, England, CONFIDENTIAL

3.3(U) Ambient Noise (U)

(U) Ambient noise is the background noise in the water observed with a sensor, not including any self-noise which may be caused by the sensor itself. The basic properties of ambient noise are usually described by the following:

- Spectrum Level - This is the omnidirectional sound pressure level per unit bandwidth. The spectrum level is expressed in dB relative to one micro Pascal (one micro newton per square meter), although many reports are still in use which express the spectrum level relative to one microbar (one dyne per square centimeter). Conversion from the latter to the former adds 100 dB.

- Directionality - This property refers to the directional characteristics at a given depth and location. Vertical and horizontal properties may be of interest. It is expressed in dB relative to a μ Pascal/$Hz^{1/2}$/steradian.

- Depth Dependence - This property is the change in omnidirectional spectrum level as a function of depth at a given location and time.

- Ambient Noise Statistics - These statistics may be either spectrum level or instantaneous value statistics. Spectrum level statistics describe the fluctuations, for a given averaging time, relative to the mean square pressure. Instantaneous value statistics describe the fluctuation of the pressure amplitude.

3.3.1(U) Sources of Ambient Noise (U). Ambient noise is produced from a number of causes, although there is a predominant cause in various parts of the frequency spectrum of interest here. Noise in the region from 10 to 500 Hz is produced by shipping and distant storms, with shipping normally predominating. Noise in the region from 1 to 30 kHz is caused predominately at the sea surface and is highly correlated to wind speed (the well-known Knudsen curves). For frequencies above 30 kHz the ambient noise is believed to be dominated by the thermal noise of the molecules in the sea. The levels associated with these causes in the open ocean are shown in figure 3.3.1-1 as a function of frequency (Wenz, 1962), for later comparison to levels in the Mediterranean.

(U) In addition to the above, there are two noise sources classified as intermittent in nature. These are the effects of marine life and rainfall. Sounds produced by biological sources have been described in section 2.4 above. The effect of rainfall is shown in figure 3.3.1-2.

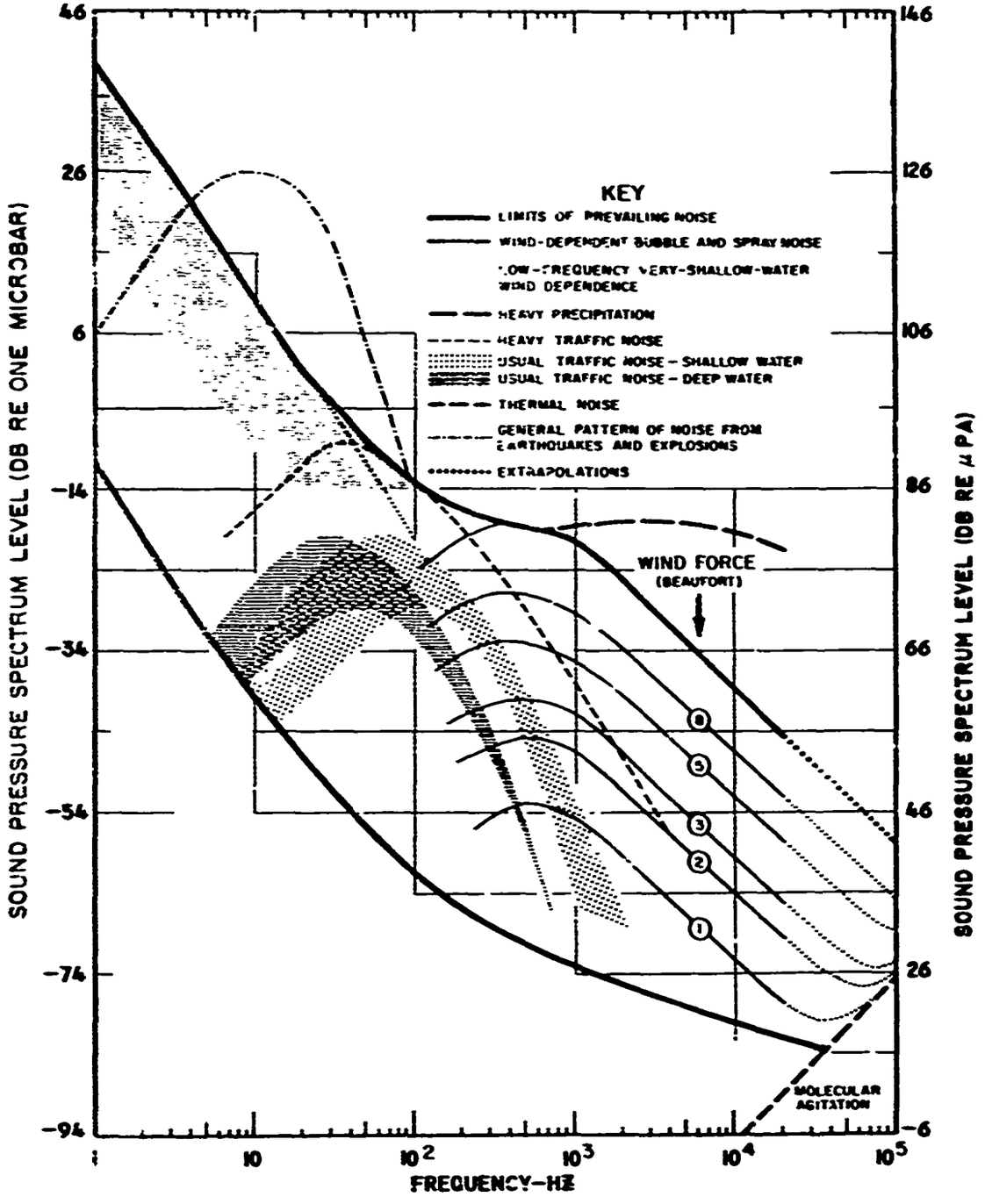

Figure 3.3.1-1. Ambient Noise Spectra in the Sea

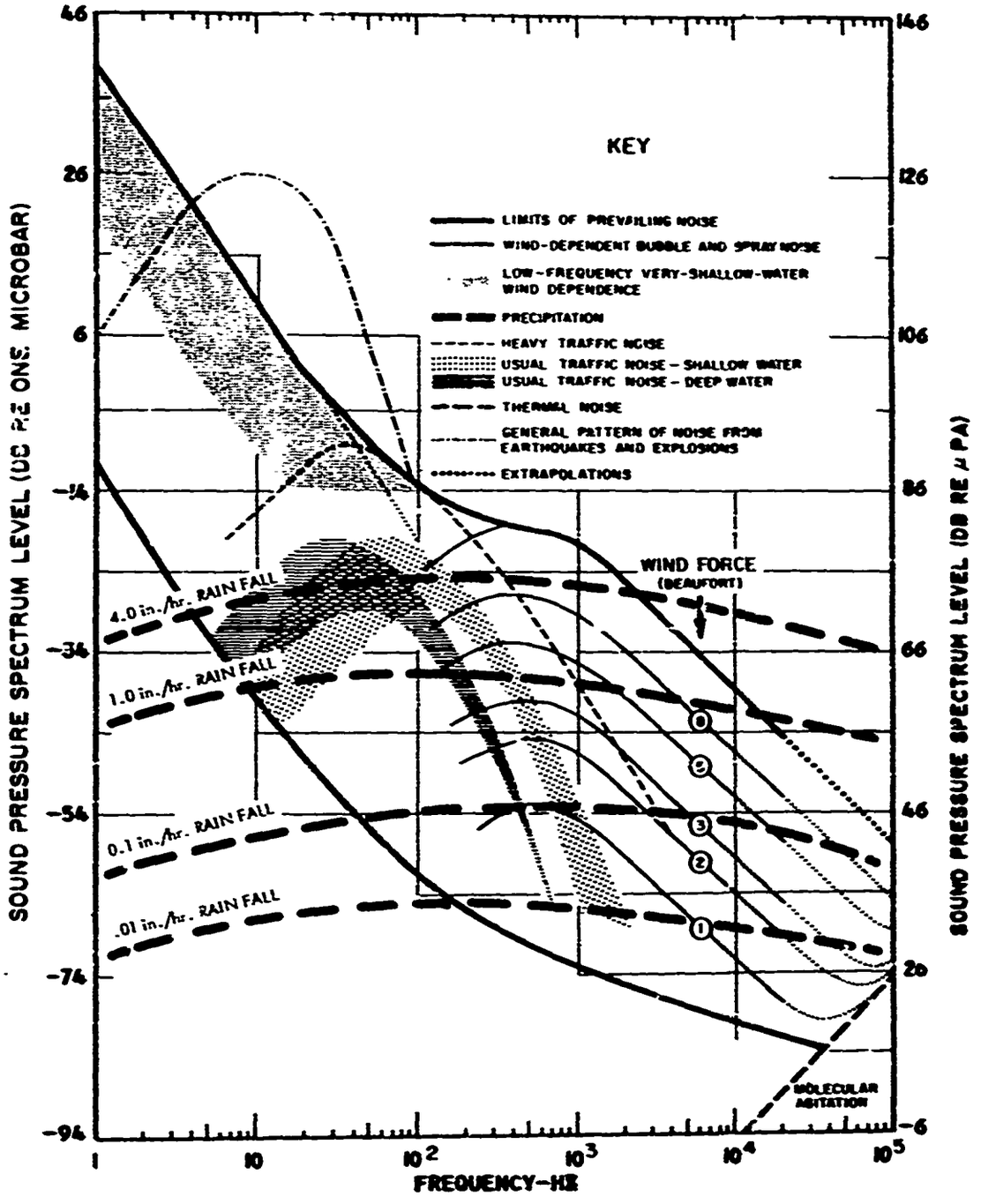

Figure 3.3.1-2(C). The Effect of Rainfall on Ambient Noise, Franz (1959) (U)

3.3.2(C) Measurements in the Mediterranean Sea (U). Ambient noise has been measured in the Mediterranean Sea at the locations indicated in figure 3.3.2-1. The parameters describing these measurements and representative data describing the results are listed in table 3.3.2-I.

(C) Results typical of the Mediterranean are shown in figure 3.3.2-2. The data were obtained in the Ionian Basin during November 1971 (MC Report No. 015, 1973) as part of the IOMEDEX exercise. The median, 10th and 90th percentile curves of the omnidirectional ambient noise spectrum levels at 149 meters depth are shown on the Wenz curves. The figure illustrates the strong influence of the heavy shipping in the Mediterranean on the spectrum levels below 400 Hz. Below 200 Hz the median noise level is 10 to 15 dB above what Wenz refers to as usual deep water traffic noise. At frequencies above 1000 Hz, the omnidirectional levels correspond to a wind force of 5 or less. The mean wind speed during the measurement period was 12 knots, corresponding to wind force 4.

(C) An illustration of the correlation of ambient noise with wind speed is shown in figure 3.3.2-3 (Martin and Perrone, 1973). The correlation is low between 20 and 200 Hz, increases rapidly between 200 and 1000 Hz and then levels off above 1000 Hz. The correlation is generally highest for the shallower hydrophones.

(C) No significant dependence of the noise levels on depth and season are displayed by any of the data. This is consistent with the fact that propagation loss is not expected to vary with season. A summary of noise measurements in the major basins of the Mediterranean is shown in figure 3.3.2-4, adapted from reference 64 (Urick and Bradley, 1970).

(C) A comparison of measurements made in 1963 (White and Horton, 1968) and later measurements (MC Report No. 007, 1972 and MC Report No. 015, 1973) shows that for frequencies of 200 Hz and above the same levels were measured, while for frequencies below 200 Hz the levels have increased 3 to 4 dB. This increase is attributable to an increase in shipping density during that period.

(C) No direct measurements of horizontal directionality are available at this time. However, the correlation of the low frequency noise to shipping clearly indicates that the directionality of low frequency noise will be related to the locations of the shipping and will be dominated by horizontal noise maxima in the direction of the closest sources relative to the receiver.

(C) Vertical directionality has also not been measured directly. The high correlation of the noise to wind speed for the higher frequencies (figure 3.3.2-3) indicates that the noise is local in origin. The vertical arrival structure is therefore determined by the local velocity structure. Low frequency noise from distant sources, on the other hand, would be expected to arrive within a few degrees of horizontal.

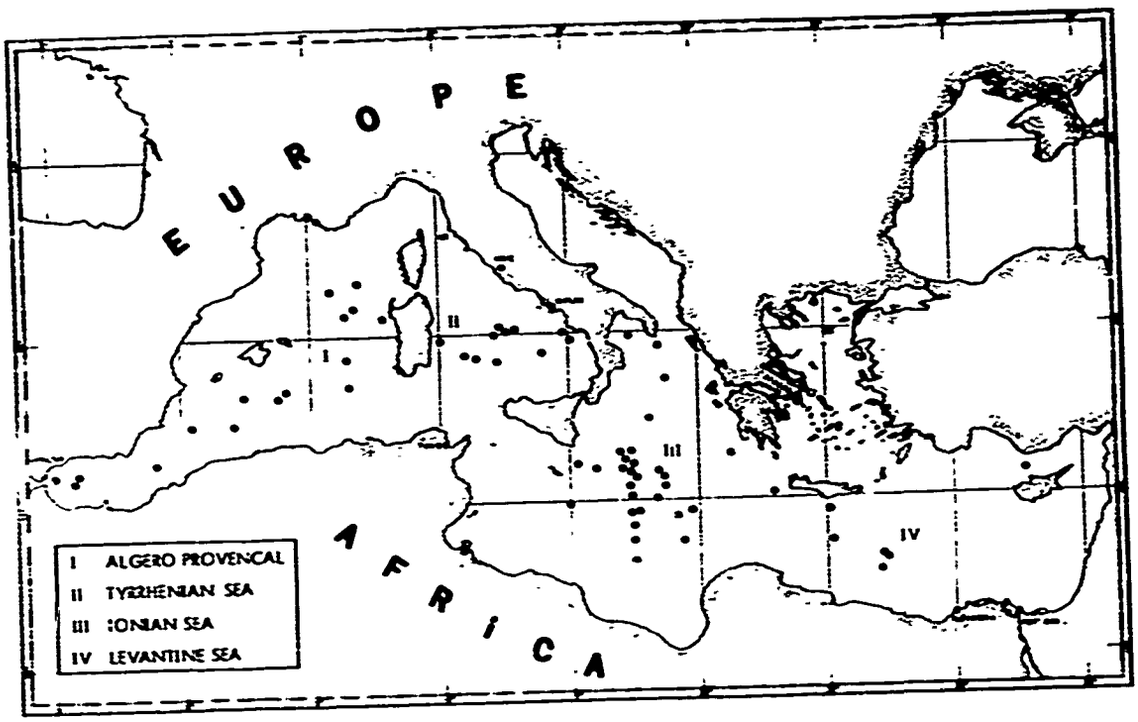

Figure 3.3.2-1. Ambient Noise Studies in the Mediterranean, 1960 to 1973

TABLE 3.3.2-I(C). NOISE SPECTRA WITH ENVIRONMENTAL AND TEST CONDITIONS (U)

Reference	SPECTRUM LEVEL dB re μPa/Hz$^{\frac{1}{2}}$							Location		
	20 Hz	50 Hz	100 Hz	200 Hz	500 Hz	1000 Hz	2000 Hz	Basin	Latitude	Longitude
Lomask (1960)	76	68	65	62	-	-	-	Tyrrhenian	40°N	15°E
	82	78	75	70	-	-	-	Tyrrhenian	40°N	15°E
Arase (1968)	82	83	80	70	60	-	-	Tyrrhenian	40°10'N	12°58'E
	90	92	85	74	65	-	-	Algerian	39°10'N	06°30'E
	93	93	85	75	67	-	-	Ionian	36°40'N	17°40'E
	92	93	87	76	65	-	-	Ionian	36°10'N	17°35'E
	84	86	79	67	60	-	-	Levantine	33°40'N	25°10'E
Hersey (1969)	84	87	79	68	59	-	-	Levantine	33°N	25°E
	92	94	88	78	65	-	-	Ionian	36°30'N	17°30'E
	90	92	87	77	-	-	-	Algerian	39°10'N	06°20'E
	81	85	80	70	60	-	-	Tyrrhenian	40°30'N	13°40'E
Hays & Murphy (1969)	-	100	89	80	70	60	57	Algero-Provencal	38°17'N	03°53'E
	-	97	88	78	70	61	60		↓	↓
	-	94	89	82	78	68	67			
	-	100	90	80	70	60	57			
	-	96	86	77	70	60	55		38°17'N	03°53'E
	-	95	90	82	77	68	65		40°33'N	07°53'E
	-	100	88	82	70	60	52		↓	↓
	-	90	83	75	65	55	48			
	-	87	83	78	68	60	57			
	-	103	95	87	75	66	64			
	-	89	87	80	68	63	63			
	-	91	88	82	71	67	67			
	-	98	88	81	70	60	54			
	-	88	83	75	65	57	54	Algero-Provencal	40°33'N	07°53'E
	-	87	84	79	69	62	61	Tyrrhenian	39°55'N	10°00'E
	-	106	95	87	76	66	60		↓	↓
	-	85	83	77	70	63	60			
	-	81	81	79	75	66	64			
	-	107	96	92	76	66	60			
	-	86	82	75	68	62	59			
	-	83	82	78	74	68	63			
	-	106	95	91	75	67	61			
	-	90	83	76	68	62	59			
	-	90	85	80	74	67	66			
	-	104	97	84	74	66	62			
	-	88	88	74	70	65	65			
	-	90	89	82	75	70	69	Tyrrhenian	39°55'N	10°00'E
White & Horton (1969)	92	92	84	75	65	59	48	Algero-Provencal	41°30'N	06°58'E
	90	89	83	75	66	60	54		41°30'N	06°58'E
	93	92	85	76	67	61	56		41°30'N	06°58'E
	93	92	87	79	68	60	53		41°30'N	06°58'E
	90	97	84	75	66	61	51		40°58'N	06°45'E
	91	98	83	74	67	62	53		40°58'N	06°45'E
	92	90	87	77	69	61	52	Algero-Provencal	40°58'N	06°45'E
	91	93	89	76	69	62	54		40°58'N	06°45'E
	82	85	82	78	70	60	52	Tyrrhenian	39°10'N	12°13'E
	78	80	76	71	62	57	52	Tyrrhenian	39°10'N	12°13'E
	83	81	79	71	62	55	42	Tyrrhenian	39°10'N	12°13'E
	82	83	80	70	65	60	55	Tyrrhenian	39°10'N	12°13'E
	90	90	85	78	72	66	59	Ionian	34°35'N	19°05'E
	94	87	83	80	76	72	66		↓	↓
	87	88	83	75	68	65	57			
	88	83	80	77	70	67	60			
	94	88	83	73	69	64	56			
	89	89	83	76	70	67	61		34°35'N	19°05'E
	90	92	86	76	66	58	52		33°45'N	19°15'E
	85	88	82	72	67	61	56		33°45'N	19°15'E
	86	91	82	74	70	61	59		35°36'N	19°47'E
	87	92	85	76	69	65	60		35°36'N	19°47'E
	87	90	83	73	65	55	48		40°00'N	17°36'E
	81	86	80	72	66	60	51		40°00'N	17°36'E
	93	89	81	73	67	62	54		40°00'N	17°36'E
	90	89	83	75	67	62	51	Ionian	40°00'N	17°36'E

TABLE 3.3.2-I(C). NOISE SPECTRA WITH ENVIRONMENTAL AND TEST CONDITIONS (Continued) (U)

Time of Day (Z)	Date Measured	Water Depth (meters)	Hydrophone Depth (meters)	Layer Depth (meters)	Sound Channel Axis Depth (meters)	Sea State	Ship Speed (kt)	Notes
Var.	Jul-Oct	915-2928	183			0		
Var.	Jul-Oct	915-2928	183			2		
Var.	6/12/68	3477	29	0	76	1		
Var.	6/16/68	2745	29	0	92	1		
Var.	6/20/68	3294	29	0	113	1		
Var.	6/22/68	3477	29	0	113	2		
Var.	6/26/68	2196	29	0	153	2-3		
Var.	6/68						10.7	Summary present
Var.	6/68						8.7	
Var.	6/68						5.2	
Var.	6/68						5.4	
0600	7/9/68	2562	107	0	101			
0600	7/9/68		137					
0600	7/9/68		305					
0500	7/10/68		107					
0500	7/10/68		137					
0500	7/10/68	2562	3005		101			
0900	7/13/68	366	92		677			
0900			183					
0900			275					
1000			92					
1000			183					
1000			275					
1100			92					
1100			183					
1100	7/13/68	366	275		677			
1230	7/14/68	1464	92		110			
1230			183					
1230			297					
1300			92					
1300			183					
1300			297					
1400			92					
1400			183					
1400			297					
1430			92					
1430			183					
1430	7/14/68	1464	297	0	110			
1300	12/1/68	2654	27	49	153	2-3		
1300	12/1/68	2654	92	49		2-3		
1800	12/1/68	2654	27	49		2-3		
1800	12/1/68	2654	92	49		2-3		
1400	12/2/68	2667	27	37		3-4		
1400	12/2/68	2667	92			3-4		
1600	12/2/68	2667	27			3-4		
1600	12/2/68	2667	92			3-4		
0900	11/10/68	3386	27			2		
0900	11/10/68	3386	92			2		
0700	11/11/68	3386	27			2		
0200	11/11/68	3386	92	37		2		
0700	11/11/68	3340	27	53		4-5		
0700			92			4-5		
1100			27			4-5		
1100			92			4-5		
1700			27			4-5		
1700	11/17/68		92			4-5		
0200	11/20/68		27			2		
0700	11/20/68		92	53		2		
1600	11/23/68		27	31		4		
1600	11/23/68	3440	92	31		4		
0400	11/27/68	915	27	46		2		
0400	11/27/68	915	92	46		2		
0900	11/27/68	915	27	46		2		
0900	11/27/68	915	92	46	153	2		

TABLE 3.3.2-I(C). NOISE SPECTRA WITH ENVIRONMENTAL AND TEST CONDITIONS (Continued) (U)

Reference	SPECTRUM LEVEL dB re μPa/Hz$^{\frac{1}{2}}$							Location		
	20 Hz	50 Hz	100 Hz	200 Hz	500 Hz	1000 Hz	2000 Hz	Basin	Latitude	Longitude
White & Horton (1969) (Continued)	88	91	83	73	67	63	57	Ionian	40°00'N	17°36'E
	95	95	90	82	75	67	58	Ionian	↓	↓
	88	82	76	69	63	58	50	Levantine	↓	↓
	80	82	79	72	66	63	58	↓	↓	↓
	87	84	83	73	64	59	55	↓	↓	↓
	79	80	80	72	62	57	52	↓	↓	↓
	85	87	87	78	66	60	57	↓	↓	↓
	77	77	78	70	63	59	53	Levantine	40°00'N	17°36'E
Sanders Associates (1969)	-	84	78	70	60	51	45	Ionian	34°50'N	17°27'E
	-	85	82	75	65	60	46	Ionian	34°50'N	17°27'E
	-	81	75	72	66	61	60	Ionian	34°50'N	17°27'E
	-	80	76	72	65	61	60	Ionian	34°50'N	17°27'E
	82	85	77	70	67	67	62	Levantine	32°50'N	26°53'E
	-	81	77	70	65	64	60	↓	↓	↓
	-	74	71	68	62	59	55	↓	↓	↓
	-	83	77	73	68	63	60	↓	↓	↓
	-	81	80	72	69	65	61	↓	↓	↓
	-	80	75	71	61	50	41	Levantine	32°50'N	26°53'E
Dale (1969)	81*	86	82	74	71	69	66	Tyrrhenian	40°10'N	12°20'E
	81	86	82	76	72	70	67	↓	40°10'N	12°20'E
	79	87	80	74	70	67	62	↓	40°10'N	12°20'E
	87	87	82	77	73	70	66	↓	40°10'N	12°20'E
	87	90	84	77	71	69	65	↓	40°05'N	12°08'E
	83	87	84	78	70	67	61	↓	↓	↓
	81	88	83	78	69	64	57	↓	↓	↓
	86	88	83	77	70	64	57	↓	↓	↓
	82	85	80	75	67	62	56	↓	↓	↓
	82	87	82	75	68	62	54	↓	↓	↓
	79	86	83	77	69	63	56	↓	↓	↓
	84	87	83	78	70	65	58	Tyrrhenian	40°05'N	12°08'E
	93	98	89	81	73	65	56	Algero-	38°20'N	02°30'E
	99	105	93	83	75	68	59	Provencal	↓	↓
	92	98	91	81	73	66	59	↓	↓	↓
	93	98	92	79	70	65	57	↓	↓	↓
	92	98	90	81	72	64	56	↓	↓	↓
	97	103	94	83	73	68	-	↓	38°20'N	02°30'E
	93	98	90	77	74	69	65	↓	41°20'N	05°45'E
	93	100	90	79	74	70	63	↓	↓	↓
	96	107	90	79	75	70	67	↓	↓	↓
	96	104	88	78	74	70	66	↓	↓	↓
	92	102	88	78	73	67	62	Algero-	↓	↓
	95	110	90	80	75	71	67	Provencal	41°20'N	05°45'E
	91	95	90	80	73	65	56	Ionian	35°55'N	18°30'E
	92	97	92	82	74	65	55	↓	↓	↓
	96	99	94	82	78	73	63	↓	↓	↓
	96	99	93	82	77	71	63	↓	↓	↓
	96	98	93	82	76	72	65	↓	↓	↓
	93	98	92	81	77	70	63	↓	↓	↓
	96	99	93	82	77	74	64	↓	↓	↓
	95	96	90	79	76	71	60	↓	↓	↓
	96	98	94	82	76	71	65	↓	↓	↓
	95	96	92	82	77	70	62	↓	↓	↓
	96	96	90	81	73	68	61	↓	↓	↓
	93	95	90	80	74	67	60	↓	↓	↓
	93	96	91	82	78	69	62	↓	↓	↓
	95	100	93	82	77	70	62	↓	↓	↓
	94	101	93	83	78	70	61	↓	↓	↓
	94	99	92	81	75	69	61	↓	↓	↓
	94	100	92	81	76	69	61	↓	↓	↓
	95	99	92	82	77	70	61	Ionian	35°55'N	18°30'E
	80	87	84	73	69	66	63	Levantine	33°07'N	27°17'E
	80	85	80	73	69	66	63	↓	↓	↓
	80	88	85	76	72	70	65	↓	↓	↓
	83	82	79	73	68	64	59	↓	↓	↓
	81	90	82	75	71	67	62	Levantine	33°07'N	27°17'E

*25 Hz

TABLE 3.3.2-I(C). NOISE SPECTRA WITH ENVIRONMENTAL AND TEST CONDITIONS (Continued) (U)

Time of Day (Z)	Date Measured	Water Depth (meters)	Hydrophone Depth (meters)	Layer Depth (meters)	Sound Channel Axis Depth (meters)	Sea State	Ship Speed (kt)	Notes
0100	11/28/68	915	27	61	153	2		
0100	11/28/68	915	92	61	↓	2		
1300	11/14/68	915	27	52		3		
1300	11/14/68	915	92	52		3		
1300	11/15/68	3294	27	37		3		
1300	11/15/68	3294	92	37		3		
1900	11/15/68	3294	27	37		3		
1900	11/15/68	3294	92	37	153	3		
0254	11/20/68		31	49		2		
0254	11/20/68		92	49		2		
0751	11/23/68		31	49		4		
0751	11/23/68		92	49		4		
1253	11/14/68		31	52		3		
↓	↓		92	↓		3		
			31			3		
			92			3		
			31			3		
1253	11/14/68		92	52		3		
1600	4/14/69	3670	92			3		
2045	4/14/69	↓	31			3		
2045	4/14/69		92			3		
2045	4/14/69		92			3		
0307	4/16/69		31			2		
0307			31			2		
0747			31			2		
↓	↓	↓	92			2		
			31			2		
			92			2		
			31			2		
0747	4/16/69	3670	92			2		
1620	4/20/69	2654	31			1-1½		
↓	↓	↓	92			1-1½		
			31			1-1½		
			92			1-1½		
			31			1-1½		
1620	4/20/69	2654	92			1-1½		
0450	4/22/69	2562	31			2-1½		
0450		↓	31			2-1½		
0630			31			2-1½		
0630			31			2-1½		
0630			92			2-1½		
0630	4/22/69	2562	31			2-1½		
0325	4/23/69	3976	31			1-1½		
0325		↓	31			1-1½		
0745			31			1-1½		
↓	↓	↓	92			1-1½		
			31			1-1½		
			92			1-1½		
			31			1-1½		
0745	4/23/69	↓	92			1-1½		
1810	4/24/69		31			1		
↓	↓		92			1		
			31			1		
			92			1		
1810			92			1		
2000			31			1		
↓	↓		92			1		
			31			1		
			92			1		
2000	4/24/69	3976	92			1		
0535	4/17/69	2745	31			1		
0535	↓	↓	92			1		
0535			31			1		
0535			92			1		
0910	4/17/69	2745	31			1		

TABLE 3.3.2-I(C). NOISE SPECTRA WITH ENVIRONMENTAL AND TEST CONDITIONS (Continued) (U)

Reference	SPECTRUM LEVEL dB re μPa/Hz$^{\frac{1}{2}}$							Location		
	20 Hz	50 Hz	100 Hz	200 Hz	500 Hz	1000 Hz	2000 Hz	Basin	Latitude	Longitude
Dale (1969) (Continued)	82	87	81	75	71	69	64	Levantine	33°07'N	27°17'E
	80	90	82	74	69	65	62		↓	
	82	86	80	73	67	65	61			
	81	88	82	75	70	67	62			
	84	86	80	73	67	66	61		33°07'N	27°17'E
	84	88	81	73	67	60	56		32°55'N	27°07'E
	83	90	83	75	68	62	58		↓	↓
	86	87	81	73	66	58	55			
	83	86	79	71	65	59	56			
	89	88	81	74	66	60	56			
	83	88	82	73	66	61	57			
	83	89	82	73	68	63	59			
	80	89	80	71	66	61	58			
	85	92	82	73	69	64	60	Levantine	32°55'N	27°07'E
	94	99	94	82	76	73	67	St. of	36°04'N	04°00'W
	93	99	93	82	77	73	66	Gibraltar	36°04'N	04°00'W
	93	96	92	81	75	72	67	St. of	36°04'N	04°00'W
	95	96	93	81	75	73	68	Gibraltar	36°04'N	04°00'W
Gerrebout & Leroy (1968)	-	-	91	85	75	70	65	St. of	36°04'N	05°17'W
	-	-	102	92	85	80	75	Gibraltar	36°04'N	05°17'W
Sanders Associates (1970)	90	92	85	74	-	-	-	Algero-	N/A	N/A
	92	93	84	75	67	60	55	Provencal	↓	↓
	94	96	90	79	72	65	58	Algero-		
	94	102	90	79	73	68	61	Provencal		
	81	84	78	69	59	-	-	Tyrrhenian		
	83	84	81	74	68	61	49	Tyrrhenian		
	83	88	82	77	69	62	60	Tyrrhenian		
	83	84	86	77	67	66	54	Tyrrhenian		
	93	95	88	77	65	-	-	Ionian		
	74	96	90	84	72	65	-	Ionian		
	-	98	89	81	73	66	-	Ionian		
	-	99	92	82	75	70	-	Ionian		
	84	86	79	68	58	-	-	Levantine		
	80	82	80	76	66	62	57	Levantine		
	-	80	79	70	64	60	58	Levantine		
	-	88	82	74	68	64	60	Levantine	N/A	N/A
Morey Macphee (1970)	111.3 .4	97.4 7.3	88.3 4.8	75.4 6	60.6 5	50.3 4	44.3 7	Ionian	35°55'N	18°30'E
Baxter Lincoln (1971)	-	93	89	76	-	-	-	Balearic	40°30'N	06°45'E
	-	99	85	73	-	-	-		↓	↓
	-	96	90	78	-	-	-			
	-	92	91	76	-	-	-			
	-	96	88	77	-	-	-		40°30'N	06°45'E
	-	98	88	77	-	-	-		37°46'N	06°15'E
	-	97	90	77	-	-	-		37°46'N	06°15'E
	-	98	84	73	-	-	-	Balearic	37°46'N	06°15'E
	-	96	85	75	-	-	-	Straits of	37°21'N	11°28'E
	-	97	85	75	-	-	-	Sicily	37°21'N	11°28'E
	-	99	92	88	-	-	-	Ionian	36°02'N	16°55'E
	-	92	88	86	-	-	-		36°02'N	16°55'E
	-	98	93	75	-	-	-		35°41'N	17°52'E
	-	92	91	75	-	-	-		35°41'N	17°52'E
	-	91	89	76	-	-	-		35°41'N	17°52'E
	-	98	88	77	-	-	-		35°35'N	17°57'E
	-	97	87	76	-	-	-		35°35'N	17°57'E
	-	96	85	75	-	-	-	Ionian	35°35'N	17°57'E
	-	93	83	78	-	-	-	Tyrrhenian	40°00'N	13°02'E
	-	93	85	75	-	-	-	Tyrrhenian	40°00'N	13°02'E
Murphy, et al. (1971)	88	96	92	80	-	-	-	Ionian	36°00'N	17°00'E
	87	92	85	76	-	-	-	Ionian	36°00'N	17°00'E
	87	92	85	75	-	-	-	Balearic	40°40'N	06°30'E

TABLE 3.3.2-I(C). NOISE SPECTRA WITH ENVIRONMENTAL AND TEST CONDITIONS (Continued) (U)

Time of Day (Z)	Date Measured	Water Depth (meters)	Hydrophone Depth (meters)	Layer Depth (meters)	Sound Channel Axis Depth (meters)	Sea State	Ship Speed (kt)	Notes
0910	4/17/69	2745	92			1		
↓	↓	↓	31			1		
			92			1		
			31			1		
0910	4/17/69		92			1		
1553	4/19/69		31			½-1		
↓	↓		92			½-1		
			31			½-1		
			31			½-1		
1553			92			½-1		
1710			31			½-1		
1710			31			½-1		
1710			31			½-1		
1710	4/19/69	2745	92			½-1		
2000	4/20/69	1373	31			2-2½		
2000	4/20/69	1373	92			2-2½		
2000	4/20/69	1373	31			2-2½		
2000	4/20/69	1373	92			2-2½		
Var.	Var.	1336	1.281			1-4		
Var.	Var.	1336	1.281			1-4		
N/A	Summer	N/A	31	N/A	N/A	N/A		Seasonal Summary Based on Arase, Dale, and White
↓	Fall	↓	↓	↓	↓	↓		
	Winter							
	Spring							
	Summer							
	Fall							
	Winter							
	Spring							
	Summer							
	Fall							
	Winter							
N/A	Spring	N/A	31	N/A	N/A	N/A		
Var.	1/2/-1/30/70	3.8125	1530			0-1		110 spectra median value
0400	7/14/70		18		115	0	0	
0400	↓		92		↓	0	0	
0400			18			0	1	
0400			92			0	1	
1900	7/14/70		458		115	0	1	
0200	7/18/70		18	12	175-229	3	5	
0200	7/18/70		92	12	175-229	3	5	
0200	7/18/70		458	12	175-229	3	5	
1500	7/20/70		18	18-54	91	3	1	
1500	7/20/70		92	18-54	91	3	1	
1340	7/24/70		18		100	2	2	
1340	7/24/70		92		100	2	2	
0600	7/26/70		18		50	2	4	
0600	7/26/70		92		50	2	4	
0600	7/26/70		458		50	2	4	
1400	7/26/70		18		50	2½	[illegible]	
1400	7/26/70		92		50	2½	6	
1400	7/26/70		458		50	2½	6	
2100	7/28/70		18		90	1	1	
2100	7/28/70		92		90	1	1	
Daily	7/24/70		18				1	
1 Aug	7/24/70		92				1	
	7/14/70		18				8 (1-13)	

TABLE 3.3.2-I(C). NOISE SPECTRA WITH ENVIRONMENTAL AND TEST CONDITIONS (Continued) (U)

Reference	SPECTRUM LEVEL dB re μPa/Hz½							Location		
	20 Hz	50 Hz	100 Hz	200 Hz	500 Hz	1000 Hz	2000 Hz	Basin	Latitude	Longitude
Murphy, et al. (1971)	92	91	86	76	-	-	-	Balearic	40°40'N	06°30'E
	94	94	88	77	-	-	-	Balearic	40°40'N	06°30'E
	83	88	79	69	-	-	-	Tyrrhenian	37°15'N	11°25'E
	91	93	82	72	-	-	-	Tyrrhenian	37°15'N	11°25'E
	86	96	89	77	-	-	-	Ionian	36°00'N	17°30'E
	89	93	86	75	-	-	-	Ionian	36°00'N	17°30'E
	89	93	87	76	-	-	-	Ionian	36°00'N	17°30'E
Weigle, Watt (1971)	97	98	91	80	73	61	-	Ionian	38.5°N	40°E
	97	98	90	80	72	60	-		38.5°N	40°E
	97	98	90	80	70	60	-		38.5°N	40°E
	97	98	90	77	70	60	-		38.5°N	40°E
	-	-	85	81	75	69	-		37.6°N	02°E
	98	99	93	81	73	65	61			
	99	101	93	81	73	65	59			
	99	101	93	81	72	62	55			
	99	101	93	81	71	61	55			
	99	101	93	81	69	60	55		37.6°N	02°E
	-	-	88	82	75	70	65		37.5°N	0.5°E
	99	100	92	82	75	70	66			
	99	100	92	81	75	70	65			
	99	100	92	82	75	70	65			
	99	101	92	82	73	68	64			
	99	101	92	82	73	68	64		37.5°N	0.5°E
	-	-	80	79	73	70	64		36.5°N	01°W
	96	98	91	82	73	69	64			
	98	99.5	95	82	78	70	65			
	98	99.5	95	85	75	71	69			
	100	101	92	82	72	70	64			
	101	102	92	80	72	68	63		36.5°N	01°W
	-	-	88	81	78	70	-		36°N	04°W
	98	97	91	81	74	71	65		36°N	04°W
	98	98	91	81	70	61	56		36°N	04°W
	98	98	91	80	67	59	55	Ionian	36°N	04°W
Frisch & Johnson (1972)	98	96	92	82	74	65	60	Ionian	36°19.6'N	17°14.3'E
	95	94	92	82	74	67.5	62.5		36°19.6'N	17°14.3'E
	93	93.5	90	79	71	65	58		35°28.7'N	17°31.9'E
	93	95.5	90	79	71	65	61		35°28.7'N	17°31.9'E
	90	92	88	78	71	68	62.5		35°28'N	17°30.9'E
	90	92	89	79	71	68	65		35°28'N	17°30.9'E
	90	92.5	86.5	77.5	73.7	66.2	55.5		34°12.9'N	17°29.8'E
	87.5	92.5	86.5	75	75	66.2	63.3		34°12.9'N	17°29.8'E
	93.7	94.5	86.3	75	69.3	63	61		33°2.3'N	17°33.3'E
	86.75	94.5	86.3	75	66.8	63.75	61.3		33°2.3'N	17°33.3'E
	90	90	87	74.5	64.5	58.3	53.3		33°3.1'N	17°32.8'E
	90	90	87	80	64.5	60	56		33°3.1'N	17°32.8'E
	91.5	92	87	76.3	67	62	54		33°2.4'N	17°28.5'E
	91.5	92	87	78.5	70	64.3	60		33°2.4'N	17°28.5'E
	92.5	92.5	86.5	73.3	67.5	61.3	59		33°2.4'N	17°28.5'E
	87.5	87	87	75	67.5	60	53		34°11'N	17°22.3'N
	90	94	90	78	70	66.5	55		34°20.2'N	17°29.4'E
	91.8	96	89	77.5	69.5	62	56.8		35°23.7'N	17°32.7'E
	91.8	92.3	88.8	78.8	71.3	65	61.3		35°23.9'N	17°24.4'E
	93.8	93.0	88	80	71.3	63.5	59.3		35°23.3'N	17°31.7'E
	93.8	94.3	88	80	71.3	63.5	59.3		35°23.3'N	17°31.7'E
	93.5	97.3	94.3	84.3	73	61.3	59		36°19.3'N	17°8.8'E
	91.8	96.5	94.8	83	72	68.5	60		36°20.6'N	17°11.8'E
	93.8	98.8	94.8	82	74	68.5	58.5		36°20.6'N	17°11.8'E
	96.5	96	91.8	82	73.5	66.3	56.3		36°19.1'N	17°12.9'E
	95	95.8	93.3	83.3	73.5	66.3	61.8		36°19.1'N	17°12.9'E
	91	94	89	79	71	61	54		36°20.6'N	17°11.8'E
	90	95	89	79	71	65	57		36°20.6'N	17°11.8'E
	90	97	89	79	69	65	58	Ionian	36°24.4'N	17°17.8'E

TABLE 3.3.2-I(C). NOISE SPECTRA WITH ENVIRONMENTAL AND TEST CONDITIONS (Continued) (U)

Time of Day (Z)	Date Measured	Water Depth (meters)	Hydrophone Depth (meters)	Layer Depth (meters)	Sound Channel Axis Depth (meters)	Sea State	Ship Speed (kt)	Notes
Daily	7/14/70		92				8	
1 Aug	7/14/70		458				(1-13)	
↓	7/20/70		18				2	
	7/20/70		92				(1-3)	
	7/26/70		18				7	
Daily	7/26/70		92				(4-9)	
1 Aug	7/26/70		458					
1600-0200	11/16-11/17/70	2617	488				12-15	
1600-0200	11/16-11/17/70	2617	1068				12-15	
1600-0200	11/16-11/17/70	2617	1732				12-15	
1600-0200	11/16-11/17/70	2617	2321				12-15	
2200-0600	11/17-11/18/70	2681	31				8-12	
			271				↓	
			586					
		↓	1144					
2200-	11/17-		1923					
0600	11/18/70	2681	2477				8-12	
2200-	11/18-	2599	18				20-22	
0700	11/19/70		284					
↓	↓		528					
2200-	11/18-		1156					
0700	11/19/70	2599	1769					
2200-	11/20-	2489	2053				20-22	
0600	11/21/70		31				15-20	
			168					
			461					
		↓	915					
2200-	11/20-		1412					
0600	11/21/70	2489	2028				15-20	
1100-	11/22/70	1354	31				4	
1300	11/22/70	1354	543				4	
1100-	11/22/70	1354	857				4	
1300	11/22/70	1354	961				4	
1716	11/7/71	~3909	1110	~0/70	~100/300	1		Include
1716	11/7/71		178			1		Spectra
0200	11/9/71		1150			1		
0200	11/9/71		188			1		
1100	11/9/71		540			1		
1100	11/9/71	~3909	130			1		
0958	11/10/71	~2268	1400			1		
0958	11/10/71		115			1		
0154	11/11/71		1130			1		
0154	11/11/71		1550			1		
1039	11/11/71		1200			1		
1039	11/11/71		280			1		
1757	11/11/71		1100			1		
1757	11/11/71		582			1		
2059	11/11/71		247			1		
0842	11/12/71		790			1		
1554	11/12/71	~2268	720			1		
0841	11/13/71	~3909	230			2		
1334	11/13/71		2200			2		
2057	11/13/71		1100			1		
2057	11/13/71		56			1		
1248	11/14/71		93			1		
1445	11/14/71		2200			1		
1445	11/14/71		650			1		
2351	11/14/71		1120			1		
2351	11/14/71		270			1		
0121	11/14/71		2200			1		
0121	11/14/71		650			1		
0121	11/18/71	3909	2520	~0/70	~100/300	1		Include Spectra

TABLE 3.3.2-I(C). NOISE SPECTRA WITH ENVIRONMENTAL AND TEST CONDITIONS (Continued) (U)

Reference	SPECTRUM LEVEL dB re μPa/Hz$^{\frac{1}{2}}$							Location		
	20 Hz	50 Hz	100 Hz	200 Hz	500 Hz	1000 Hz	2000 Hz	Basin	Latitude	Longitude
Frisch & Johnson (1972) (Continued)	91	95	90	79	70	62	57	Ionian	36°19'N	17°13'E
	91	95	90	79	70	60	49		36°19'N	17°13'E
	92	97	90	79	72	68	61		36°57'N	17°23'E
	89	92	89	78	71	65	60		35°53'N	17°16'E
	88	89	89	75	73	74	59		35°53'N	17°16'E
	89	91	88	82	74	72	63		38°35.3'N	18°7.7'E
	89	91	88	81	73	69	59	Ionian	38°35.3'N	18°7.7'E
Marshall (1973)	85	108	83	74	-	-	-	Ionian	38°40'N	17°12'E
	86	108	85	74	-	-	-			17°12'E
	90	93	89	79	-	-	-			18°40'E
	88	91	86	78	-	-	-			
	86	90	85	77	-	-	-			
	85	88	82	74	-	-	-			
	84	88	82	73	-	-	-	Ionian	38°40'N	18°40'E
Martin Perrone (1973)	88	96	91	77.5	70	64	57	Ionian	36°18'N	17°12'E
	88	96	91	77.5	70	64	57			
	88	96	91	77.5	70	66	60			
	88	96	91	77.5	71	68	63			
	88	96	91	77.5	72	68	64			
	88	96	91	77.5	73	69	64			
	88	96	91	77.5	73	70	65			
	90	96	92	77	71	65	60			
	90	96	92	77	71	65	60			
	90	97	92	78	72	66	61			
	90	97	92	79	73	68	63			
	90	98	92	80	74	70	65			
	90	98	92	80	74	71	67		36°18'N	17°12'E
	90	91	86	75	69	61	55		34°15'N	17°30'E
	90	91	84	72	68	61	55		34°15'N	17°30'E
	-	91	85	74	70	64	60		34°15'N	17°30'E
	-	91	85	74	70	62	55	Ionian	34°15'N	17°30'E
Gaul, et al. (1972)	93	100	92	81	-	-	-	Ionian	36°30'N	17°30'E
	99	90	86	77	-	-	-		38°30'N	18°40'E
	92.5	98.5	91	79	-	-	-		36°30'N	17°30'E
	92.5	99.5	90	81	-	-	-			
	87	93	86	76	-	-	-			
	-	92	85	74	-	-	-			
	88	98	90	79	-	-	-			
	86	95	88	77.5	-	-	-			
	84.5	92.5	86	76	-	-	-	Ionian	36°30'N	17°30'E
MC 015 (1973)	87.2	92	88.4	75.6	67.6	61.6	52.4		36°18'N	17°12'E
	89.6	94.4	89.6	77.2	69.6	65.6	58		36°18'N	17°12'E
	92.8	98.4	93.6	79.2	73.2	69.6	62.8		36°18'N	17°12'E

TABLE 3.3.2-I(C). NOISE SPECTRA WITH ENVIRONMENTAL AND TEST CONDITIONS (Continued) (U)

Time of Day (Z)	Date Measured	Water Depth (meters)	Hydrophone Depth (meters)	Layer Depth (meters)	Sound Channel Axis Depth (meters)	Sea State	Ship Speed (kt)	Notes
0610	11/18/71	~3909	300	0/70	~100/300	½		Include Spectra
0610	11/18/71	↓	1320	↓	↓	½		↓
2050	11/18/71	↓	55	↓	↓	2		↓
0123	11/19/71	↓	180	↓	↓	2		↓
0123	11/19/71	~3909	2330	↓	↓	2		↓
1323	11/22/71	~2433	366	↓	↓	2		↓
1323	11/22/71	~2433	1270	0/70	~100/300	2		Include Spectra
Cont.	11/6-	2433	2135	67	100			Median
↓	11/14/71	↓	3119	↓	↓			↓
↓	11/8-	↓	137	↓	↓			↓
↓	11/16/71	↓	613	↓	↓			↓
↓	↓	↓	1116	67	100			↓
↓	11/8-	↓	2377	~67	~100			↓
Cont.	11/16/71	2433	2652	67	100			Median
Cont.	11/6-	630	82, 149	50	120		3-7	Divided by W.S. Group
↓	11/15/71	↓	320, 472	↓	↓		8-12	↓
↓	↓	↓	613	↓	↓		13-17	↓
↓	↓	↓	↓	↓	↓		18-22	↓
↓	↓	↓	↓	↓	↓		23-27	↓
↓	↓	↓	↓	↓	↓		28-32	↓
↓	11/6-	↓	↓	↓	↓		33-37	↓
↓	11/15/71	2630	613	↓	120		8-12	↓
↓	11/7-	3320	113,180	↓	100		13-17	↓
↓	11/22/71	↓	350, 503	↓	↓		18-22	↓
↓	↓	↓	643	↓	↓		23-27	↓
↓	11/7-	↓	↓	↓	↓		28-32	↓
↓	11/22/71	3320	643	↓	100		33-37	Divided by W.S. Group
↓	11/18/71	3080	31	↓	280		12	Include Spectra
↓	↓	↓	92	↓	280		12	↓
↓	↓	↓	122	↓	280		12	↓
Cont.	11/18/71	3080	1464	50	280		12	↓
	11/11/71		150					Typical Data From Iomedex Mean Values
	11/11/71		137					↓
	11/9-		82					↓
	11/14/71		150					↓
	11/9-		613					↓
	11/14/71		3123					↓
	11/17-		113					↓
	11/24/71		180					↓
	11/17-		644					↓
	11/24/71							Mean Spectra
	11/6-							Median Values
	11/15/71							↓
	11/6-							↓
	11/15/71							Detailed Spectra Available In Iomedex Data Library Through LRAPP

TABLE 3.3.2-I(C). NOISE SPECTRA WITH ENVIRONMENTAL AND TEST CONDITIONS (Continued) (U)

Reference	SPECTRUM LEVEL dB re μPa/Hz½							Location		
	25 Hz	50 Hz	100 Hz	200 Hz	500 Hz	1000 Hz	2000 Hz	Basin	Latitude	Longitude
McCloskey, et al. (1972)	93.8/92.9	99.1/96.3	89.2/88.3	76.2/75.4	-	-	-	Ionian	36°25.5'N	17°28.7'E
	94.4/93.8	98.5/96.2	89.3/88.4	75.7/75.0						
	- / -	-	-	-						
	95.8/95.0	99.8/97.6	84.9/89.2	77.3/76.3						
	95.0/94.1	99.0/96.5	84.5/83.7	77.9/76.9						
	92.1/92.6	96.8/94.9	82.4/82.0	74.9/74.3						
	91.4/91.4	95.5/95.5	89.1/88.9	76.9/76.5						
	92.5/92.4	95.4/95.4	89.4/89.3	76.3/75.9						
	-	-	-	-						
	93.5/93.3	96.4/96.7	84.5/85.4	77.5/78.1						
	92.3/92.4	95.0/95.7	83.9/85.1	78.1/78.9						
	90.9/90.8	93.7/94.2	82.7/83.7	76.3/76.8						
	92.4/92.4	96.8/95.2	90.2/89.6	76.3/76.4						
	93.6/94.0	96.7/96.1	90.6/90.1	76.0/76.2						
	-	-	-	-						
	99.0/94.8	97.4/95.8	86.1/85.2	77.4/77.9						
	93.7/93.8	97.6/95.0	86.3/85.6	79.8/79.1						
	92.2/92.1	95.3/93.1	83.4/84.1	75.8/76.8						
	92.9/95.9	99.1/99.2	90.4/86.9	77.9/75.5						
	93.8/91.8	99.1/93.9	90.9/87.5	77.8/75.1						
	-	-	-	-						
	94.7/92.5	99.6/94.7	86.2/82.5	78.9/76.1						
	94.0/92.0	98.8/94.0	86.5/82.4	80.1/77.3						
	92.2/90.7	97.0/92.6	84.1/80.8	77.2/75.3						
	92.7/89.8	98.2/93.7	88.8/88.8	76.1/75.9						
	94.2/90.7	99.4/93.7	89.7/89.5	76.0/75.7						
	-	-	-	-						
	94.9/91.9	100.3/94.9	84.6/85.2	77.2/77.6						
	93.8/91.1	98.8/94.1	84.5/85.4	78.3/79.1						
	92.1/90	96.9/93.2	82.6/84.3	75.5/76.9						
	90.7/90.5	93.6/99.0	88.9/87.8	75.6/77.0						
	91.5/92.2	93.5/94.7	89.6/89.2	75.4/77.3						
	-	-	-	-						
	-	-	-	-						
	91.5/91.9	93.0/94.5	84.6/84.0	77.5/79.1						
	90.0/90.5	91.4/92.8	83.2/82.7	75.0/74.6						
	91.2/90.1	98.1/96.7	89.1/88.1	77.1/76.6						
	92.8/91.6	98.9/97.0	90.4/89.3	78.1/76.9						
	-	-	-	-						
	-	-	-	-						
	92.4/91.8	98.2/97.4	85.3/84.7	79.8/79.3						
	91.0/90.1	96.4/95.9	84.0/83.1	77.4/76.5						
	92.9/89.9	97.6/95.4	88.9/88.6	77.4/76.1						
	-	-	-	-						
	-	-	-	-						
	-	-	-	-						
	94.4/91.2	98.0/95.5	84.9/84.5	79.7/78.0						
	92.3/89.3	96.0/93.4	83.3/83.1	76.8/75.2						
	92.1/91.2	96.0/94.0	90.2/88.1	72.4/75.5						
	-	-	-	-						
	-	-	-	-						
	-	-	-	-						
	93.4/92.3	96.3/94.1	86.1/83.7	80.3/77.6						
	91.6/90.4	94.2/91.9	84.5/82.3	77.1/74.5						
	93.1/92.8	98.1/96.1	90.3/88.4	77.8/77.6						
	-	-	-	-						
	-	-	-	-						
	-	-	-	-						
	94.7/91.8	98.6/94.5	86.6/84.3	81.1/79.0						
	92.5/90.5	96.4/92.9	84.7/82.9	72.5/76.0						
	-	-	-	-						
	-	-	-	-						
	-	-	-	-						
	-	-	-	-						
	89.0/-	93.4/-	81.5/-	76.8/-						
	86.8/-	92.0/-	79.2/-	73.2/-	-	-	-	Ionian	36°25.5'N	17°28.7'E

TABLE 3.3.2-I(C). NOISE SPECTRA WITH ENVIRONMENTAL AND TEST CONDITIONS (Continued) (U)

Time of Day	Date Measured	Water Depth (meters)	Hydrophone Depth (meters)	Layer Depth (meters)	Sound Channel Axis Depth (meters)	Sea State	Ship Speed (kt)	Notes
(0-1200)/(1200-2400)	8/26/72	3340	301	29-33	~144		Avg Range 0-10	10 sec Data Samples Averaged for 12 Hours (0-1200) (12-2400)
			333					
			944					
			1556					
			2167					
	8/26/72		2779		~144			
	8/27/72		301		~164			
			333					
			944					
			1556					
			2167					
	8/27/72		2779		~164			
	8/28/72		301		~168			
			333					
			944					
			1556					
			2167					
	8/28/72		2779		~168			
	8/29/72		301		~156			
			333					
			944					
			1556					
			2167					
	8/29/72		2779		~156			
	8/30/72		301		~144			
			333					
			944					
			1556					
			2167					
	8/30/72		2779		~144			
	8/31/72		301		~120			
			333					
			944					
			1556					
			2167					
	8/31/72		2779					
	9/1/72		301					
			333					
			944					
			1556					
			2167					
	9/1/72		2779					
	9/2/72		301					
			333					
			944					
			1556					
			2167					
	9/2/72	3340	2779					
	9/3/72	3431	301		~120			
			333		140			
			944					
			1556					
			2167					
	9/3/72		2779					
	9/4/72		301					
			333					
			944					
			1556					
			2167					
	9/4/72		2779		140			
	9/5/72		301		128			
			333					
			944					
(0-1200)/(1200-2400)			1556					
			2167					
	9/5/72	3431	2779	29-33	128			

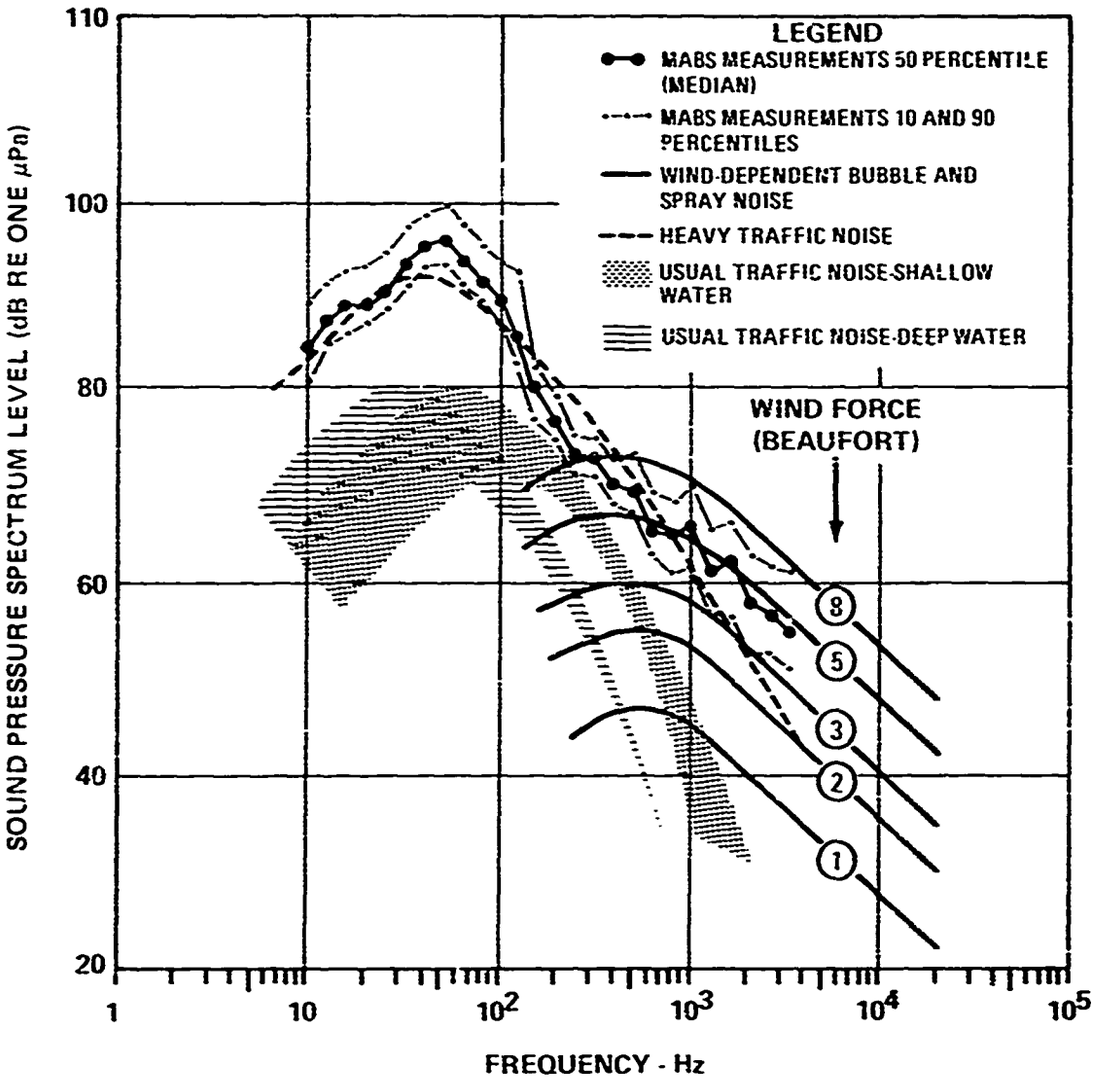

Figure 3.3.2-2(C). Comparison of Omnidirectional Ambient Noise Levels (10th, 50th, and 90th Percentiles) Measured 6 to 15 November at Site A by the MABS 149 Meter Hydrophone With Average Open Ocean Ambient Noise (Wenz, 1962). Average Wind Force During the Measurement Period was 4 on the Beaufort Scale. (U)

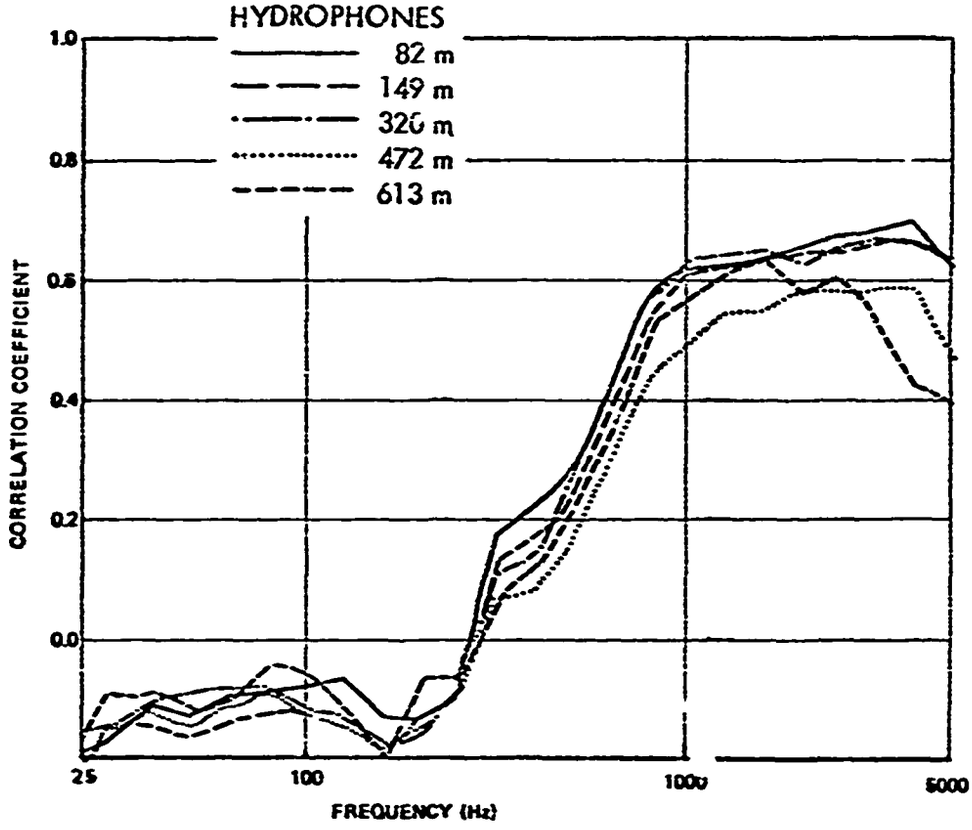

Figure 3.3.2-3. Cross Correlation of Ambient Noise and Wind Speed, Zero Time Lag, (Martin and Perrone, 1973)

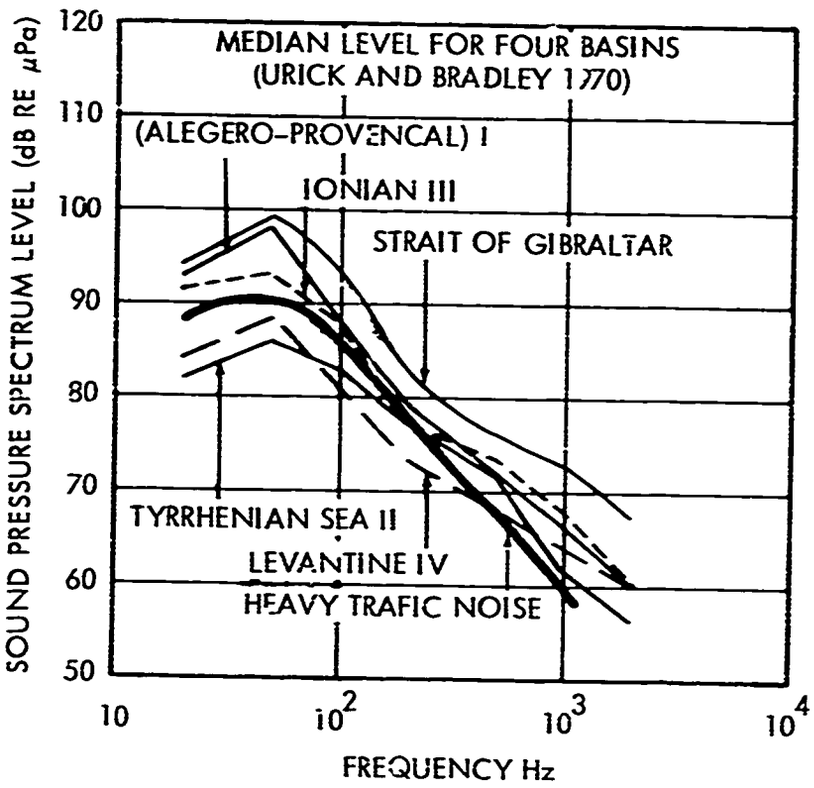

Figure 3.3.2-4(C). Median Ambient Noise Levels in the Major Basins

REFERENCES

1. Arase, E.M. and Arase, T. On the statistics of ambient noise. Columbia University, Hudson Laboratories, Informal Document No. 126, UNCLASSIFIED

2. Arase, E.M. and Arase, T. 1965. A review of recent research in underwater ambient noise, (U). JUA, Vol. 15, No. 3, p. 589, CONFIDENTIAL

3. Arase, E.M. and Arase, T. 1970. Ambient noise in the ocean, 1965-1970, (U). 26th Navy Symp. on Underwater Acoustics, Vol. 1, Nov., CONFIDENTIAL

4. Arase, E.M. and Arase, T. 1971. A review of underwater ambient noise research in the period 1965-1971, (U). JUA, Vol. 21, No. 4, p. 541, Oct, CONFIDENTIAL

5. Arase, E.M. and Arase, T. 1968. Ambient noise measurements in the Mediterranean Sea (U). Proc. 26th Navy Symp. Underw. Ac., Vol. 2, USL Symp. Rep. no. 995, p. 900, New London, Conn. (Also as Hudson Lab. Tech. Rep. no. 152, 1968) CONFIDENTIAL

6. Arase, E.M. and Arase, T. 1968. Deep-sea ambient-noise statistics. JASA, Vol. 44, No. 6, p. 1679, UNCLASSIFIED

7. Arase, E.M. and Arase, T. 1972. Transmission loss in the Ionian Sea (IOMEDEX), (U). Stevens Institute of Technology, Technical Memorandum 163, UNCLASSIFIED

8. Basin, M.A. and Brackmann, W.H. Jr. 1963. Self-noise investigations of modular line array sonar systems, (U). JUA, Vol. 13, No. 3, p. 671, CONFIDENTIAL

9. Baxter, II, L. Spectra of ambient noise in the Mediterranean Sea. Woods Hole Oceanographic Institution, WHOI - Ref. No. 71-64, CONFIDENTIAL

10. Buvik, L.M. and Leroy, C.C. 1967. An analysis of traffic surveys made in the Strait of Gibraltar and its eastern approaches, (U). SACLANT ASW Res. Cen. Tech. Rep. No. 84, La Spezia, (NATO CONFIDENTIAL)

11. Chesapeake Instrument Corp. 1969. Proposal for ambient noise and propagation studies in the Mediterranean Sea with interim towed array sonar system, (U). Snadyside, Md., SECRET

12. Crouch, W.W. 1968. Amplitude statistics of ambient sea noise, (U). U.S. Navy Underwater Sound Laboratory, USL Tech. Memo No. 2063-07-68, CONFIDENTIAL

13. Dale, J.C. 1969. Acoustic survey and data reduction (U). Sanders Associates Report, SECRET

14. Duykers, B. and Bom, N. 1965. Acoustical measurements in the Gibraltar area (U). SACLANT ASW Res. Cen. Tech. Memo. No. 101, La Spezia, NATO CONFIDENTIAL

15. Dyer, I. 1970. Statistics of sound propagation in the ocean. JASA, Vol. 48, No. 1 (Part 2), p. 337, Unclassified

16. Fenner. D.F., Banchero, L.A., Lackie, K.W. and Watrous, B.A. 1973. IOMEDEX sound velocity analysis, current measurements, and environmental data summary, (U). NAVOCEANO Technical Note No. 6160-8-73, UNCLASSIFIED

17. Franz, G.J. 1959. Splashes as sources of sound in liquids. J. Acoust. Soc. Am. 31:1080

18. Frisch, W. and Johnson, C. 1972. Ambient noise measurements in the Ionian Basin of the Mediterranean with sonodiver (U). NUC Tech. Note No. 783, New London, Conn.

19. Frisch, W. and Johnson, C. 1972. IOMEDEX data summary and report. NUC TN 704, UNCLASSIFIED

20. Gaul, R.D., White, A.E. and Fadness, A.E. 1972. IOMEDEX synopsis, (U). Maury Center for Ocean Science, Long Range Acoustic Propagation Project, MC Report 07, CONFIDENTIAL

21. Gerrebout, J. and Leroy, C. 1968. Background-noise at audio-frequencies in the Strait of Gibraltar (U). SACLANT ASW Res. Cen. Tech. Rep. No. 89, La Spezia, NATO CONFIDENTIAL

22. Hasse, R. . 1971. Ioned experiment preliminary data report, (U). Naval Underwater Systems Center, NUSC Pub. No. 6002, CONFIDENTIAL

23. Hays, E.E. and Murphy, E.L. 1969. Mediterranean sound transmission, (U). Woods Hole Oceanogr. Inst. Ref. No. 69-69, Woods Hole, Mass., CONFIDENTIAL

24. Hersey, J.B. 1969. Mediterranean Sea environmental atlas for ITASS, (U). Maury Center for Ocean Science, Ocean Science Program, MC Report 002, SECRET-NOFORN

25. Hontz, R.W. and Higgins, M.E. 1970. Ambient sea noise spectra at selected locations in the North Atlantic, (U). NADC, Johnsville, Penn., CONFIDENTIAL

26. Houston, M.H. and Vidale, M.L. 1969. Estimates of ambient noise in the deep ocean. Part II, General Oceanology Rept. no. GO-5, DDC no. AD-513-209, SECRET

27. Howard, J.R. 1972. Horizontal distribution of ocean ambient noise, (U). Proc. 29th Navy Symp. Underw. Acous. 2, p. 51, CONFIDENTIAL

28. Johannessen, O.M. and Mellberg, L.W. 1972. Layered oceanic microstructure, its effects on sound propagation. SACLANT ASW Res. Cen. Tech. Rep. no. 206, La Spezia

29. Keller, E. A. and Weinstein, M.S. 1971. Prime factors affecting ASW surveillance in the Mediterranean, (U). Raff Associates, Inc., Report No. 71-5, SECRET

30. Kingsbury, F.J., Owsley, N.L., and Sumpf, R.M. 1972. Vertical line array ambient noise measurements, final report, (U). NUSC Tech. Rep. 4293, New London, Conn. CONFIDENTIAL

31. Kirklin, R.H. 1974. IOMEDEX data report, (U). Tracor Document No. T-73-RV-5151-C, CONFIDENTIAL

32. Langis, J. 1966. Analysis of merchant traffic in the Strait of Gibraltar, (U). SACLANT ASW Res. Cen. Tech. Rep. No. 58, La Spezia, NATO CONFIDENTIAL

33. Leroy, C.C. 1967. Sound propagation in the Mediterranean Sea, (U). SACLANT ASW Research Centre Tech. Rep. No. 103

34. Lomask, M. and Frassetto, R. 1960. Acoustic measurements with the bathyscaph. JASA 32, 1028

35. Long Range Acoustic Propagation Project, Office of Naval Research 1971. IOMEDEX, LRAPP operation order, (U). MC Plan 06, CONFIDENTIAL

36. Marshall, S.W. 1973. Ambient noise and signal-to-noise profiles in IOMEDEX, (U). NRL Rep. No. 2638, Washington, D.C., CONFIDENTIAL

37. Martin, R.L. and Koenigs, P.D. 1973. Analysis of propagation loss and signal-to-noise ratios from IOMEDEX, (U). NUSC Technical Report 4483

38. Martin, R.L. and Perrone, A.J. 1973. Ionian Basin ambient-noise measurements, (U). NUSC Tech. Rep. No. 4471, New London, Conn., CONFIDENTIAL

39. Maury Center for Ocean Science 1973. IOMEDEX, summary report, (U). Long Range Acoustic Propagation Project, MC Report 015

40. Maury Center for Ocean Science 1972. Mediterranean TASSRAP exercise final report, (U). Long Range Acoustic Propagation Project, MC Report 007, SECRET-NOFORN

41. McCloskey, T.J., LCDR, and Gottwald, J.T. 1972. Mediterranean TASSRAP exercise final report, (U). Maury Center Report 007, SECRET-NOFORN

42. Mellen, R.H. 1952. Thermal noise limit in the detection of underwater acoustic signals. JASA 24:478

43. Morey, C.F. and Macphee, J.V. 1970. Results of Hazeltine Corporations acoustic experiment during January 1970, (U). Hazeltine Corp. Rep. No. 2287, Braintree, Mass., SECRET

44. Murphy, E., et al., 1971. Ambient noise measurement on Atlantis II Cruise No. 59 in the Mediterranean in July 1970, (U). Woods Hole Oceanogr. Inst. Ref. No. 71-14, 1971, also in Proc. 8th Navy Symp. Mil. Oceanogr., 2, p. 372, 1971), CONFIDENTIAL

45. NAVOCEANO Contribution to IOMEDEX Operation Summary Report

46. Pastore, M.J., and Elash, E.S. 1972. Low-frequency, directional (azimuthal) ambient-noise measurements in the Mediterranean Sea, (U). NUSC Tech. Rep. 4199, New London, Conn., SECRET-NOFORN

47. Pastore, M.J. 1970. Preliminary results of ITASS noise measurements, (U). NUSC/NL Tech. Memo. No. 2040-00390-70, New London, Conn., SECRET-NOFORN

48. Pastore, M.J., Cannon, T.F., and Holland, J.P. 1971. Additional results of ITASS noise measurements, (U). NUSC Tech. Memo. No. PA3-00333-71, New London, Conn., SECRET-NOFORN

49. Pastore, M., Cannon, T. and Finlon, K. 1971. ITASS/EMP, (U). 8th U.S. Navy Symposium on Military Oceanography, Vol. 2, 559-566, CONFIDENTIAL

50. Pastore, M.J. 1972. Low-frequency omnidirectional ambient-noise measurements in the Mediterranean Sea, (U). NUSC Rep. No. 4197, New London, Conn., CONFIDENTIAL

51. Polin, B. 1971. Observed nonstationary characteristics of ocean ambient noise, (U). JUA, Vol. 21, No. 3, 409-422, CONFIDENTIAL

52. Sander, E.L., Moses, E.J., and Jennette, R.L. 1972. Spectra of radiated surface ship noise at low frequency, (U). Proc. 29th Symp. on Underwater Acoustics, Vol. 2, p. 97, CONFIDENTIAL

53. Sanders Associates, Inc. 1969. Ambient sea noise tape data analysis, (U). Rep. No. SAN-MRT-69-1272, Nashua, N.H., SECRET

54. Sanders Associates, Inc. 1969. Acoustic survey and data reduction, (U). Rep. No. SAN-MTA-69-1439, Nashua, N.H., SECRET-NOFORN

55. Sanders Associates, Inc. 1970. Acoustic survey and data reduction, Phase II. NADC-CN, N00019-70-C-0468

56. Sanders Associates, Inc. 1970. Acoustic survey and data reduction, Phase II, (U). Rep. No. SAN-RTA-70-6931, Nashua, N.H., SECRET

57. Scheu, H.E. and Bowan, J.I. 1971. Shipping survey procedures for use by aircraft in IOMEDEX, (U). Raf[illegible] Associates, Inc., Report 71-11, CONFIDENTIAL

58. Schumacher, W.R., Thorp, W.H., and Friedel, F.C. 1971. Low-frequency propagation loss experiment in the Mediterranean Sea, (U). Proc. 8th Navy Symp. Mil. Oceanogr., 2, p. 464, CONFIDENTIAL

59. Stasko, N.J. 1971. The optimal location of deep passive acoustic sensors in the Mediterranean Sea-Tyrrhenian Basin, (U). U.S. Naval Postgraduate School, Thesis, SECRET-NOFORN

60. Steinberg, B.N. 1971. Passive integrated Mediterranean plan final report, (U). Naval Air Development Center, Vol. 2, SECRET-NOFORN

61. Stone, J. 1960. Problems associated with the measurement of ambient noise directivity by means of linear additive arrays. Columbia University, Hudson Laboratories, Contribution No. 80

62. Strarup, T., and Tacconi, G. 1966. Measurement of the 2-25 Hz horizontal electric background noise component parallel and close to the coast-line near the Strait of Gibraltar, (U). SACLANT ASW Res. Cen. Tech. Memo. No. 114, La Spezia, NATO CONFIDENTIAL

63. TRW Systems Group 1972. Some brief notes on ambient noise experiments, (U). SECRET

64. Urick, R.J. and Bradley, D.I. 1970. A compilation of ambient noise measurements in the Mediterranean Sea, (U). NOL Tech. Rep. No. 70-191, White Oak, Md., CONFIDENTIAL

65. Urick, R.J., Lund, G.R. and Tulko, T.J. 1972. Measurements of the depth profile of deep water ambient noise, (U). 29th Navy Symposium on Underwater Acoustics, Vol. 2, 117-128, 31 Oct - 1 Nov. 1972, CONFIDENTIAL

66. Vidale, M.L., and Houston, M.H. 1968. Estimates of ambient noise in the deep ocean. General Oceanology Rep. No. 4, DDC No. AD-513-205, CONFIDENTIAL

67. Weigle, F.G. and Watt, H.S. 1971. Ambient noise measurements in the Western Mediterranean with NUSC autobuoy in November 1970, (U). Proc. 8th Navy Symp. Mil. Oceanogr., Vol. 2, p. 398, 1971. (Also as NUSC Tech. Rep. 4205, New London, Conn.) CONFIDENTIAL

68. Wenz, G.M. 1962. Acoustic ambient noise in the ocean, spectra and sources. JASA, Vol. 34, No. 12, p. 1936

69. Wenz, G.M. 1971. What price small-sample, short-term measurements of ambient noise in the ocean?, (U). (L) JUA, Vol. 21, No. 1, 147-152, CONFIDENTIAL

70. White, E.A., Jr. and Horton, D.M. 1969. Ambient noise measurements and predicted signal-to-noise levels in the Mediterranean Sea, Autumn 1968, (U). Tracor, Inc., Washington, D.C., SECRET

71. Wilson, W.D. 1962. Extrapolation of the equation for the speed of sound in sea water. J. Acoust. Soc. Am., Vol. 34, p. 866

APPENDIX 1

(C) This appendix contains, in figures A-1 through A-59, representative seasonal sound velocity profiles for each of the ASW prediction areas shown in figure 3.1.1-1. As discussed in section 3.1.1, in many of these regions, sound velocity profiles were not available for one or more seasons. All sound velocity profiles have been extended either to the mean deep bottom depth (as given on NAVOCEANO Chart NA8 p 2401) or to an appropriate regional bottom depth. In either case, bottom depths are corrected using the tables of Mathews (1939).

(C) Most of the sound velocity profiles given in this appendix are "representative" or "model" profiles for Mediterranean Sea two-degree squares as selected by the AESD sound speed profile retrieval system (Audet and Vega, 1974). Therefore, these profiles are more or less typical of seasonal oceanographic conditions in given two-degree squares. Since two-degree squares only roughly approximate Mediterranean ASW prediction areas, and since the boundaries of these areas (figure 1.0-1) were purposefully maintained to the maximum extent possible in circumscribing the regions depicted in figure 3.1.1-1, a seasonal profile in any given sound velocity region may not differ markedly from a profile for the same season in an immediately adjacent region. However, the overall annual variation in sound velocity within a given region, i.e., the composite of the four seasonal profiles, is always significantly different from that observed in adjacent regions.

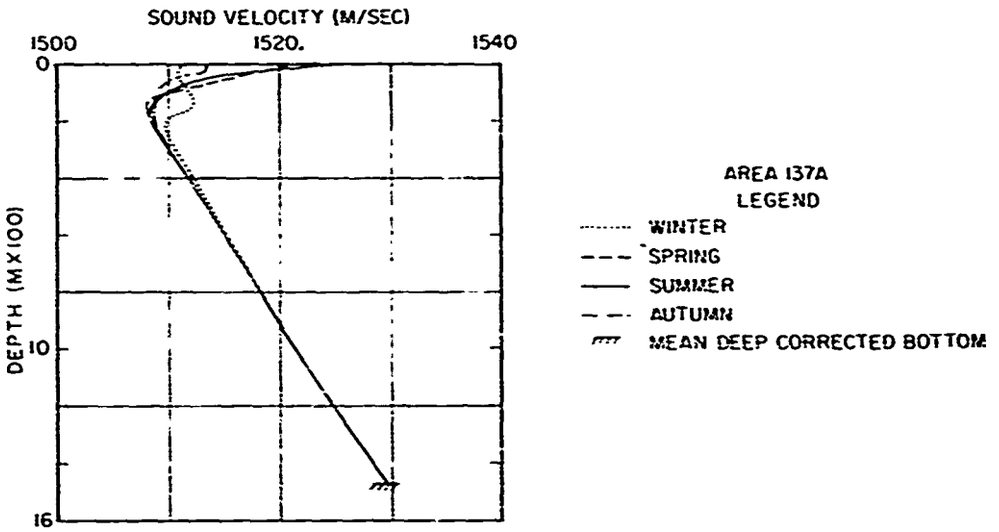

Figure A-1. Representative Seasonal Sound Velocity Profiles for Region 137A

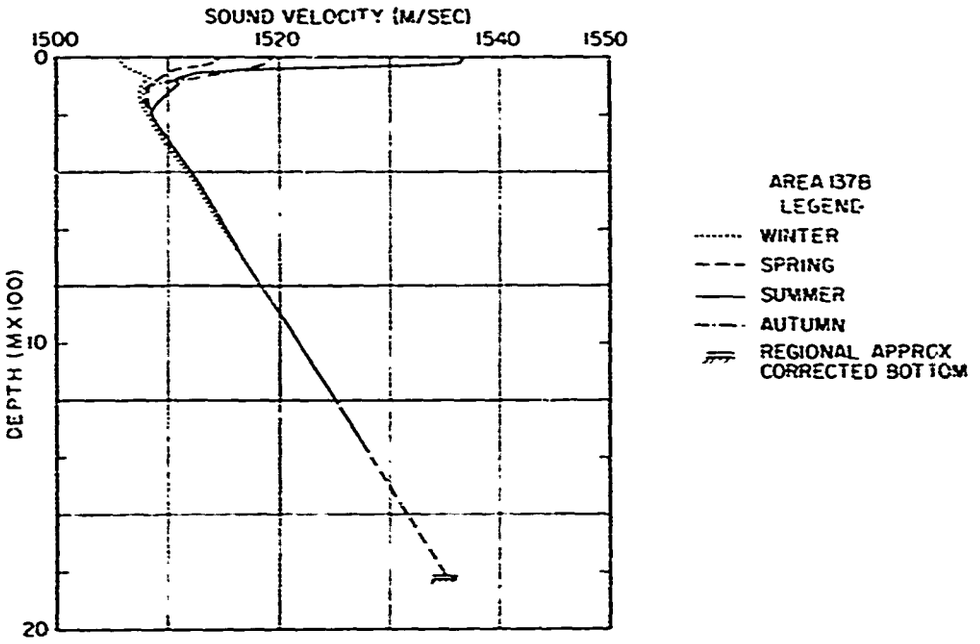

Figure A-2. Representative Seasonal Sound Velocity Profiles for Region 137B

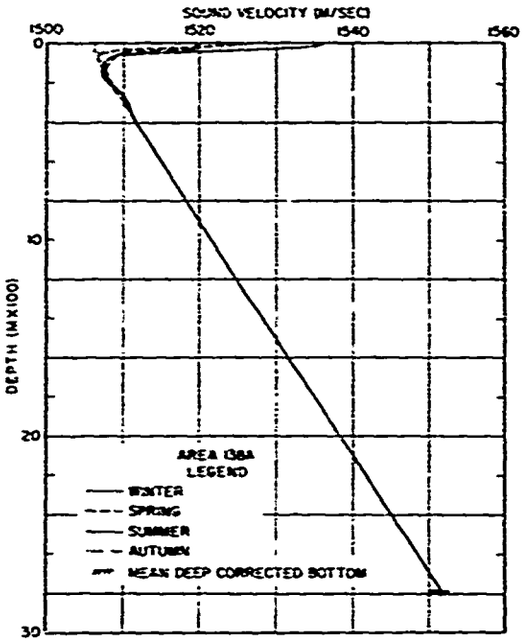

Figure A-3. Representative Seasonal Soumd Velocity Profiles for Region 138A

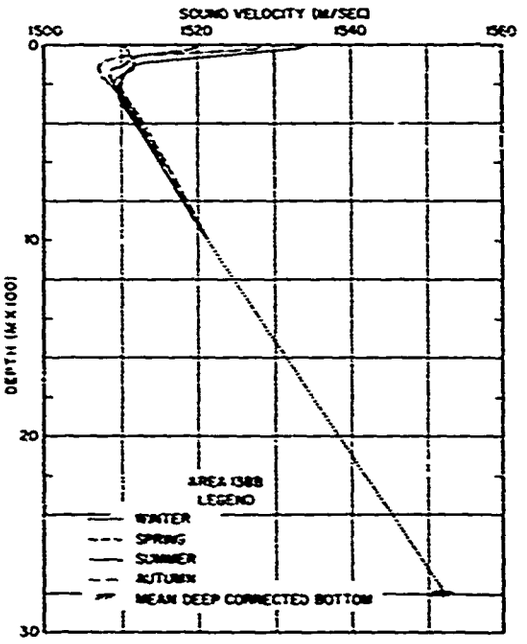

Figure A-4. Representative Seasonal Soumd Velocity Profiles for Region 138B

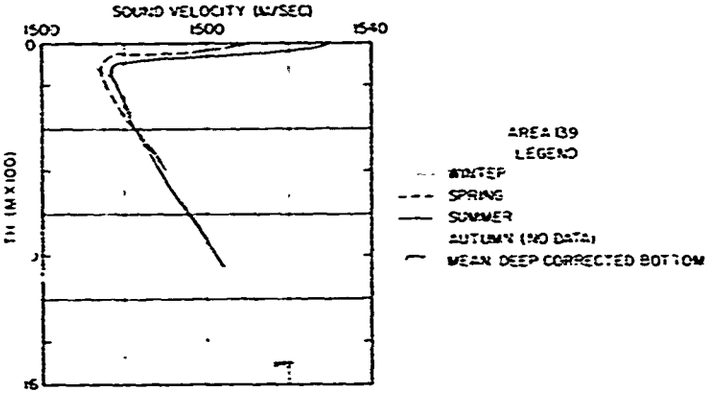

Figure A-5. Representative Seasonal Sound Velocity Profiles for Region 139

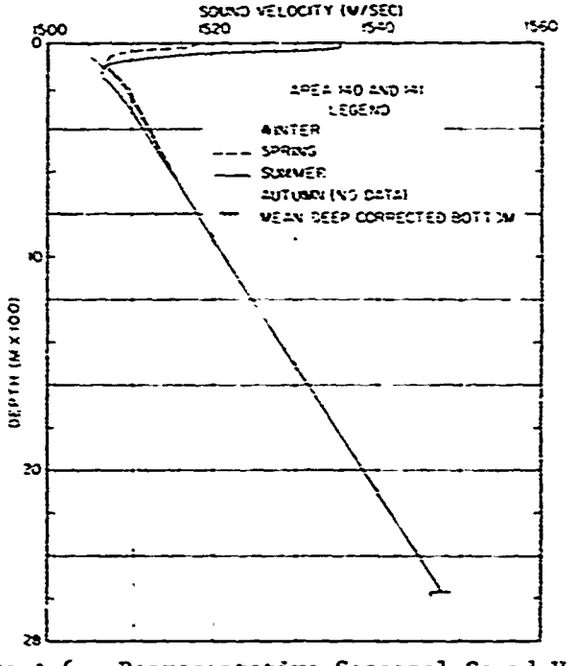

Figure A-6. Representative Seasonal Sound Velocity Profiles for Regions 140 and 141

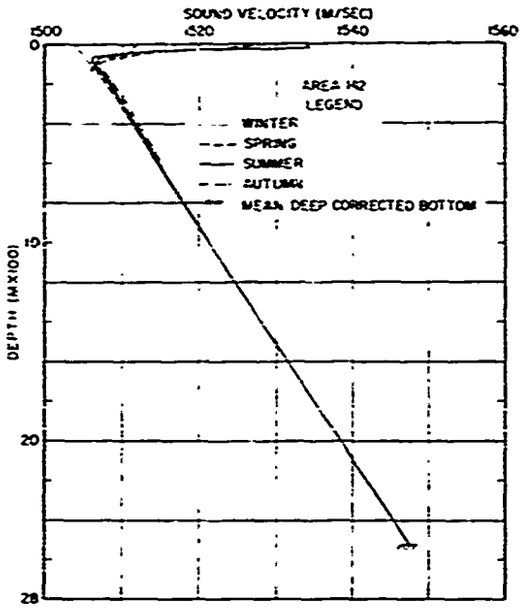

Figure A-7. Representative Seasonal Sound Velocity Profiles for Region 142

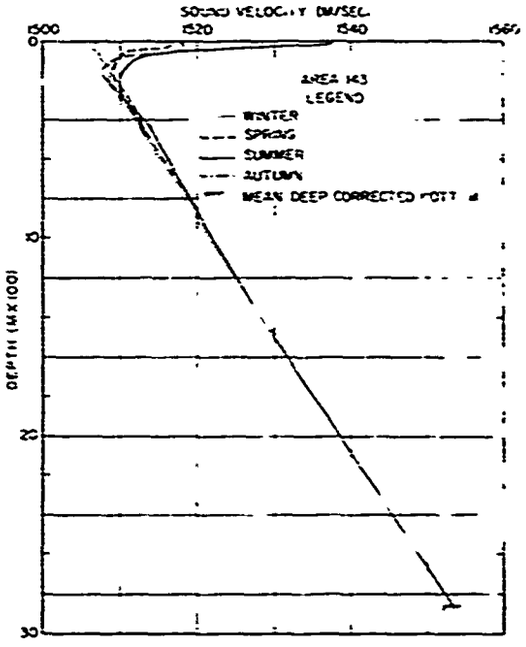

Figure A-8. Representative Seasonal Sound Velocity Profiles for Region 143

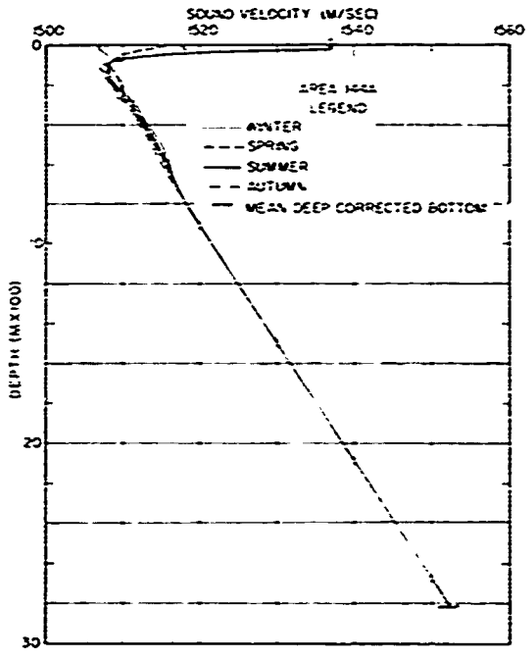

Figure A-9. Representative Seasonal Sound Velocity Profiles for Region 144A

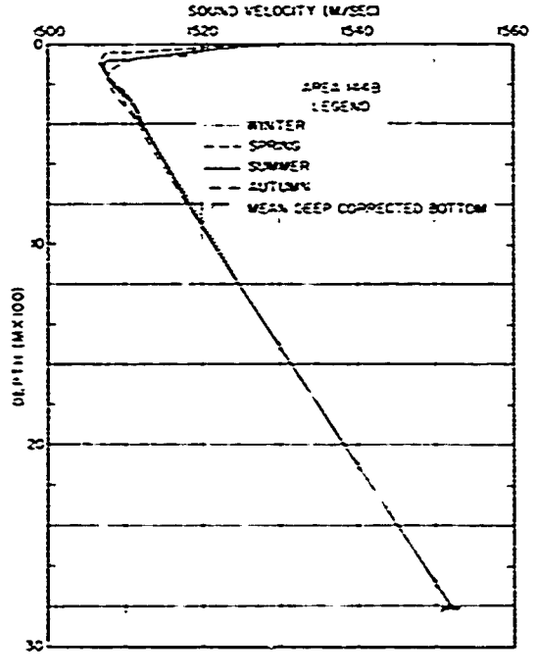

Figure A-10. Representative Seasonal Sound Velocity Profiles for Region 144B

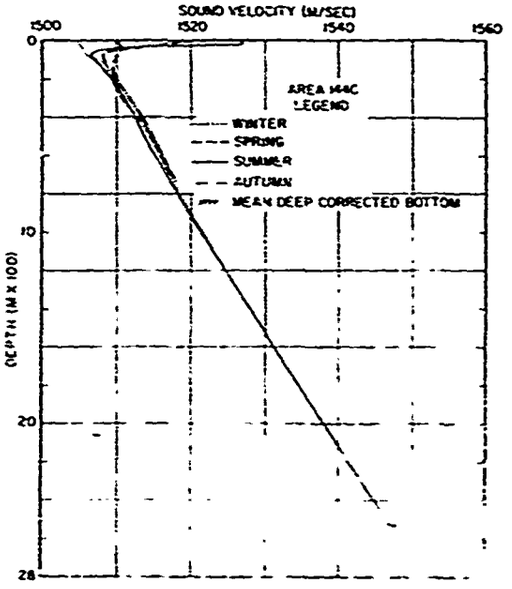

Figure A-11. Representative Seasonal Sound Velocity Profiles for Region 144C

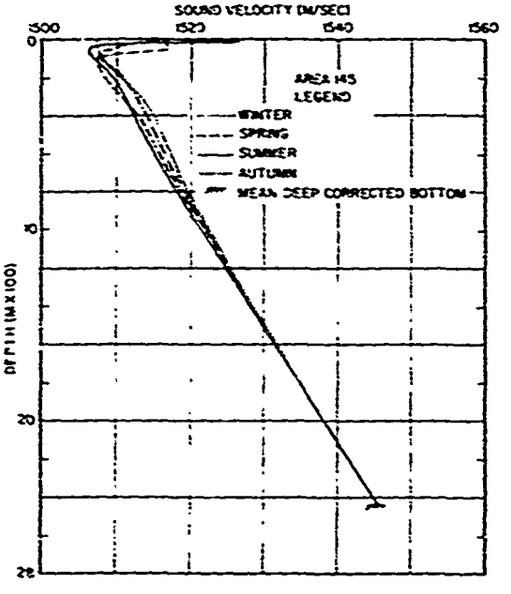

Figure A-12. Representative Seasonal Sound Velocity Profiles for Region 145

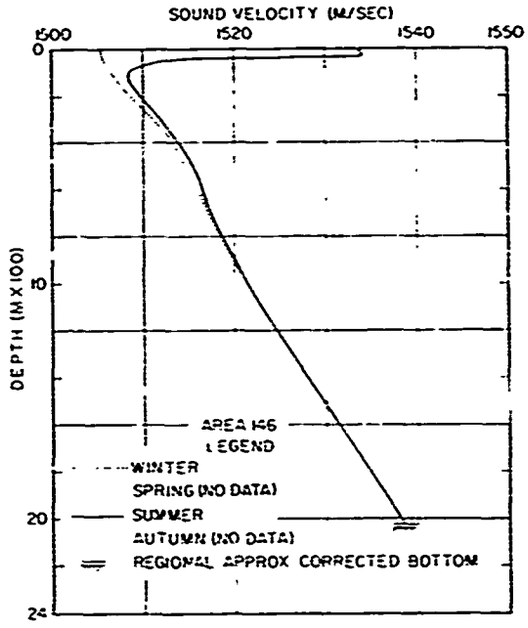

Figure A-13. Representative Seasonal Sound Velocity Profiles for Region 146

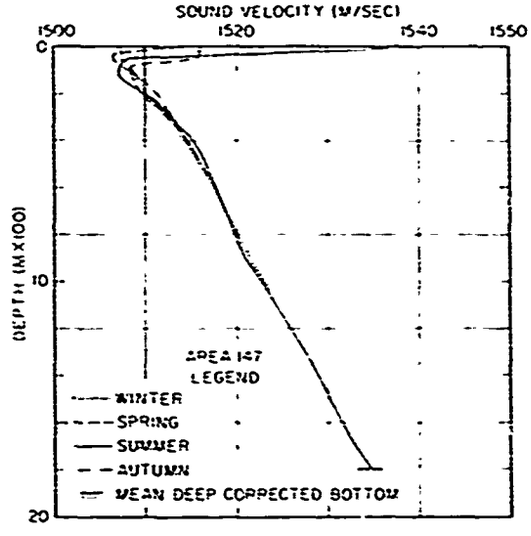

Figure A-14. Representative Seasonal Sound Velocity Profiles for Region 147

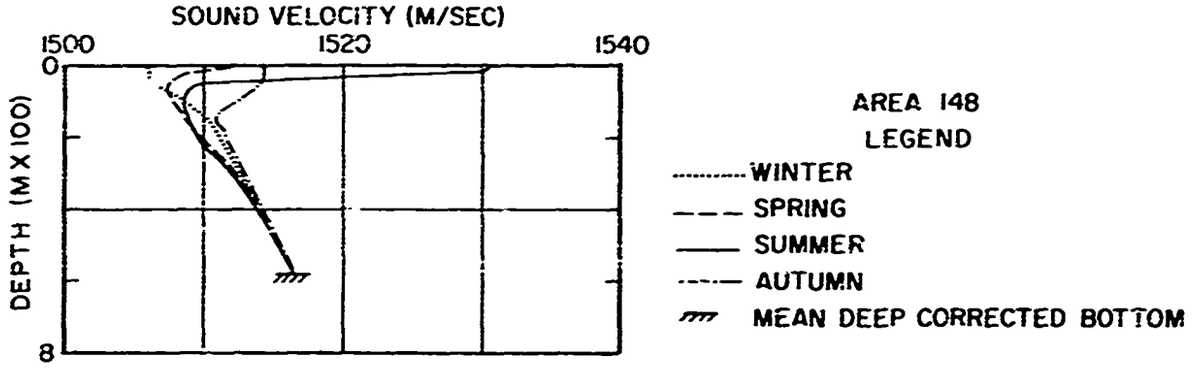

Figure A-15. Representative Seasonal Sound Velocity Profiles for Region 148

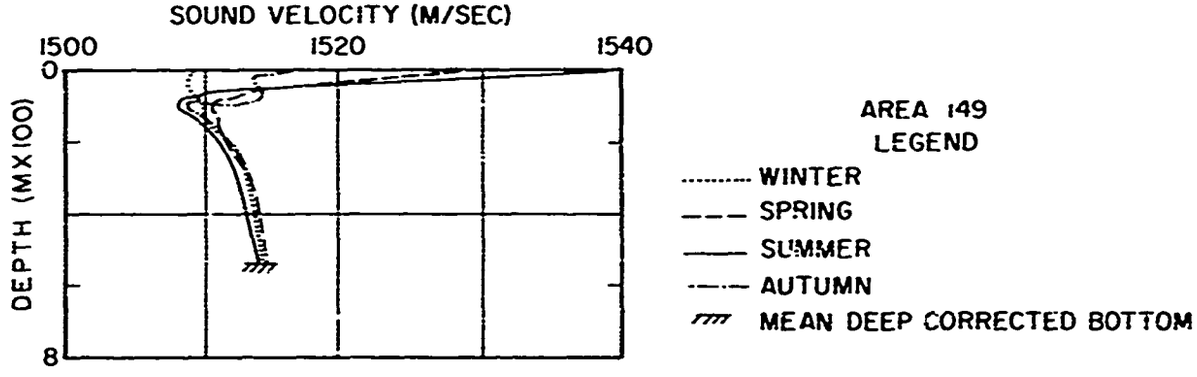

Figure A-16. Representative Seasonal Sound Velocity Profiles for Region 149

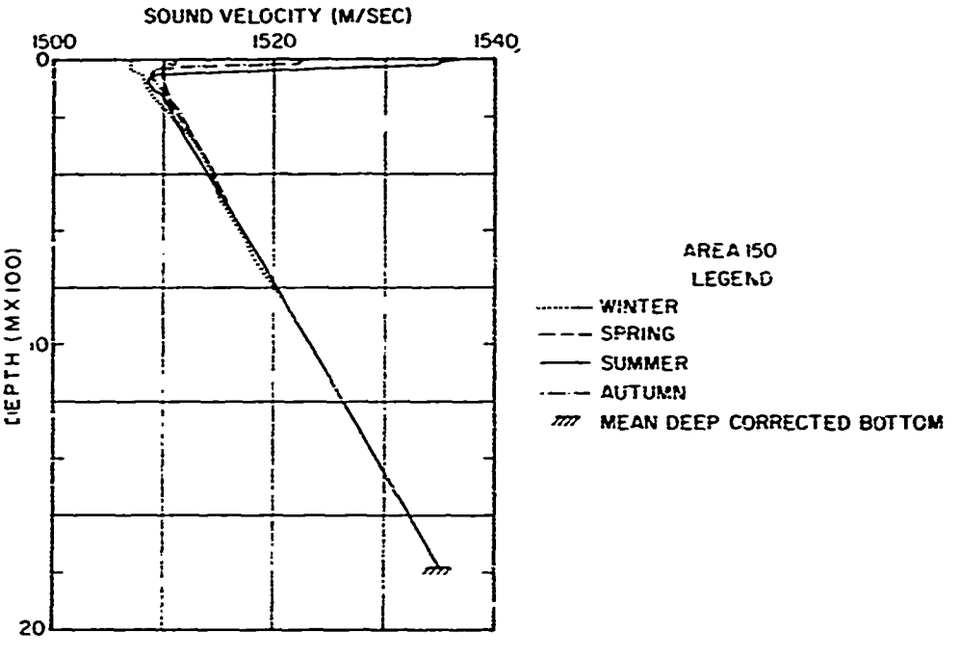

Figure A-17. Representative Seasonal Sound Velocity Profiles for Region 150

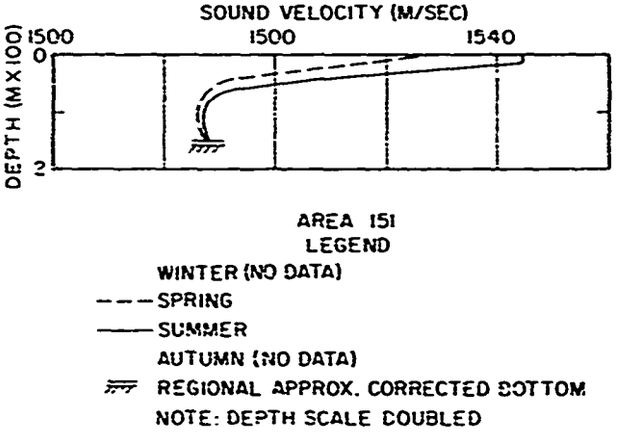

Figure A-18. Representative Seasonal Sound Velocity Profiles for Region 151

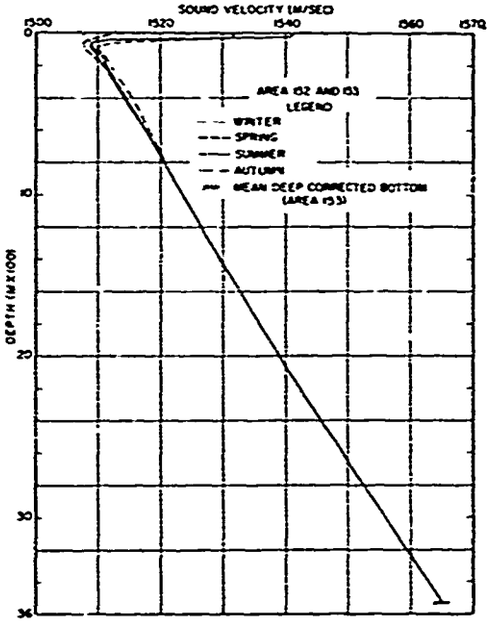

Figure A-19. Representative Seasonal Sound Velocity Profiles for Regions 152 and 153

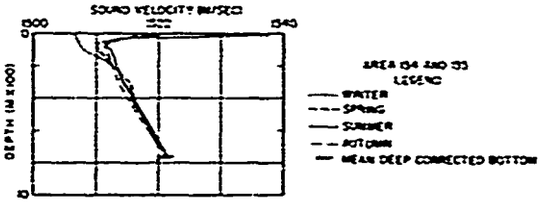

Figure A-20. Representative Seasonal Sound Velocity Profiles for Regions 154 and 155

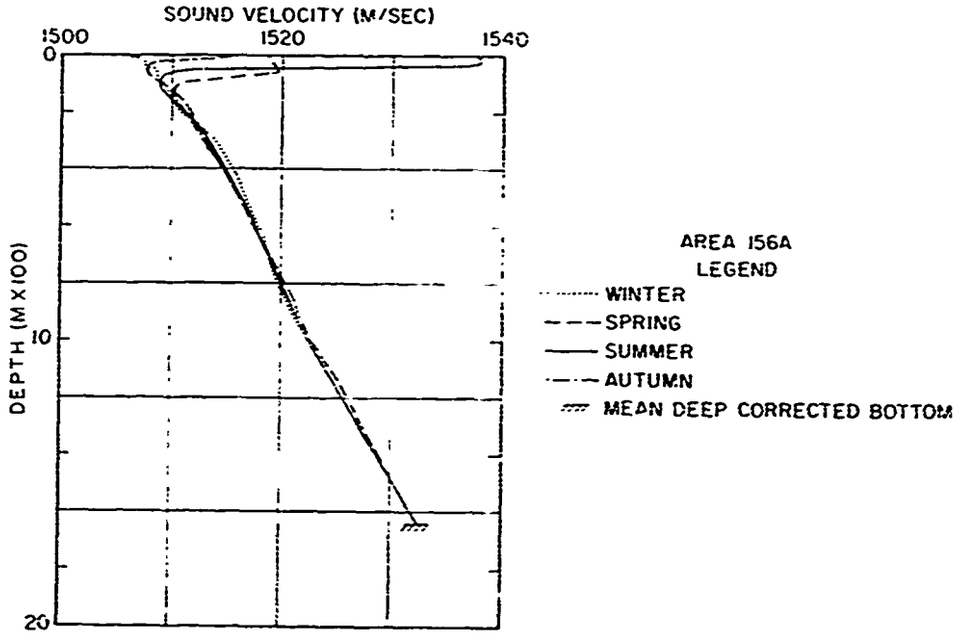

Figure A-21. Representative Seasonal Sound Velocity Profiles for Region 156A

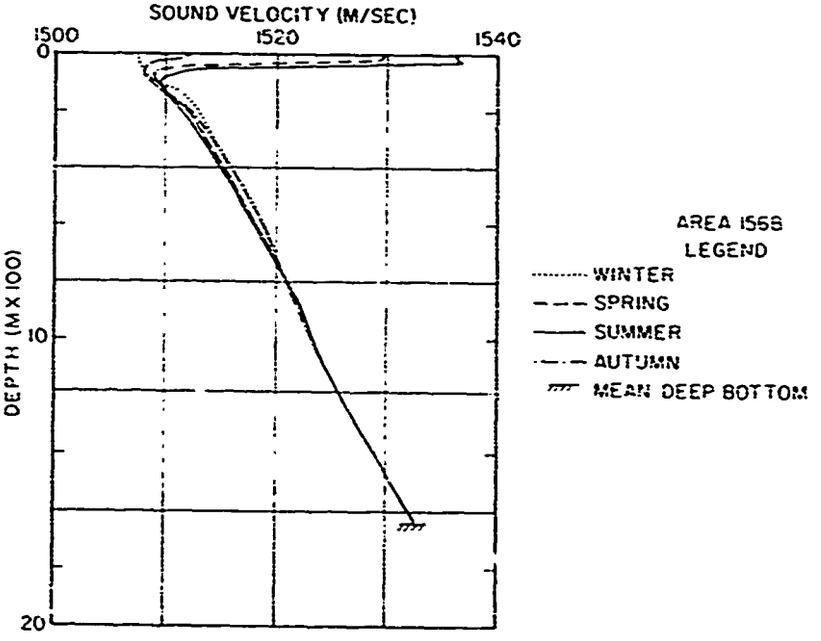

Figure A-22. Representative Seasonal Sound Velocity Profiles for Region 156B

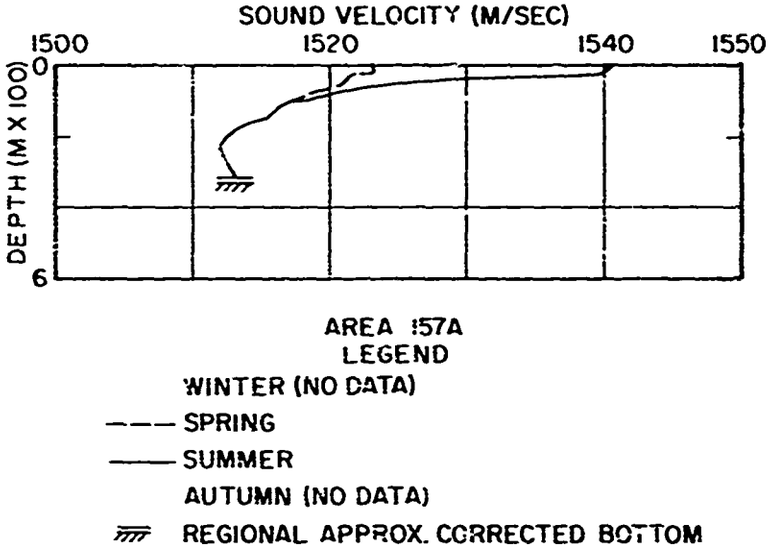

Figure A-23. Representative Seasonal Sound Velocity Profiles for Region 157A

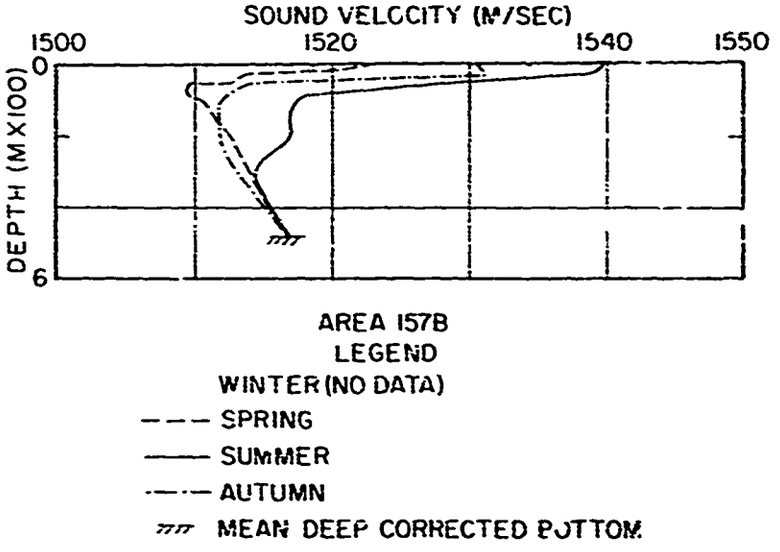

Figure A-24. Representative Seasonal Sound Velocity Profiles for Region 157B

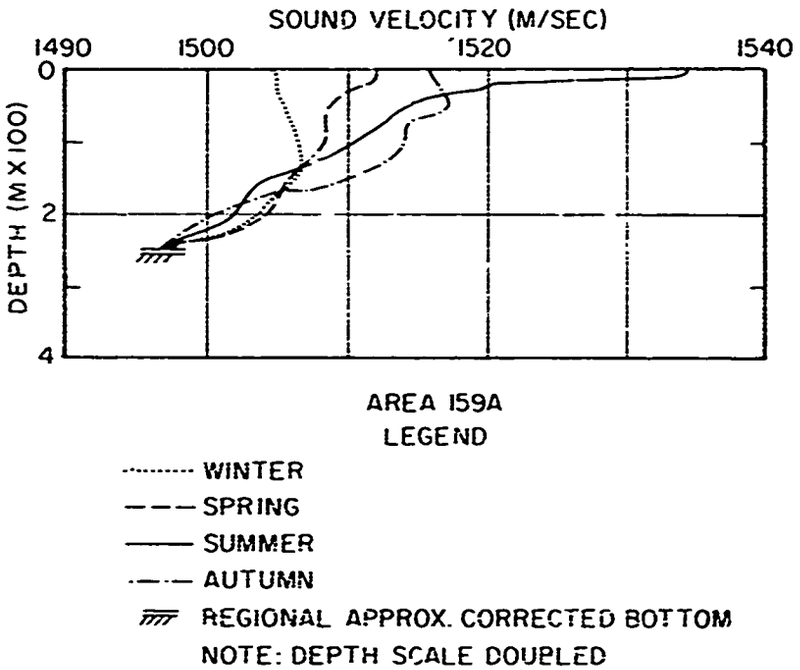

Figure A-25. Representative Seasonal Sound Velocity Profiles for Region 158

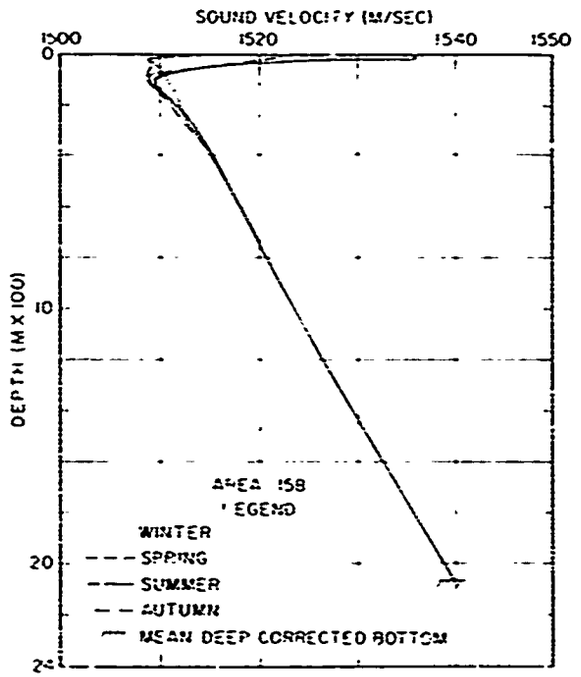

Figure A-26. Representative Seasonal Sound Velocity Profiles for Region 159A

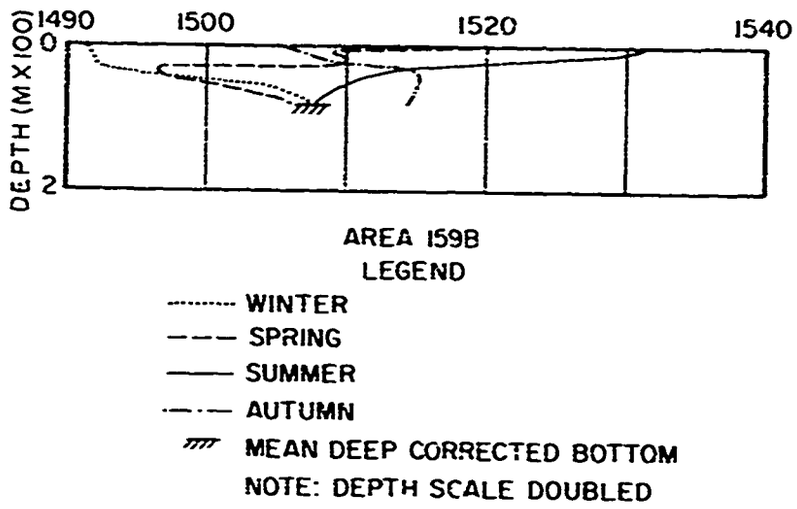

Figure A-27. Representative Seasonal Sound Velocity Profiles for Region 159B

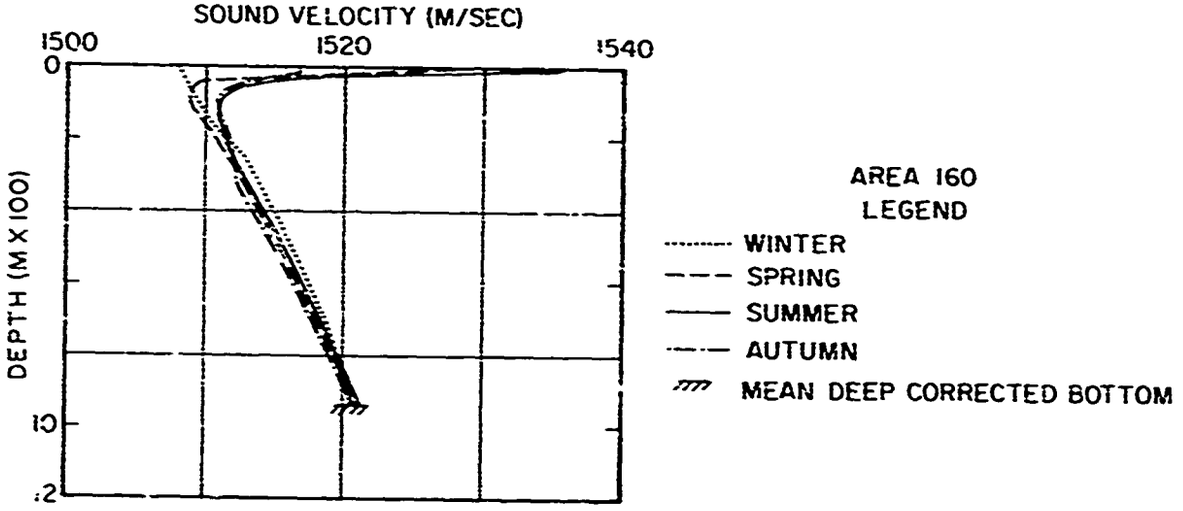

Figure A-28. Representative Seasonal Sound Velocity Profiles for Region 160

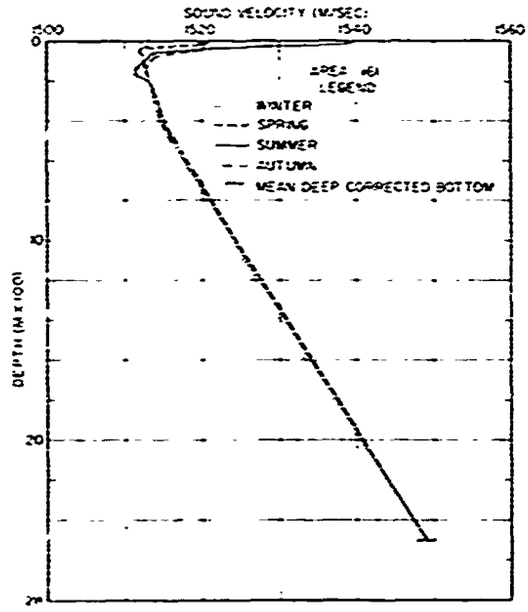

Figure A-29. Representative Seasonal Sound Velocity Profiles for Region 161

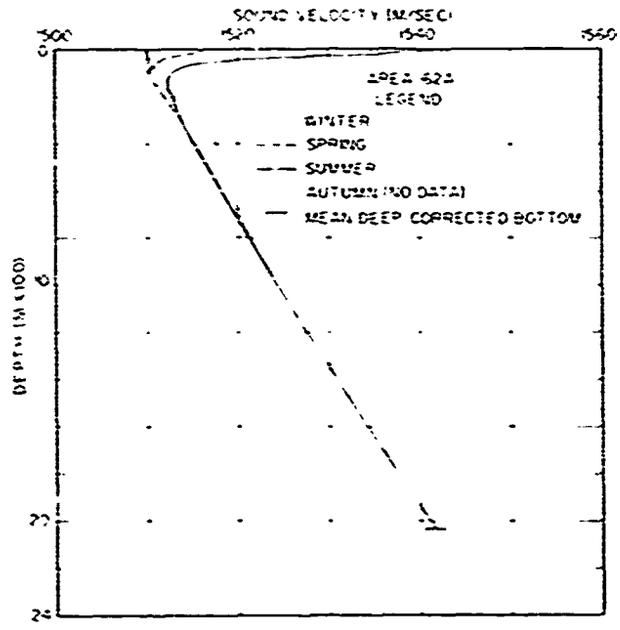

Figure A-30 Representative Seasonal Sound Velocity Profiles for Region 162A

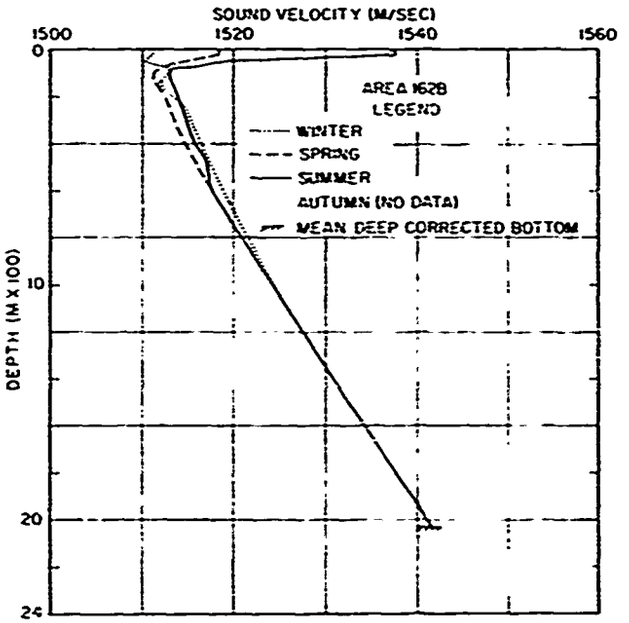

Figure A-31. Representative Seasonal Sound Velocity Profiles for Region 162B

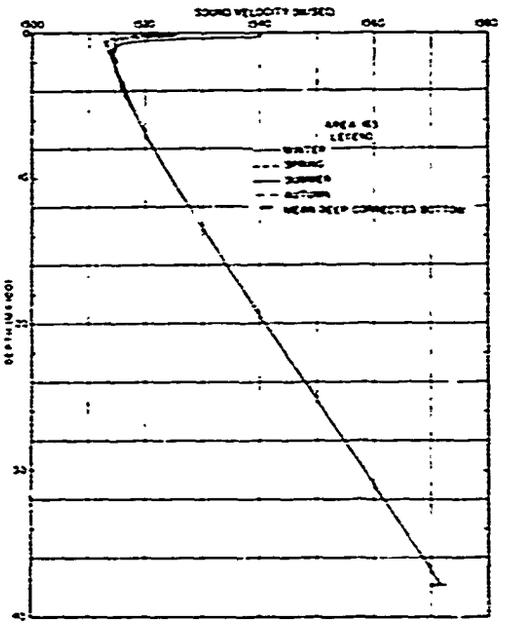

Figure A-32. Representative Seasonal Sound Velocity Profiles for Region 163

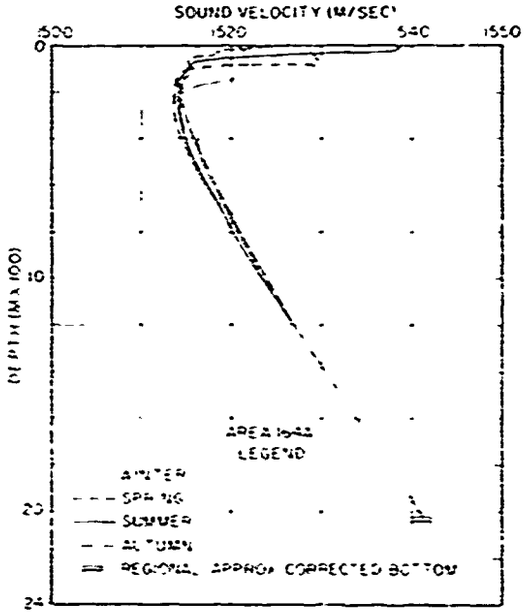

Figure A-33. Representative Seasonal Sound Velocity Profiles for Region 164A

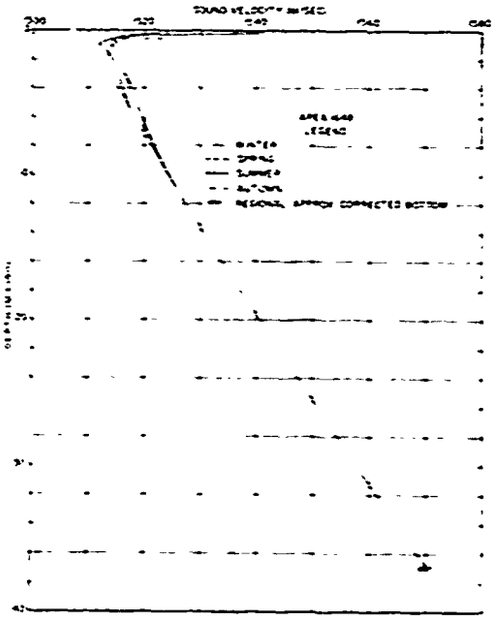

Figure A-34. Representative Seasonal Sound Velocity Profiles for Region 164B

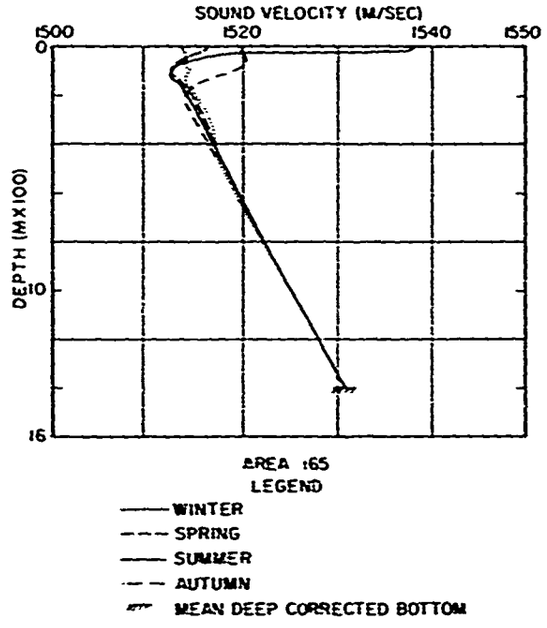

Figure A-35. Representative Seasonal Sound Velocity Profiles for Region 165

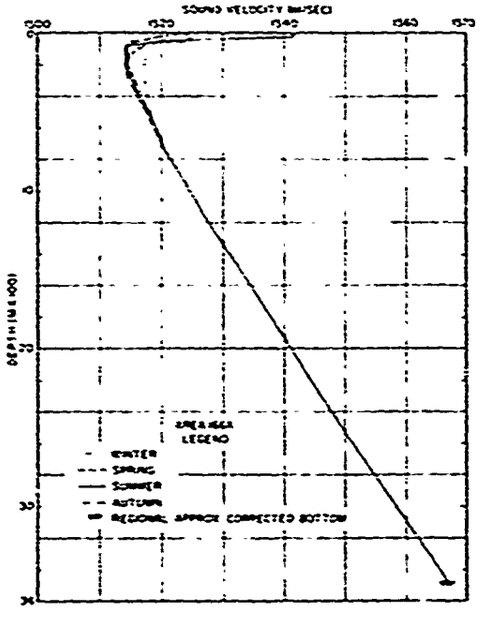

Figure A-36. Representative Seasonal Sound Velccity Profiles for Region 166A

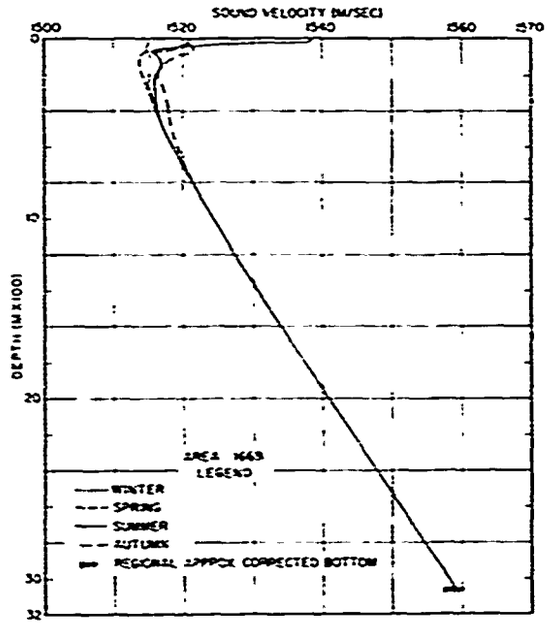

Figure A-37. Representative Seasonal Sound Velocity Profiles for Region 166B

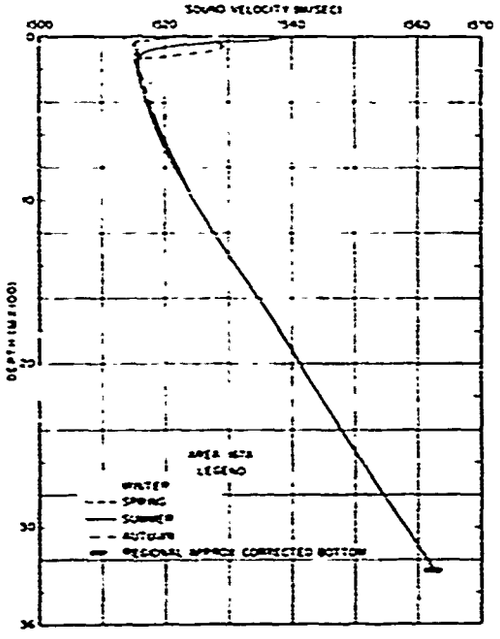

Figure A-38. Representative Seasonal Sound Velocity Profiles for Region 167A

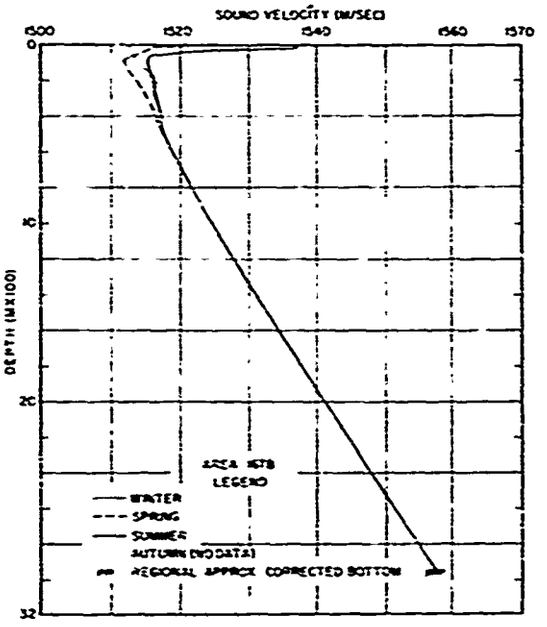

Figure A-39. Representative Seasonal Sound Velocity Profiles For Region 167B

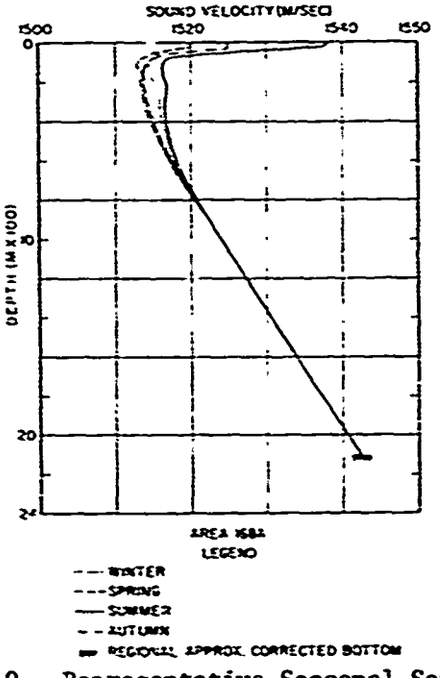

Figure A-40. Representative Seasonal Sound Velocity Profiles for Region 168A

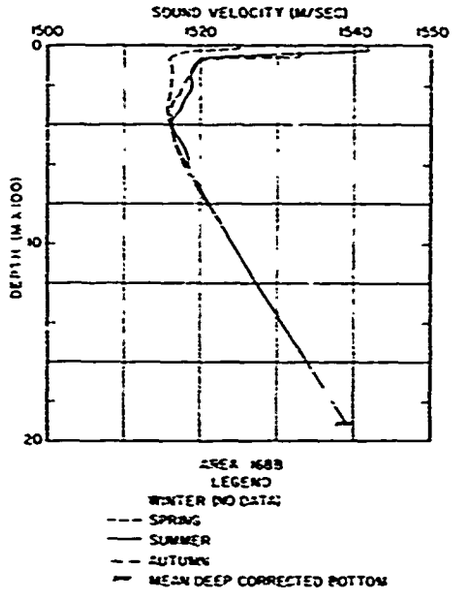

Figure A-41. Representative Seasonal Sound Velocity Profiles for Region 168B

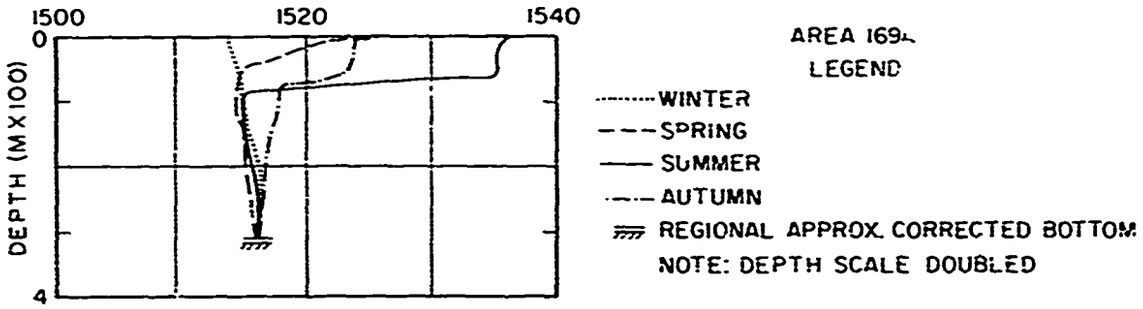

Figure A-42. Representative Seasonal Sound Velocity Profiles for Region 169A

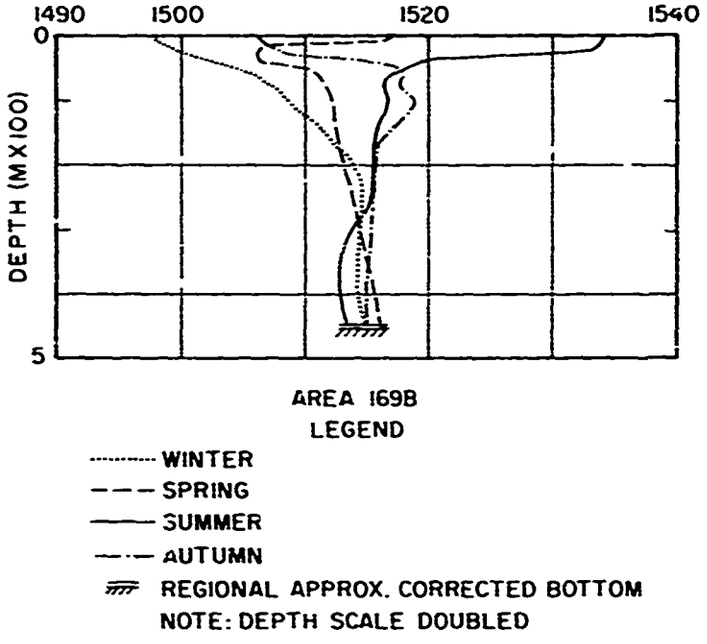

Figure A-43. Representative Seasonal Sound Velocity Profiles for Region 169B

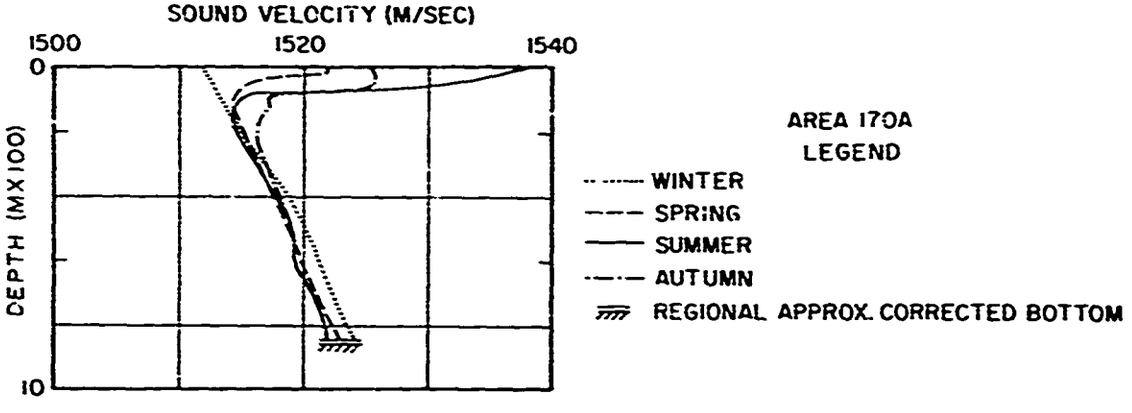

Figure A-44. Representative Seasonal Sound Velocity Profiles for Region 170A

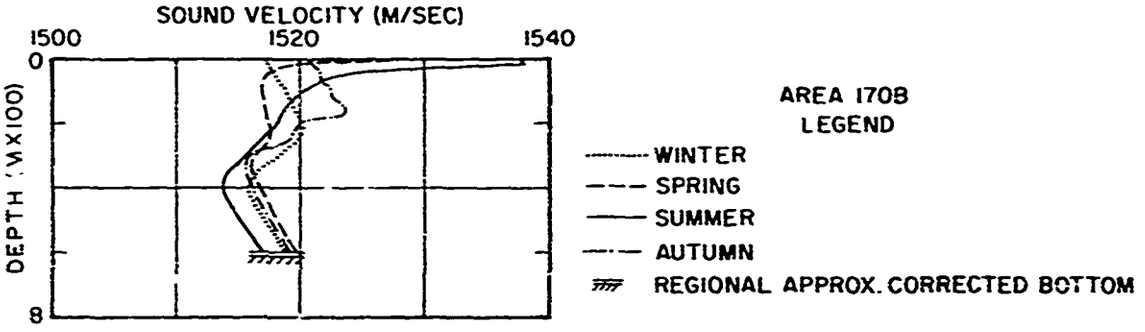

Figure A-45. Representative Seasonal Sound Velocity Profiles for Region 170B

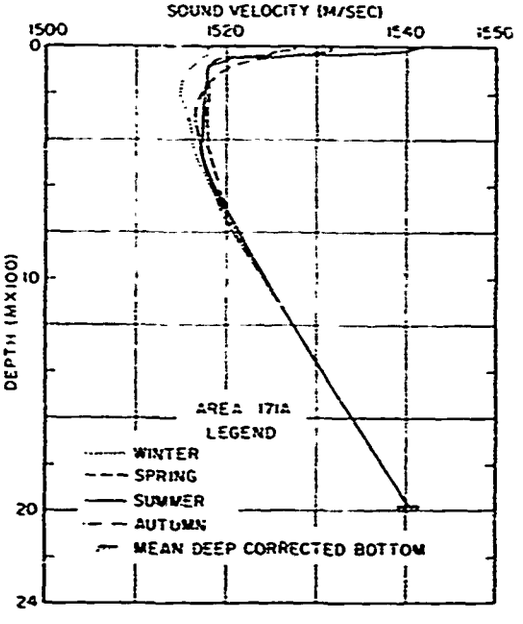

Figure A-46. Representative Seasonal Sound Velocity Profiles for Region 171A

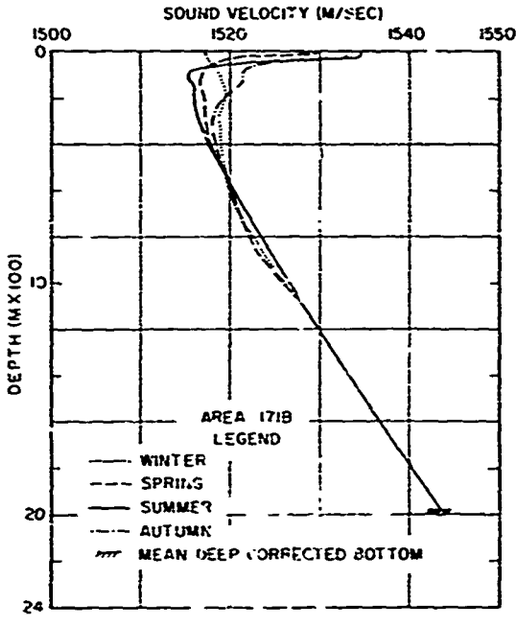

Figure A-47. Representative Seasonal Sound Velocity Profiles for Region 171B

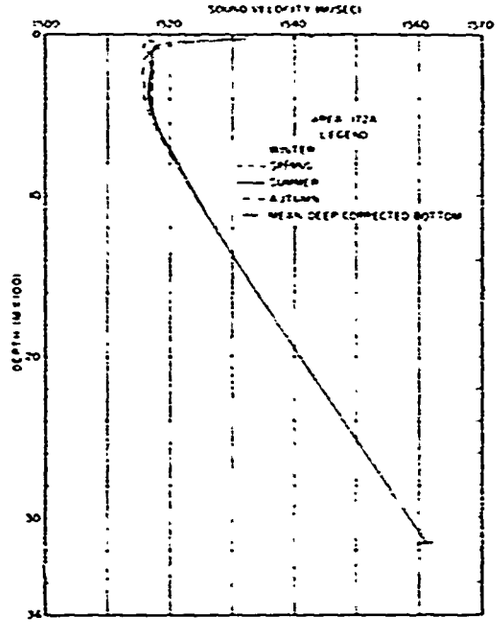

Figure A-48. Representative Seasonal Sound Velocity Profiles for Region 172A

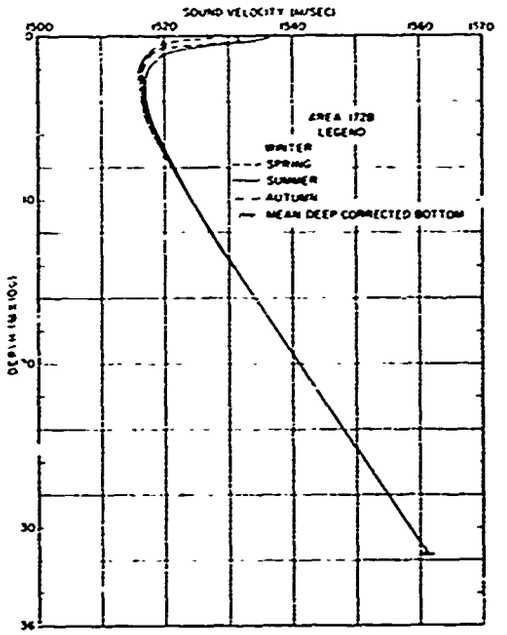

Figure A-49. Representative Seasonal Sound Velocity Profiles for Region 172B

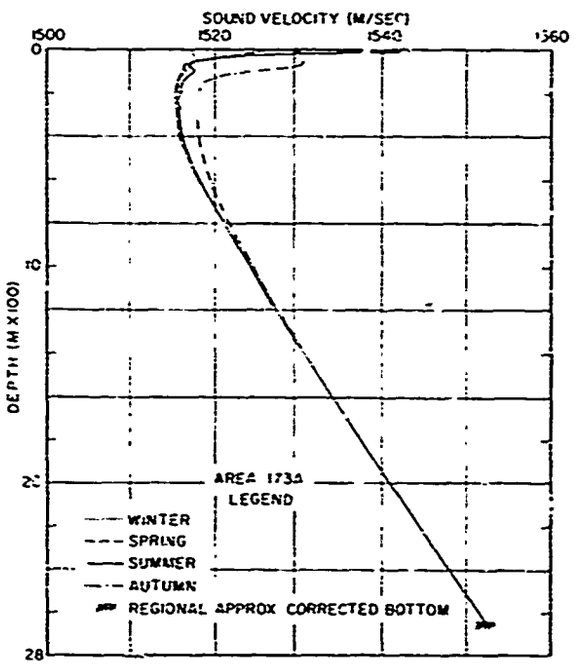

Figure A-50. Representative Seasonal Sound Velocity Profiles for Region 173A

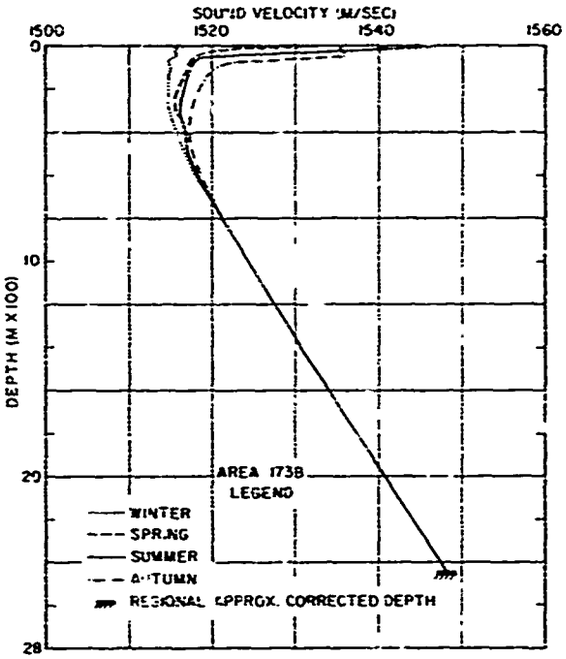

Figure A-51. Representative Seasonal Sound Velocity Profiles for Region 173B

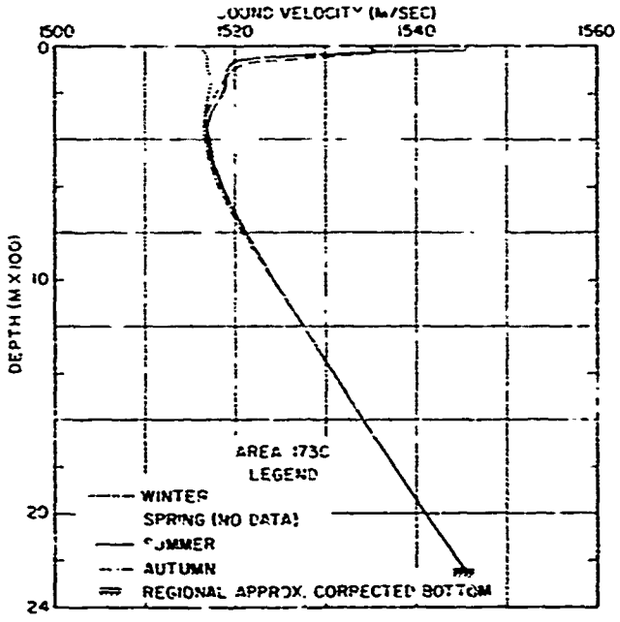

Figure A-52. Representative Seasonal Sound Velocity Profiles for Region 173C

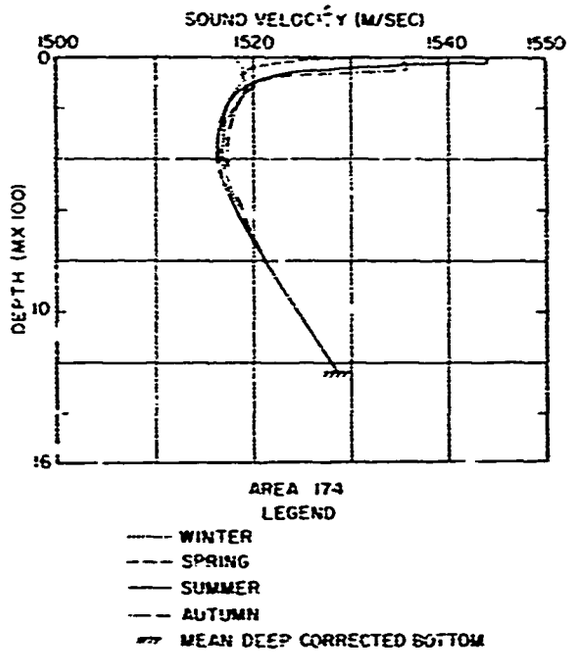

Figure A-53. Representative Seasonal Sound Velocity Profiles for Region 174

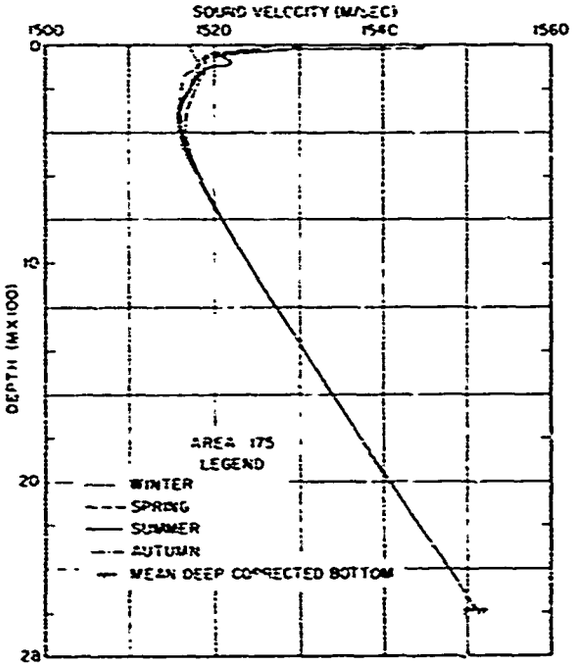

Figure A-54. Representative Seasonal Sound Velocity Profiles for Region 175

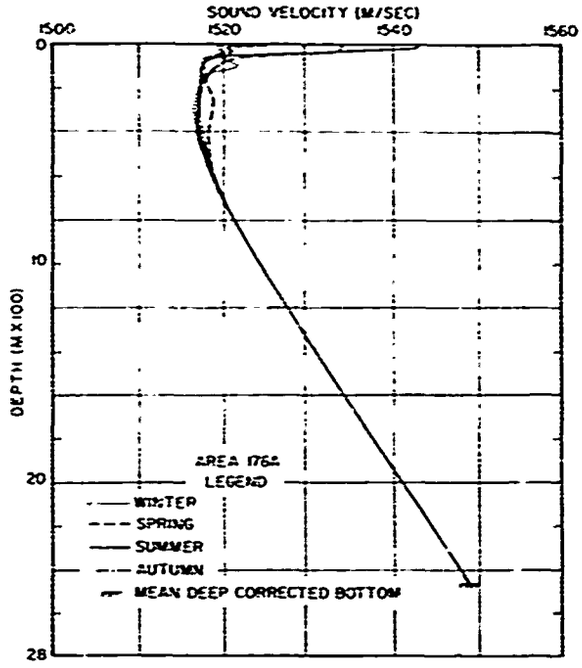

Figure A-55. Representative Seasonal Sound Velocity Profiles for Region 176A

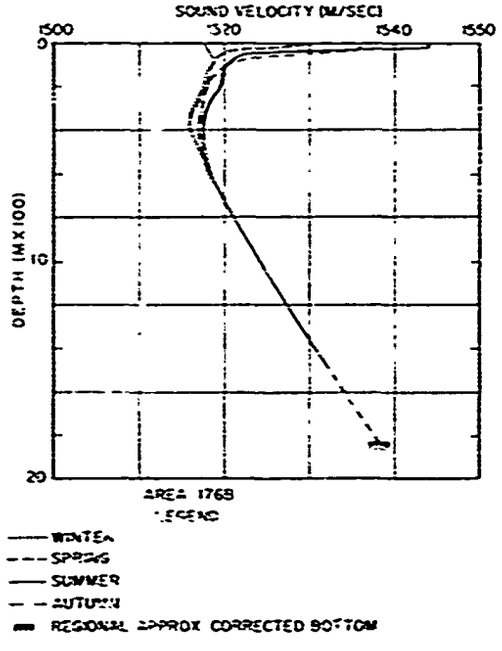

Figure A-56. Representative Seasonal Sound Velocity Profiles for Region 176B

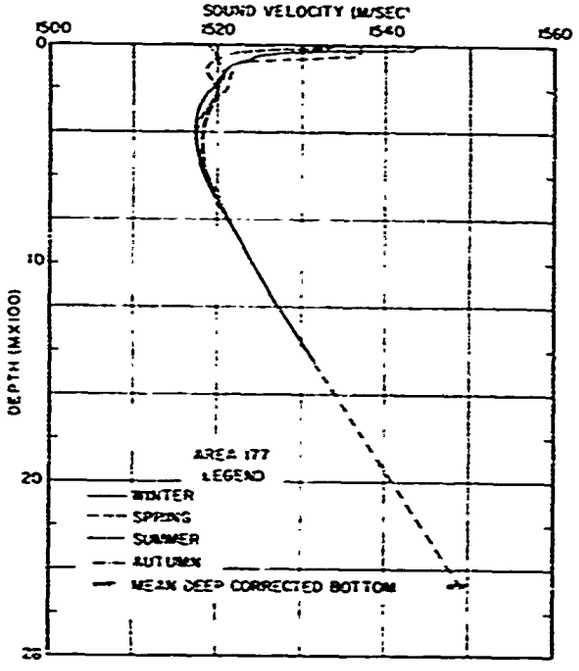

Figure A-57. Representative Seasonal Sound Velocity Profiles for Region 177

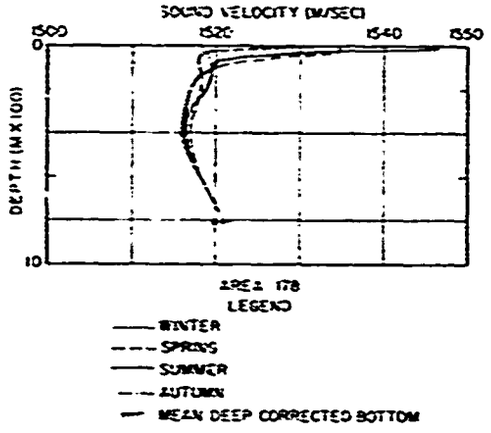

Figure A-58. Representative Seasonal Sound Velocity Profiles for Region 178

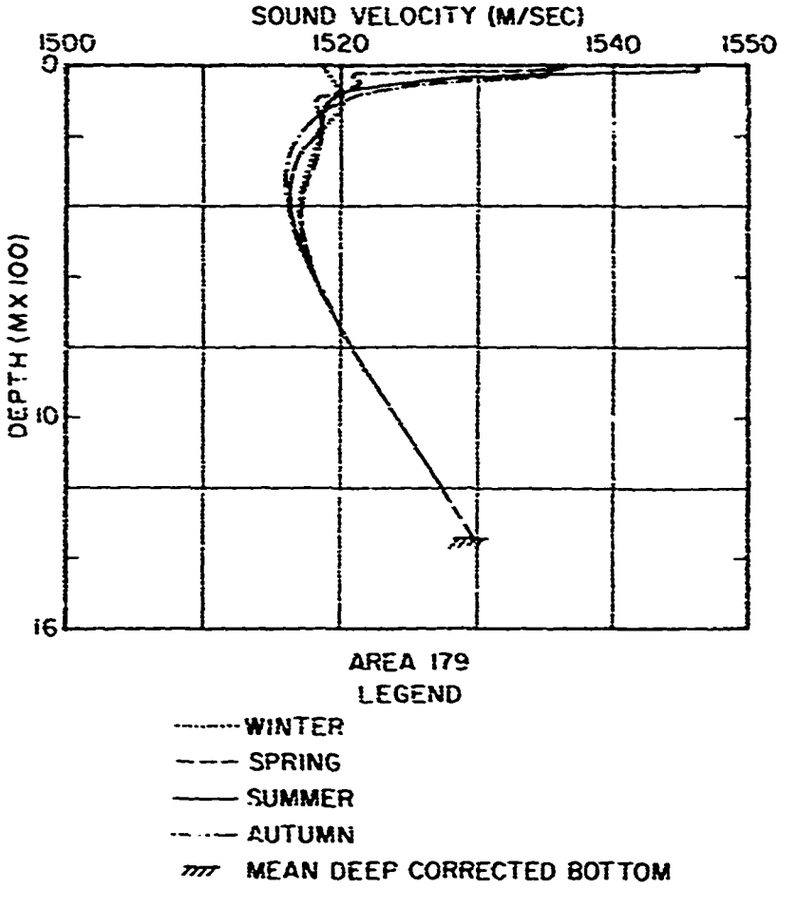

Figure A-59. Representative Seasonal Sound Velocity Profiles for Region 179

DISTRIBUTION LIST

CNO (OP-094) (1)
CNO (OP-095) (2)
CNO (OP-096) (1)
CNO (OP-098) (1)
CNM (PM-4) (4)
COMNAVELEXSYSCOM (PME-124) (4)
COMNAVSEA (4)
COMNAVAIRSYSCOM (4)
ONR (102-OSC) (3)
ONR (200) (1)
ONR (AESD) (1)
COMNAVOCEANO (2)
OCEANNAV (2)
COMNISC (1)
CNA (1)
NADC (1)
NOL (1)
NRL (1)
NUC (1)
NUSC (1)
NSRDC (1)
CINCLANTFLT (1)
CINCUSNAVEUR (1)
COMSIXTHFLT (2)
CTF-67 (5)
CTF-69 (5)
FNWC (1)
FWC ROTA (1)
COMOCEANSYSLANT (1)
COMOPTEVFOR (1)
U.S. Naval Academy (1)
U.S. Naval Post Graduate School (1)
Naval Coastal Systems Laboratory (1)
Advanced Research Projects Agency (1)
National Science Foundation (1)
APL/JHU (1)
APL/UW (1)
ARL/UT (1)
ARL/PSU (1)
Catholic University (1)
SCRIPPS INSTITUTION of OCEANOGRAPHY (1)
GURC (1)
Texas A & M University (1)
WOODS HOLE OCEANOGRAPHIC INSTITUTE (1)
A.D. Little, Inc. (1)
Anacapa Sciences (1)

Analysis and Technology (1)
B and K Dynamics (1)
Bell Laboratories (1)
Bendix-Electrodynamics Div. (1)
Bolt, Beranek and Newman (1)
Bunker Ramo (1)
Cambridge Acoustical Associates (1)
Chesapeake Instrument Corp. (1)
Computer Sciences, Inc. (1)
Control Data Corp. (1)
E-Systems (1)
Edo Corporation (1)
General Dynamics/Electric Boat Co. (1)
General Electric Corp. (1)
Goodyear Aerospace (1)
Hazeltine, Inc. (1)
Honeywell, Inc. (1)
Hughes Aircraft (1)
Hydrospace Challenger, Inc. (1)
Hydroacoustics, Inc. (1)
Hydrotronics (1)
IBM (1)
Magnavox (1)
MAR, Inc. (1)
Mechanics Research, Inc. (1)
Ocean Data Systems, Inc. (1)
Operations Research, Inc. (1)
Planning Systems, Inc. (1)
Radian, Inc. (1)
Raff Associates (1)
Raytheon Corp. (1)
Rockwell International (1)
Sanders Associates (1)
Seismic Engineering Co. (1)
Spectral Dynamics Corp. (1)
Sperry (1)
System Planning Corp. (1)
Tetra Tech (1)
Texas Instruments (1)
Tracor, Inc. (1)
TRW, Inc. (1)
Undersea Research Corp. (1)
Underwater Systems Inc. (1)
Unitech, Inc. (1)
Vitro, Automation Industries (1)
Western Electric Co. (1)
Westinghouse (1)
Xonics (1)
DDC (12)

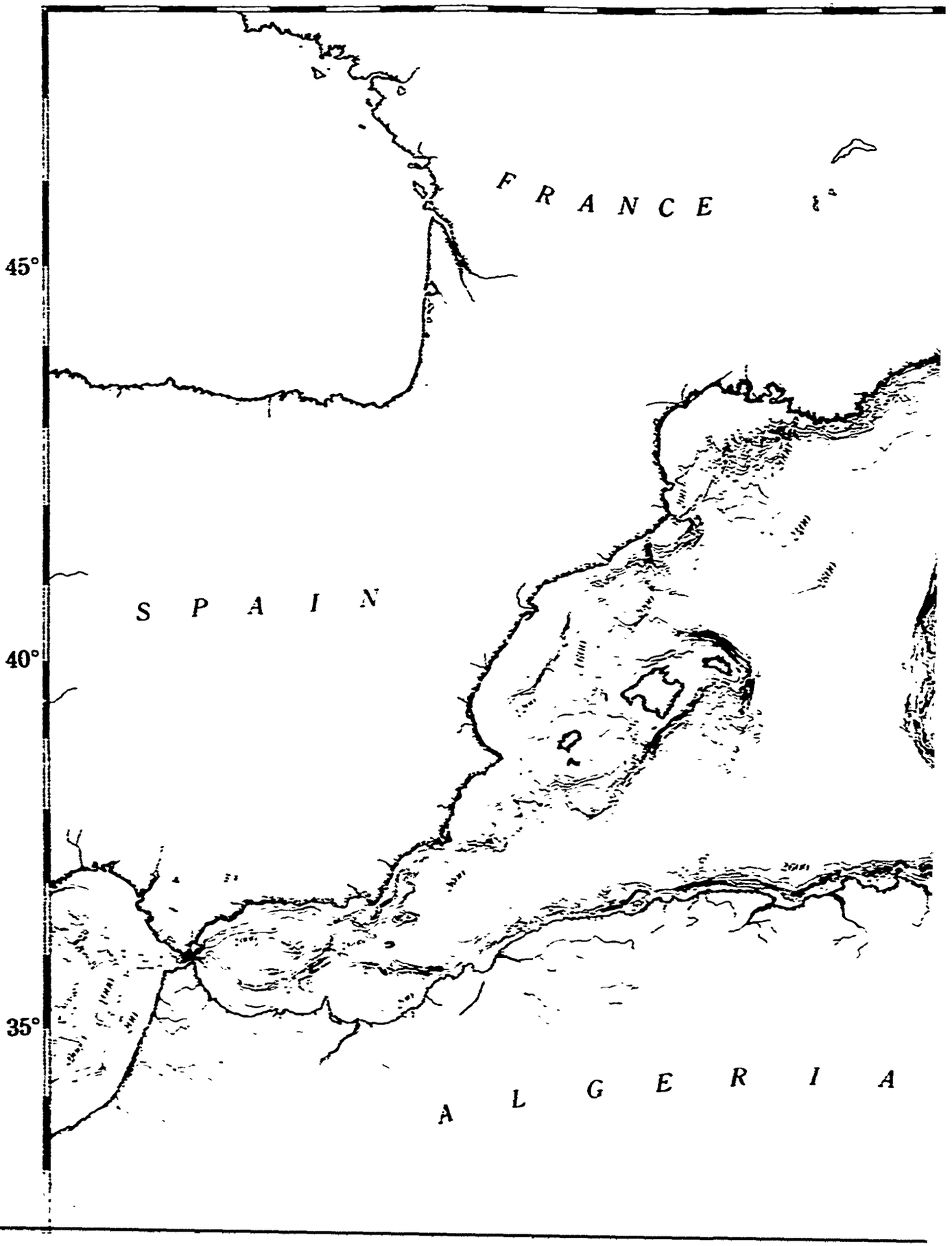
FRANCE
45°
SPAIN
40°
35°
ALGERIA

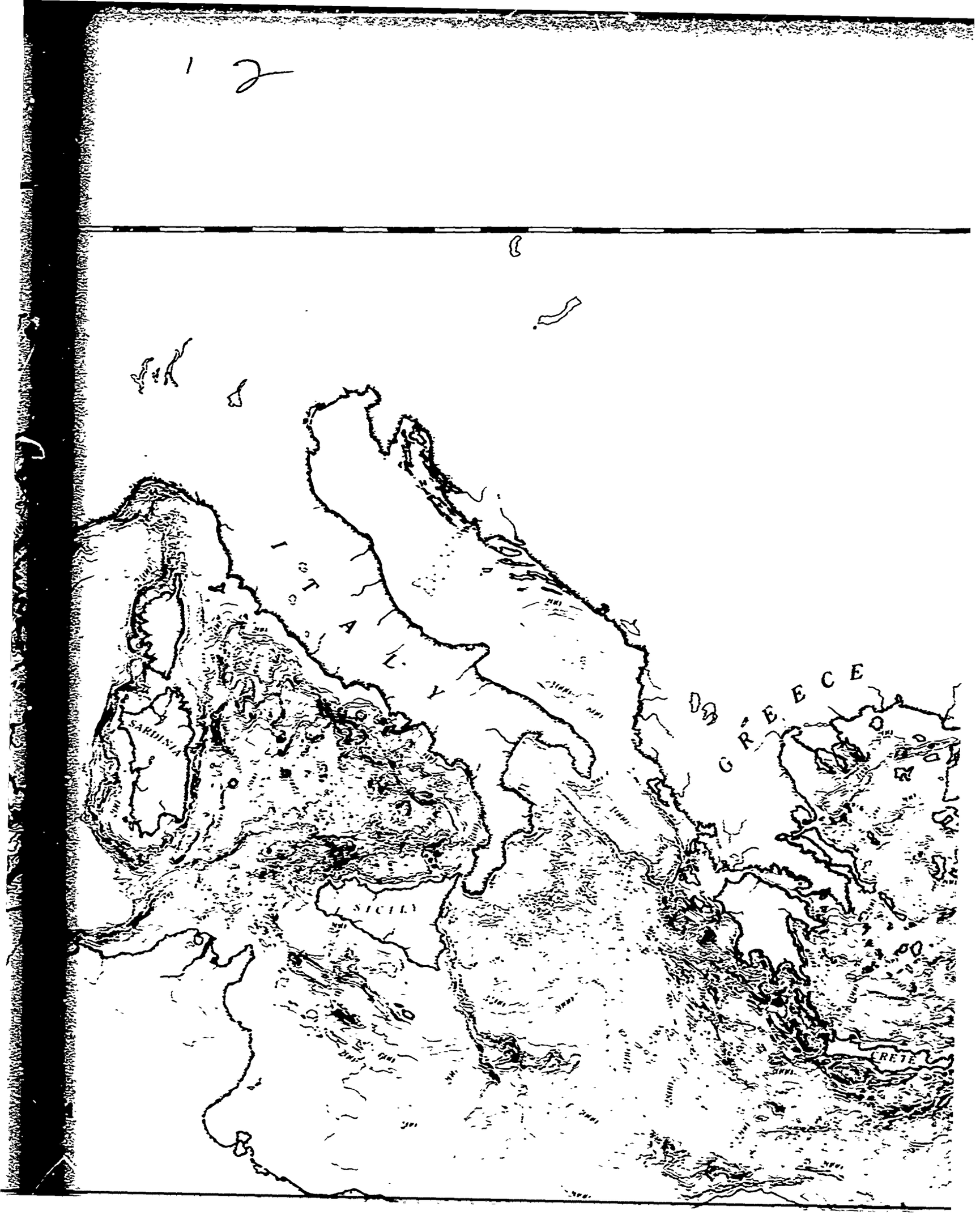
ITALY
SARDINIA
SICILY
GREECE
CRETE

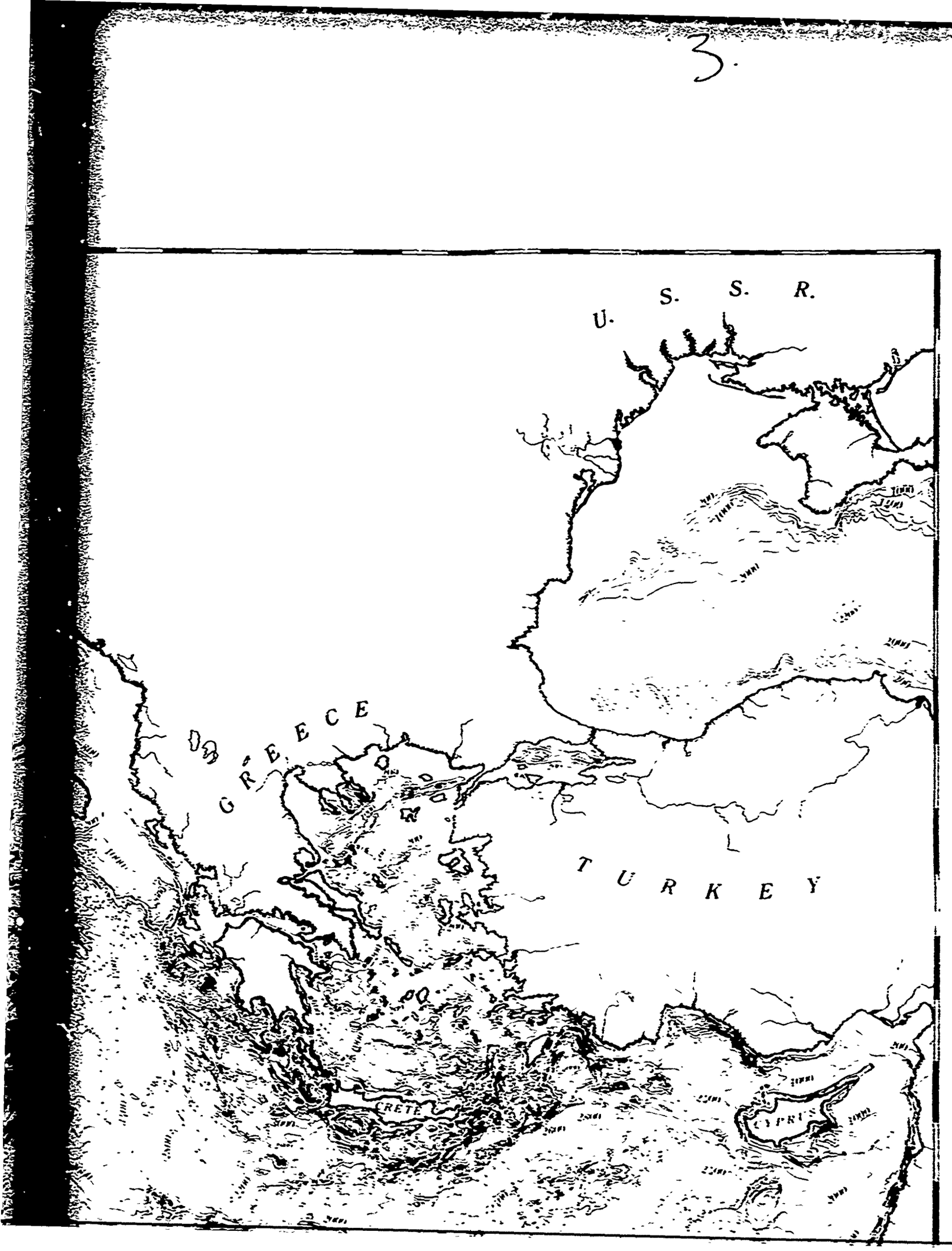
U. S. S. R.
GREECE
TURKEY
CRETE
CYPRUS

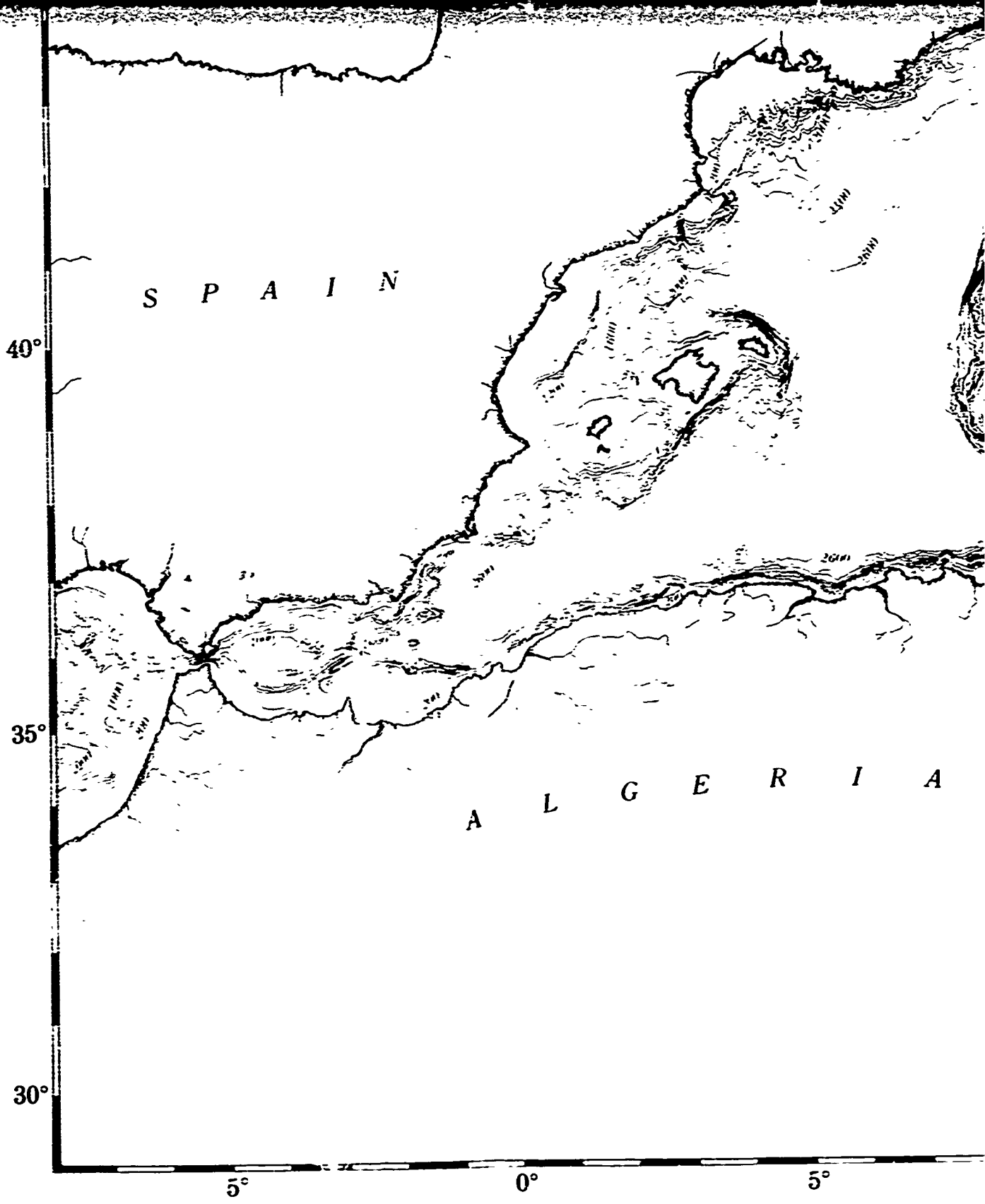

4

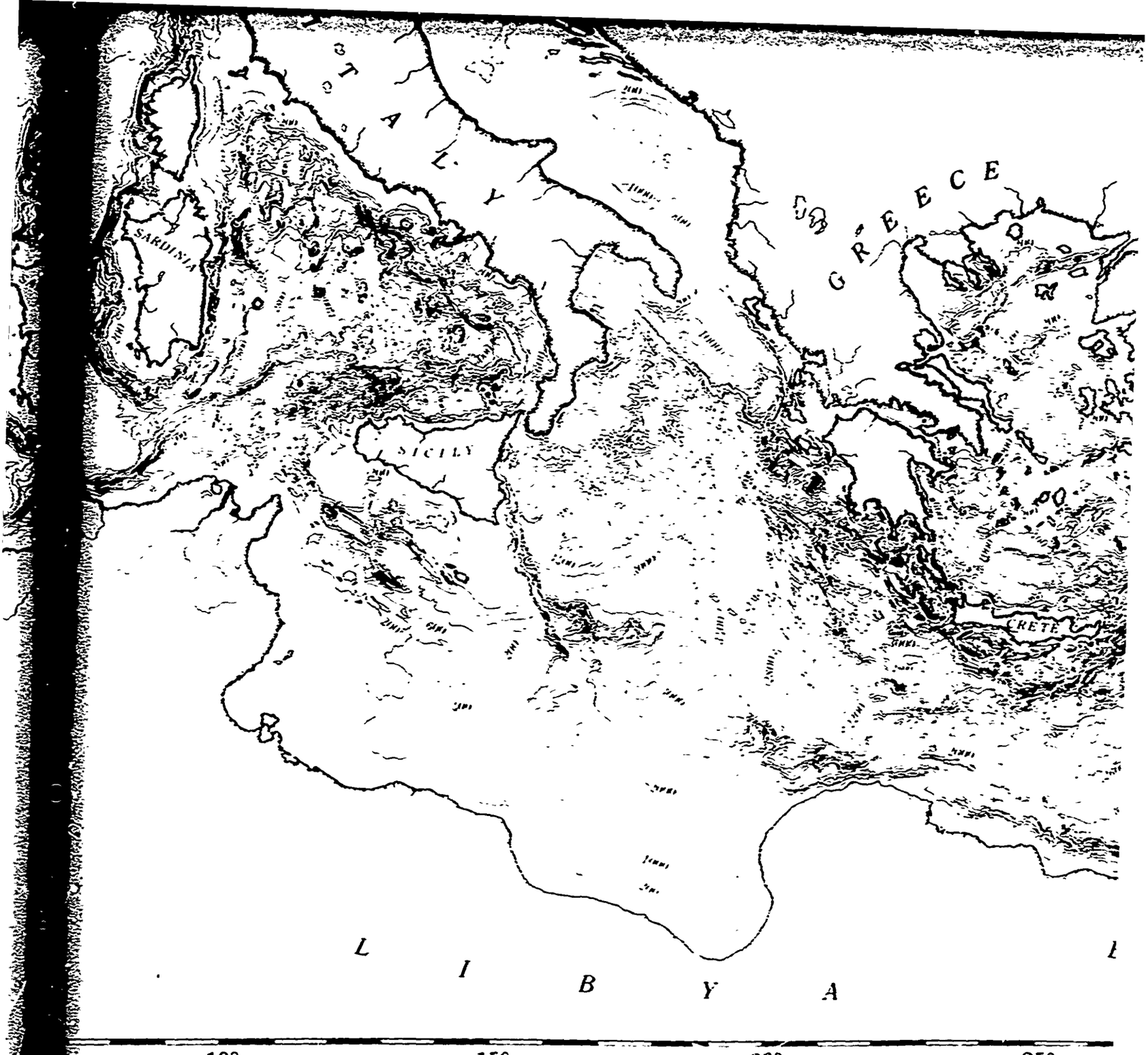

Figure 2.3.1-1. Mediterranean Sea Bathymetry
(Soundings in Meters)

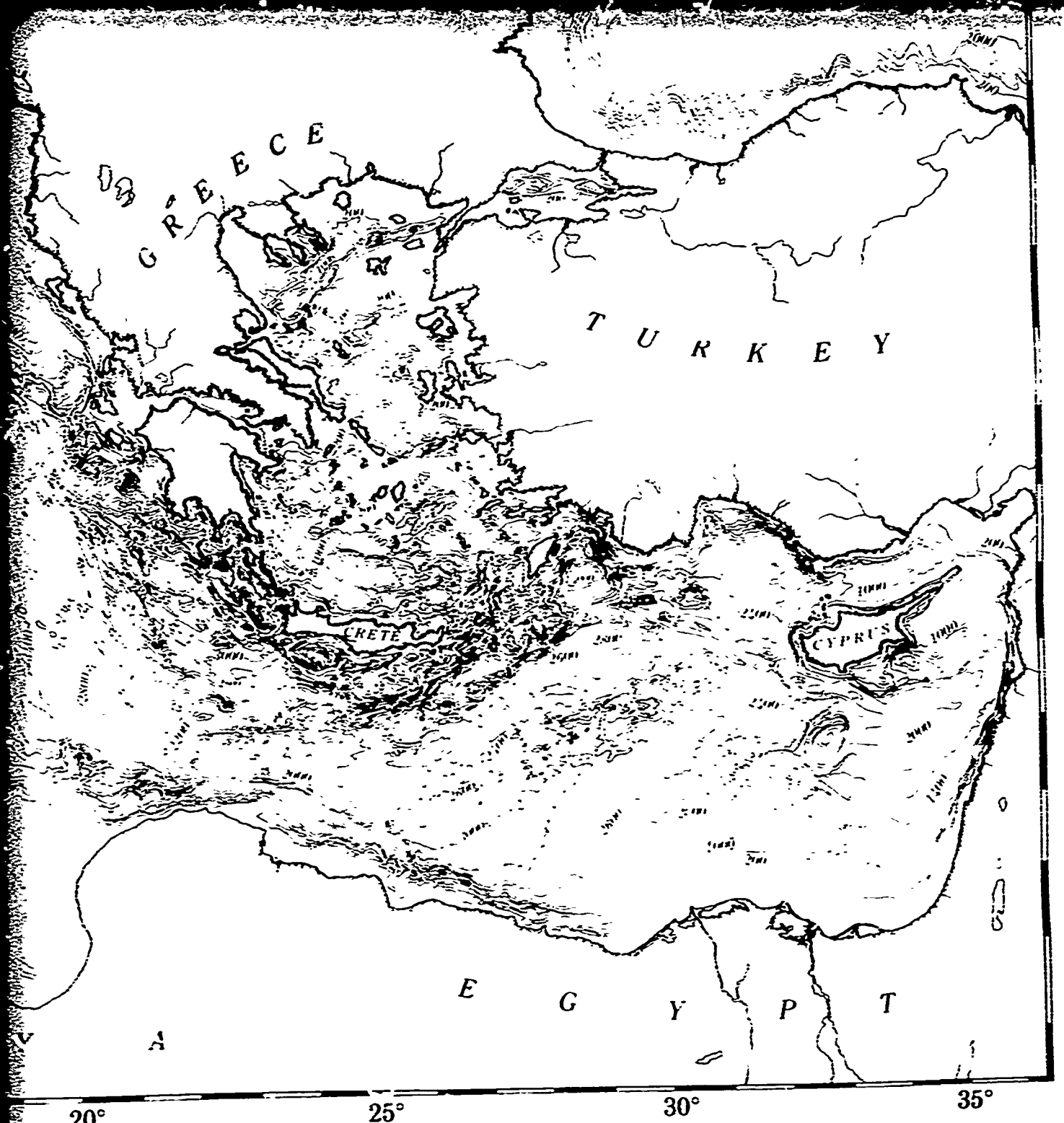

ry

UNCLASSIFIED

6

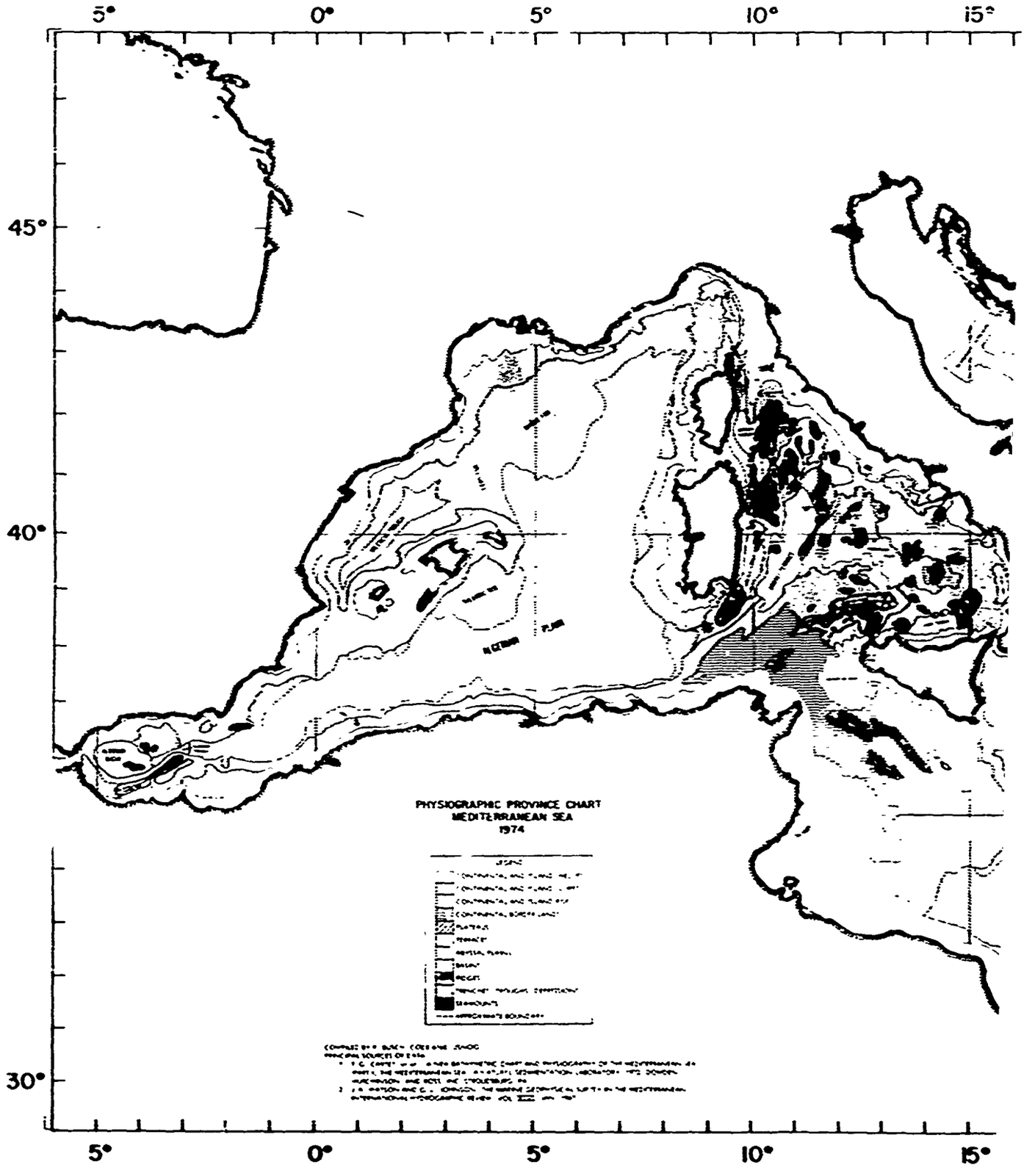

Figure 2.3.2-1. Physiographic Provi

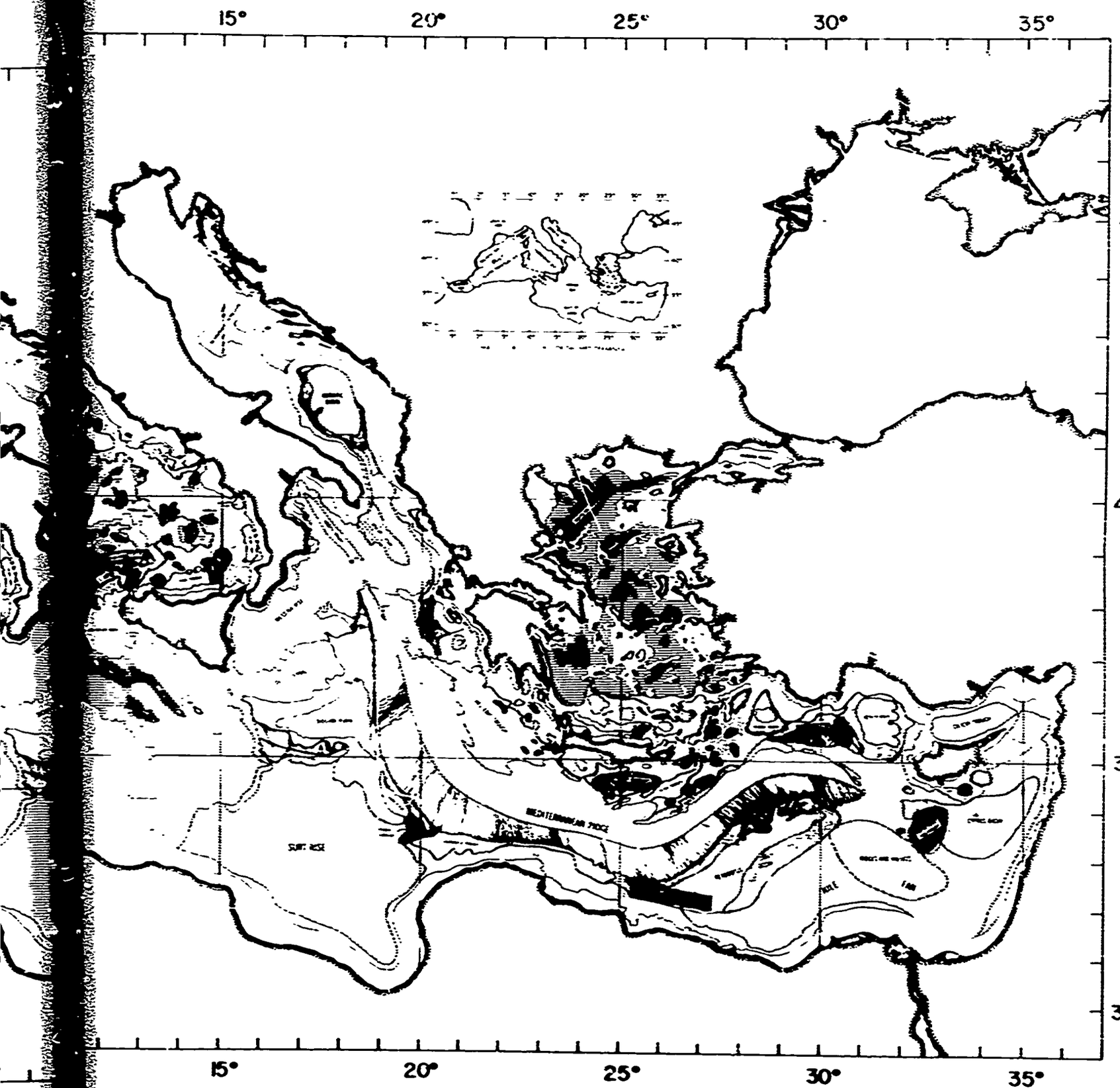

iographic Province Chart of the Mediterranean Sea

vince

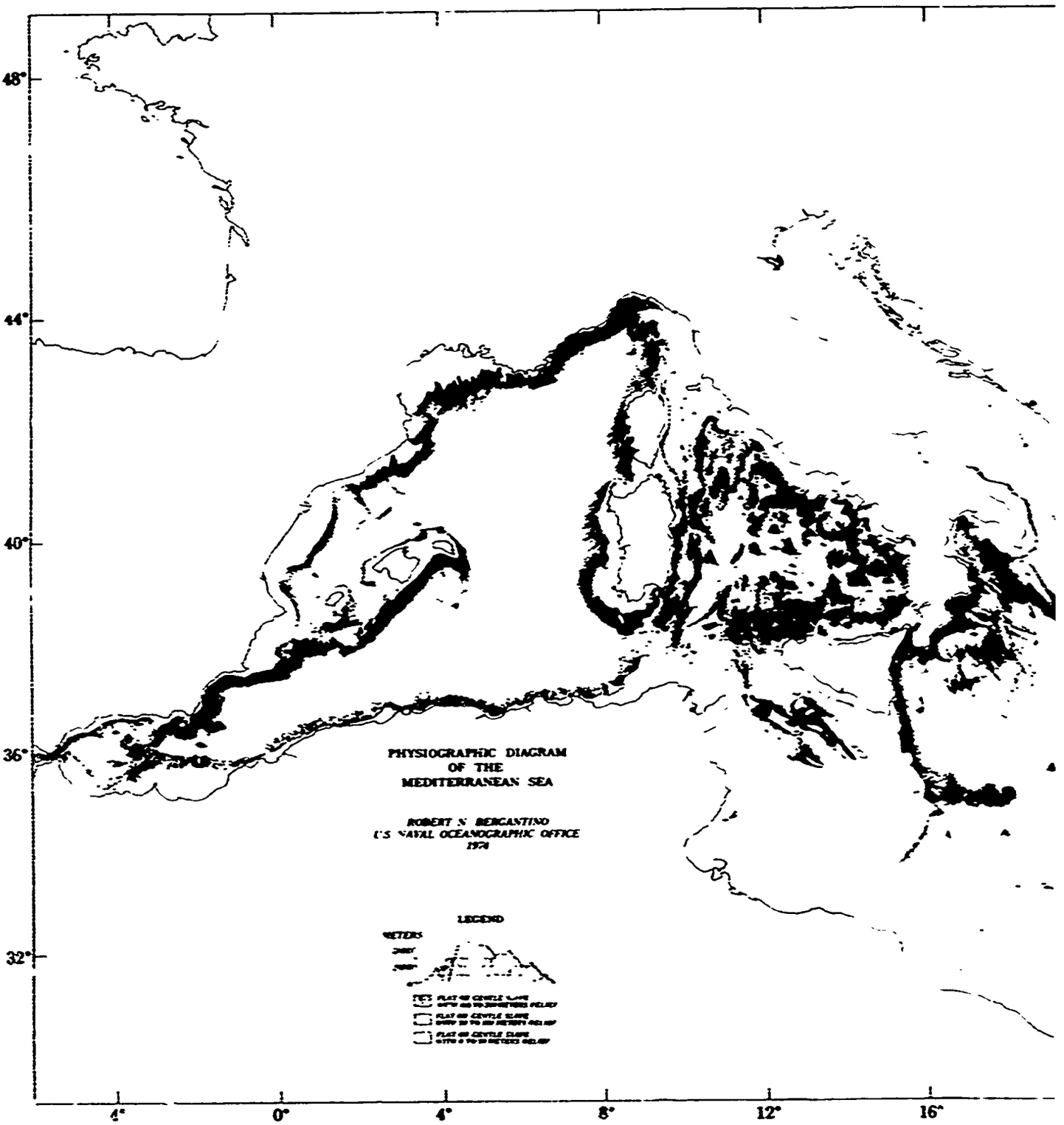

Figure 2.3.2-2. Physiographic Diagr

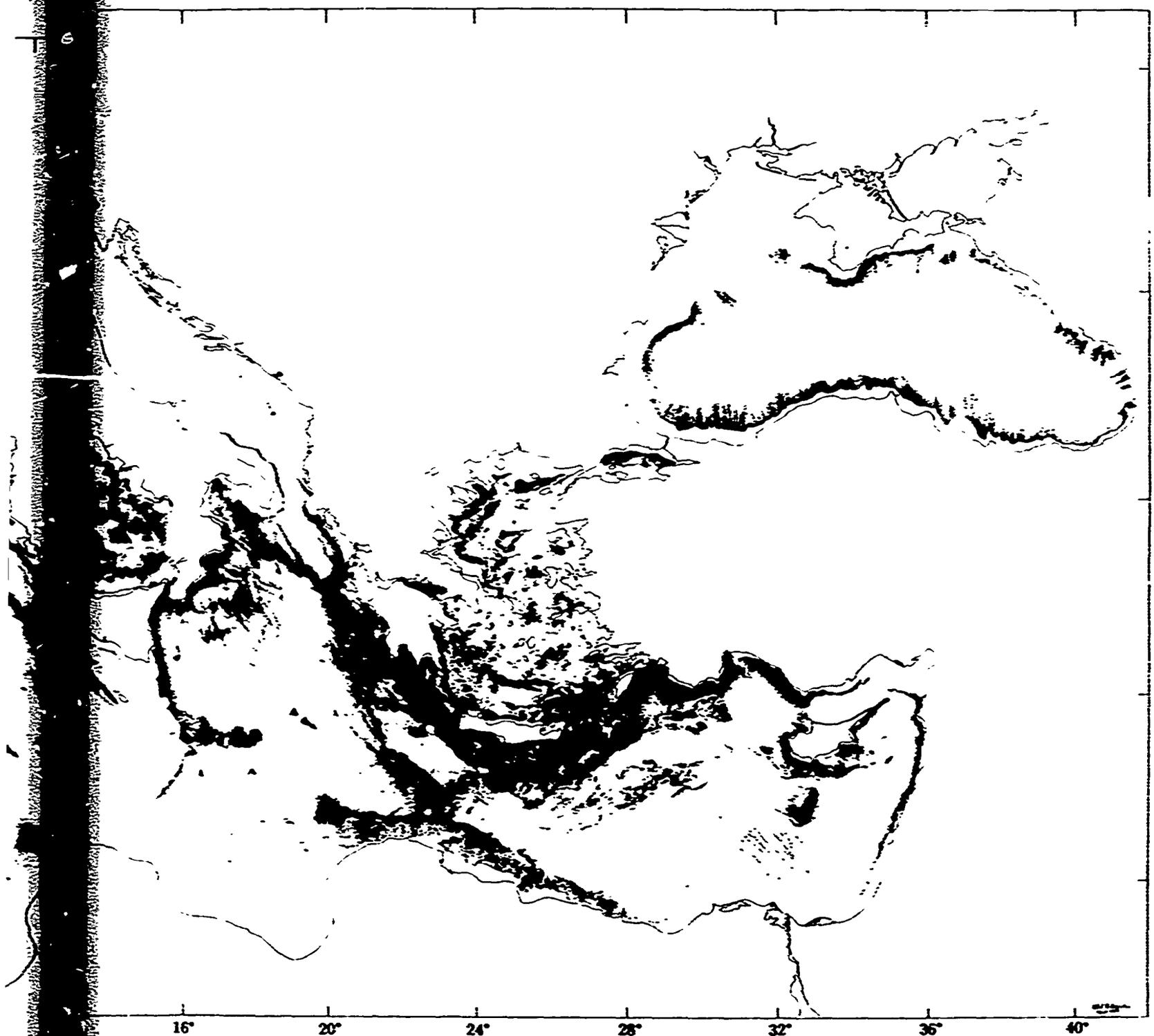

Physiographic Diagram of the Mediterranean Sea

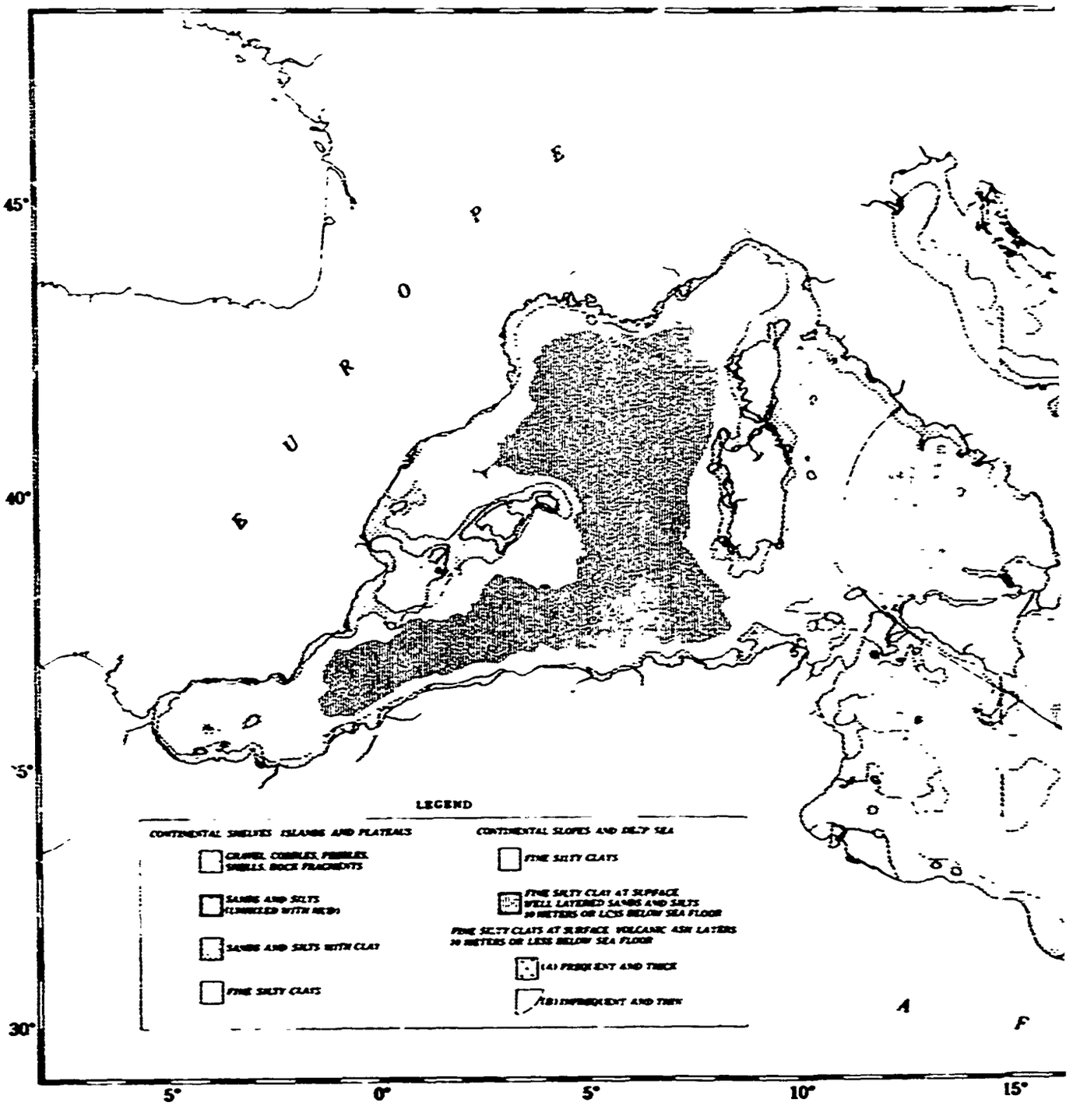

Figure 2.3.3-1. Bottom Sediments in t

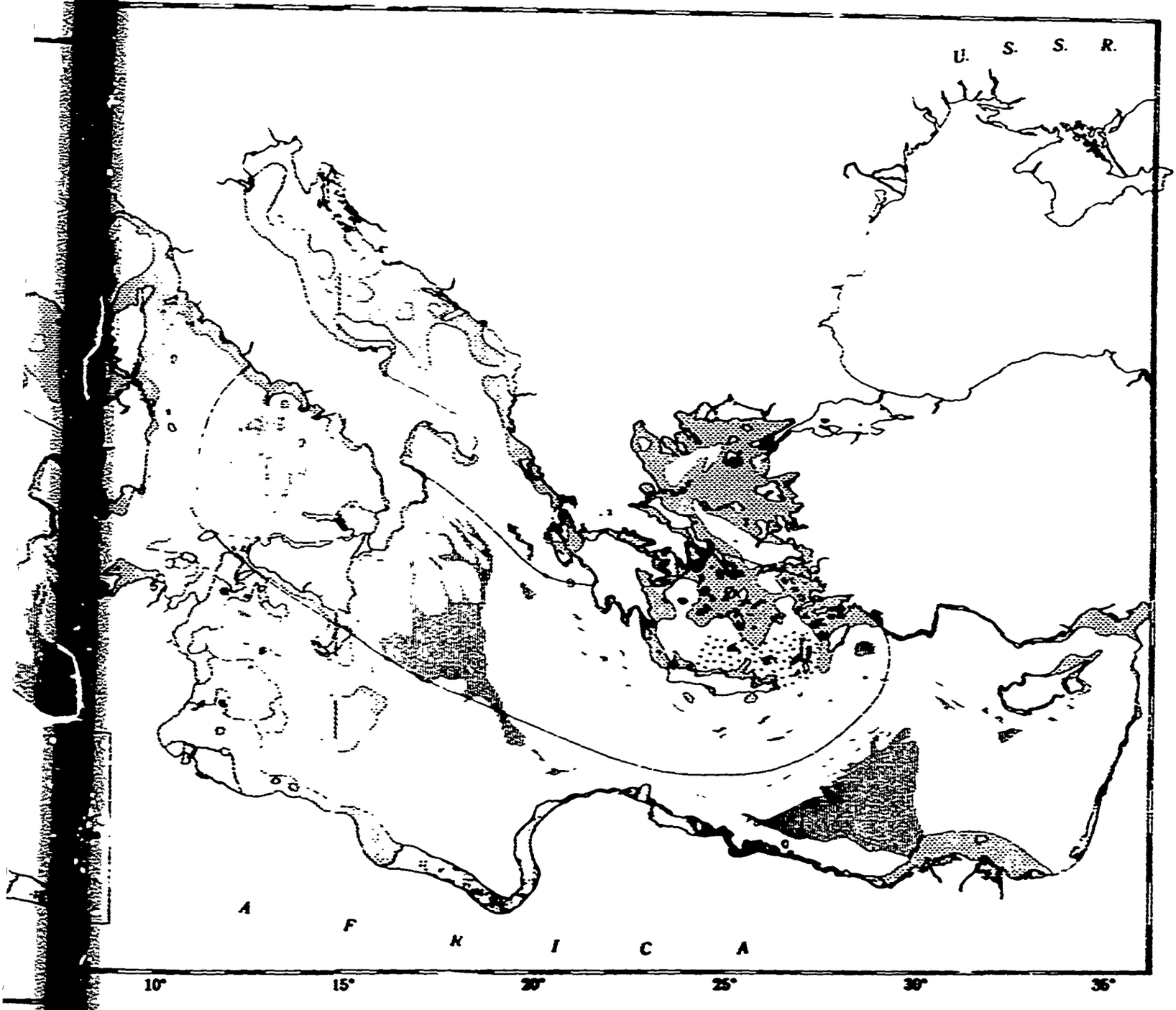

3.3-1. Bottom Sediments in the Mediterranean Sea

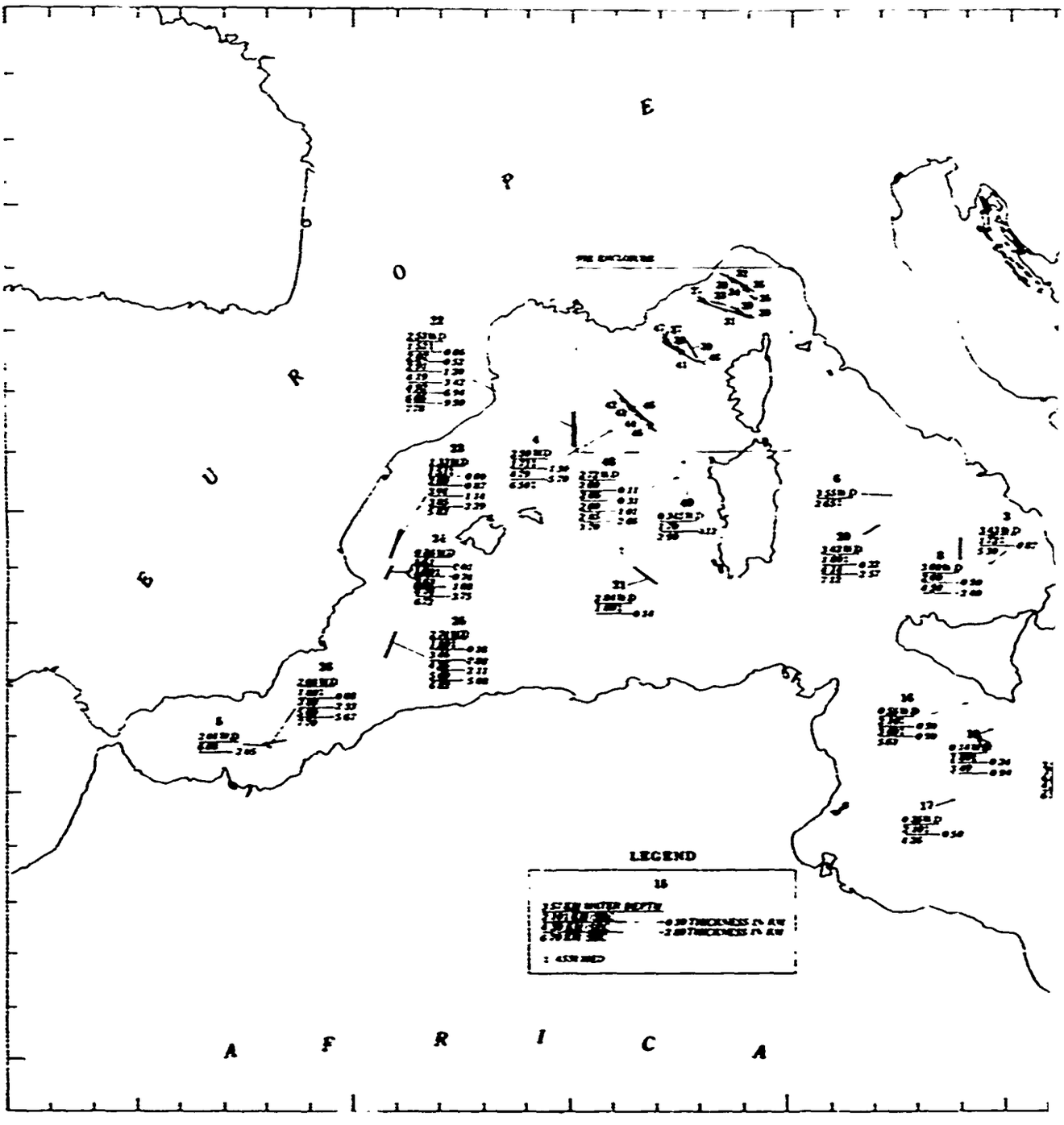

Figure 2.3.4-1a. Mediterranean S

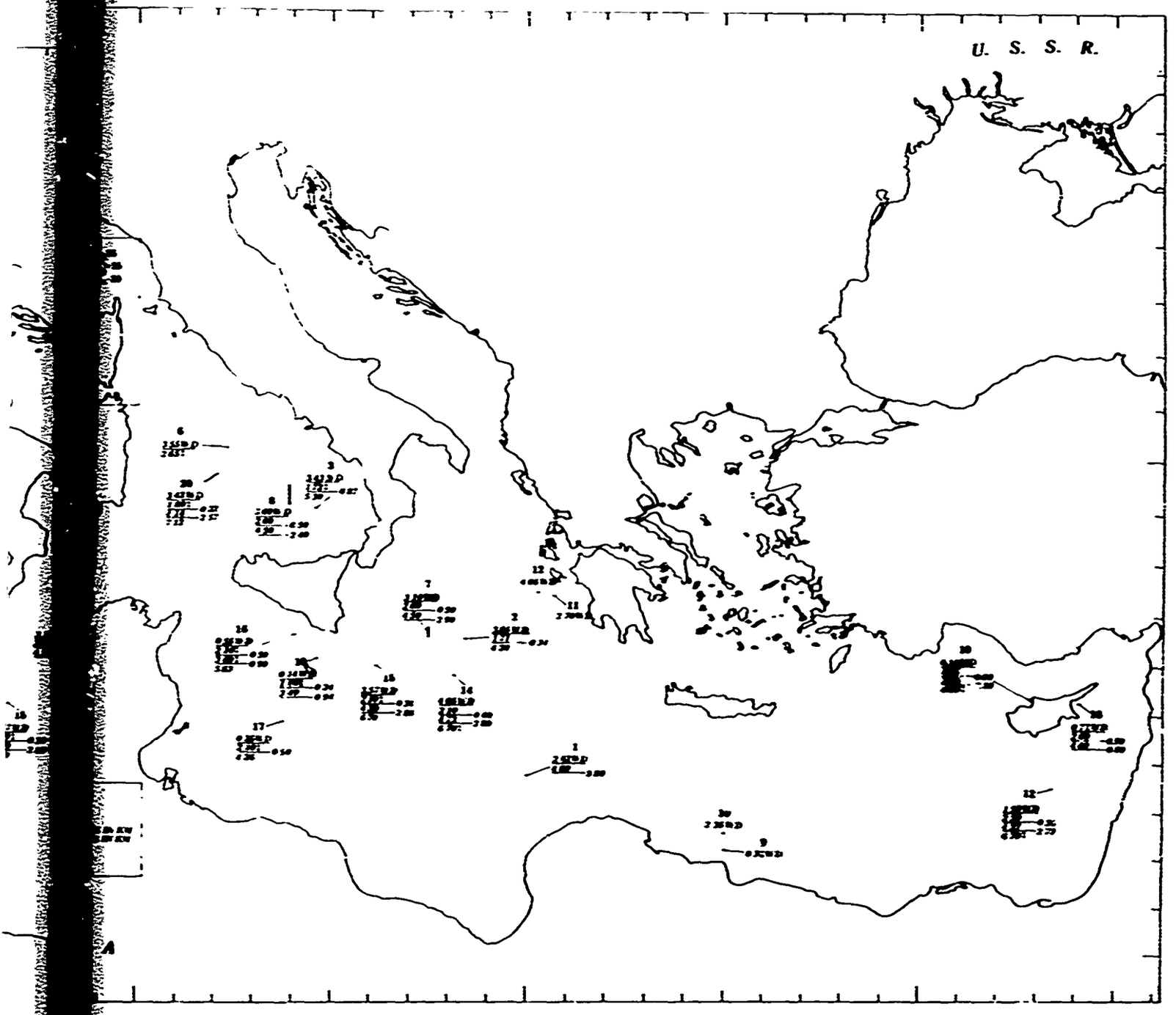

2.3.4-1a. Mediterranean Subbottom Structure

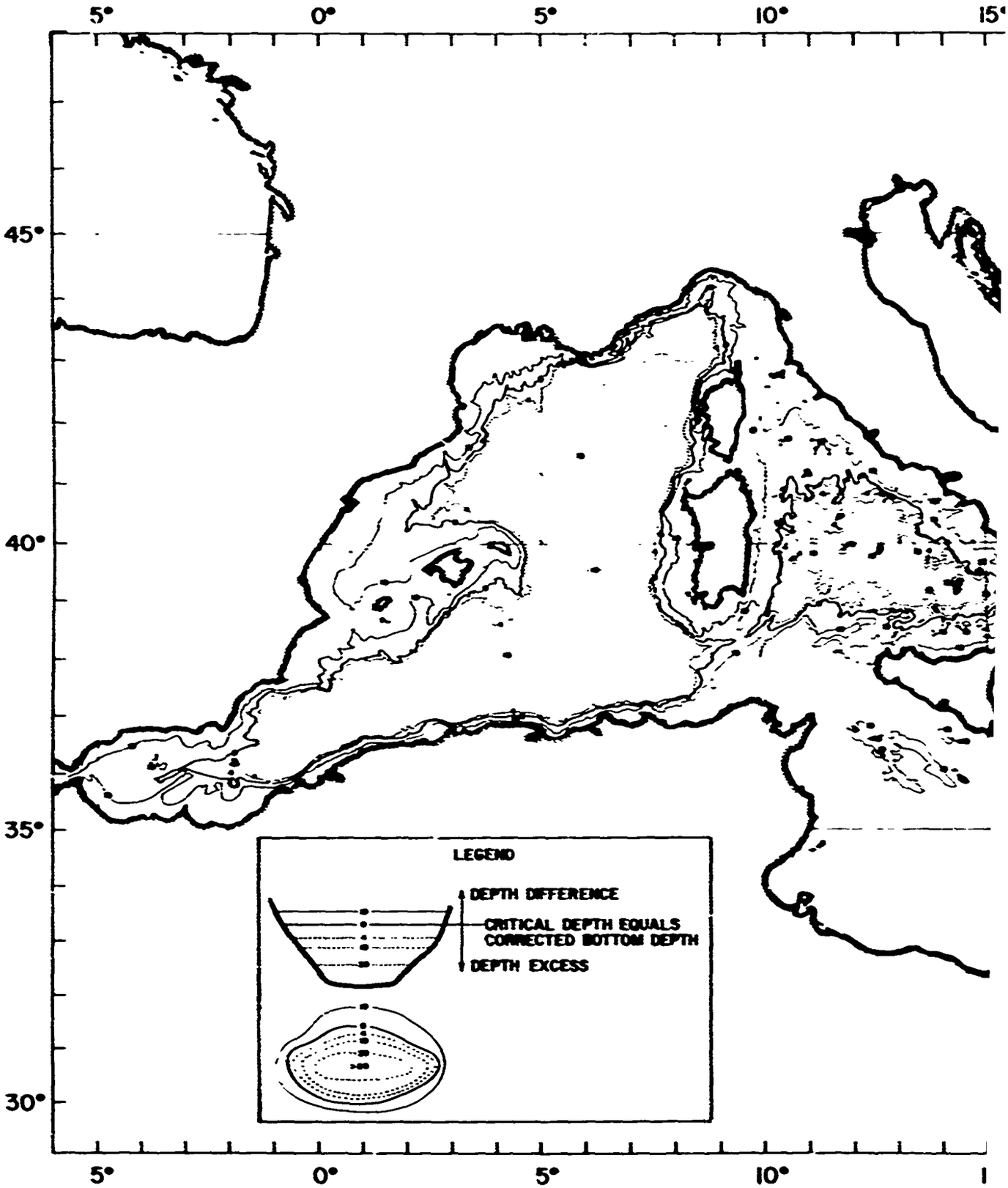

Figure 3.1.4-11(C). Topograp
Critical Depth for S

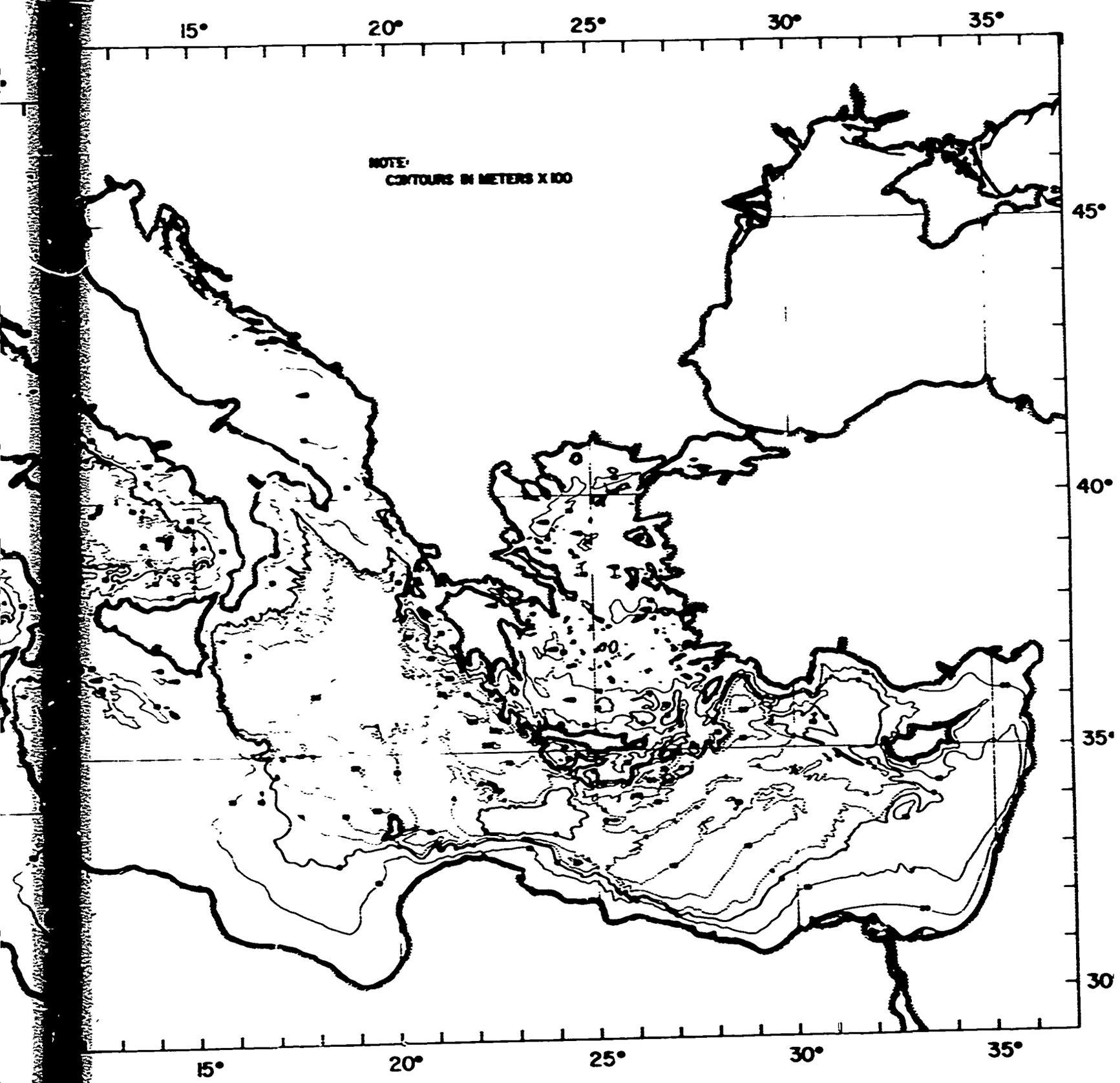

). Topography Shoaler and Deeper than Average Depth for Summer (July-September) (U)

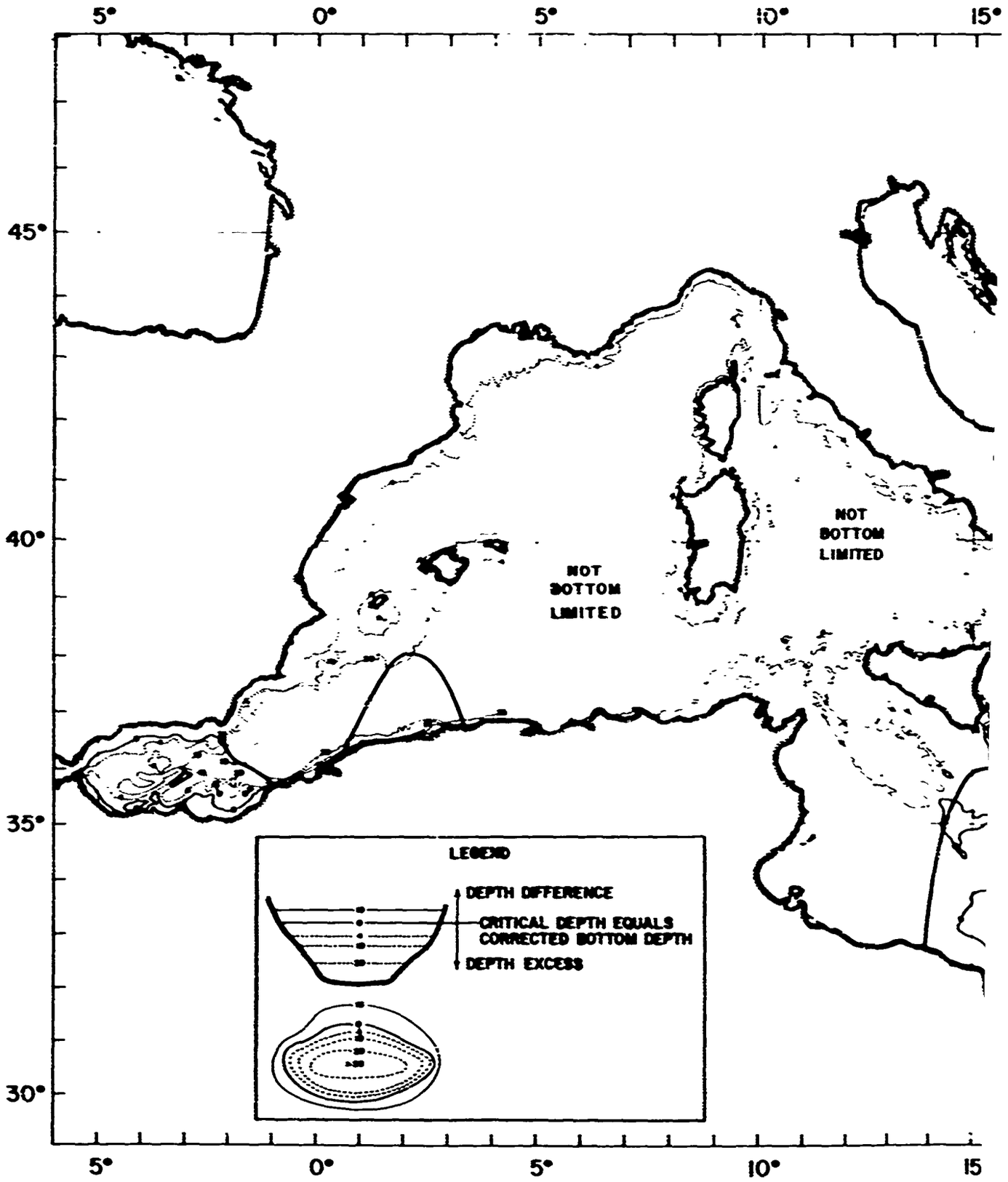

Figure 3.1.4-10(C). Topography S
Critical Depth for Winte

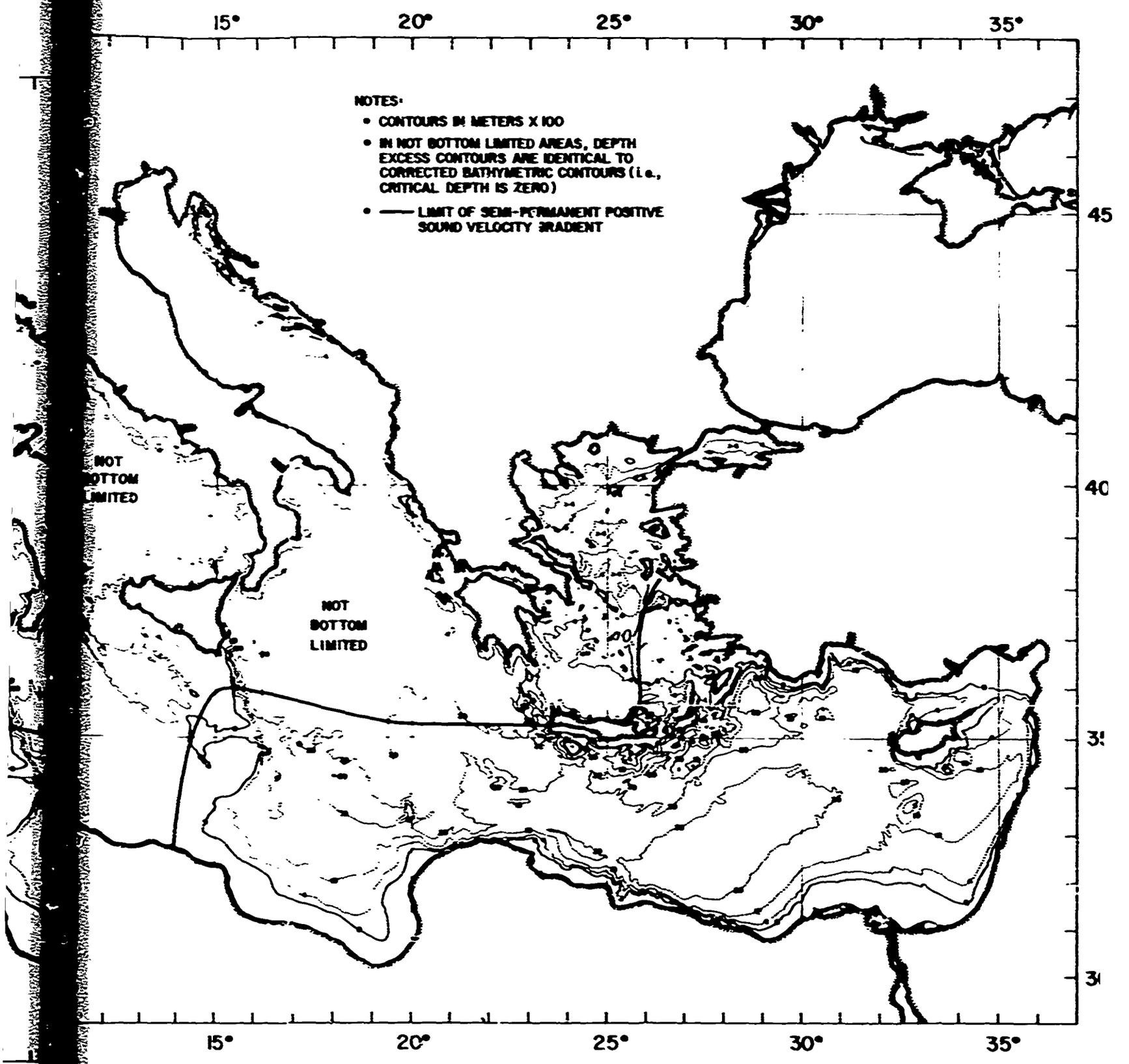

). Topography Shoaler and Deeper than Average Depth for Winter (January-March) (U)

DEPARTMENT OF THE NAVY
OFFICE OF NAVAL RESEARCH
875 NORTH RANDOLPH STREET
SUITE 1425
ARLINGTON VA 22203-1995

IN REPLY REFER TO:

5510/1
Ser 321OA/011/06
31 Jan 06

MEMORANDUM FOR DISTRIBUTION LIST

Subj: DECLASSIFICATION OF LONG RANGE ACOUSTIC PROPAGATION PROJECT (LRAPP) DOCUMENTS

Ref: (a) SECNAVINST 5510.36

Encl: (1) List of DECLASSIFIED LRAPP Documents

1. In accordance with reference (a), a declassification review has been conducted on a number of classified LRAPP documents.

2. The LRAPP documents listed in enclosure (1) have been downgraded to UNCLASSIFIED and have been approved for public release. These documents should be remarked as follows:

   Classification changed to UNCLASSIFIED by authority of the Chief of Naval Operations (N772) letter N772A/6U875630, 20 January 2006.

   DISTRIBUTION STATEMENT A: Approved for Public Release; Distribution is unlimited.

3. Questions may be directed to the undersigned on (703) 696-4619, DSN 426-4619.

BRIAN LINK
By direction

Subj: DECLASSIFICATION OF LONG RANGE ACOUSTIC PROPAGATION PROJECT (LRAPP) DOCUMENTS

DISTRIBUTION LIST:

NAVOCEANO (Code N121LC – Jaime Ratliff)
NRL Washington (Code 5596.3 – Mary Templeman)
PEO LMW Det San Diego (PMS 181)
DTIC-OCQ (Larry Downing)
ARL, U of Texas
Blue Sea Corporation (Dr.Roy Gaul)
ONR 32B (CAPT Paul Stewart)
ONR 321OA (Dr. Ellen Livingston)
APL, U of Washington
APL, Johns Hopkins University
ARL, Penn State University
MPL of Scripps Institution of Oceanography
WHOI
NAVSEA
NAVAIR
NUWC
SAIC

Declassified LRAPP Documents

Current availability key: NS - NRL Stennis; ND - NRL D.C.; AU - ARL:UT; ADXXXXXXX-DTIC

Report Number	Personal Author	Title	Publication Source (Originator)	Pub. Date	Current Availability	Class.
HLR167; CU-195-69-ONR-266-PHYS	Hardy, W. A.	PROJECT APTERYX: FINAL REPORT (U) (HUDSON LABORATORIES OPERATION 245)	Columbia Univ./ Hudson Labs	690301	NS; ND AD511326	C
MCR002	Unavailable	MEDITERRANEAN SEA ENVIRONMENTAL ATLAS FOR ITASS (U)	Maury Center for Ocean Science	691001	NS; ND AD511976	C
NUSCNL3018	Unavailable	TECHNICAL PLAN FOR IMPLANTMENT OF THE TEST BED ARRAY FOR THE LONG RANGE ACOUSTIC PROPAGATION PROGRAM (LRAPP) (U)	Naval Underwater Systems Center	700810	NS; ND	C
Project469 149429855R700	Balaban, M. M.	LRAPP TEST BED ARRAY CABLE FAILURE ANALYSIS (U)	TRW Systems Group	710730	AD0516710; NS; ND	C
BKDCN667	Bernard, P. G., et al.	TECHNICAL DIAGNOSTIC ANALYSIS OF LRAPP TEST BED PROGRAM FAILURE (U)	B-K Dynamics, Inc.	710802	AD0516656; NS; ND	C
NUSCPUB6002	Unavailable	IOMED EXPERIMENT. PRELIMINARY DATA REPORT (U)	Naval Underwater Systems Center	711206	NS; ND	C
ADL ED 15316; ADL-116-672	Unavailable	SQUARE DEAL EXERCISE PLAN (U)	Arthur D. Little, Inc.	720301	ND	C
ADLR4560372	Sullivan, D. L., et al.	PRELIMINARY ANALYSIS OF ACODAC MEASUREMENTS NEAR MADEIRA ON 13-16 OCTOBER 1971 (U)	Arthur D. Little, Inc.	720331	AD0595812; NS; ND	C
MCR07	Gaul, R. D., et al.	IOMEDEX SYNOPSIS ON ENVIRONMENTAL ACOUSTIC EXERCISE IN THE IONIAN BASIN OF THE MEDITERRANEAN SEA NOVEMBER 1971.	Maury Center for Ocean Science	720401	NS; ND	C
P1243	Unavailable	FINAL REPORT ACOUSTIC TEST ARRAY (U)	Raytheon Co.	720831	AD0522104; NS; ND	C
Unavailable	Unavailable	CHART-BATHYMETRIC-SQUARE DEAL EXERCISE (U)	Naval Oceanographic Office	730601	AU	C
TM SA23-C275-73	Wilcox, J. D.	A DESCRIPTION OF THE LRAPP ATLANTIC TEST BED ARRAY FOR MOTION PREDICTION STUDIES (U)	Naval Underwater Systems Center	731212	ND	C
Unavailable	Unavailable	CHURCH ANCHOR AMBIENT NOISE REPORT (U)	Texas Instruments, Inc.	740501	AU	C
Unavailable	Hoffman, J., et al.	CHURCH ANCHOR CW PROPAGATION LOSS AND SIGNAL EXCESS REPORT(U)	Texas Instruments, Inc.	740701	AU; ND	C
MCR104	Unavailable	MEDITERRANEAN ENVIRONMENTAL ACOUSTIC SUMMARY (U)	Maury Center for Ocean Science	740701	NS; ND ADC000411	C
OSTP-39	Romain, N. E.	OSTP-39 NER: ANALYSIS OF DATA FROM A FIELD TRIAL OF THE LAMBDA ARRAY (U)	Westinghouse Electric Corp. and Bell Laboratories	740930	ND	C
MC-103	Unavailable	MEDITERRANEAN ENVIRONMENTAL ACOUSTIC DATA CATALOG (U)	Office of Naval Research	750501	ND	C
Unavailable	Unavailable	SQUARE DEAL SUS TRANSMISSION LOSS (U)	Arthur D. Little, Inc.	750725	AU	C

ENCL (1)